



Loughborough University

Department of Chemical Engineering

Bioprocessing of Bacteriophages and Bacteriocins: Continuous Culture and Downstream Purification

Doctoral Thesis

Submitted by

Francesco Mancuso

Supervised by

Dr D. J. Malik and Dr B. Benyahia

A Doctoral Thesis. Submitted in partial fulfilment of the requirements
for the award of Doctor of Philosophy of Loughborough University

To my family

Abstract

Antimicrobial resistance poses a major problem to health and new alternatives to antibiotics are required. Bacteriophages are viruses able to selectively kill bacteria and they can be exploited to treat infections. Another alternative to antibiotics that can be used to treat bacterial infections are bacteriocins, which are proteins produced by bacteria, meant to kill other strains competing for the same nourishment source. Future industrial demand for large quantities of bacteriophages and bacteriocins imposes the development of a scalable production platform.

In this PhD thesis, research on bioprocessing of bacteriophages K and T3 and one bacteriocin belonging to the subcategory of colicins, E9, has been conducted. The aims were to find the parameters involved in production of phages and colicin E9 using shake flasks and then exploiting them to perform continuous production of both phages and colicin E9 and showing the different outcomes when using complex medium (LB) and a synthetic medium (SM) using glucose as only carbon source.

For the colicin E9 bioprocessing, tests for expression were carried out to measure when and for how long to induce for optimal protein production and the best conditions for production were an induction of 3 h with 1 mM of IPTG in LB medium and >10 h of induction with 1 mM of IPTG in SM. These parameters were used for continuous production of colicin E9 that was carried out using a chemostat. Optimal dilution rates were used to ensure maximum productivity and a production of 1 mg mL⁻¹ of colicin E9 was achieved using either LB and synthetic medium. Then, the influence of flowrates and of different growth media on the first step of purification was assessed using affinity chromatography, showing that the synthetic medium allowed higher recovery of the product in the chromatography step.

Bioprocessing of the phages K and T3 was carried out in shake flasks and 5L fermenters, researching the best parameters for producing the highest titres. The effect on the final titre of a variety of multiplicities of infection (MOI), the ratio of phages out of bacteria at the moment of infection, was evaluated. For both phages the MOI that ensured the highest phage titre, 10¹¹ PFU mL⁻¹, was 0.01. The parameters measured were then used for continuous production of bacteriophage T3.

Continuous phage T3 production was carried out using a novel reactors layout, composed by 3 separated stages. This set up allowed to divide the production of the host cells, carried out in the first reactor, from the infection, carried out in the second reactor, and from the final amplification step, carried out in the third reactor. The synthetic medium with glucose as only carbon source and the dilution rate (D, the volume of media that flows in the reactor per hour) were used to control the growth rate of the host, which strongly influenced the final production of bacteriophages. Different D

were tested, from 0.1 to 0.6 h⁻¹ and the independent control of the dilution rate of the first and the second reactor allowed to produce phage lysates at the same concentrations as in batch process, reaching a constant production of 2x10¹¹ PFU mL⁻¹ when D = 0.5 h⁻¹ was used in the first reactor.

Moreover, research on the downstream process of phage bioprocessing was conducted, aiming to reduce the host cell protein burden from phage samples using scalable techniques. The purification of bacteriophages from complex medium was performed using ultrafiltration in batch mode in a stirred cell (SC) and in using tangential flow filtration (TFF). The high shear stress produced SC decreased the viability of the tailed phage K of ~2 log₁₀ in 2 h and the positive effects of purification were cancelled by the loss of titre. Phage T3, which has a short tail, showed no side effects due to shear stress. TFF was then tested and both phage K and T3 were purified without significant viability loss. Size exclusion chromatography was used to assess the final protein concentration and showed a decrease of host cell protein load in both phages samples purified by ultrafiltration. Samples of both phages were mixed with a positively charged resin used for anion exchange chromatography and it was shown that phages that have been filtered using ultrafiltration can bind 10 times more than phages of the lysate.

The main aim of purification phages produced from Gram-negative bacteria, such as T3, was to reduce the endotoxin levels (or lipopolysaccharide, LPS). Endotoxins are a major contaminant that can cause serious problems if administered and must be removed from drug products. The target was to bring the LPS levels from the initial concentration of 5x10⁶ EU mL⁻¹ (Endotoxin Units per mL) below the limit of 5 EU mL⁻¹. Endotoxin removal was performed using ultrafiltration and liquid-liquid extraction (LLE).

The first method tested was the TFF ultrafiltration, carried out in batch mode or in diafiltration mode. Batch ultrafiltration showed a decrease of LPS of ~2 log₁₀, either starting from a phage T3 sample from LB or from SM. Diafiltration TFF reached ~3 log₁₀ reduction of LPS in both LB or SM samples, but in LB samples it took 20 h and in SM samples only 4 h, showing how a chemically defined medium could improve the purification of phages produced from Gram-negative hosts.

The other method tested to further reduce LPS concentration was liquid-liquid extraction, using 1-octanol as organic phase. Many different conditions of LLE were tested, such as length of contact time between aqueous and organic phases, different mixing methods and number of extractions. Liquid-liquid extraction using octanol ensured a reduction of endotoxins of 4 log₁₀ from the initial concentration. This technique was then followed by ion exchange chromatography, which allowed to reach a final concentration of 10² EU mL⁻¹.

Finally, analysis on how endotoxins concentrations affected the aggregation of phage T3 were performed, showing how phage T3 aggregates in presence of endotoxins whilst it has a low polydispersity at low endotoxins concentrations.

This thesis showed how is it possible to produce bacteriophages and an antimicrobial protein at high concentrations using a continuous production mode and a chemically defined medium. The positive effects of the synthetic medium on the downstream steps were also illustrated, such as a lower burden for ion exchange columns and a faster reduction of endotoxin concentration from the samples.

Acknowledgments

I would like to thank my supervisors Dr. Danish J. Malik and Dr. Brahim Benyahia for their constant support and help throughout these three years.

During these three years I was lucky to be with two incredible men who became my friends: a special thanks to Andrea, we shared the same office, the same laboratories and the same house for 30 months! He has offered countless songs to all of us to cheer all of us up also during the most intense days; he taught about Neapolitan culture and spread the love for Naples, the song and the delicious food. And thanks to Salvo, the best chemist in the world. We started together, we helped each other during all these years and he was the lab partner that everybody would like to have. I'll never forget our endless days in the lab talking about music, politics and scientific cuisine. Nor I will forget what an amazing cook he is!

A big thanks to Gurinder, who was always there for a chat, a laugh and for support. She always made the lab a very pleasant place where to stay despite her questionable music taste. Thanks to Nimit, Ansa, Zhara, Jiahui and Kerry.

Thanks to Serena, Raffa and Federica who made me feel less homesick and to Isabel and the Portuguese gang. Special mention to Mamba, he's THE man!

I always want to thank all the guys Volleyball team and the Nuoto Sincronizzato Team, who incited me to stay active and to celebrate after every game; and all the Italians in Loughborough, we spent a lot of nice moments.

Thanks to my parents and my brother, who were only physically far away but I felt very close all the time; to my girlfriend Alessia was one of the people that most suffered for this PhD, that took us apart for 3 years and to her goes all my gratitude for the support despite was not easy.

Thanks to the technicians and staff at the Chemical Engineering Department, they helped me A LOT.

Publications

Mancuso, F., Shi, J., Malik, D. J. (2018). High Throughput Manufacturing of Bacteriophages Using Continuous Stirred Tank Bioreactors Connected in Series to Ensure Optimum Host Bacteria Physiology for Phage Production. *Viruses* 2018, 10(10), 537; <https://doi.org/10.3390/v10100537>

Cinquerrui, S., Mancuso, F., Vladislavljević G. T., Bakker, S. E., Malik D. J. (2018). Nanoencapsulation of Bacteriophages in Liposomes Prepared Using Microfluidic Hydrodynamic Flow Focusing. *Front. Microbiol.*, 12 September 2018 | <https://doi.org/10.3389/fmicb.2018.02172>

Malik D.J., Sokolov I.J., Vinner G.K., Mancuso F., Cinquerrui S., Vladislavljevic G.T., Clokie M.R.J., Garton N.J., Stapley A.G.F., Kirpichnikova A. (2017). Formulation, Stabilisation and Encapsulation of Bacteriophage for Phage Therapy. *Adv Colloid Interface Sci.* 2017 Nov;249:100-133. doi: 10.1016/j.cis.2017.05.014

Conference posters and presentations

Mancuso, F., Shi, J., Malik, D. J. (2018). Effect of dilution rate on continuous production of phages using two chemostats in series. 5th World Congress on Targeting Infectious Diseases: Targeting Phage & Antibiotic Resistance 2018, Florence.

Mancuso, F., Benyahia, B., Malik, D. J. (2017). A scalable ultrafiltration process for phage purification. Centennial Celebration of Bacteriophage Research, Institut Pasteur, Paris, France.

List of figures

Figure 2. 1 Schematic drawing of a single tailed phage	12
Figure 2. 2 A schematic to show the steps in a phage infection cycle.	13
Figure 2. 3 Schematic diagram of the cellstat, composed of two reactors connected in series. (Husimi et al., 1982b).	26
Figure 2. 4 Level sensors are used for the control of valves.....	27
Figure 2. 5 Schematic of a virustat.....	29
Figure 2. 6 Principles of dead-end filtration (a) and cross flow filtration (b).	33
Figure 2. 7 Schematic of batch tangential flow filtration.	34
Figure 3. 1 Schematic showing layout of the continuous phage production process.....	52
Figure 3. 2 Schematic diagram showing (a) the UF stirred cell and (b) the shear distribution in the vicinity of the stirrer.	53
Figure 3. 3 Diagram of the filtration unit. It could be used to perform batch UF or diafiltration.	54
Figure 4. 1 Test expression of colicin in E. coli BL21(DE3)pLysS, in LB (left) and synthetic medium (right) at different conditions.....	62
Figure 4. 2 Batch growth and colicin E9 production in LB broth.....	63
Figure 4. 3 Batch growth and colicin E9 production in SM.....	64
Figure 4. 4 Batch production of colicin E9 in LB (empty circles, ○) and in SM (empty squares, □).....	64
Figure 4. 5 Continuous production in LB at 37°C, residence time 3 hours.....	65
Figure 4. 6 Continuous production in SM at 30°C, residence time 10 hours.....	66
Figure 4. 7 Production of colicin E9 in LB (open circles, ○) and SM (open diamonds, ◇).	67
Figure 4. 8 Breakthrough curves of colicin E9 lysates from LB medium operated at 10 CV h ⁻¹	69
Figure 4. 9 Breakthrough curves of colicin E9 lysates from synthetic medium operated at 10 CV h ⁻¹ . 70	
Figure 5. 1 Growth curve of S. aureus in BHI broth.	74
Figure 5. 2 Growth curve of E. coli in LB broth.	75
Figure 5. 3 One-step growth data for phage K grown in BHI broth at 37°C.	76
Figure 5. 4 One-step growth data for phage T3 grown in LB broth at 37°C.	77
Figure 5. 5 Growth curve of S. aureus and amplification of phage K in BHI using different MOIs.	78
Figure 5. 6 Growth curve of S. aureus and amplification of phage K in BHI adding 2% ammonium sulphate, using a bioreactor with 2L working volume.	79
Figure 5. 7 Growth curve of E. coli and amplification of phage T3 in LB using different MOIs.	81
Figure 5. 8 Growth curve of E. coli in synthetic medium.	83

Figure 5. 9 One-step growth data for phage T3 grown in synthetic medium..	84
Figure 5. 10 Final concentration of phage T3 after infection using different MOI in shake flasks.	85
Figure 5. 11 Host bacterial cell productivity in reactor 1 (R1), as a function of different dilution rates in R1, filled squares (■). Concentration of host bacterial cells in R1, filled circles (●).....	86
Figure 5. 12 Glucose conversion as a function of dilution rates in R1.	87
Figure 5. 13 Phage productivity (■) in Reactor 2 (R2) as a function of the dilution rate (D1) in Reactor 1 (R1)..	88
Figure 5. 14 Effect of bacteria physiology and dilution rate D2 on phage titres in the second reactor (R2)..	89
Figure 5. 15 Final phage titres in Reactor 3 (R ₃) after overnight amplification following infection in R ₂ using dilution rates (D ₂).	90
Figure 6. 1 Percentage rejection of different MW dextrans in the stirred cell using Millipore membranes of 100 kDa or 300 kDa MWCO at high or low shear.....	97
Figure 6. 2 Percentage rejection of different MW dextran solutions in the stirred cell with Alfa Laval membranes of 100 kDa at high or low shear.	98
Figure 6. 3 Time series data showing viability of phage K in the stirred cell exposed to different shear stress levels over time.	99
Figure 6. 4 Cryo-TEM image of phage K after UF in the SC.....	100
Figure 6. 5 Time series data showing viability of T3 phages in the stirred cell exposed to different shear stress levels over time.	101
Figure 6. 6 Cryo-TEM image of T3 phages after UF.....	101
Figure 6. 7 Viability of phage K purified using a 100 kDa MWCO membrane using the crossflow apparatus measured over time.....	102
Figure 6. 8 Viability of phage T3 purified using a 100 kDa MWCO membrane using the crossflow apparatus measured over time.....	103
Figure 6. 9 Permeate flux of sterile BHI (empty squares, □) and phage K lysate in BHI (empty diamonds, ◇) in the CFF apparatus.....	104
Figure 6. 10 Permeate flowrates of sterile LB (empty squares, □) and phage T3 lysate in LB (empty diamonds, ◇) in the cross-flow apparatus. Transmembrane pressure $\Delta P = 0.5$ bar.	105
Figure 6. 11 Gel filtration chromatography of Phage K lysate (solid line) and Phage K after batch UF (dashed line).	106
Figure 6. 12 Gel filtration chromatography of Phage T3 lysate (solid line) and Phage T3 after batch ultrafiltration (dashed line).....	107

Figure 6. 13 Ion exchange isotherm curves of phage K before (phage K lysate, filled squares, ■) and after batch ultrafiltration (empty squares, □).....	108
Figure 6. 14 Ion exchange isotherm of phage T3 before (phage T3 lysate, filled squares, ■) and after batch ultrafiltration (empty squares, □).....	109
Figure 7. 1 Permeate fluxes for batch ultrafiltration of phage T3 lysates produced in LB (□) or SM (○).....	113
Figure 7. 2 Endotoxin concentration before and after batch ultrafiltration in LB broth (filled columns) and SM (empty columns).....	114
Figure 7. 3 Permeate fluxes for diafiltration of phage T3 lysates produced in LB or SM.	115
Figure 7. 4 LPS concentration in LB lysate (□) and SM lysate during diafiltration (○).....	116
Figure 7. 5 Endotoxin concentration after LLE using different volume ratios of 1-octanol/phage T3. Filled squares (■) represent LPS concentration in phage T3 lysates and filled diamonds (◆) represent LPS concentration in phage T3 after batch ultrafiltration.	117
Figure 7. 6 Endotoxin concentration in phage T3 lysate after multiple LLE cross-current equilibration steps.	118
Figure 7. 7 Endotoxin concentration in phage T3 lysate over time using enhanced mixing.	119
Figure 7. 8 Size distribution and aggregation state of phage T3 samples after different purification methods: LLE in 1-octanol (dotted line), diafiltration (continuous line) and batch ultrafiltration (dashed lines).	120
Figure 7. 9 Cryo-TEM image of phage T3 after batch ultrafiltration.....	121
Figure 7. 10 Particle size distribution and aggregation state of phage T3 sample, before (dashed line) and after diafiltration followed by addition of pure endotoxins (continuous line).	122
Figure 7. 11 Isothermal curves of adsorption of pure LPS to QA resin	123
Figure 7. 12 Isothermal curves of adsorption of different phage T3 samples to QA resin.....	124
Figure 7. 13 Loading and elution of phage T3 sample (after LLE) and endotoxin from QA ion exchange column. Filled circles (●) represent endotoxin units (EU) and the dashed line the NaCl concentration.	125
Figure 7. 14 Schematic model of interaction between phage T3, LPS molecules (green circles) and QA resin.....	129
Figure S. 1 Viscosity of BHI measured using a rheometer with cone-plate configuration.....	150
Figure S. 2 Viscosity of LB measured using a rheometer with cone-plate configuration.....	151
Figure S. 3 Technical drawing of top part of the crossflow filtration apparatus.	152
Figure S. 4 Technical drawing of bottom part of the crossflow filtration apparatus.	153

Figure S. 5 Operative tangential flow filtration apparatus. 154

Figure S. 6 Adsorption rates of phage T3 at different dilution rates. Filled circles (●) represent adsorption at $D1= 0.5 \text{ h}^{-1}$, filled squares at $D1= 0.4$ (■) and filled triangles (▲) at $D1=0.6 \text{ h}^{-1}$ 156

Figure S. 7 One-step of phage T3 at different dilution rates. Filled circles (●) represent adsorption at $D1= 0.5 \text{ h}^{-1}$, filled squares at $D1= 0.4$ (■) and filled triangles (▲) at $D1=0.6 \text{ h}^{-1}$ 157

Figure S.8 CsCl separation for phage K (a) and phage T3 (b) with the typical bands due to different gradients. 157

Figure S. 9 Calibration curve correlating dextran refractive index to their concentration in the solution. 158

Figure S. 10 Calibration curve correlating peristaltic pump power to flowrate of deionised water. 158

Figure S. 11 Calibration curve correlating Analox voltage outcome to glucose concentration (mM). 159

Figure S. 12 Elution of protein standards in SEC using S-100 column. The proteins eluted are IgG (160 kDa), BSA (67 kDa) and cytochrome C (12,4 kDa). 160

List of tables

Table 4.1 Dilutions and relative concentrations of colicin E9 producing a clear spot on a lawn of *E. coli*.61

Table 5.1 Summary of titres of Phage K using different Multiplicities of infection.....80

Table 5.2 Summary of titres of Phage T3 using different Multiplicities of infection.....81

Table 5.3 Summary of conditions tested and final titres of Phage T3 in reactor 3.....93

Table 7.1 Final concentrations of endotoxins before and after different purification methods.....128

Table S.1 Composition of synthetic medium for continuous production of *E. coli*.....155

Abbreviations

AAC	Chloramphenicol acetyltransferases
Ads	Adenovirus

Amp	Ampicillin
AMR	AntiMicrobial Resistance
AFMPS	Federal Agency for Medicines and Health Products
ANSM	Agence Nationale de Sécurité du Médicament et des Produits de Santé
ATCC	American Type Culture Collection
BHI	Brain Heart Infusion
CFF	Cross Flow Filtration
CFU mL ⁻¹	Colony Forming Units per mL
CIM	Convective Interactive Media
CLB	Colicin-like bacteriocins
Cm	Chloramphenicol
CV	Column Volume
D	Dilution Rate
DNA	Deoxyribose Nucleic Acid
DoE	Design of Experiments
dsDNA	Double Stranded DNA
dsRNA	Double Stranded RNA
EMA	European Medicines Agency
FDA	US Food and Administration
GRAS	Generally Recognized As Safe
HTT	High-Throughput Technologies
ICTV	Virus Taxonomy International Commission
IEC	Ion Exchange Chromatography
IL	Interleukin
IPTG	Isopropyl β -D-1-thiogalactopyranoside
LAB	Lactic Acid Bacteria
LAL	Limulus Amoebocyte Lysate
LB	Lysogeny Broth
LER	Low Endotoxin Recovery
LPS	Lipopolysaccharide
Mab	Monoclonal Antibodies

Man-PTS	Mannose-Phosphotransferase Systems
MOI	Multiplicity Of Infection
MRSA	Methicillin-resistant Staphylococcus aureus
NTA	Nanoparticle Tracking Analysis
OD	Optical Density
ODL	Odilorhabdins
PFU mL ⁻¹	Plaque-Forming Units per mL
pI	Isoelectric Point
QbD	Quality by Design
QC	Quality Control
RCT	Randomised Control Trials
SEC	Size Exclusion Chromatography
SEM	Scanning Electron Microscope
SCF	Self-Cycling Fermentation
TEM	Transmission Electron Microscope
TFF	Tangential Flow Filtration
TNF	Tumor Necrosis Factor
UF	Ultrafiltration
v/v	Volume per Volume
w/v	Weight per volume

Greek Symbols

η	Coefficient of dynamic viscosity	Pa s ⁻¹
τ	Shear stress	Pa
ω	Angular velocity	Rad s ⁻¹

Table of contents

Abstract	iii
Acknowledgments.....	v
Publications	vii
Conference Posters and Presentations	vii
List of Figures	viii
List of Tables	xi
Abbreviations.....	xi
Table of Contents	xiv
1. Introduction	1
1.1. Background	1
1.2. Aims And Objectives	1
1.3. Research Novelty	2
1.4. Thesis Outline	3
2. Literature Review	5
2.1. Antimicrobial Resistance: What Is It And Why Is It a Problem?.....	5
2.2. New Antibiotics, Proteins And Viruses Against AMR: State of the Art.....	7
2.2.1. Alternative Compounds And New Antibiotic Classes	7
2.2.2. Bacteriocins: What Are They And How Can Be Used	7
2.2.3. Bacteriocins Infecting <i>E. coli</i> : Colicins	9
2.2.4. Bacteriophages as Valid Alternative	10
2.3. Phage Therapy	14
2.3.1. Phage Trials – Case Reports.....	16
2.3.2. Modelling of Phage Therapy	17
2.3.3. Problems Related to Phage Therapy	19
2.3. Bioprocessing of Bacteriophages And Bacteriocins.....	21
2.3.1. Production of Bacteriophages	22
2.3.2. Downstream Processes	30
2.4. Production of Phages For Clinical Trials: the Phagoburn Experience.....	46
2.5. Future Applications	46
2.5.1. Applications In Industry and Health	46

2.5.2.	Encapsulation and Stabilization of Phages and Bacteriocins	47
3.	Materials and Methods	48
3.1.	Strains, Media and Buffers	48
3.2.	Bacteriophage Stocks Production	48
3.3.	Bacterial Growth Curve	49
3.4.	Bacteriophage Characterization	49
3.4.1.	Viable Phages Particle and Bacterial Cells Enumeration	49
3.4.2.	Phages One-Step Growth Experiment	49
3.4.3.	Phages Adsorption Experiment	50
3.4.4.	Quantification of Phage Concentrations and UV Reading	50
3.4.5.	Transmission Electron Microscopy	51
3.4.6.	Phage Size and Distribution.....	51
3.5.	Continuous Production of Bacteriophages	51
3.6.	Filtration	52
3.6.1.	Filtering Unit – Stirred Cell, Membranes and Rejection Experiments.....	52
3.6.2.	Shear Stress	53
3.6.3.	Tangential Flow Filtration (TFF)	54
3.7.	Removal of Endotoxins.....	55
3.7.1.	Liquid-Liquid Extraction Using Octanol.....	55
3.7.2.	Endotoxin Quantification	55
3.8.	Chomatography	56
3.8.1.	Size Exclusion Chomatography	56
3.8.2.	Ion Exchange Chomatography.....	56
3.8.3.	Isothermal Curves	56
3.9.	Bacteriocin Bioprocessing	57
3.9.1.	Production	57
3.9.1.2.	Test Expression	57
3.9.1.3.	Production in Flasks	57
3.9.1.4.	Continuous Production of Colicin E9	58
3.9.2.	Purification	58
4.	Production and Purification of Colicin E9	60
4.1.	Production of Colicin E9	60

4.1.1.	Molecular Biology Background.....	60
4.1.2.	Test Expression of Colicin E9 In LB And SM.....	61
4.1.3.	Growth Curves and Batch Production Of Colicin E9 In Lysates from LB and SM	62
4.1.4.	Continuous Production of Colicin E9 Using Chemostat Mode In LB And SM ...	65
4.2.	Purification of Colicin E9 Using Nickel Column.....	68
4.2.1.	Difference in Adsorption to Nickel Column of Colicin Produced In LB or SM...	68
4.3.	Discussion	71
5.	Production of Bacteriophages K and T3 in Batch and in Continuous Mode	73
5.1.	Life Cycle Parameters of Bacteriophages and Hosts	73
5.1.1.	Growth Curves of <i>S. aureus</i> and <i>E. coli</i>	73
5.1.2.	One-step Growth of Phage K and Phage T3	76
5.2.	Batch Amplification of Bacteriophages Using Different Multiplicity of Infection (MOI).....	78
5.3.	Continuous Production of Bacteriophage T3 Using Synthetic Medium (SM)	81
5.3.1.	Characterization of <i>E. coli</i> and Phage T3 Growth in SM	82
5.3.2.	Continuous Production of Phage T3 Using 3 Reactor Stages: Reactor 1 (R ₁) and Growth of the Host Culture	85
5.3.3.	Continuous Production of Phage T3 Using 3 Reactor Stages: Reactor 2 (R ₂) – Infection Reactor	87
5.3.4.	Continuous Production of Phage T3 Using 3 Reactors Stages: Reactor 3 (R ₃) – Amplification Tank.....	89
5.4.	Discussion	91
6.	Purification of Phage Lysates Using Ultrafiltration	95
6.1.	Ultrafiltration Using a Stirred Cell for Purifying Bacteriophage Lysates.....	95
6.1.1.	Characterization of Membranes and Shear Stress in the Stirred Cell	95
6.1.2.	Phage Recovery After UF in the SC and Viability of Phages Over Time.....	98
6.2.	Cross-Flow Filtration (CFF): Batch Ultrafiltration (UF)	102
6.2.1.	Viability of Phage K in CFF	102
6.2.2.	Viability of Phage T3 in the CFF	103
6.2.3.	Permeate Flux Using CFF.....	103
6.3.	Assessment of Purity of Samples.....	105

6.3.1	Size Exclusion Chromatography to Assess Purity of Retentate Phage Samples	106
6.4.	Ion Exchange Isotherms of Phage K and Phage T3 Before and After UF	107
6.5.	Discussion	110
7.	Removal of Endotoxins From Phage T3 Lysates	112
7.1.	Ultrafiltration (UF) to Reduce Endotoxin from Phage Lysate	112
7.1.1.	Batch Ultrafiltration	112
7.1.2.	Purification of T3 Phage Lysate Using Diafiltration	114
7.1.3.	Comparison of Endotoxin Levels After Diafiltration for LB and SM	115
7.2.	Removal of Endotoxin from T3 Phage Lysates Using Liquid-Liquid Extraction	116
7.2.1.	Effect of Different Volume Ratios of Octanol: Lysate on Endotoxin Removal	116
7.2.2.	LLE Using Multiple Equilibrium Stages	118
7.2.3.	LLE Using Multiple Equilibrium Stages Using Higher Mass Transfer Mixing	118
7.3.	Measurement of Aggregation of T3 Phages in the Presence of Endotoxin	120
7.4.	Removal of Endotoxin from Phage Lysates Using Anion Exchange Resins	122
7.4.1.	Ion Exchange Equilibrium Isotherm Data	122
7.5.	Discussion	126
8.	Conclusions and Future Work	131
8.1.	Future Work	131
8.1.1.	Bacteriocins	132
8.1.2.	Bacteriophages	132
9.	References	134
10.	Supplementary Results	150
10.1.	Viscosity of BHI and LB Broth	150
10.2.	Tangential Flow Filtration System	152
10.2.1.	Technical Drawing: Top	152
10.2.2.	Technical Drawing: Base	153
10.2.3.	Tangential Flow Filtration Experimental Set-up	154
10.3.	Composition of the Synthetic Medium	155
10.4.	Adsorption of Phage T3 at Different Dilution Rates	156
10.5.	One-step of Phage T3 at Different Dilution Rates	157
10.6.	Cesium Chloride Purification for Phage T3 and Phage K	157

10.7.	Calibration Curves	158
10.7.1.	Dextran Refractive Index	158
10.7.2.	Peristaltic Pump	158
10.7.3.	Analox	159
10.7.4.	Protein Standards at SEC	160

1. Introduction

1.1. Background

Antimicrobial resistance describes the ability of bacteria to develop immunity towards antibiotics available (Brown-Jaque et al., 2015) and it is a global problem causing every year an increasing number of deaths (Who, 2014; Ecdc, 2015).

Bacteriophages and antimicrobial proteins have been recently used as alternatives to antibiotics (Bull et al., 2002; Joerger, 2003; Pirnay et al., 2012). Bacteriophages, or phages, are small viruses that selectively infect and kill bacteria. They are the most abundant entity in the biosphere, with an estimated population of 10^{30} virions in the biome (Domingo-Calap et al., 2016). They are composed of proteins and nucleic acids and rely on the host replicative machinery for propagating. They are extremely selective and they have the ability to kill their host after replication and this is why they were used as antimicrobial agents before the discovery of antibiotics (Atterbury, 2009). In Eastern Europe, treatment of infections using bacteriophages was not abandoned after the discovery of antibiotics and it is nowadays still well practiced. Another alternative to antibiotics is represented by bacteriocins, proteins produced by bacteria to achieve competitive advantage over the same strains potentially competing for the same nutrients (Joerger, 2003). Bacteriocins such as nisin have been always used in the food industry and the producer strain has the condition of generally recognized as safe (GRAS), but there are many other families of bacteriocins that are being studied for their potential use as antimicrobial proteins in farms, the food industry and potentially can be used in healthcare as drugs.

There are studies showing the effect of bacteriophages *in vivo* (Capparelli et al., 2007; Jeon et al., 2016) and on human patients (Rose et al., 2014; Schooley et al., 2017). The Phagoburn project is the first clinical trial conducted on a large scale, involving 30 patients, trying to assess the effect of bacteriophages on humans (Jault et al., 2018). The encouraging results of this study show that the general trend and the direction towards Western medicine is moving: in the future a large-scale production of phages and antimicrobial proteins will be required (Merabishvili et al., 2009; Pirnay et al., 2015) and there will be soon the need for a robust method of production bacteriophages and antimicrobial proteins.

1.2. Aims and objectives

This thesis will deal with the bioprocessing, from production to purification, of the antimicrobial protein colicin E9, belonging to the family of bacteriocins produced by *Escherichia coli* strains, and the

production and purification of model bacteriophages K and T3. Phage K infects *Staphylococcus aureus*, phage T3 infects *E. coli* and they belong to the *Myoviridae* and *Podoviridae* families.

The aim is to define the fundamental parameters to move from a batch production using shake flasks to a continuous production using bioreactors connected in series. Chemically defined media will be compared with the commonly used complex media from a production and from a purification perspective, to see if the synthetic medium can ensure the same production rate of the complex medium and if it provides any advantage during the downstream process over the complex medium. The objectives of the downstream part of the thesis are finding the optimal conditions for the phage purification using membrane filtration, comparing batch ultrafiltration with diafiltration and to achieve maximum recovery. Additionally, the effects of media composition on final purification were assessed. Finally, methods for removing endotoxins from phage T3 samples were explored, using different techniques such as membrane filtration, liquid-liquid extraction and chromatography. Endotoxins are poisonous contaminants largely present in phage samples and the aim was to assess the best method to reduce endotoxin levels below 5 EU mL⁻¹.

1.3. Research novelty

Despite production of highly concentrated proteins being a well-established protocol, colicin E9 is a protein only recently investigated for antimicrobial properties and large-scale production was not designed for it. It was produced using a complex medium and synthetic medium and in batch and continuous mode.

The protocol for phage amplification and purification is optimal only for lab scale and hardly scalable. New methods and technologies are required to produce and purify bacteriophages in large scale. Studies on large scale production of phages and continuous production of phages have been already undertaken, mostly using 2-stage reactors (Husimi et al., 1982a; Nabergoj et al., 2018) or a self-cycling fermenter (Sauvageau and Cooper, 2010; Storms, 2012). Continuous production of bacteriophage T3 was performed using a synthetic medium and a new layout of the bioreactors. Using 3-stage reactors it is possible to grow the cells in the first reactor, infect them in the second reactor and amplify bacteriophages in the third reactor. All the stages are connected but can be individually controlled by changing the dilution rate. This layout ensures a final high titre of bacteriophages.

Host physiology and its effects on phage production during steady state growth were analysed and the best conditions to continuously produce phage T3 were assessed. Methods of purification from broth composed by complex media were analysed, focusing on membrane filtration using the dead-end or the tangential flow system. A correlation between shear stress and viability of phages are

described, depending on phage morphology. The advantages of removal of impurities is demonstrated, measuring the isotherms of the phage lysates binding to anion exchange resins. Removal of endotoxins using 1-octanol, ion exchange and a combination of the two methods was studied. Despite effective removal of LPS using 1-octanol has been already demonstrated (Schooley et al., 2017; Szermer-Olearnik and Boratyński, 2015), the removal of LPS using 1-octanol was monitored over time to assess the optimum timing for the process. Interaction of endotoxins with phage T3 and the effect of endotoxin contamination on the aggregation of phage particles was analysed.

1.4. Thesis outline

Chapter 1 – Introduction

The first chapter of the thesis deals with the background and the reasons why research on phages has been performed. It describes the aims and objectives and explains the novelty of the research.

Chapter 2 - Literature review

The chapter discusses the problems of antimicrobial resistance and deals with the research on alternative antimicrobial proteins such as bacteriocins and phage therapy. Examples of *in vivo* experiments and effective clinical trials carried out are reported and the problems related to the use of these alternatives are discussed. Furthermore, it reports the state of the art of production and purification of proteins and bacteriophages, highlighting the issues and the bottlenecks of the process. It points at the techniques that can increase the processing volumes that will be used in the results chapters.

Chapter 3 – Materials and methods

The chapter shows the list of bacterial host strains, bacteriophages and materials used and the protocols followed to perform experiments are reported. The experimental methodologies, the continuous production of the bacteriocin and phages, the stirred cell and the tangential flow devices employed in the research are described.

Chapter 4 – Production and purification of colicin E9

The chapter deals with the production of colicin E9 using complex and synthetic media. It introduces the production in shake flask and in bioreactor, using batch mode and continuous mode and a comparison of the production using complex medium with synthetic medium was performed. The differences of the two growth media in the first step of purification were evaluated using an affinity chromatography column.

Chapter 5 – Production of phages K and T3 in batch and continuous mode

The main parameters of hosts and phages were measured and then exploited for amplification of phages in batch using flasks and bioreactors, trying to improve the final titre. The effect of infecting the host at different multiplicity of infection and adding divalent salts on the final titre were evaluated. Continuous production of bacteriophage T3 was performed in synthetic medium, using a three-stage reactor and analysing the effect of the host physiology on phage production and final yield of the reactor.

Chapter 6 – Purification of phage lysates using ultrafiltration

The chapter deals with the purification process of the phage lysates using membrane filtration, comparing the effects of dead-end filtration and tangential flow filtration. The effect of shear stress on the viability of tailed and non-tailed phages was assessed when performing dead-end filtration and tangential flow filtration, performing batch ultrafiltration. The final purity of phage sample was evaluated using gel chromatography.

Chapter 7 – Removal of endotoxins from phage T3 lysates

This chapter deals with the purification of phage T3 lysates from endotoxins, or LPS, using batch ultrafiltration and diafiltration, liquid-liquid extraction and anion exchange. Differences in the process and the final amount of LPS in LB or synthetic medium were evaluated. The effect of aggregation of phage T3 particles in relation of the concentration of LPS in the sample was analysed.

Chapter 8 – Conclusions and future work

The chapter contains the conclusive remarks of the experiments and topics to be explored in future work.

2. Literature Review

2.1. Antimicrobial Resistance: what is it and why is it a problem?

Antimicrobial resistance (AMR) is the ability of bacteria to become resistant to the killing effect of one or more antibiotic classes available. One of the most important causes of antimicrobial resistance is the overuse and misuse of antibiotics: use of antibiotics imposes a selectivity pressure on bacterial populations, favouring the emergence of resistant ones. The prescription of antibiotics has become routine practice in hospitals, even in cases where they are not needed such as colds due to viral infections (Davies and Shallcross, 2014).

Bacteria can be quite simply divided into two groups: Gram-positive and Gram-negative bacteria. This is based on the outcome of a precise staining protocol performed on an unknown strain and it gives an idea of the cell wall structure of the bacteria by detecting peptidoglycan present in the cell wall of Gram-positive bacteria. Gram-positive bacteria, indeed, have a thick membrane that is stained by crystal violet dye whilst the Gram-negative bacteria have a two-membrane cell wall stained by safranin used as counter stain. It is very important when it comes to the antibiotic to be used, because they react to external factors in different ways: Gram-negative bacteria are more resistant to antibiotics due to the bilayer membrane (Delcour, 2009a).

There are many classes of antibiotics which target different metabolic pathways of the prokaryotic cells (and not the eukaryotic ones). Among these there are the cephalosporins and penicillins, that block bacterial cell wall synthesis; the tetracyclines and macrolides, that stop the protein synthesis by binding to the 30S or 50S ribosomal unit; the quinolones, that inhibit DNA replication of bacteria (Coates et al., 2011).

At present, most of the Gram-negative bacteria can inactivate antibiotics, by producing enzymes that hydrolyse or change the conformation of the molecule. Metallo- β -lactamases, for instance, can vanquish the effect of carbapenems, cephalosporins, penicillins and monobactams and currently there are about 300 β -lactamases that have been identified. Moreover, bacteria can change the target molecule, for instance aminoglycoside-modifying enzymes prevent the binding to the 30s ribosomal unit while chloramphenicol acetyltransferases (AACs) prevent the binding to the 50s one.

Another resistance mechanism is the expression of efflux pumps on the cytosol membrane (Delcour, 2009b), pumping out the antibiotic at the same speed that it enters, before reaching the target (Kapoor et al., 2017).

Most of the time there are cases of resistance also using the methicillin and vancomycin, which are considered the last resort antibiotics against *Staphylococcus aureus* and *Enterococcus* infections. Reports of these resistant bacteria are so common that nowadays they are just called MRSA and VRE,

methicillin-resistant-*S. aureus* and vancomycin-resistant-*Enterococci*, respectively (Siddiqui and Bernstein, 2010).

The most common bacteria showing increasing rates of resistance are: *Escherichia coli*, *Staphylococcus aureus*, *Pseudomonas aeruginosa* and *Enterococcus* spp. as well as bacteria that previously were easily treated with antibiotics, such as *Streptococcus pneumoniae*, *Klebsiella pneumoniae*, *Acinetobacter baumannii* – all together they are also referred with the acronym ESKAPE (O'Neill, 2016).

Another problem is the infection of patients suffering from burns or chronically-ill patients. A chronic infection might be characterized by various flora, that can change over time. Another complication is that chronic wounds present an ideal environment for biofilm growth. A biofilm is an aggregation of bacterial cells surrounded by extracellular matrix adhering to a surface and forming a layer that is very resistant to antibiotic treatment (Chan and Abedon, 2015). Diseases such as cystic fibrosis and complications disease-related like diabetic foot ulcers are exposed to polymicrobial biofilms.

Most of the antibiotic resistant infections are nosocomial and it has huge consequences on healthcare associated costs, because people stay longer in hospitals, increasing the cost of hospitalization (Michaelidis et al., 2016).

Not all people heal from the infections, and number of deaths from antibiotic resistant infections is always increasing (de Kraker et al., 2011; Shlaes and Bradford, 2018). In Europe and the US, antimicrobial resistance is the cause of the death of 50,000 people each year; even if a precise estimate from other parts of the World is not available, at the moment at least 700,000 lives are lost every year because of complications related to antibiotic resistance (O'Neill, 2014). The number of deaths due to infection is estimated to reach 10 million by 2050 (de Kraker et al., 2016).

The obvious thing to do is to teach people how to properly use antibiotics and to organize better antimicrobial stewardship (Thabit et al., 2015). Nevertheless, the process can only be slowed down as the trend is going in the direction of a new era where antibiotics cannot cure infections.

Antimicrobial resistance is nowadays a major concern in medicine, and the fact that until 2012 only two new classes of antibiotics have been brought to market helps illustrate how difficult it has become to develop new treatments for bacterial infections (Coates et al., 2011). The rate of discovery of new antibiotic classes by pharmaceutical companies has slowed down for many reasons. One relates to a lack of metabolic targets (Becker et al., 2006) and the other is lack of economic drivers. In 2012 the Food and Drugs Administration (FDA) changed the regulation for antibiotics development incentivising the discovery of new molecules, and new antibiotics have been released to market but they are not as profitable as a new drug meant to treat diseases such as diabetes, cancer or neurodegenerative diseases (Shlaes and Bradford, 2018; Ventola, 2015). Despite the difficulties, there is a constant search

for new compounds for treating infections from resistant bacteria, not only chemical compounds, but also proteins and viruses.

2.2. New antibiotics, proteins and viruses against AMR: state of the art

2.2.1. Alternative compounds and new antibiotic classes

Pharmaceutical companies pointed to the research of new antibiotics by modifying and improving old and previously working molecules, but this strategy cannot be pursued any longer and it will not result in finding new antibiotics very soon.

There are some new molecules that are under development now. Tedizolid is a new drug developed to treat infections caused by Gram positive bacteria and it binds to the 50s subunit of the ribosomes. Dalbavancin is closely related to vancomycin and it targets MRSA, and oritavancin is active against VRE. They all require quite a high dose (1000 and 1200 mg). Ceftazidime is a new cephalosporin, delafloxacin is a new fluoroquinolone and eravacycline is related to tetracycline (Thabit, 2015). In 2018 a new class of antibiotics was discovered: the odilorhabdins (ODLs). This new class targets ribosomes and interferes with protein production in a way that is different from all other antibiotics and they have effect on both Gram-negative and Gram-positive bacteria. These ODLs have been already tested *in vitro* and *in vivo* showing efficacy and low toxicity. They have all the potential to be tested in clinical trials soon (Pantel et al., 2018).

2.2.2. Bacteriocins: what are they and how can be used

Bacteriocins are antimicrobial peptides naturally produced by both Gram-positive and Gram-negative bacteria. They are produced to kill only bacteria closely related to the producer and are used when there is competition for nutrients in the same environment. They have different biochemical properties and their activity varies and it might be narrow effective on closely related species or quite broad and have effect on several species (Joerger, 2003). The first bacteriocin was identified in 1925 by Gratia, who described an antimicrobial protein from *E. coli* and gave it the name of colicin (Balciunas et al., 2013). However, the term bacteriocin is mostly used to describe the peptides that have antimicrobial properties synthesised by lactic acid bacteria (LAB), that are Gram-positive bacteria. Since LAB have always been associated with food, they are considered safe (GRAS) (García et al., 2010; Shin et al., 2015). Nisin, one of the most studied bacteriocins, is mostly active on Gram-positive pathogens (Joerger, 2003) and its bactericidal effect has been known for a long time (Hirsch, 1950).

The fact that bacteriocins are very specific and powerful makes them a valid alternative to conventional antibiotics, as they do not target other bacteria unlike antibiotics (Drider et al., 2006). Historically, there were four classes of bacteriocins (Klaenhammer, 1993):

- I class: thermostable peptides of molecular weight <5k Da (e.g. nisin)
- II class: thermostable peptides of molecular weight <10k Da. This class has three sub-classes: IIa, IIb and IIc
- III class: thermolabile peptides of molecular weight >30 kDa
- IV class: large peptides, also complexed with lipids and carbohydrates

A more modern classification divides bacteriocins in three classes and is based on genetic and biochemical properties (Drider et al., 2006):

- Class I or lantibiotics: composed of small, post-translationally modified peptides. They contain unusual amino acids like lanthionine. Nisin is one of the most studied in this class;
- Class II: composed of heat-stable bacteriocins with molecular mass <10 kDa;
- Class III: composed of thermo-sensitive proteins with molecular mass >30 kDa.

The differences between antibiotics and bacteriocins are many. Bacteriocins are proteins and they are generally inactivated by proteases like trypsin and pepsin (Balciunas et al., 2013). The mechanism of action is still not fully understood and there are different models proposed (Cascales et al., 2007; Hammami et al., 2013). What is sure is that bacteriocins begin their lethal action by binding to a receptor on the membrane, such as the mannose-phosphotransferase systems (man-PTS, present on genera like *Listeria*, *Enterococcus* and *Lactobacillus*). After the binding, the bacteriocin enters the cell and forms ion-permeable channels that will become eventually pores (Hammami et al., 2013). After they enter in the cell, they have different mechanisms of action, as they can have nuclease activity by cleaving DNA or they can also hydrolyse rRNA, block protein synthesis, inhibit the macromolecular synthesis or create pores in the membrane and cause death by ion leakage (Cascales et al., 2007). Bacteriocins show effect at nanomolar concentrations and are non-toxic to humans (Hammami et al., 2013). The effect and the therapeutic potential of bacteriocins were positively shown by previous researchers and there are many patented bacteriocins (Walker and McCaughey, 2016). It has been shown that colicins prevent the colonization of the urinary tract (Trautner et al., 2007) and there are many *in vivo* studies in pigs (Cutler et al., 2007), mice (Bosák et al., 2018), rabbits and chicken embryos (Behens et al., 2017) showing positive effects of bacteriocins despite using different administration routes, and most importantly their safety. Colicins can be used in the poultry and cattle industry, for food preservation, and they have even been proposed for bioremediation (Gillor et al., 2004).

Bacteriocins have potential applications in veterinary medicine, agriculture and aquaculture but they are mostly used for food biopreservation. For instance, nisin can be used to preserve dairy products, meat and vegetables because of its wide effect on spoilage bacteria such as *Staphylococcus aureus* and *Clostridium tyrobutyricum* (García et al., 2010).

The most known and used bacteriocins are the colicins, produced by *E. coli*, but there are many other bacteria producing bacteriocins such as *Pseudomonas pyogenes*, producing pyocins, or *Enterobacter cloacae* (cloacins), *Yersinia pestis* (pesticins), *Klebsiella* species (klebicin or klebocins), *Serratia marcescens* (marcescins), *Photobacterium luminescens* (lumicins) or the Gram-positive *Bacillus megaterium* (megacins) (Cascales et al., 2007).

2.2.3. Bacteriocins infecting *E. coli*: Colicins

Gram-negative bacteriocins can be divided in three classes:

- Peptide bacteriocins antibacterial proteins (30–80 kDa) as well as smaller peptides (1 - 10 kDa), named microcins.
- Colicin-like bacteriocins (CLBs), toxins active against *Klebsiella*, *Yersinia pestis*, *Pseudomonas aeruginosa* and other Gram-negative bacteria. After they bind to the membrane receptor, they bind to the Ton-like or Tol-like system – these systems usually are used by Gram negative bacteria to intake vitamins or siderophores - to be translocated into the cell.
- Tailocins, which look like tails of the phage family *Myoviridae* or *Siphoviridae*. They are thought to derive from phages, but they are not simply defective phages. They can bind to LPS and can change conformation and make damages, leading to lysis of the targeted cell. Tailocins are not protease sensitive (Behens et al., 2017).

The producers are mainly found among the *Enterobacteriaceae*, which produce bacteriocins in response to stress. Since the first Gram negative bacteriocin was discovered and found to be active against *E. coli*, all the bacteriocins that kill Gram negative bacteria are called Colicin-like bacteriocins (CBLs). Colicins are also the most prominently studied bacteriocins from Gram negative bacteria and are produced by 30–50% of the strains isolated from human hosts (Cascales et al., 2007). It is not easy to classify all the CLBs, but they can be categorized depending on the receptor they use to bind before being internalized and lysing the cells. There is the group A that comprises the colicins binding to the Tol system proteins, such as colicins A, E1 to E9, K, L, N, S4, U and Y, while the group B comprises the colicins binding to the TonB system: the colicins B, D, H, Ia, Ib, M, 5 and 10. Colicins are toxins sized 40-70 kDa that specifically target *E. coli* (Behens et al., 2017). Typically, the toxic domains of colicins

work as pore-forming ionophores or nucleases, however activity of degrading lipid II or the peptidoglycan (colicin M), blocking protein synthesis by cleaving tRNA (colicins D and E5) or 16S RNA (colicins E3, E4 and E6) has also been shown.

Chapter 4 deals with the production of colicin E9 which is well characterized. Colicin E9 has a molar weight of ~55 kDa and it binds to the Tol system. Colicin E9, like all the other bacteriocins, binds to the immunity protein Im9 that gives protection to the producer strain on the colicin itself. Im9 is peculiar in terms of the binding strength to E9: the dissociation constant (K_d) of the complex E9-Im9 is 10^{-16} M (Wallis et al., 1995). Its mechanism of action is well studied and E9 kills *E. coli* strains thanks to its DNase activity (Cascales et al., 2007).

Colicins are sensitive to proteases as well as most bacteriocins. They are regarded as a potential antimicrobial alternative to antibiotics, but there are some challenges in the potential use of colicins as antimicrobials, such as quick clearance from the body and the necessity of a high dosage. The positive aspect is that colicins are more potent than antibiotics and the short time of exposure might delay the appearance of resistance of any sort.

2.2.4. Bacteriophages as valid alternative

Besides research into new chemical compounds, there is constant ongoing research into different bactericidal agents, such as proteins and viruses able to inhibit the growth or kill bacterial pathogens. A bacteriophage (also known as phage) is a virus which is able to selectively infect and kill bacterial cells without disrupting other microflora. The word “bacteriophage” comes from two words, “bacterium” and “fagein”, from the Greek language, and it means “eater” and describes the capacity of a phage to infect and lyse a bacterial cell releasing a new progeny of viruses which will continue to infect other bacteria. Phages are the most abundant living organism in the world and they outnumber bacteria by a factor of 10 (Domingo-Calap, 2016).

The use of bacteriophages for treating bacterial infections is called phage therapy and it is routinely used in Eastern Europe in countries like Poland, Georgia and Russia. There are important hospitals and research centres on phage therapy, frequented by people from Western Europe when treatment of an infection with antibiotics fails. One of the most important phage therapy centre is the Eliava Institute in Tbilisi. Phage therapy is gaining increasing interest in the Western world in recent years due to increasing levels of antibiotic resistance in pathogenic bacteria.

2.2.4.1. History of bacteriophages

The first evidence for a viral-like agent with antibacterial properties was reported by M. E. Hankin in 1896 (Hankin, 1896). It was found in the Ganges and Jumna rivers in India, it was temperature sensitive, capable of passing through a porcelain filter, and could reduce titres of the bacterium *Vibrio cholerae* in laboratory cultures. Hankin suggested that it might help to decrease the incidence of cholera in people using water from these rivers, but no further research was conducted for almost 20 years after this record. The discovery of bacteriophages is attributed to Frederick Twort and Felix d'Herelle, who independently studied and described this particular kind of virus. Frederick W. Twort was a British microbiologist and in 1915 published his discovery in a paper (Twort, 1915). He described an infecting agent that can pass through 0.2 µm filters and modify the morphology of bacterial cultures. Unfortunately, he never continued his studies because he was called to his duty by the British Army. Felix d'Herelle was a French-Canadian microbiologist who made the same discovery in 1917, while he was working at the Pasteur Institute and published his research in the paper: "*Le bacteriophage: son rôle dans l'immunité*". He described many biological features of phages and immediately imagined the great potential of phages as antimicrobial agents.

2.2.4.2. Bacteriophage biology and other uses

Phages can be described as obligate intracellular parasites of bacteria as they do not have an independent metabolism. These viruses are extremely diverse and can be found all over the biosphere and almost every species of bacteria has its own infecting phage. A bacteriophage is composed of a DNA or RNA molecule, single or double stranded (ss or ds), encapsulated in a protein or lipoprotein head. Their dimensions vary from 10 to 400 nm and they are visible only using the Transmission Electronic Microscopy (TEM). Bacteriophages are classified based on their morphology (Luria et al., 1943). The International Committee on Taxonomy of Virus (ICTV) is in charge of classifying phages based on virus morphology and genome composition. At present there are ten different families of phages. More than 95% of phages are in the order of *Caudovirales*, that are dsDNA phages. The order of *Caudovirales* is composed of three main families and classification is based on the tail morphology. Around 60% of them belong to the *Siphoviridae* family, with a long and flexible tail; ~25% belong to *Myoviridae*, with a contractile tail and the last 15% are composed by *Podoviridae* and have a short tail. In all the dsDNA phages the genome is highly packed inside the head and represents the 20-25% of the phage mass (Earnshaw and Harrison, 1977). The capsid structure is resistant enough to maintain the genome in a condensed state until it is injected into the bacterial cell. The phage structure is extremely simple, and all parts have an essential role in the life cycle of the phage. All the *Caudovirales*

have an icosahedral capsid (20 faces and 12 vertexes) and the size depends on the length of the chromosome inside it. Usually the capsid diameter varies between 45 and 100 nm. The vertexes are usually composed of pentamers of the capsid protein and the rest of the surface is made by hexamers of the same protein (or a very similar protein) (Kutter and Sulakvelidze, 2005). The linking protein between head and tail (portal protein) is an important viral structure because it is involved in many phases of the replicative cycle. It controls the DNA injection and the attachment of the tail to the head during the assembly of the virion. The tail has the important function of attaching the phage to the bacterial cell wall membrane during phage infection; it is usually made by proteins and it is the main structure through which the DNA passes during the injection and its length varies between 2 and 800 nm (Fig. 2.1).

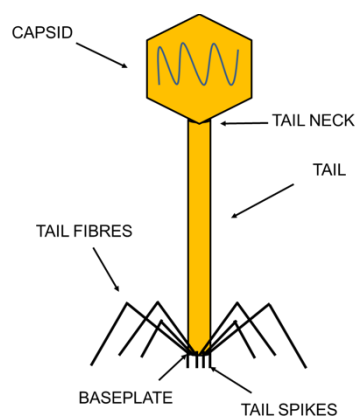


Figure 2. 1 Schematic drawing of a single tailed phage

2.2.4.3. Life cycle

The study of phage life cycles was undertaken by Delbruck and Ellis, who developed the “one step growth” experiment (Ellis and Delbrück, 1939). A typical bacteriophage growth curve is characterized by two distinct phases: the latency period and the rise. During the latency period there is no increase in free phage numbers following infection, but after the burst there is a steep growth and increase in the number of free virions. After the growth there is a *plateau* that corresponds to a new latency period for a new cycle. The total number of new phages, or burst size, is the total number of phages released by a bacterial host.

The latency period represents the time when the phage takes over the replication machinery of the bacterial cell and starts replicating inside the cell. In the first part of latency there are no virions present in the cell and this period is called eclipse. It is easily demonstrated by lysing bacterial cells during this stage. After the eclipse, the number of complete and mature virions increases inside the cell until the burst.

The act of infection is characterized by different moments:

- Adsorption: it is the first and most important phase of the infection, because it depends on the binding of the phage to a specific target on the bacterial membrane. This can be a protein, a pilus or flagellum, LPS etc. The phage recognizes the receptors through the fibres of the tail. This phase usually follows a first-order kinetics that can be described by the equation:

$$P = P_0 \exp(-Bkt) \quad (2.1)$$

Where k is the adsorption rate constant (mL/min); B is the concentration of bacterial cells (CFU mL⁻¹); t is the time interval (min) in which the titre falls from P_0 to P (final) (PFU mL⁻¹) (Clokic and Kropinski, 2009).

- Penetration: after the stabilization of the phage on the membrane, the phage DNA passes from the capsid to the cell. If the phage has a contractile tail, it contracts and pushes the DNA into the cell.
- Replication: the phage takes over the replicative machinery of the host cell and starts replicating its genome and assembling new bacteriophage particles

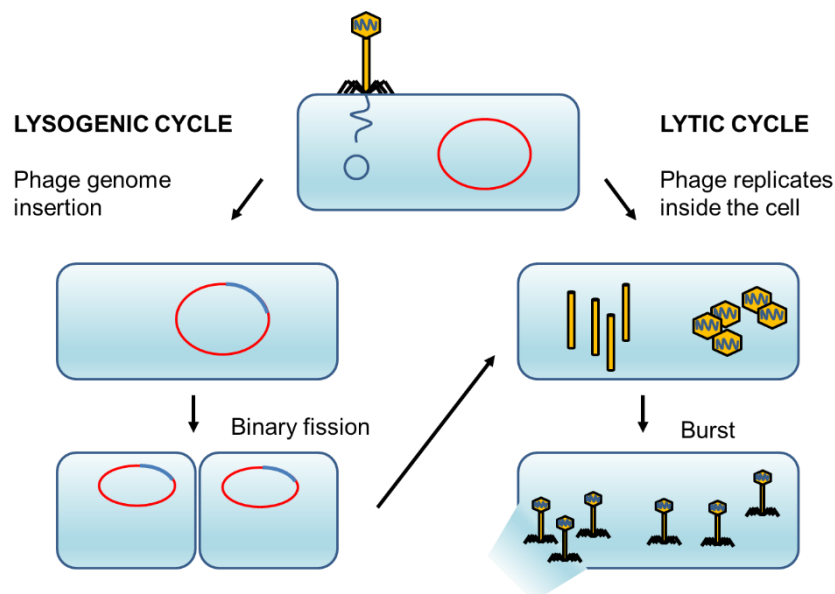


Figure 2. 2 A schematic to show the steps in a phage infection cycle. Phages can follow the lytic cycle which leads to the lysis of bacterium or the lysogenic cycle where the phage DNA is incorporated in the bacterial genome.

There are two different kinds of bacteriophages: lytic and temperate ones (Fig. 2.2). Many phages, such as T2, T4 and T7 are obligate lytic phages and start their replicative cycle right after DNA injection into the host cell (Fig. 2.2). There are other phages though, like λ , which are temperate. A temperate bacteriophage injects its DNA into the bacterial cell, and this DNA will circularize and in a subsequently

may integrate in the bacterial genome. A temperate phage can stay integrated in the genome of a host cell (at this stage it is called a prophage) for many replicative cycles and its genome will be replicated as well. The prophage will excise its genome and start the lytic cycle only if there are stressful conditions from the environment, such as an increase of temperature or a deficiency of nourishment (Fig. 2.2). A lytic phage skips the prophage phase and directly takes over the replicative machinery of the bacterial cell and replicates until the progeny will lyse the cell and spread in the environment (Bertani, 1953).

2.3. Phage therapy

Phages, upon initial discovery, were used for fighting infections but the results were not consistent due to a lack of understanding of how phages worked as well as manufacturing problems related to phage titre and purification issues and they were no longer used in the West after the discovery of antibiotics. There were many problems during initial attempts at using phages, the most important ones were: 1) Host range: phages have a narrow range of susceptible hosts and phages were not sufficiently tested against all prevalent strains before being used; 2) Phage preparations were mostly crude lysates of phages or in the best case not completely purified. Thus, the presence of contaminants such as bacterial debris present in phage preparations overshadowed the therapeutic action of phages; 3) Attempts to remove host bacteria: in order to purify phage stocks, rough methods were adopted such as heating the samples or adding poisoning compounds. In this way phage preparations were rendered useless, either due to inactivation of phages or the toxicity of the preparation; 4) Rapid clearance of phages: phages are recognized by antibodies as an external agent to be cleared and this reduced the efficacy of chronic treatments; 5) Lysogeny: many phages had not been characterized after being discovered and many were temperate and not optimal for phage therapy; 6) Failure to establish proof of efficacy: no systematic studies were available to demonstrate that the results were reliable and repeatable. The first trials made to use phages to treat infections gave apparently good results, but the data were not sufficiently rigorous and not reproducible. Lack of control groups and absence of high quality double blinded clinical trials are often cited as weaknesses in demonstrating the efficacy of phage therapy (Carlton, 1999). All the reasons that brought failure during initial attempts at phage therapy can be attributed to a lack of biological knowledge of the phages: the first microbiologists used phages without knowing the nature of phages (the first TEM picture of a phage was taken after 1940) (Pirnay et al., 2012).

After the Second World War, with the discovery of antibiotics, phage therapy research largely stopped in Western countries. Bacteriophages were not completely abandoned but have been used for many other reasons: due to their simple genome and their ability to transfer genetic material among bacteria they have been used as gene vectors. Molecular biology made huge improvements in the studying of phages, especially the model phages of *E. coli* T2 and T4 (Hershey and Chase, 1952). Another model phage of *E. coli*, λ , was used to prove the restriction modification system (Bertani and Nice, 1953), to better understand the genetic regulation and the composition of different bacterial organisms (Lewin, 2009). In Western countries phages are considered no more than a potentially usable drug for the future, but in ex-Soviet countries phage therapy is currently used and one of the most important centres in the world of Phage therapy is in Georgia, the Eliava Institute.

There are many records of effective use of phage therapy in humans and they have been used both in Western and in Eastern Europe and for treating all kinds of infections. After their discovery in 1917, d'Herelle continued his studies on phages in France, at the Pasteur Institute, and tested different phage preparations on many patients. His research has been reported in papers and books that have been translated from French to English. In a 1961 review in French by J.F. Vieu of the Bacteriophage Service of the Pasteur Institute summarized the fundamentals of phage therapy in France at that time, when phages were used to treat mostly *Staphylococcus*, *Pseudomonas*, *E. coli* and *Serratia* (Vieu, 1961). Many of the details described are still valid, such as the choice of lytic phages or the need for purification of samples from other proteins before intrathecal and venous administration. In Poland, phage therapy has been used to treat thousands of patients, especially at the Hirsfeld Institute of Immunology and Experimental Therapy in Wroclaw. The reported cure rates ranged from 75 to 100%, but for many reasons it is not possible to consider these results as a proof of phage therapy efficacy. The reasons are that the treatments were not blinded, and the details were not scientifically reported and often the antibiotics were used together with phages. The lack of scientific rigour has been cited in many attempts of using phage therapy (Carlton, 1999).

Phage therapy research reached the United States as well. Here d'Herelle worked at Yale University from 1928 to 1933. Another leading centre on phage research was the Michigan Department of Health where *Staphylococcus* infection was the most targeted pathogen because it occurred on the skin. Several well-known pharmaceutical firms started producing phages, but they had the same problems reported so far: lack of quality control and poor stability of phage titre. Besides, they could not prove the efficacy of their cocktails, mostly because the additives contained in the preparation drastically reduced the amount of viable phages.

As mentioned earlier, countries from ex-Soviet Union are the ones with considerable expertise in phage research and phage-based therapies because they kept using them even after the discovery of antibiotics. The language barriers – most of the works had never been translated- and the imposition of military secrecy limited the transfer of skills and knowledge to the Western countries. In Georgia the most important centre was and still is the Eliava Institute in Tbilisi, which was founded after 1930 by George Eliava, in association with d’Herelle. In this centre, up to 1200 people used to work, selecting and producing phages against diarrhoea and wounds to be used by the Army. Other cocktails of phages were available to ordinary people, even without any medical prescription, such as “Instestiphage” which targets about 20 different intestinal pathogens. Another one is “Pyophage”, containing phages targeting *Staphylococcus*, *Streptococcus*, *Pseudomonas*, *Proteus* and *E. coli*. The most interesting fact about these products is that they are not static phage mixtures but are continuously updated in response to changes in pathogenic targets. Thus, they are not identical though time or from place to place. In Tbilisi, they are updated every six months adding new phages able to target newly emerging pathogen strains. Each batch is tested by the manufacturer and then by their Medication Certification Lab: they are required to be active against a certain specified fraction of the strains for each type before state approval is received for them to be marketed. The main targets of Russian research on phage therapy were diarrheal infections, infections associated with battle and trauma, particularly targeting gangrene. For instance, during the war of Finland (1938 – 1940), the Russian Army treated gangrene infections with phages. During World War II, Russian soldiers were successfully treated using phages in their wounds. In one study, of those receiving anti-*Clostridium* phages following battlefield wounds, around 80% survived versus only around 60% survival among those not receiving phage treatments. The main centre where phages were studied was the Central Institute of Epidemiology and Microbiology in Moscow and the technologies to apply phages as liquids, tablets, creams, aerosols or in tablets form were first developed there (Abedon et al., 2011).

2.3.1. Phage trials – case reports

Besides the experiences in Eastern Europe, there are many cases of phage application on infections e.g. in the UK and US (Kutter et al., 2010). Most of the recent trials aim to show the safety of phage therapy in patients rather than focusing on efficacy, e.g. in ulcer infections (Rhoads et al., 2009), or otitis (Wright A et al., 2009) or diarrhoea (Sarker et al., 2016). Recent case reports of phage therapy treatment of a single patient have shown promising results treating infections (Schooley et al., 2017; Jennes et al., 2017). In these cases, cocktails of phages were isolated, characterized and developed to

be administered to individual patients not responding to antibiotic treatment. This is a common outcome: a personalized treatment targeting the infection-causing bacterium against which the phages are effective usually works, while a pre-made cocktail may not work effectively (Pirnay et al., 2011). These approaches have different economic implications: a personalized phage cocktail will be more expensive than a “general” cocktail that might be distributed to the market. The number of phage therapy trials carried out has increased only in the last few years, showing the struggle to overcome the legislative and technical issues that caused delays (and sometimes even affected the results of the studies).

2.3.1.1. PhagoBurn

A recent clinical trial used phage cocktails to treat *P. aeruginosa* soft tissue infection in burn patients; the trial was called the PhagoBurn project and founded by the European Commission. It started in 2013 and ended in 2017 and the project was intended to treat patients with burns infected with *P. aeruginosa* not responding to the normal antibiotic cycle. It involved hospitals from France, with the Percy Military Hospital, Belgium, with the Queen Astrid Military Hospital and Switzerland, with the Centre Hospitalier Universitaire Vaudois and University of Lausanne (Jault et al., 2017). A paper reporting the scientific outcomes of the study has been recently published (Jault et al., 2018), remarking how this has been the first blind trial based on GMP-produced phage antimicrobials that showed firstly safety in humans and also a decrease in bacterial load in patients infections. It must be pointed out that the control antibiotic – 1% sulfadiazine silver emulsion cream – had a better and faster result, but this does not diminish the importance of this trial.

There is also a final report highlighting the main challenges and overall results of this study. Other preparative aspects and outcomes of this clinical trial, such as the production, purification and validation process or the absence of adverse events during the test will be discussed later.

2.3.2. Modelling of phage therapy

One of the main problems for phage therapy development might be that previous knowledge from fighting infections with antibiotics cannot be used for bacteriophages, and there is a need for a new model. The nature of the phage as a “self-replicating drug” makes the pharmacokinetics different, because, theoretically, only one administration of phages may be enough to treat the infection, as long as the bacterial concentration is high enough to let the phages replicate. This concept was introduced for the first time by Payne *et al.* (Payne and Jansen, 2001), who explained in their paper

the idea of thresholds in phage therapy. They described the definitions of “active therapy” and “passive therapy”. A passive therapy, is typical of normal drugs, relies only on the “dose” of the medicine: the concentration of active compound must be enough to provide the therapeutic effect. A typical feature of a passive therapy is the need for continuous administration of the drug at regular intervals. On the other hand, an active therapy is less dependent on the dosage, because the drug can replicate itself, perpetuating its replication and maintaining (and increasing) a high dose of compound, enough to overcome the disease. In this case, in theory, only one administration of the drug is necessary to treat the patient.

This concept wholly describes the importance of dosage in phage therapy: a sufficiently large dose of phages can eradicate the bacteria even without the need of replication of the virus – passive therapy. A smaller infective dose may have two different outcomes: maybe the dose is enough to give a transient inundation effect or can be sufficient to lead to active replication of phages that subsequently fully subdues the bacterial infection. It is therefore important to develop a suitable theoretical framework for understanding the non-linear kinetics of phages as “self-replicating pharmaceuticals” (Tsonos et al., 2014).

In phage therapy, pharmacokinetics (the route of the drug into the body, from assumption to the clearance) and pharmacodynamics (the actual effect of the drug on the body) cannot be fully separated because they are fundamentally interrelated. Phages infecting susceptible bacterial cells, reproduce and subsequently infect other susceptible cells. Therefore, the rate of phage growth is dependent on the host population, in that the phage population can only increase when the bacterial concentration is sufficiently high (Cairns et al., 2009).

The rate of phage growth is dependent on the host concentration and Payne and Jansen (2001) discussed the concept of a *proliferation threshold*, that is the concentration that the bacterial population must exceed in order for the total number of phages to increase. Likewise, there is an *inundation threshold* which is the minimal concentration of phages above which the bacterial population declines. The parameters to consider for modelling the behaviour of phages are at least the growth rate of bacteria, latent period and burst size of phages and phage and bacteria thresholds. There are other parameters that need to be considered in order to make a more accurate model, such as the “binding rate of phages to the susceptible bacteria” or the “mutation rate of bacteria” or the “phage decay rate”, but they are still considered an “extra” because it is not always easy to determine these parameters.

A new model for interaction of phage-bacteria populations was proposed by Malik (2017). It was based on the model of Levin and Bull and the one of Cairns but the effect of controlled release of phages

was introduced. The model demonstrated the conditions under which phage therapy may be successful and this model showed how phage concentration at the site of infection is an important parameter in phage therapy. Loss of phage activity may result in poor phage therapy outcome. This model also highlights how important is to fully understand phage parameters (adsorption rate, latency and burst) and host parameters (growth rate) to build a robust model able to predict the behaviour of the populations involved.

2.3.3. Problems related to phage therapy

2.3.3.1. Regulatory constraints for phage pharmaceuticals

There are not only biological constraints issues in the way of phage therapy development. From a legislative point of view, there are at least two main problems: the difficulties to patent phage cocktails and the absence of a precise law that regulates phage therapy. A clear legislative framework is needed for the regulation of phage based drugs, from phage selection, manufacturing and purification and the quality control requirements of the production (Pirnay et al., 2014). Before the PhagoBurn trial, all the tests and applications of phages on human patients were allowed only in compliance with article 37 of the Declaration of Helsinki. This states: “In the treatment of an individual patient, where proven interventions do not exist, or other known interventions have been ineffective, the physician, after seeking expert advice, with informed consent from the patient or a legally authorised representative, may use an unproven intervention if in the physician’s judgement it offers hope of saving life, re-establishing health or alleviating suffering. This intervention should subsequently be made the object of research, designed to evaluate its safety and efficacy. In all cases, new information must be recorded and, where appropriate, made publicly available” (WMA Declaration of Helsinki, 2013). This article states how phage therapy may be used as a last resort treatment, but it does not address the wider issues and is strictly related to the single patient case.

Another challenge for phage therapy is the time needed to introduce a new drug to the market. Time frames for conventional medicinal product development and marketing take years and are not compatible with a flexible and tailor-made phage therapy concept. A phage-based drug should be “updated” as new resistance arises, perhaps using a similar regulatory framework as for vaccines, that slightly change every year, but they do not incur the need for a new request of clinical trial. The main advantage of phages over antibiotics or any classical drugs is their capacity to rapidly (in an order of days to weeks) evolve to kill the new (or the phage-resistant) pathogenic bacterial strains. For this reason, phage preparations may not follow the conventional medicinal product development and

licensing pathway that takes many years (Pirnay et al., 2012). Verbeken argued that bacteriophages should be considered as advanced therapy medicinal products (Commission Directive 2003/63/EC), which includes gene therapy, somatic cell therapy and tissue engineered products. However, the European Commission has indicated that the existing regulatory framework is adequate for bacteriophage therapy. Therefore, the current European regulation framework on medicinal products may be the way forward for bacteriophage therapy in the European Union (Verbeken et al., 2007).

Even if the phage cocktails would be considered in the same way as vaccines, the legislation would be too slow anyway. Vaccines are annually updated and licensed, and development times of many months may be too long in view of the enormous challenges related to rapidly progressing bacterial resistance. The real power of phage therapy lies in the possibility that the search for a potent natural phage against a resistant infection and the preparation of a classic galenic preparation (e.g., physiological water or a basic ointment) containing phages is practically feasible in the time frame of days to weeks (Pirnay et al., 2015)

The PhagoBurn project allowed significant advancements in the regulatory framework of phage therapy: thanks to PhagoBurn a serious discussion was opened between the French regulators (ANSM) and the Belgian (AFMPS) and Swiss (Swissmedic) authorities in the years 2013-2014. This discussion was the basis for the first regulatory workshop held in June 2015 in London at the European Medicine Agency (EMA). At the moment, the EMA will not change the regulation adjusting it for phage therapy, but in this workshop the issues and requests of medical doctors and researches have been brought to the attention of the Agency. In the final remarks and conclusions, the Agency is “looking forward to gathering more robust evidence on the value of bacteriophage treatments and further discussing the scientific and regulatory aspects relating to the biological characterisation of the phages” (EMA, 2015).

2.2.3.1. Technical problems of phage therapy

One of the few studies conducted before PhagoBurn was performed on a limited number of patients in the Queen Astrid Military Hospital (Brussels, Belgium). It showed interesting and encouraging results, but also a long list of problems (Rose et al., 2014). This test was performed in accordance with article 37 of the Declaration of Helsinki. A cocktail of three lytic phages against *P. aeruginosa* and *S. aureus* (called BFC-1), was developed to treat infections of burned wounds (Merabishvili et al., 2009). One issue derived from the negative perception of the bacteriophages: they were perceived as a “virus” and their healing effect was not sure. This caused reluctance among patients and specially hospital staff. As an evidence of it, the inclusion criterions were quite strict: only patients with a proven infection of antibiotic resistant *P. aeruginosa* or *S. aureus* were considered; patients in critical

conditions and pregnant women were excluded. Eventually, only 9 people took part in this test and 10 burns were to be treated. Furthermore, a non-fault insurance was provided to the patients, assigning to phages a class risk of 5 out of 7, quite high for non-human viruses. Misunderstandings with hospital staff were quite frequent as the phage samples were administered right after antibiotics and it took time for nurses to get used to handling bacteriophages.

Nevertheless, despite all these difficulties, the authors reported improvements in the conditions of 8 out of 10 wounds treated with their phage cocktail. Most importantly, no adverse reactions were reported at any time.

PhagoBurn gave some insights into these kinds of problems: the inclusion criteria were too difficult to achieve and only 27 patients out of the 60 expected were included (Jault et al., 2017).

Besides the difficulties of administering phage sample to patients and the outcomes, there is a serious issue that must always be addressed. Bacteriophages could be dangerous and can, paradoxically, spread antimicrobial resistance. It is well known that temperate phages can carry genomic sequences coding for toxins and the most famous are the cholera toxin that the phage CTX ϕ can integrate in *Vibrio cholerae* or the shiga-like toxin in *E. coli* O157:H7 (Canchaya et al., 2003). Besides, phages can induce the expression of virulence factors involved in any stage of bacterial infection, such as adhesion proteins or resistance to phagocytosis (Verheust et al., 2010). Phages can spread new genetic traits among bacteria: this process is called “horizontal gene transfer” and is mediated by transduction, which happens when a portion of bacterial genome is packed together with viral genome and then is transferred to other bacteria. Therefore, it is important to characterize phages and to screen their genome before using them in order to avoid complications. Phages can be a great tool against antimicrobial resistances, but they will need to be used properly.

2.3. Bioprocessing of bacteriophages and bacteriocins

Increasing commercial interest in phage therapy will require production of increasing amounts of phages. At present, continuous production of phages has not been explored in any detail, however, there are some studies and patents available on eukaryotic virus and protein production. The production of phages has been studied from many perspectives such as the evolution of the relationship between phages and the host (Bull et al., 2006; Horne, 1970; Ziv et al., 2013) and with many different phages and host bacteria. An important challenge is the downstream purification, including clarification of the lysate and purification of the final product from contaminants such as intracellular proteins and LPS etc.

Bacteriocins can be produced as recombinant proteins inducing the expression of a plasmid in a host strain. Usually recombinant proteins are produced in bacterial host strains, but also eukaryotic and mammalian cells are used as well (Assenberg et al., 2013; Demain and Vaishnav, 2011; Wurm, 2004).

This is an efficient protocol vastly used in the pharmaceutical industry. Thus, for recombinant proteins such as the bacteriocins, research can focus on optimization, finding the best conditions for expressing and purifying the highest concentrations of the protein of interest.

2.3.1. Production of bacteriophages

Independently from the amount of product needed, phage production will always depend on the biological features of the phage, the bacterial host strain and the purification of the final product. There are different reports on how phages have been produced, depending on the amount of the final volume. Small scale preparations are made in laboratories and often never repeated (Boratynski et al., 2004; Merabishvili et al., 2009; Pirnay et al., 2014, 2015; Rose et al., 2014). Large scale preparations usually are carried out using different production method: in batch (Bourdin et al., 2014), semi-continuous (Sauvageau and Cooper, 2010; Storms, 2012) or continuous (Husimi et al., 1982b; Nabergoj et al., 2018). Key features and downsides of these methods will be described in the following paragraphs.

2.3.1.1. State of the art of phage production

Bacteriophages have been widely used for non-therapeutic purposes for a long time but mainly for research: phage λ (lambda) is one of the most studied models in molecular biology (Lewin, 2009). The most obvious consequence of this fact is that only small volumes of purified phages were needed for such work. The production of bacteriophages typically follows a well-established protocol which has been widely used with small changes according to the host and phage features (Adams, 1959). The method requires the infection of a host growing in the logarithmic phase, followed by lysis after few hours (or less, depending on the characteristics of the phage). The phage lysate is then centrifuged and the supernatant – containing the phages – is then filtered with a 0.22 or 0.45 μm membrane filter. Then the aggregating agent PEG₈₀₀₀ is added to the filtered phage suspension at a final working concentration ranging between 8 and 10% w/v and left for several hours (sometimes overnight) at 4°C. After that, the sample is centrifuged at $\sim 3000 \times g$ for 45-60 minutes always at 4°C, then the pellet is collected, and the supernatant is discarded. The resuspended pellet is then ultracentrifuged in a

CsCl gradient at 10000 x *g* for at least 3 hours. Then the phage is concentrated in one band and it is collected using a syringe. The sample is finally dialysed against NaCl.

This protocol is considered the gold standard for phage production and purification and it is possible to achieve the highest purity and a titre of at least 10¹² PFU mL⁻¹. Although such a procedure delivers a pure and highly concentrated phage suspension, there are many disadvantages including issues with scale-up of such a process (Bonilla et al., 2016). The protocol is time consuming and requires a skilled operator and only produces small volumes.

As mentioned earlier, bacteriophages have recently been used in randomised control trials (RCT) for phage therapy; mostly *in vivo* studies have focused on animal models (Malik et al., 2017) and only on a few occasions involved human patients (Jault et al., 2018; Rose et al., 2014; Schooley et al., 2017). A study looking at small scale-production of phages described the methods for selection, production and purification of lytic phages, specific against *P. aeruginosa* and *S. aureus* (Merabishvili et al., 2009). The amount of phages produced was at lab scale and much more effort was put into the quality control of the final product, which was controlled for the pyrogenicity, sterility and cytotoxicity in order to be tested on humans. Bacteriophage genome and proteome were controlled in order to assure the absence of toxin-coding genes and the lytic nature of phages (Merabishvili et al., 2009).

Currently, if the volume required needs to be larger, the method of production would not change, only the scale of the reactor would increase, from a small flask to a bigger fermenter (Bourdin et al., 2014). Before proceeding with amplification of bacteriophages it is important to understand what the life cycles of the phage and the host are. Bacterial life cycles can be studied with a growth curve which shows how long the different phases of the growth last and the right moment of infection of the phage or induction of the plasmid can be found.

2.3.2. Batch and continuous processes of phages and recombinant proteins

Many pharmaceutical processes, including recombinant proteins and bacteriophages are produced in batch because it is a well-known and established process. However, pharmaceutical industry is moving towards continuous production for many reasons. Despite batch processes ensure high titre of phages and highly concentrated proteins, they have a long downtime between two runs due to cleaning and new sterilization of the reactor before the new run. Continuous manufacturing allows fast processing of high volumetric throughput with smaller process footprint and at lower production cost. The most important pharmaceutical companies have been strongly investing for changing the method of production to continuous: Pfizer, Novartis, Johnson & Johnson, GSK (Burcham et al., 2018). Continuous

production can be applied either to bacteriophages and to proteins and has also economic benefits: it ensures higher productivity and a smaller footprint (Jozala et al., 2016). Nevertheless, despite all these benefits, the commercialization is limited and the pharmaceutical industry is not keen in adopting the continuous manufacturing (Peebo and Neubauer, 2018). This is because there are many technical issues and challenges that slowed the process. The most difficult part is the standardization of the process, process control and characterization and handling of the final product at the end of the process. During the design of the continuous process, there is a need to anticipate technical problems that a batch process would not have. It is important to prevent or quickly deal with issues such as overfilling of the vessel, material spills or backflow of materials into other vessels. Online process control of many parameters is important: there is a need to adopt sensors and new technologies for a continuous and, most importantly, sterile monitoring (Center for Health policy at Brookings, 2015). The FDA encouraged research and development of continuous processing of drugs in many conferences, highlighting that “continuous manufacturing is fully consistent with FDA’s QbD” (Konstantinov, 2014).

Usually there is a trade-off in continuous processing: the final product often does not have the highest product concentration possible, but this is compensated with the high volumes produced. In continuous bioprocessing, where the product is made by a microorganism, it is important to ensure long-term sterility and genetic stability to always obtain the same product (Peebo and Neubauer, 2018). In the case of phage amplification, if phages and bacteria are in contact for too long, there will be mutation of the host and eventually of the phage and the genetic shift will lead to a different product.

It is against this background that the present work is presented: here it is shown how it is possible to continuously produce antimicrobial proteins and bacteriophages. While a simple layout of production is mostly recommended for bacteriocins, phages show a complexity that can be addressed by using a three-stage process. Different previous studies have shown ways to continuously cultivate proteins or phages, using one or two reactors connected in series. Here we briefly describe them, highlighting their results but also the critical points.

2.3.2.1. Continuous production in one vessel: the chemostat

A chemostat is a reactor in which cells can grow at steady state. Fresh medium is constantly added at a constant flowrate while the spent one, together with cells and products, is taken out at the same flowrate. A chemostat is good for protein bioprocessing because it allows cells to grow under controlled conditions. So, once steady-state is reached, production can continue for a long time

(Peebo and Neubauer, 2018). Chemostats have been widely used for production of recombinant proteins, such as insulin precursor (Liu et al. 2013), serum albumin (Blondeau et al. 1994), antibodies (Maurer et al. 2006; Buchetics et al. 2011), interferons (Srivastava & Mukherjee 2005; Vaiphei et al. 2009) and many enzymes such as trypsinogen (Paulová et al. 2012), phosphatases (Hidayat et al. 2006) and β -glucanase (Velur Selvamani et al. 2014). Production of bacteriocins can be carried out in the same way, using *E. coli* as the host, either using a complex medium or a synthetic medium and testing different dilution rates to achieve the best productivity (van Heerden and Nicol, 2013).

Bacteriophage amplification in a chemostat, however, is not convenient. When bacteria and bacteriophages are mixed together in the same reactor the phages quickly lyse the bacterial population. It is impossible to control inlet and outlet flowrates to avoid this situation and to have a good yield of bacteriophages. For this reason, chemostats have been used for research purposes instead of production: the chemostat is a good model for studying evolution of phage-bacteria populations inside the same environment. Culturing phages and bacteria in a chemostat allows the study of host-prey interactions and the evolution of mutations of both the viruses and the bacteria (Ziv et al. 2013; Horne 1970; Kick et al. 2017).

2.3.2.2. Production of bacteriophages using two reactor stages: the cellstat and the self-cycling fermentation

A patent of 2012 describes and protects a process for continuous production of bacteriophages (Baldwin and Summer, 2012), where “host bacteria are grown in a vessel and then the host and virulent bacteriophage are fed into a reactor vessel where the phage attach to, infect and lyse the host bacteria providing multiple replications of it and coincidentally concentrating the phage”. Even though this concept can theoretically work, many biological and quality flaws are present: for example, there is no control of either phage mutants or growth of resistant bacteria, whose number will eventually dominate over the susceptible bacteria and will contaminate the process.

A continuous process for phage production using two reactors was developed in order to study and continuously control the mutation rates of phages and host cells, but no further studies have been conducted to achieve the best optimization of the process (Husimi et al., 1982b). The “cellstat” is a bioreactor designed to continuously grow bacterial cells (Fig. 2.3). It is used as a source of physiologically unchanged, exponentially growing host cells. It has been used to study the evolution of bacteriophages and cells populations (Husimi, 1989).

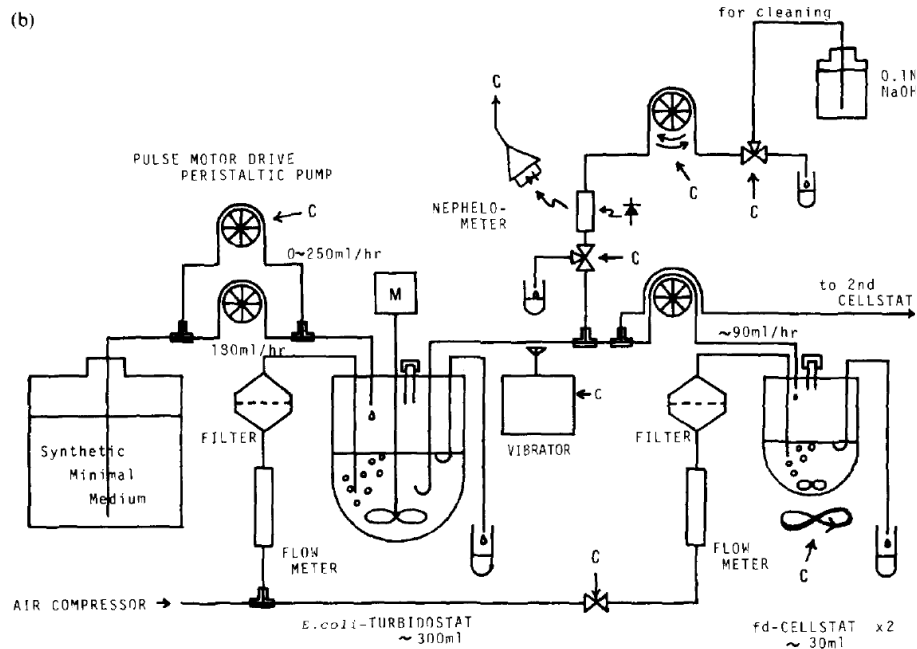


Figure 2. 3 Schematic diagram of the cellstat, composed of two reactors connected in series. (Husimi et al., 1982b).

The host cells, passing in a continuous stream through the reactors, are used to propagate bacteriophages and the flow rate of host cells is adjusted to a value that keeps the mean residence time of bacteria in these reactors much shorter than the generation time of eventually emerging mutant host cells. In such a way, coevolution of the host and the virus, which could lead to the takeover of phage-resistant host cells, is theoretically prevented. Bacteriophages are usually not washed out under these conditions because their growth rate is much higher than that of the host cell. What happens under real conditions is that some host cells and phage particles may theoretically remain in the fermenter for an infinite amount of time while others may leave the fermenter immediately upon entrance. The first situation can lead to coevolution of host cells and phages while the second leads to the harvest of uninfected or non-lysed host cells, which lowers the volumetric productivity of phages.

In order to achieve a high titre production of a batch process and to shorten the timing of the entire production, a semi-continuous process has been tested (Sauvageau and Cooper, 2010). The first stage, in which the host cells are grown, was operated under the principles of self-cycling fermentation (SCF). SCF is a non-steady state, cycling process in which a control parameter linked to cell growth is used in a feedback control loop to trigger cycling once growth has ended (Fig. 2.4). Just before the cell population enters stationary phase, half of the contents of the fermenter is removed and replaced with fresh medium. This process presents two different advantages: the first is keeping the population

in exponential growth and the second and more important, it synchronizes the population. The second stage, in which the host is infected by the phage, is also operated in an automated cycling mode in order to provide semi-continuous harvests, which reduces the proportion of down-time relative to production time. Each harvest did not present any loss of titres compared with batch infections carried out under similar conditions. The independent operation of both the first and second stages reduced the chances of co-evolution and there was no evidence for the selection of either more susceptible hosts or for more virulent phages.

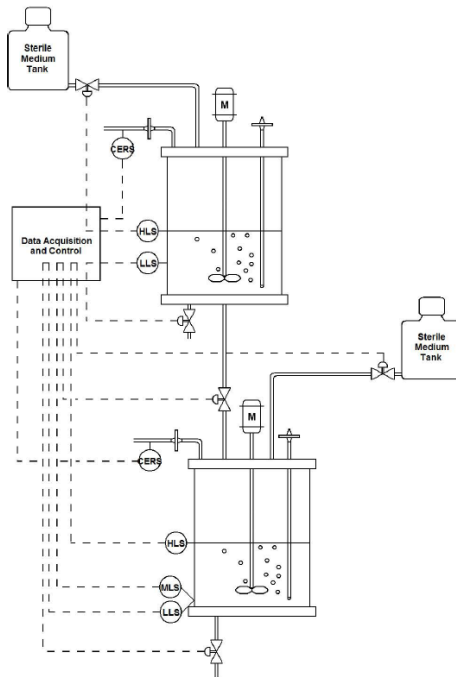


Figure 2. 4 Level sensors are used for the control of valves (low: LLS, mid: MLS, high: HLS). The carbon dioxide sensors (CERS) are used to measure CER and as the feedback control parameter for cycling of both stages. (Sauvageau and Cooper, 2010)

Papers dealing with the continuous production of phages are still relatively few and mostly published for research purposes (Gori 1965; Jacobson & Jacobson 1966), but there is an increasing interest in production due to the future need for phage therapy applications (Nabergoj et al., 2018; Sauvageau and Cooper, 2010).

Nabergoj assumed that the 2-stage reactor scheme was optimal, however, there is a major issue: the bacteriophages replicate at a higher rate than bacteria. The final titre will be affected by this difference of growth rate: phages will lyse all the bacteria before these could reach the optimal cell concentration and each host cell will not release as many phages as it could at the moment of lysis. Sauvageau understood the problem and tried to overcome it with the Self Cycling of the culture: using this method, bacteria are infected exactly at their mid-log phase of growth and can produce high

concentrations of phages (Sauvageau and Cooper, 2010) (Fig. 2.4). This is an interesting way of producing phages because it addresses the different growth rate problem and combines the advantages of batch and continuous processes. On the other hand, Nabergoj realized the importance of the dilution rate (D) of both the reactors in the amplification of the bacteriophages (Nabergoj et al., 2018). He uses a cellstat, that is composed of two chemostats connected in series: in the first one bacteria are grown at steady state and in the second one there is the infection with phages, like described by Husimi (1982). Dilution rate (D) is the ratio between the flow of medium in the reactor and the volume of the reactor and is a parameter used to describe how many volumes per hour are exchanged in the reactor. When bacteria grow in a continuous reactor, for a long enough time, they synchronize and reach steady state. So, by adjusting D is possible to decide how long cell are going to grow in the reactor and the physiology and growth rate is related to dilution rate. However, the problem of different growth rates between host and phage is only partially overcome: a higher productivity has been traded off with a lower titre of the final sample, because the phage T4 used is produced at a lower concentration than what he gets from batch culture. So, Nabergoj pointed to an interesting way to control growth rate of cells and related it to phage production, but it did not reach the highest productivity possible.

2.3.2.3. Continuous production of phages using three reactor stages

It is interesting to point out that both Sauvageau and Nabergoj, although using different methods of production, realized the need to identify the parameters involved in the continuous production of bacteriophages that might influence the final yield (Storms et al. 2014; Nabergoj et al. 2017). Control of the dilution rate in a cellstat is a way to control physiology of the host cell but it does not assure a high yield by itself; thus, in this thesis a third reactor is introduced. With three bioreactors connected in series the first reactor is used to propagate the host bacteria cultivated at steady state to the desired concentration and with controlled physiology, the second reactor is used to infect the host with the phages allowing a small number of bacteria to be infected and in the third reactor phage amplification is completed, which should allow overall better control of phage propagation.

The main difference compared with approaches used in the past is the function of the second bioreactor, which is used to control the infection process allowing time for phage to adsorb to exponentially growing bacteria and injecting their DNA in the host. The dilution rate in reactor 2 (D_2) is kept high – residence time is matter of minutes – to avoid the complete lysis of all the bacteria but enough to ensure release of some new phages to maintain steady concentration of phages in reactor

2. The three reactors are independent but the performance of the second and the third reactors depend on the operative conditions of the first one, which controls the bacterial host physiology.

A multi-stage reactor was previously described by Jacobson having different features (Jacobson, 1966) (Fig. 2.5). The system was called a Virustat and was composed of independent reactors for the host and the phages but there are key differences between what was done in the past and what is proposed here. The main one is the self-inoculation nature of the virustat, which is not the case here.

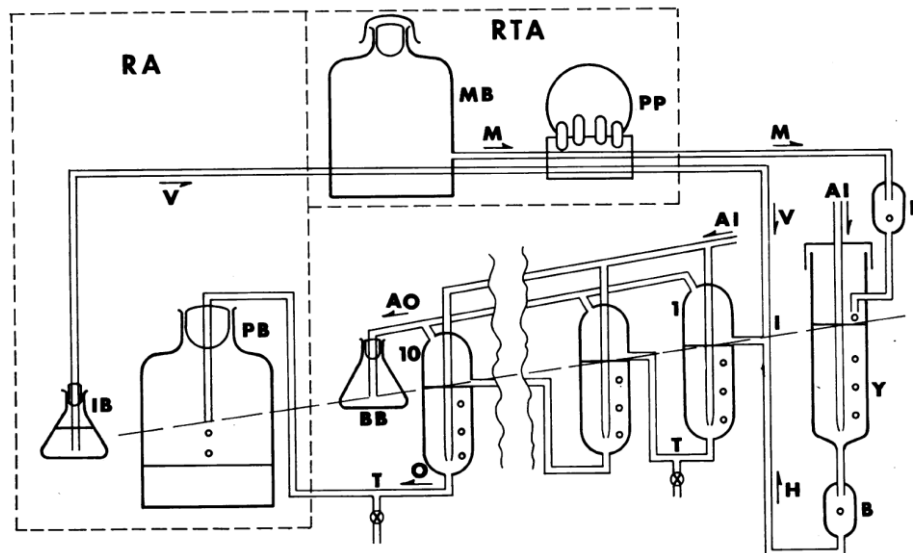


Figure 2. 5 Schematic of a virustat. The dotted boxes enclose the refrigerated area (RA) and the room temperature area (RTA). Shown in these areas are the medium reservoir bottle (MB), peristaltic pump (PP), inoculum reservoir bottle (IB), and production reservoir bottle (PB). Then the bacterial growth tube (Y), backflow traps (B), blow-over bottle (BB), air intake (AI) and output (AO) manifolds, three Cells (first and last are labelled 1 and 10, with a schematic hiatus after the second), and tees for host-cell inoculation (I) and for sampling (T). Arrows indicate path of air, and of medium (M), host cells (H), virus inoculum (V), and production output (O). The long-dashed line indicates the gradual liquid level drop, somewhat exaggerated, driving the gravity flow from bacterial growth tube to production reservoir bottle inlet. (Jacobson, 1966)

The three-stage reactor system for phage production is the novelty of the present work. Three independent reactors were connected in series to achieve a high titre of phages. The first is dedicated to the growth of the host bacteria, the second is used as a mixing tank and initial reaction stage for infecting bacteria with phages and the third is the final amplification reactor, where the phages were propagated and the reactor operated in batch mode, achieving high phage yields. Furthermore, evaluation of phage production using a defined medium with glucose as the limiting nutrient has not been done before. Modelling of the three reactors in series has also been carried out (Mancuso et al., 2018).

2.3.2.4. Optimization of the production

Optimization of production systems used to be performed in shake flasks. Nowadays, High-Throughput Technologies (HTT) are used, such as multiwell plates or small reactors, with volumes ranging from 0.2 to 10 mL. HTT allow collection of a large amount of data in a short time and using a limited amount of resources. One of the most relevant factors is the growth medium where cells grow and produce the protein of interest: medium optimization is often where the main effort is put during early stages of production. Nowadays it is possible to use design of experiments (DoE) to analyse the effect of multiple factors at the same time instead of checking the effect of each by changing them one by one (Tripathi and Shivastava, 2018).

The need of a robust production platform leads to the concept of quality-by-design (QbD). Briefly, QbD ensures the quality of the product, it is a systematic and risk-based approach to pharmaceutical production, that aims to improve understanding and the control of the process. QbD identifies the quality features that the product needs and changes and optimizes the parameters until the product get to the ideal characteristics (Yu, 2008).

2.3.3. Downstream processes

One of the main and most expensive parts of phage production is the purification of the lysate. After the amplification of bacteriophages, the final product will be impure because of the presence of residual media, resistant bacterial cells and cell debris such as membrane portions, nucleic acids and proteins. It is important to have a phage solution perfectly purified and concentrated.

The gold standard for lab-scale production of phages is firstly clarification by centrifugation and microfiltration, to remove the larger particle size impurities. After this initial clarification step is the elimination of impurities including small molecules such as nucleic acids and proteins or other host membrane elements that are potentially undesirable in the product including LPS (lipopolysaccharide), which causes inflammatory reactions if injected in the blood stream and its concentration is required to be below 5 endotoxin-units/kg/h (endotoxins will be described in section 2.3.5).

2.3.3.1. State of the art of phage purification

A good way to purify phages from impurities is a well-established but quite old protocol (Adams, 1959). The procedure is rather long consisting of centrifugation of the phage lysate and then filtering

the supernatant using a 0.22 or 0.45 μm filter to remove cellular debris (\sim 1-2 hours); PEG precipitation of the phages (\sim 16 hours); ultracentrifugation in a CsCl gradient ($>$ 4 hours) and finally dialysis ($>$ 24 hours). There might be some slight changes to speed up the process but phage purification is time consuming, especially if it is required to remove endotoxins (Bonilla et al., 2016). Chromatography is a very efficient downstream purification method, but it is a major processing bottleneck. Many kinds of chromatographic separations have been evaluated to purify virus-like particles and bacteriophages including size-exclusion (SEC), ion-exchange (IEC) using well characterized model phages, and often with filamentous phages.

A straightforward ion exchange chromatographic separation is different due to the low isoelectric point (pI) of the phage (it is around pH 4 for model phages) and around pH 2 for endotoxins; this means that both phages and endotoxins remain negatively charged under typical operating conditions. Other methods based on separation through size differences cannot effectively separate phages from endotoxins: the dimensions of phage and endotoxins are similar in magnitude (Petsch and Anspach, 2000). Hence, finding a method that is general and can be applied to any kind of phage is difficult.

Ion exchange chromatography using Convective Interactive Media (CIM) monolith columns have been shown to concentrate and separate phages (Smrekar et al., 2011a). With this method phages and the other impurities are eluted from the column at different concentration gradients of salt buffers, proving high resolution of the column. CIM has the advantage that the process is fast (usually taking between 20-45 minutes whereas a conventional SEC can take hours), granting a significant advantage if large volumes of phages are to be purified.

Alternative methods to remove endotoxins from phage preparations, include the precipitation of the lysate with a combination of PEG, NaCl and Triton X-100 (Branston et al., 2015). A 5-log reduction of endotoxin concentration was achieved but required more than one washing step and it may not be the best solution for large-scale production of high titre of bacteriophages (this topic will be dealt with more thoroughly later).

To summarize, many parameters need to be controlled in order to have purified final product: pH, pyrogenicity and sterility are important. To-date there is no gold standard to achieve this target and different solutions depend on each individual case. Methods to scale-up purification need to be used. Filtration can be used to purify large volumes of lysate and then concentrate it prior the chromatographic step. In the next paragraphs, techniques and methods that can be used to purify phages and that were exploited in the experiments of this thesis will be described. The aim was to apply scalable techniques to phage purification.

2.3.3.2. Filtration

Filtration is a pressure driven method of separation based on membranes. The membrane pore size is different depending on the nature of the compound or body that must be retained:

- Microfiltration is mostly used for clarification and sterilization of biological solutions. The membrane pore size is usually between 0.05 and 10 μm (Kelly and Zydney, 1997).
- Ultrafiltration (UF) is a branch of filtration where the membranes have pore sizes between 1 and 20 nm. UF mostly used for protein concentration and buffer exchange instead of gel chromatography and it is easily scalable (van Reis and Zydney, 2007).
- Nanofiltration or reverse osmosis, is used to separate solvents, salts and small organics from divalent ions.

2.3.3.2.1. Ultrafiltration (UF)

UF is generally used for protein concentration and buffer exchange, it is an alternative to size exclusion chromatography, especially at an industrial scale (van Reis and Zydney, 2007). UF for phages is comparable to small human virus purification processes. These viruses, called Adenoviruses (Ads) have an average size of 90-100 nm. They are often used as viral vectors for vaccine and gene therapy and membranes between 300 and 1000 kDa can be used and obtain up to 100% of virus recovery (Nestola et al., 2014).

Depending on the direction of the feed flow with respect to the membrane, it is called dead-end filtration (or normal flow) if the flow is perpendicular to the membrane whilst it is called tangential flow filtration (TFF) or cross flow filtration (CFF) if the flow is parallel to the membrane surface (Fig. 2.6).

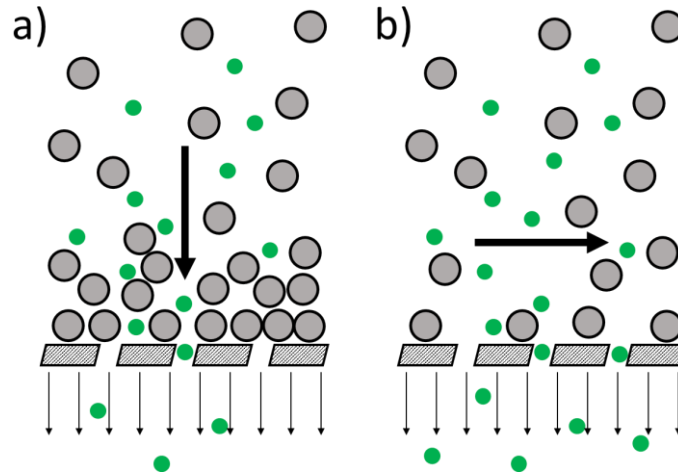


Figure 2. 6 Principles of dead-end filtration (a) and cross flow filtration (b). In dead-end filtration a layer of filter cake builds up, while in cross flow filtration the flow sweeps the surface area of the membrane.

2.3.3.2.2. Dead-end filtration – or normal flow filtration

Dead-end filtration is the classical filtration and it is used when the solute is at a low concentration. It is based on the difference of pressure between the two sides of the membrane and the selectivity of the membrane is related to the solute sieving coefficient (van Reis and Zydney, 2007):

$$S = \frac{C_f}{C_F} \quad (2.2)$$

Where C_f is the solute concentration in the filtrate and C_F is the feed solution.

Volumetric filtrate flux at the beginning is described by:

$$Lp = \frac{J}{\Delta P} \quad (2.3)$$

As it depends on the membrane hydraulic permeability, where J is the filtrate flux (L/m^2h) and ΔP (bar) is the transmembrane pressure.

Dead-end filtration is mostly used for retaining only poorly concentrated components and it is used mainly at small scale because the membrane is subjected to concentration polarization effects and can get quickly fouled. Membrane fouling is a common phenomenon during filtration that leads to a decreased filtration efficiency. It is caused by the adsorption within or on the pores of the membranes or the formation of a layer on the external surface of the membrane (Kelly and Zydney, 1997). Polysulfone membranes tend to adsorb more proteins than regenerated cellulose ones, resulting in lower process permeability (van Reis and Zydney, 2007).

Concentration polarization is the concentration of retained solutes at the filtration surface of the membrane. Polarization effects can be controlled by applying high shear rate across the membrane surface.

Filtration rate is affected by pH and ionic strength of the solution (Becht et al., 2008) and property differences of components to be filtered can be exploited for selective filtration (Burns and Zydney, 1998; Saksena and Zydney, 1993).

2.3.3.2.3. Tangential flow filtration (TFF)

For large scale applications, tangential flow is used as it allows processing of larger volumes: the membrane is constantly washed by the constant flow across the membrane surface and the fouling is slowed (van Reis and Zydney, 2007) as a constant shear rate is applied on the surface of the membrane (Gésan-Guiziu et al., 1999).

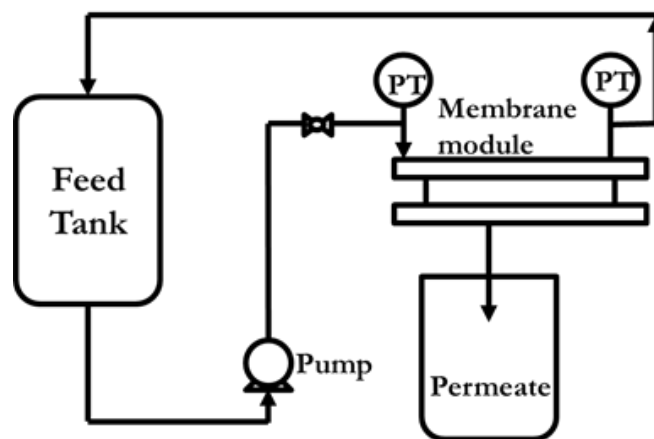


Figure 2. 7 Schematic of batch tangential flow filtration. Sample from the feed tank is pumped into the module with flat sheet membrane or hollow fibre. The ΔP across the membrane allows filtration; the filtrated sample ends up in the permeate whilst the retentate is circulated back into the feed tank

Tangential flow filtration is subjected to membrane fouling as well: the solute is forced onto the membrane and it builds up forming a cake layer. The difference with dead-end filtration is that here the process stream sweeps this layer back into the bulk flow. The cake layer grows until the rate of solute deposition equals the rate of solute diffusion back into the feed stream (Dosmar, 2006).

There are different ways to perform tangential flow filtration (TFF) or cross flow filtration (CFF): using flat sheet membranes, hollow fibres or cassettes.

2.3.3.2.4. Diafiltration

Diafiltration is a method specially used for buffer exchange operations. Diafiltration can be discontinuous if the solution is concentrated and then diluted with buffer, and after a few cycles the

buffer is exchanged. Diafiltration can be continuous when fresh buffer is continuously added at the same flowrate as the permeate (Jungbauer, 2013).

Diafiltration has been used for purification of monoclonal antibodies (Mab) (Guo et al., 2016) or for the purification of adenoviruses (Nestola et al., 2014). It has been used for preparing a phage sample as well, for a phage trial, especially for medium exchange before proceeding to further purification (Schooley et al., 2017).

2.3.3.3. Chromatography

Chromatography is a technique that allows separation of a molecule dissolved in a mobile phase, by interacting with a stationary phase that is chemically modified to exploit the chemical and physical differences between biomolecules. Molecules are separated on the basis of their size, electrical charge, hydrophobicity or binding specificity (Cummins et al., 2011). Chromatography ensures high resolution especially when it comes to separating components with similar features and in the final polishing steps, where a high degree of purification is required. Despite the constant research of alternative, non-chromatographic methods for purification, chromatography still maintains a dominant role in separation and purification (Hanke and Ottens, 2014).

2.3.3.3.1. Factors affecting column performance

Many kinds of chromatography exist, but there are common features that affect the column performance. The pore size of the stationary phase influences the surface available for the protein in the mobile phase. The particle size influences the mass transfer of the protein, but if the particle size is too small there might be a big pressure drop causing low permeability. The performance can change if the support material is compressible and the column packing influences the number of theoretical plates, affecting the resolution of the column.

Operation conditions that can influence the outcome of the separation are the composition, flowrate and temperature of the solvents used and must be empirically optimized for each product. The solvent should not damage either the protein of interest or the matrix and the temperature should not be too high so as not to denature the protein. Usually, all the large-scale separations are conducted mostly at 4°C.

2.3.3.3.2. Ion exchange chromatography

Ion exchange chromatography allows separation of molecules based on the charge. It is routinely used for proteins and enzymes, but also for peptides, antibodies, nucleic acids and carbohydrates and it is

easily scalable (Cummins et al., 2011). A specific technology for ion exchange chromatography for phage separation has been developed by BIA Separations (Smrekar et al., 2011b). This company put in the market convective interaction media (CIM) monolith columns, that are different from standard columns packed with beads and can process large biomolecules such as viruses and plasmid DNA (Etzel and Riordan, 2009). The main advantage of monoliths is their hollow structure which allows the solute to be transported into the large open pores through convection rather than diffusion, allowing faster flow rates during operation with a low pressure drop. Monoliths can be used to isolate, concentrate and purify different kind of viruses (Oksanen et al., 2012). Breakthrough profiles are used to assess the packed column performance and is an important parameter to assess before scaling up production of proteins (Skidmore and Chase, 1990). Breakthrough profiles can be modelled to predict the interaction between protein and stationary phase (El-Sayed and Chase, 2010).

2.3.3.3.3. Affinity and adsorption chromatography

Affinity chromatography achieves separation due to the interaction of a molecule with the stationary phase and is mostly used as a first step for purifying recombinant proteins due to high selectivity and capacity. It can exploit the interaction between a histidine tag with metal chelators, antibody-antigen interaction, nucleic acids-heparin interaction (Duong-Ly and Gabelli, 2015).

Affinity chromatography can be scaled-up and a large scale recovery of recombinant proteins is possible using expanded bed adsorption chromatography, which allows clarification of the lysate, retention and concentration of the protein in one single step (Johansson et al., 1996).

It is used for bacteriophages but not for production purposes, only for separating bacteriophages during phage display (Ceglarek et al., 2013; Zhao et al., 2018).

2.3.3.3.4. Gel filtration chromatography

Gel filtration chromatography, or size exclusion chromatography (SEC) is a method of separation based on the size and it is usually performed as a final polishing step for protein purification. It separates all the few impurities left from adsorption chromatography and sometimes some reagents from a previous purification step (Amons and Schier, 1981; Gräslund et al., 2008; Wingfield, 2016).

SEC has also been used to allow the proper folding of the recombinant protein produced in the form of an inclusion body, which is an aggregation of insoluble polypeptides usually due to the high concentration in the cell. The formation of inclusion bodies is a problem because the protein, losing the right folding, loses its activity. There are many reports of proper refolding after running the protein through a size exclusion column (Batas and Chaudhuri, 1996; Li et al., 2004; Werner et al., 1994).

Gel filtration can also be used for purifying bacteriophages, but, most of the time phages are bigger than the pore size of the matrix in the columns and they flow out in the void volume, but the impurities are separated from the virions.

Gel filtration is not a scalable process but can be used as an analytical method for assessing the purity of phage samples after ultrafiltration (Boratynski et al., 2004). Gel filtration has also been used to purify the filamentous phage M13/fd for phage display under mild conditions (Zakharova et al., 2005).

2.3.4. Purifying proteins and bacteriophages

Chromatography has been developed mostly to purify antibodies (Hanke and Ottens, 2014), small molecules or recombinant proteins (Asenjo and Andrews, 2009) and lately human viruses used as viral vectors for gene therapy such as adenoviruses (Burova and Ioffe, 2005; Tomono et al., 2016). Bacteriophages have a size between 50 and 300 nm and except for *Podoviridae* phages, they cannot be approximated to a globular protein because of the tail that can be long ~100 nm.

Despite this introduction, there are ways to use standard chromatography columns for phage separation and there are also peculiar columns designed specifically for phage processing (Oksanen et al., 2012).

2.3.4.1. Performance measurements – ion exchange and affinity chromatography

- Adsorption isotherms

When the protein is in contact with the resin, it binds to it reaching an equilibrium between the protein in solution and the amount adsorbed to the resin. There are different curves describing the adsorption isotherms:

- Linear isotherm, not widely used in bioseparations
- Freundlich isotherm, mostly used for antibiotics
- Langmuir isotherm that is the most commonly used for protein adsorption

- Breakthrough curves

Breakthrough curves measure the dynamic capacity of the medium and give an indication of when the column gets to saturation during the loading. When this happens the protein of interest does not bind anymore to the matrix, but the eluate has the same concentration of the feed.

The gradient of the curve indicates the specificity of the binding: the steeper the curve the more specific is the binding.

Factors that may influence the adsorption and the breakthrough curve are the flow rate and the column height. A fast flow rate decreases the rate of mass transfer while a slow flow rate increases the residence time in the column.

2.3.4.2. Isotherm curves and equilibrium capacity of a resin with bacteriophages

Adsorption isotherm curves have mostly been studied for ion exchange chromatography when applied to proteins (Felsevalyi et al., 2011), but they can be used for measuring the affinity of phages to a resin (Bales et al., 1991).

Equilibrium binding capacity and kinetics can be studied, i.e. the time required to reach equilibrium and the adsorption capacity at equilibrium can be measured. Rarely equilibrium capacity reaches saturation when bacteriophages are binding to a porous medium because of the large size of the viruses which is in the order of nanometres, and many functional groups are left not available to phages (Bales et al., 1991).

Adsorption on a porous medium is usually influenced by temperature, pH and ionic strength of the solvent. Quaternary amine resins can be used as their positive charge will attract the negatively charged capsids (Cademartiri et al., 2010). Purity of phage sample can influence the binding capacity of the resin, as phage lysate in contact with a resin will have more impurities competing to bind to the resin. On the contrary, a purified phage sample will be able to bind more virions to the resin allowing phage purification and concentration.

2.3.5. A major contaminant from Gram-negative bacteria: Endotoxins

As mentioned in section 2.3.3, endotoxins may be a dangerous contaminant in phage production. Endotoxin is the name of one of the components of the membrane of Gram-negative bacteria. It is also called lipopolysaccharide (LPS) and it is constitutively produced by diderm bacteria, among the most known are *E. coli*, *P. aeruginosa* and *Salmonella*. The major function of LPS is a structural and stabilizing effect on the membrane. Endotoxins are composed of three defined parts: a hydrophobic part, called (i) Lipid A, a hydrophilic one, (ii) the core oligosaccharide and (iii) a heteropolysaccharide, also called Antigen O (Raetz and Whitfield, 2008). Lipid A is composed of a diglucosamine backbone and a hydrophobic domain of acyl chains in amide and ester linkages with saturated fatty acids. It is

the most conserved part of endotoxin. The acyl chains are usually six for *E. coli* strains and seven for *Salmonella* (de Oliveira Magalhães et al., 2007). The core oligosaccharide has a conserved structure, usually composed of 8-12 sugar units. The core region close to the lipid A and the lipid A are partially phosphorylated, giving to the LPS a net negative charge at physiological pH. The O-antigen is composed of repeated units of sugars, which are strain specific and can have up to 40 units thus giving the hydrophilic feature to the LPS. The O-antigen is a major antigenic determinant (it is recognized by antibodies) and it has immunological specificity. (de Oliveira Magalhães et al., 2007; Ongkudon et al., 2012).

2.3.5.1. Virulence of endotoxins

Endotoxins have a very powerful biological effect even at the slightest concentrations: even at 1ng mL^{-1} they can cause fever, septic shock, failure of organs and even death. They do not have a direct effect on the organs, but endotoxins can induce an inflammatory reaction: monocytes and macrophages are activated and proinflammatory mediators are released, such as tumor necrosis factor (TNF), interleukin (IL)-6 and IL-1(de Oliveira Magalhães et al., 2007). These compounds cause cell metabolic disfunctions, activation of coagulation cascade and induction of shock.

LPS is a very potent activator of the immune system, although it is still not clear what are the actual molecules that activate the inflammatory response (Mueller et al., 2004). The toxic effects are thought to be due to the Lipid A moiety, but the macromolecular structure might have a more important role than the chemical composition: aggregates forming an inverted cubic structure are active, while lamellar aggregates exhibit low or no ability to activate the immune system (Brandenburg et al., 1993; Seydel et al., 2003). Lipid A is the major target to eliminate during purification of phage samples from endotoxins.

2.3.5.2. Problems of endotoxins in manufacturing

Due to these effects, the legislation on therapeutic agents is strict and the limits for injecting LPS is $5\text{ EU mL}^{-1}\cdot\text{kg}\cdot\text{h}$ (FDA, 2012). The main problem of endotoxin is in its amphiphilic nature because it is composed of lipids and sugars and it is hard to find a physical or chemical property for separating them from phages. Besides, endotoxins have a hydrophobic region of 10-20 kDa that gives rise to a high tendency to aggregate into micelles and they can reach sizes of the order of $1\ \mu\text{m}$. Endotoxins therefore do not have a defined size in solution and the extent of aggregation is impossible to predict quantitatively (Branston et al., 2015). Another consequence of aggregation is the possibility of

favouring the formation of an even more dangerous form of LPS as the aggregates of endotoxins are stronger activators of the immune system, while monomers of lipid A are not able to activate any response (Mueller et al., 2004). Endotoxins are pH and temperature stable, which makes their removal particularly challenging.

Although it is always preferable to have LPS levels below the 5 EU mL⁻¹ limit, it is technically not always necessary: it all depends on the final use of the bacteriophages. For instance, for respiratory or intestinal applications there are different limits of endotoxins compared with phages that will be given systemically and will enter the blood stream. It is also important to respect the limits in case of injections or topic applications – in case of wounds phages could enter in the blood stream.

2.3.5.3. Methods for detecting of endotoxins

There is a standard test for detecting the presence and the concentration of endotoxins in biological samples, using the amoebocyte lysate from the horseshoe crab (abbreviated in LAL) (*Limulus polyphemus*) (European Pharmacopoeia, 2010). This method is based on the feature of the blood of horseshoe crabs that forms clots when in contact with LPS (Levin and Bang, 1968). It has been recognized as ideal and it is fast, cheap, sensitive and accurate, does not involve use of animals and it replaced the rabbit pyrogen test. The rabbit pyrogen test was developed in 1920's and was the first method approved by US Food and Drugs Administration (FDA) for LPS detection. It is based on the rise of temperature in rabbits after intravenous injection of a solution containing endotoxins (Hoffmann et al., 2005).

Mechanism of LAL assay: bacterial endotoxins catalyse the activation of the Factor C, which stimulates the Factor B, which converts the proclotting enzyme into a clotting enzyme. Finally, there is the formation of a gel (B. and Jalal, 2010). The simplest form of this assay is the clotting one (developed by Sigma with the name of E-Toxate) and it is a semi-quantitative test, since it is not too accurate in measuring the LPS concentration. Other tests based on the LAL have been developed to better quantify the concentration of endotoxins in biological samples: the endpoint chromogenic LAL assay (Thermo scientific, GenScript, Lonza Bioscience); the kinetic turbidimetric LAL assay (Lonza Bioscience) and the latest is the kinetic chromogenic-LAL assay (Lonza Bioscience) (Su and Ding, 2015).

This is not a perfect method and some components of the sample or solvents used to extract LPS might give false negatives or false positive outcome of the test. It has been shown that the LAL reacts with some polymeric forms of glucose: for instance the β -(1,3)-D-glucan, although not pyrogenic, can

activate the coagulation hence causing a response without the presence of endotoxin (Roslansky and Novitsky, 1991). The false negative effect is when an organic solvent such as octanol (Szermer-Olearnik and Boratyński, 2015) or triton X are used to remove LPS. The sample must be completely purified also from the solvent, because it inhibits the Factor C, which is essential for activating the reaction of LAL.

There are other methods to detect LPS based on endotoxin-affinity components, but at present are listed only as promising alternatives. There are studies on biosensors that may use proteins, peptides or aptamers to detect LPS, but at the moment they lack in sensitivity and they are still far from being commercialized (Su and Ding, 2015).

2.3.5.4. Methods for eliminating endotoxins

Purification of biological products from LPS is an important step in therapeutic production, especially those coming from *E. coli* fermentation. At present, a unique method for eliminating endotoxins is not available, as it strongly depends on the type of the product and many papers have been published on the topic, but they all dealt with lab scale amounts of phages (Van Belleghem et al., 2017; Boratynski et al., 2004; Szermer-Olearnik and Boratyński, 2015). Common techniques are ultrafiltration, ion exchange chromatography, size exclusion, affinity chromatography, hydrophobic interactions, liquid-liquid extraction. Currently, most of the papers published on endotoxin removal deal with purification of therapeutic proteins produced in *E. coli*. Only few of them have focused on removal of endotoxins from bacteriophages samples. As bacteriophages are small viruses, could be approximated as big proteins bigger than 500 kDa; *Podoviridae* are easily approximated to a globular protein because the short tail makes the capsid the main part of the entire phage, whilst for *Siphoviridae* and *Myoviridae* the presence of a long tail makes things more difficult. This is the reason why technology developed for proteins are not always transferable to phages but need modifications.

2.3.5.4.1. Microfiltration and ultrafiltration

Filtration is a commonly used method for clarification of bacterial suspensions and it has also been used for removing endotoxins. The main issue of filtration is that lipopolysaccharide particles do not have the same size and they can aggregate to form micelles depending on the composition of the medium/buffer in which they are suspended (Li and Luo, 1998). Hence, it is not straightforward to select the right membrane pore size to be used.

Microfiltration – with membrane pores between 0.1 and 0.45 μm - has been mostly used to purify water from possible contaminations of bacteria. Since endotoxins are too small for microfiltration,

modified filters of 0.22 μm can be used to retain LPS using electric charge instead of size. A positively charged filter can remove up to 99% of endotoxins present in a solution, compared to a negatively charged one. The pH plays an important role as well: using the same filter and the same solution, the removal is more efficient at pH 4 than one at pH 7 (Gerba and Hou, 1985). This property has been widely used and many researchers have evaluated efficacy of LPS removal from liquid solutions (Doorne, 1993; Schomm et al., 1998; Bononi et al., 2008). The main difference between these studies on endotoxin contamination of water and purification of LPS from a protein/phage amplification certainly is the concentration: in water the endotoxin concentration is very diluted while in a phage lysate they can get up to 10^7 EU mL^{-1} .

Ultrafiltration – with membrane pores between 5 and 750 kDa - has been one of the first methods used for removing endotoxins from protein solutions (Sweadner et al., 1977). Ultrafiltration has been proven to be effective in removing LPS from a protein solution using the micelle-forming property given by adding Ca^{2+} ions to the sample (Li and Luo, 1998): using a 300 kDa membrane, the protein passed in the permeate while the LPS were retained in the retentate.

There is a report of purification of a recombinant protein, the histone H1.5, produced in *E. coli* from endotoxins using a 100 kDa membrane. The protein was ~ 30 kDa and the LPS were retained in the retentate and the permeate protein reached endotoxin concentration below 0.5 EU mL^{-1} (Pyo et al., 2001). It is also possible that a concentrated sample favours the formation of big aggregates of LPS while a diluted sample affects it and makes it easier for endotoxins to be in monomeric form. This property can be exploited in ultrafiltration: a diafiltration process where buffer is exchanged may perform better than a simple ultrafiltration process where the permeate is not replaced by fresh buffer and the sample is concentrated. In this case, a 30 kDa membrane may be enough to remove 99.8% of endotoxins in an *E. coli* preparation (El-Moghazy, 2011).

2.3.5.4.2. Liquid-liquid extraction (LLE)

Liquid-liquid extraction is a promising method for eliminating endotoxins from a phage suspension, due to the lipophilic part of the endotoxin. An organic solvent can be used to partition the LPS in the solution thereby removing it, leaving phage viability unaffected and removing most of the endotoxins.

Using Butanol and Octanol as organic extractant

1-butanol or 1-octanol were tested for removing LPS from phage samples (Szermer-Olearnik and Boratyński, 2015). In this work, samples of *E. coli* phage T4 were mixed with 40% butanol or octanol and after 1-3 hours of shaking, the two phases were separated using a separation funnel or centrifugation at $4000 \times g$, 10 minutes. Octanol gave the best results in extracting endotoxins

compared to butanol. Despite octanol is considered immiscible in water, it still retains a solubility of 0.3 g/L which is enough to impair the LAL assay. A step of dialysis using a membrane of 12-14 kDa against 25% ethanol was therefore performed to remove all the octanol left. Before the dialysis step, resistance of the phage to ethanol was tested and a concentration lower than the maximum resistance capacity of the phage was used for exchanging the octanol left in the sample. After 5 cycles of 4 hours in ethanol followed by 4 cycles of 4 hours in 150 mM NaCl were performed to remove the ethanol in the sample and then the concentration of endotoxin was measured. Losses of titres of phage T4 were minimal and the final titre was always around the same order of magnitude of the initial sample. Endotoxin levels decreased by 3 to 5 log₁₀, not far from the 5 EU mL⁻¹ limit. Szermer-Olearnik et al. (2015) point the endotoxin concentration in the organic phase was higher than the initial concentration in phage T4 lysate; moreover, they affirmed that a purified sample showed a low polydispersity but unfortunately, the authors did not investigate further to explain these findings.

Using Triton X-100 as organic extractant

Triton X-100 has been tested for removing endotoxins. Triton is a non-ionic surfactant that is composed of a hydrophilic polyethylene oxide chain and an aromatic hydrocarbon hydrophobic group. The use of Triton has been described in many papers dealing with non-chromatographic methods for endotoxin removal. In their work, Branston et al. (2015), added up to 2% Triton to PEG₆₀₀₀ and 500 mM NaCl before precipitating samples of phage Ff produced from *E. coli*. Compared to samples without Triton, the ones with the surfactant decreased the endotoxin concentration by almost 6 log₁₀ after three rounds of precipitation.

Endotoxin contamination is a problem either for phage amplification or for protein expression using *E. coli*. The recombinant protein E2, derived from the bovine viral diarrhoea virus has been produced using an *E. coli* system (Cavallaro et al., 2011). The problem of lipopolysaccharide contamination was overcome using two-phase extraction with Triton X-114, which led to a reduction of endotoxins below detectable levels (>3 EU mL⁻¹). Other Gram-negative bacteria have been tested, such as *Klebsiella*, with encouraging results and better yields compared to gel filtration, anion exchange or ultrafiltration (Adam et al., 1995).

There is, however, a new phenomenon recently discovered, called “low endotoxin recovery” (LER). It consists in a lower efficacy of the LAL assay of detecting LPS due to the masking effect caused by external agents in the buffer, sometimes resulting in an erroneous measurement of endotoxins (Schwarz et al., 2017). The paper of Schwarz and colleagues highlights the importance of the purification step after two-phase extraction before performing the LAL test, as pointed out by Szermer-Olearnik & Boratyński (2015). This observation has been cited only a few times in other

papers (for instance Aida & Pabst 1990). Endotoxin has been shown to interact with other proteins. The most known are the lipopolysaccharide-binding protein (LBP), transferrin and of course the enzyme in the *Limulus* amoebocyte lysate (LAL). There are reports of interactions with lysozyme (Ohno and Morrison, 1989) and lactoferrin (Ward et al., 1997), but also haemoglobin (Kaca et al., 1994). It is probable that the presence of divalent cations like Ca^{2+} might form stable calcium bridges between LPS and proteins (Petsch and Anspach, 2000). While divalent cations such as Ca^{2+} stabilize endotoxins and make them into big aggregates of more than 100 kDa and form micelles, the use of surfactants such as Triton X-100 destabilizes their conformation and makes them into smaller sized macromolecules and with the hydrophobic parts more exposed to the solution. This effect strongly inhibits the LPS-mediated activation of Factor C, that is the main component of the LAL coagulation cascade.

The amphiphilic nature of the endotoxins allows a change in morphology and characteristics, and this complicates the purification because it is not possible to design a single method that might be good for all preparations.

2.3.5.4.3. Chromatography for removing LPS

Chromatography methods are widely used also in the purification of phages from LPS but none of them is used uniquely. The most common is affinity chromatography: columns packed with L-histidine, poly-L-lysine, polymyxin B can be chosen (Petsch and Anspach, 2000). The type of buffer, salt and pH influence the removal efficacy: it has been demonstrated that LPS binds to proteins at different isoelectric points. It was shown that removing LPS from basic proteins is harder than removing LPS from acidic proteins (de Oliveira Magalhães et al., 2007). Commercially available kits are composed of columns filled with resin that adsorbs LPS and the sample is collected in the flow through. One of these media is the Endo-trap kit (Hyglos, Germany) or Pierce Detoxigel and Bioprocessing Prosep Remotx, based on polymyxin B ligand, although they are not always effective (Wilson et al., 2001).

LPS affinity for histidine has been exploited for purifying a recombinant protein produced by *E. coli*. In a case report, the protocol was maintained the same till the first purification step using a nickel column, in which the protein is retained and isolated from the major lysate impurities and finally eluted. After this step, the His-tag was cleaved and the sample loaded again in the nickel column: this time all the histidine residues, bound to the LPS, were retained into column and the purified protein was collected in the non-adsorbed elution fraction (Mack et al., 2014).

Similarly, the negative charge of endotoxin molecules can be used in anion exchange chromatography to retain the endotoxins in the column and collect the desired protein in the elution. Nevertheless, it is probable that the LPS binds to the protein of interest or to the phage and they are both retained in the column and then eluted together (Bourdin et al., 2014). It is also important to determine the optimal pH and divalent ions in the sample, which might affect the charge (Dullah and Ongkudon, 2017).

2.4. Production of phages for clinical trials: the PhagoBurn experience

PhagoBurn was the first complete randomised clinical trial carried out with human patients. 28 patients were treated with phages using a protocol for production that was not very different from the state of the art described above. PhagoBurn was the first phage therapy trial that used GMP-like produced phages. These results came after overcoming difficult challenges and took almost two years to have GMP-standard phage cocktails. A series of quality control (QC) tests were used and routinely performed to guarantee safety of phage samples (Jault et al., 2017):

- Viability:* - titration: enumeration of phage virions.
- Identity:*
- host range: range of bacteria infected;
 - full genome sequence: knowing phage DNA using High-Throughput sequencing;
 - DNA restriction profile: digestion of genome using specific enzymes and migration using electrophoresis;
 - Genotyping: differences of phage genomes using PCR;
 - Protein profile: protein characterization using SDS-page;
 - Morphotype by electron microscopy;
- Purity:*
- Sterility and bioburden: presence and quantification of bacterial contamination
 - Endotoxins: detection of lipopolysaccharides using chromogenic quantitative and kinetic LAL assay
 - Host cell DNA
 - Total proteins
 - Visual aspect
- Chemistry:* - pH

2.5. Future applications

2.5.1. Applications in industry and health

In the past few years a lot of effort has been put into research for alternatives to antibiotics. Phage therapy is closer to market compared with bacteriocins, and the PhagoBurn project is a recent example of it. Although bacteriocins have been used for years for food preservation, phages have been studied for a longer time and the research on them is more advanced. There are many patents of phage cocktails for many infections, suggesting that there is industrial interest in using phages. Furthermore, the number of companies producing and supplying phage-based products is increasing.

There are many products already available on the market, such as Ecolyse, for preventing corrosion in the pipelines or Listshield that protects from *Listeria* infections, to name a few.

Nevertheless, bacteriocins are promising antimicrobials as well and, even if not for human applications, they have considerable potential as antimicrobials in food and animal feedstocks and for agriculture applications.

2.5.2. Encapsulation and stabilization of phages and bacteriocins

Despite the promising properties of phages and bacteriocins, and all the effort put in phage therapy research, there are still important research gaps. Bacteriophages and bacteriocins are quite sensitive to pH (not too far from neutral) and upon administration there is the need to protect them against hostile environment and from getting cleared quickly from the body.

Encapsulation might be a solution for these problems (Malik et al., 2017). Phages can be encapsulated in pH-responsive polymers for gastrointestinal delivery (Vinner et al., 2017) or in liposomes which, depending on the composition can be delivered in the intestine or even the lungs (Cinquerrui et al., 2018; Nieth et al., 2015). Bacteriophages can be incorporated in food packaging to extend the shelf life (García et al., 2010) or directly in an edible coating for food (Amarillas et al., 2018).

Encapsulation of bacteriophages can ensure a prolonged and constant release of phages. A mathematical model demonstrated that only maintaining a constant dose of phages at the site of infection can eradicate the pathogens and cure the patient. Too low a dose of phages, that is a common issue that usually occurs without encapsulation, is not enough to treat the infection (Malik et al., 2017).

Bacteriocins as well have been used as a food preservative and they have been integrated in films for food packaging (Balciunas et al., 2013; Drider et al., 2006; Parada et al., 2007; Sidhu and Neha, 2017). The major issue of their therapeutic potential is that they are protease and pH sensitive. So, in this case their encapsulation and stabilization is a crucial step to deliver bacteriocins into the target site of infection (Fahim et al., 2016; Heunis et al., 2010; Yamakami et al., 2013).

3. Materials and Methods

3.1. Strains, media and buffers

The strains used were *Staphylococcus aureus* (ATCC 19685) and *Escherichia coli* (ATCC 11303) and their respective bacteriophages, K (ATCC 1985-B1) and T3 (ATCC 11303-B3). Brain Heart Infusion (BHI – Oxoid) was used to grow *S. aureus* and propagate Phage K and Lysogeny Broth (LB - Fisher Scientific) was used for *E. coli* and Phage T3. Phage buffer (or SM buffer, containing 50mM of Tris-HCl to the final pH of 7.5, 100 mM NaCl, 10mM MgSO₄) was used to suspend bacteria and phages.

Continuous production of bacteriophage T3 was performed using either LB broth and a defined medium, slightly modified from a paper dealing with production of *E. coli* (Li et al., 2010) only the carbon source was changed to glucose at a working concentration 2.94 gL⁻¹ (16mM). Briefly, all the salts were prepared separately and mixed together followed by sterilization at 121°C: working concentration of KH₂PO₄ (13.3 g L⁻¹), MgSO₄ (0.59 g L⁻¹), (NH₄)₂HPO₄ (4 g L⁻¹), Citric acid (1.55 g L⁻¹), Fe(III) citrate (0.10 g L⁻¹), with added trace elements at concentrations (details provided as supplementary information, Table S1). Glucose was filtered using a 0.22 µm pore size in-line syringe filter (Millipore, USA) and added to the salt solution prior to use in order to avoid any caramelization reactions in the autoclave. All salts and chemicals were purchased from Fisher Scientific UK. Starter cultures were prepared using lysogeny broth (LB Miller, Fisher UK) and LB plates (LB broth Miller, Fisher Scientific, UK and 1.5 % Microbiological Agar, Oxoid, UK).

Complex media were used for phage stock production and for experiments of characterization of bacterial and viral activity, while synthetic medium was used only for characterization experiments.

The colicin E9 genetic sequence was integrated in the plasmid pET21a and kindly donated by Daniel Walker from University of Glasgow. Production was carried out in competent cells of *E. coli* BL21(DE3)pLysS (Promega, UK).

3.2. Bacteriophage stocks production

Production of phage stocks was performed using this protocol: the bacterial hosts, both *S. aureus* and *E. coli* were grown in BHI or LB at 37 °C until OD₆₀₀ reached ~0.2-0.3 value and then infected with bacteriophages using a multiplicity of infection (MOI) of 0.01. When the culture was clear (generally after 4-6 hours) the suspension was centrifuged 15 minutes at 4000g and the supernatant filtered through a 0.22 µm pore size filter. The resulting phage suspension was kept at 4°C until next use.

3.3. Bacterial growth curve

S. aureus was grown in BHI broth and *E. coli* in LB, using 125ml flasks in a shaking incubator at 120 rpm, at 37 °C and no extra aeration was added. The growth was followed by turbidity and CFU mL⁻¹ count. 50 mL of fresh broth were inoculated with an overnight culture of *S. aureus* or *E. coli* previously grown and the growth was monitored until the stationary phase was reached. The volume for the inoculation is calculated starting from the OD₆₀₀ of the overnight culture, to start from an OD₆₀₀ of 0.05. It ranged from 1 to 2 mL depending on the OD₆₀₀ of the overnight culture. The moment of the inoculum was the T₀ and samples were collected every 30 minutes and the OD₆₀₀ was checked and spot test performed until the OD₆₀₀ showed the same value for three times consecutively.

3.4. Bacteriophage characterization

3.4.1. Viable phages particle and bacterial cells enumeration

The titre was determined by plaque assay (Adams, 1959). The result was expressed in plaque forming units per mL (PFU mL⁻¹). Briefly, the phage suspension was serially diluted down to 10⁻⁸ in SM buffer and 10 µL of the dilution was spotted onto a lawn of host bacteria in soft agar (made of BHI or LB and 0.8% w/v agar). Each dilution was spotted 4 times and counted, and the result reported is the mean ± SD.

Bacterial growth was monitored by turbidity, using a spectrophotometer at 600 nm and counting the colony forming units per millilitre (CFU mL⁻¹) using the spot test. Briefly, at any time it was required, 1.5 mL of bacterial culture were sampled and 1mL was aliquoted in 1 cm path length plastic cuvette (Sarstedt, UK) and the rest was serially diluted down to 10⁻⁸ in SM buffer and 10 µL of each dilution was spotted on top of a Petri dish. Both bacteria and phage plates were incubated overnight at 37°C and colonies or plaques were counted after 16 h of incubation. Each measurement of plaque assay or cell viability was conducted in triplicate (technical repeat) and the values presented are the average values from the spot tests ± SD.

3.4.2. Phages one-step growth experiment

The one-step experiment allowed to analyse the life cycle of the phages (Clokic and Kropinski, 2009). Since the replication of the phages ends with the burst of a bacterial cell and the release of new virions,

the shape of the curve will look like a step, hence this name. The one-step experiment was performed during continuous production of phage T3 to monitor if the phage life cycle parameters changed when the host flowed out R_1 at steady state (D_1 0.4 h^{-1} , 0.6 h^{-1} or 0.5 h^{-1}). After steady state was achieved (typically after 3-4 h), 1 mL of the bacteria was collected from R_1 and after being infected with T3 at MOI 0.1 the experiment started. Phages were left to adsorb for 5 minutes, then the phage and bacteria mixture were centrifuged for 2 minutes at $10000 \times g$, the supernatant discarded, and the pellet was resuspended in 1 mL SM buffer. This step was repeated twice to remove all the unadsorbed phages. The infected bacteria were then diluted in 9 mL of spent nutrient broth previously taken from outlet of R_1 and filtered from bacteria to maintain the same growing conditions of bacteria. Samples were then taken every 10 minutes, diluted and spotted using the double layer method. A graph of the results is in the supplementary results chapter.

3.4.3. Phages adsorption experiment

Adsorption experiment was performed during continuous production of T3 to monitor the adsorption kinetics of phage T3 at determined physiological states of the host *E. coli*. The experiment was performed as described in “Bacteriophages, methods and protocols” (Clokie and Kropinski, 2009). Bacteria flowing out the first reactor (R_1) (at Dilution rate $D_1 = 0.4 \text{ h}^{-1}$, 0.5 h^{-1} or 0.6 h^{-1}) were infected with T3 at MOI 0.1 to assess the adsorption rate. Briefly, before the infection, 950 μL of medium was aliquoted in 1.5 mL tubes and few drops of chloroform were added to each tube. After the infection 50 μL of sample were collected every minute for 10 minutes and added to the tubes and vortexed for 30 seconds. Samples were diluted and spotted using double layer method. Graph of the results is in the supplementary results chapter.

3.4.4. Quantification of phage concentrations and UV reading

An Epoch plate reader was used together with a Take3 plate (both from BioTek Instruments, Inc., US) to measure the samples absorbance at 260 and 280 nm. 2 μL of sample was spotted on the plate and measured after alignment of the plate. All the measures were duplicated to ensure reproducibility of the method. Gen5 software was used to collect and analyse data.

3.4.5. Transmission electron microscopy

Cryo-TEM has been used to take images of Phage K before and after purification in the stirred cell unit. An 8 μ L aliquot of sample was spotted on a carbon coated copper grid (HC300Cu, Holey Carbon film on Copper 300 mesh, EM RESOLUTIONS) dried with filter paper and quickly dipped in a liquid mixture of ethane/propane cooled by liquid nitrogen. The sample was then kept in liquid nitrogen throughout the analysis. TEM images were taken on a JEOL 2200 TEM cryo-capable equipped with a Gatan digital imaging camera at 200 KV.

3.4.6. Phage size and distribution

A NanoSight LM10 (Malvern Instruments Ltd, UK) using nanoparticle tracking analysis (NTA) was used to determine the average size and size distribution of bacteriophages T3. NTA measurements were performed in a sample chamber equipped with a 640 nm laser to track the NPs. The optimal particle concentration ranged between 10^8 and 10^{10} PFU mL⁻¹. The sample was injected into the sample chamber using a sterile 1 mL syringe (Codan) and sample flow was maintained through the chamber until all air bubbles were removed. The temperature was monitored with a thermometer (RTD Pt100, OMEGA, UK). The software used for capturing and analysing the data was NTA 3.0 (Malvern Instruments Ltd, UK). For each sample particles were tracked over a period of 60 s and each measurement was repeated five times. The focus was set to achieve a uniform perfect spherical particle view. Before capturing the video, the camera had to be set-up to ensure all the particles in the sample were clearly visible with no more than the 20 % saturation. The single gain mode was used throughout the whole measurement process. Statistical analysis was carried out using the NTA software.

3.5. Continuous production of bacteriophages

All the experiments were conducted using a Biostat B (Sartorius Stedim Plastics GmbH) employing a 1L water cooled jacketed glass bioreactor. The host bacterium propagation reactor (R_1) working volume was 0.5 L; bacteria were grown in batch mode at 37°C for 3 hours prior to start-up of continuous operation. Calibrated peristaltic pumps (101 U/R, Watson Marlow) were used for the process. A pump was used to withdraw host bacteria containing suspension from R_1 and transfer it at a constant rate to bioreactor 2 (R_2) (Fig. 3.1). The level in R_1 was kept constant by continuously supplying fresh substrate from the substrate feed tank (volume 10 L) using a level controller actuating a peristaltic pump. This ensured the volume in R_1 was kept constant. Following attainment of steady

state in R_1 at a given dilution rate D_1 (h^{-1}) (this typically took $\sim 3\text{-}4$ hs, data not shown), R_2 was inoculated with phages at an initial inoculum of (10^8 PFU). A third pump was switched on to transfer bacteria and phages to the semi-batch reactor (R_3) acting as a holding tank to complete phage amplification (Fig. 3.1). Experimental runs were carried out at different dilution rates of R_1 and different working volumes of R_2 (information in supplementary information, chapter 9). Optical density at 600 nm was monitored at-line using a spectrophotometer (Shimadzu UV mini 1240); pH and temperature were continuously monitored with probes inside R_1 .

Dilution rates used for R_1 (D_1) were 0.1, 0.2, 0.3, 0.4, 0.5 and 0.6 h^{-1} and these were changed using a peristaltic pump that ensured flowrates between 50 and 250 mL h^{-1} . Flowrates once set were kept constant, the dilution rate of reactor 2 (R_2) was adjusted by changing the working volume of the reactor. Dilution rates tested in the second reactor were 3, 4 and 6 h^{-1} and the volume of the third reactor allowed collection of output from R_2 for periods between 5 - 10 hs.

Bacteria were aseptically sampled from the outlet flow of R_1 and phages from the outlet flow of R_2 . In R_3 samples were monitored every hour for a period of at least 4 h and then after overnight running of the process for a period of typically ~ 16 h (data not shown). CFU counts were performed using spot tests and PFU counting was performed using the double layer method.

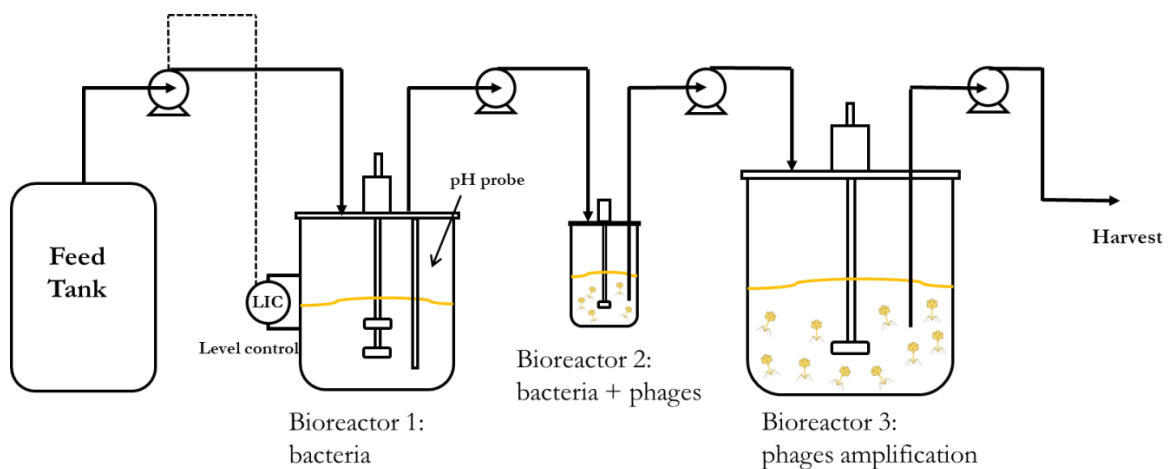


Figure 3. 1 Schematic showing layout of the continuous phage production process.

3.6. Filtration

3.6.1. Filtering unit – stirred cell, membranes and rejection experiments

Pressure driven dead end filtration experiments were conducted using a 50 mL solvent resistant stirred cell, fitting membranes of 47 mm of diameter (Millipore, cat. no. XFUF 04701, Fig. 3.2). The

membrane used for ultrafiltration (supplied by Merck Millipore UK and Alfalaval) were made of polyethersulfone (PES). The pore sizes used were 100 and 300 kDa and the membranes were characterized with rejection experiments made using dextran (PSS Polymer Service) of different molecular weight (5200, 23800, 48600, 148000, 668000 Dalton). Briefly, a solution of 2 g L⁻¹ of dextran was put in the stirred cell and 1 bar pressure applied. Permeate was collected and the concentration of the dextran was determined by measuring the refractive index (RI – Rudolph Research Analytical, US). The rejection is calculated by the formula:

$$R (\%) = 1 - (C_p/C_f) * 100 \quad (3.1)$$

where C_p and C_f are the concentrations of the permeate and the feed.

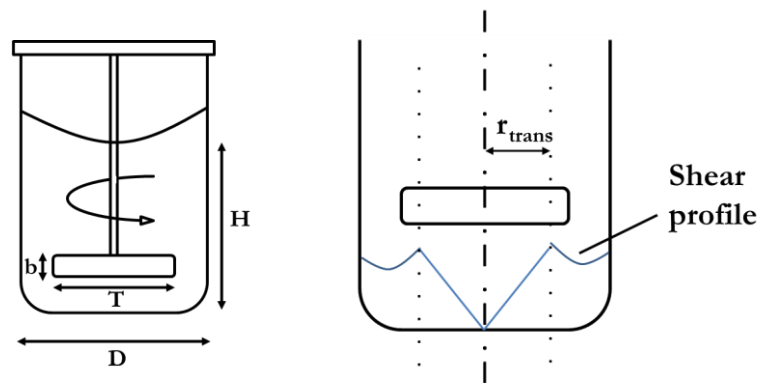


Figure 3. 2 Schematic diagram showing (a) the UF stirred cell and (b) the shear distribution in the vicinity of the stirrer. r_{trans} is the critical radius, where the shear is maximum, D is the length and b is the height of the impeller, T is the diameter of the cell.

3.6.2. Shear stress

The rotation of the impeller creates a shear inside the sample in the stirred cell. The forces inside the cell have been previously described by Kosvintsev and colleagues (Kosvintsev et al., 2005):

$$r_{trans} \frac{D}{2} 1.23 \left(0.57 + 0.35 \frac{D}{T} \right) \left(\frac{b}{T} \right)^{0.036} n_b^{0.116} \frac{Re}{1000 + 1.43Re} \quad (3.2)$$

$$\delta = \sqrt{\frac{\eta}{\rho\omega}} \quad (3.3)$$

$$\tau = 0.825 \eta \omega r \frac{1}{\delta} \quad r < r_{trans} \quad (3.4)$$

$$\tau = 0.825 \eta \omega r_{trans} \left(\frac{r_{trans}}{r} \right)^{0.6} \frac{1}{\delta} \quad r > r_{trans} \quad (3.5)$$

Where r_{trans} is the critical radius, where the shear is maximum, D is the length and b is the height of the impeller, T is the diameter of the cell, Re is the Reynolds number, η is the viscosity, τ is the torque and ω is the angular velocity. The viscosity of the medium was calculated with a Rheometer AR100-N (TA instrument, US), at 20 °C, using a cone-plate configuration.

3.6.3. Tangential flow filtration (TFF)

3.6.3.1. Batch ultrafiltration

TFF was performed with a filtration device, built by the technicians of the workshop of AACME department, that allowed to allocate an 87 cm² PES flat sheet membrane (Alfalaval, Sweden). The backpressure was constantly kept at 0.5 bar. The sample was moved by a peristaltic pump and the permeate was collected in a second tank whilst the retentate was recirculated into the feed tank (Fig. 3.3). Permeate fluxes were measured after conditioning the membrane washing it with 0.1 M NaOH for 30 minutes and then with water for 1 hour.

3.6.3.2. Diafiltration

Diafiltration was operated using the same filter and set-up for batch ultrafiltration but fresh buffer was constantly added at the same rate of permeate flow (Fig. 3.3). The volume of the feed was maintained constant by a level controller activating a peristaltic pump (101 U/R, Watson Marlow) that moved SM buffer into the tank.

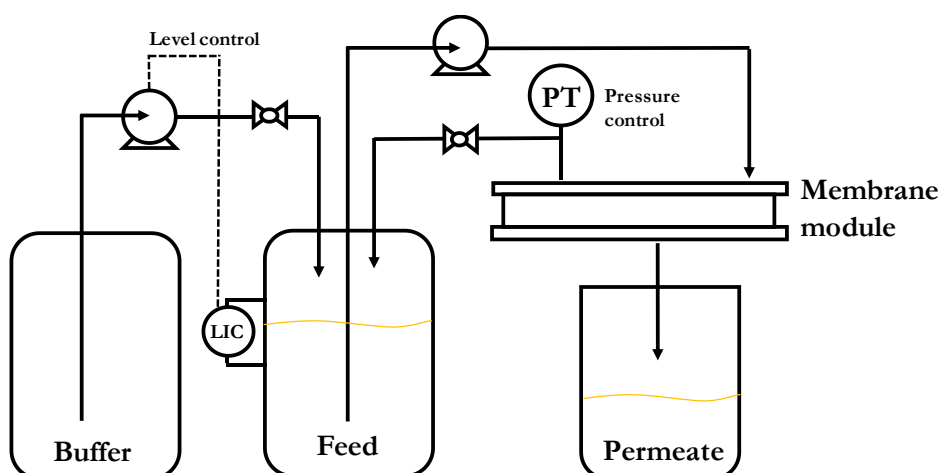


Figure 3. 3 Diagram of the filtration unit. It could be used to perform batch UF or diafiltration. In diafiltration mode a level controller activated a peristaltic pump to add fresh buffer in the feed tank at the same flowrate of feed filtration. A control valve could shut the diafiltration mode and switch to batch mode.

3.7. Removal of endotoxins

Endotoxins are only partly removed by ultrafiltration. Another method of removing lipopolysaccharide is by liquid-liquid extraction using 1-octanol as extracting solvent. It exploits the amphiphilic nature of endotoxins as they are expected to be at least partly dissolved in the octanol phase.

3.7.1. Liquid-liquid extraction using octanol

Phage T3 samples were the only involved in these experiments because they were a product of Gram-negative bacteria and they were contaminated with endotoxins released during the lysis of the cell membranes. Samples were mixed with 1-octanol (Fisher, UK) at different concentrations (ranging from 10% to 90% v/v) for 60 minutes at 300 rpm and let rest overnight at room temperature. The day after, phage samples – distributed to the bottom – were collected using a separation funnel. Alternatively, the phage suspension was added to 50% 1-octanol and mixed for 24 hours using a baffle mixer from Micropore Technologies Ltd. (Teesside, U.K.) and samples collected every hour.

Finally, the samples were purified from 1-octanol as described by Szermer-Olearnik and Boratyński (2015) by dialysing against a solution of water-ethanol 15% v/v using a 12 kDa membrane. The first wash was performed 16 hours at 40 °C and then two more washes of 4 hours each against the same buffer were performed. After this, samples were dialysed against 150 mM of NaCl to remove the ethanol: once for 16 hours and two more times for a period of 3 hours each. The amount of octanol in the samples after the dialysis was measured to be less than 100 ppm by gas chromatography.

3.7.2. Endotoxin quantification

Lipopolysaccharide (LPS) presence in T3 samples were assessed using the Pierce™ LAL Chromogenic Endotoxin Quantitation Kit (Thermo Fisher, UK) or the Limulus Amebocyte Lysate Chromogenic Endpoint Assay (Hycult Biotech, UK), following the supplier instructions. Briefly, the kit has a modified Limulus Amebocyte Lysate (LAL) which releases a proenzyme in case of presence of endotoxins: the positive sample will be coloured in yellow and the adsorption at 405 nm will be directly proportional to the amount of LPS in the sample. Serial dilutions of the samples were analysed with the kit and the final concentrations of endotoxins were extrapolated using a standard curve, as the protocol shows.

3.8. Chromatography

3.8.1. Size exclusion chromatography

A S-100 h size exclusion column (GE Healthcare) was connected to an AKTA Pure system (GE Healthcare) and used to assess the purity of the samples after the filtration step. The column was equilibrated with 20 mM Tris (Sigma-Aldrich) at pH 7.5 and 150 mM of NaCl (Thermo Fisher) and 0.5 mL of sample was injected and run in the same buffer. During the loading and the elution processes, 260 and 280 nm absorbance was constantly monitored. Albumin and lysozyme were used as standard to ensure the correct function of the column.

3.8.2. Ion exchange chromatography

The anion exchange methacrylate-based CIM QA – 1 mL (quaternary amine, BiaSeparations, Slovenia) was connected to an AKTA Pure System (GE Healthcare, UK). The buffer used for equilibrating the column and loading the sample was Tris-HCl (pH 7.5) with different concentration of NaCl (ranging from 20 mM to 100 mM). The elution buffer was Tris-HCl (pH 7.5) and NaCl concentration was increased up to 2M, with a constant gradient or stepwise. To clean the column NaOH 0.5M was used for 10 bed volumes. During the loading and the elution processes, 260 and 280 nm absorbance was constantly monitored. All the fractions coming out the loading and from the elution process of the column were titred to determinate the amount of phages (as in section 3.4.1).

3.8.3. Isothermal curves

Anion resin (Diaion PA306S) was used to study the binding capacity of Phage K and Phage T3 at pH 7. A solution of known concentration of phages filtered through 100 kDa membrane or phages from the crude lysate was added to a solution at pH 7 with 0.1 grams of resin in the chloride form (prepared following the protocol in "Ion Exchange: theory and practice" 2nd edition, C.E. Harland). After 24 hours the supernatant was titred (as in section 3.4.1) and the binding capacity of the resin was calculated.

3.9. Bacteriocin bioprocessing

3.9.1. Production

3.9.1.1. *Escherichia coli* heat shock transformation

The plasmid was transformed in competent cells of *E. coli* BL21(DE3)pLysS (Promega, UK) using thermal shock (Rahimzadeh et al., 2016). 50 ng of plasmid DNA were added to 50 μ L of competent cells and chilled on ice for 30 min, then heat-shocked at 42 °C for 60 s and cooled for 5 min in ice. 250 μ L of LB were added to the cells and they were incubated for 1 h at 30 °C, gently shaking at 100 rpm. 100 μ L of cells were then spread on LB agar plates containing 50 μ g mL⁻¹ ampicillin (Amp) and 10 μ g mL⁻¹ chloramphenicol (Cm) and incubated overnight at 37 °C in static incubator.

3.9.1.2. Test expression

A 50 mL overnight culture, in a 250 mL flask, of *E. coli* BL21(DE3 pLys)S, carrying the plasmid was prepared in LB, adding 50 μ g mL⁻¹ Amp and 10 μ g mL⁻¹ Cm. The day after fresh LB + 50 μ g mL⁻¹ Amp was inoculated 1:100 and incubated until OD₆₀₀ reached 0.6. The culture was aliquoted in six 250 mL flasks with 50 mL working volume and, after induction with IPTG, different growth conditions were monitored with constant agitation of 120 rpm: 3 hours at 37°C, 6 hours at 28°C and overnight at 25°C. Each of these conditions was tested with different final concentrations of IPTG, either 0.3 mM or 1 mM. From each flask at the end of the induction time 1 mL of sample was collected, centrifuged for 10 minutes at 10000 $\times g$ and the supernatant was discarded. The pellet was then stored at -20 °C for preparing the cells for SDS PAGE gel (described in section 3.9.2.4).

3.9.1.3. Colicin production in flasks

Colicin E9 was overexpressed from *E. coli* BL21(DE3 pLys)S carrying the plasmid. 2 litres of LB + 50 μ g mL⁻¹ Amp broth were inoculated (1:100) in 5 L flasks from an overnight culture and cells were grown at 37°C in a shaking incubator to an OD₆₀₀ = 0.6. Protein production was induced by the addition of 1.0 mM isopropyl β -D-1-thiogalactopyranoside (IPTG) and cells were grown at 37°C for a further 3 h before harvesting by centrifugation. Pellets were then kept at -20 °C until further use.

3.9.1.4. Continuous production of Colicin E9

A 1 litre reactor (Sartorius Stedim Plastics GmbH) was used to grow at 37 °C the *E. coli* with E9 plasmid, diluting 1:100 an overnight culture. The working volume was 500 mL and 50 µg mL⁻¹ Amp was added to the LB broth medium. When the OD₆₀₀ reached the value of 0.6, IPTG was added to a final concentration of 1 mM. The pump withdrawing bacteria from the reactor was activated after 3 hours setting the dilution rate D to 0.33 h⁻¹. A second pump controlled by a level controller switch and connected to a feed tank containing 10 litres of LB + 50 µg mL⁻¹ Amp + 1 mM IPTG was also activated to maintain the working volume in the reactor at 500 mL. The outlet bacteria were then harvested by centrifugation. Pellets were then stored at -20 °C until further use.

3.9.2. Purification

3.9.2.1. Quantification of colicin concentrations by double layer and UV reading

Concentrations of purified colicin E9 was assessed monitoring the activity through spot test. 10 µL of serial dilutions of the protein were spotted on top of a lawn of *E. coli* on an agar plate, let dry and incubated overnight at 37 °C in a static incubator. 2 µL of the same sample were at the same time measured at 260 and 280 nm on Take 3 plate (Biotek instruments) and the reading allowed the calculation of the concentration in mg mL⁻¹ through the Lambert-Beer law (Swinehart, 1962) ($\epsilon = 57410 \text{ M}^{-1} \text{ cm}^{-1}$; Absorbance 0.1% (=1 g/l) 0.807, assuming all pairs of Cys residues form cystines) and the 260/280 ratio allowed to confirm the purity of the sample: a value of the ratio around 0.5 would be indication of a pure protein sample. This double measurement allowed to use the spot test to know the concentration of the colicin using spot test when the protein sample was affected by other chemical components due to encapsulation.

3.9.2.2. Breakthrough curves

Colicin lysate, after sonication and filtration through 0.22 µm was loaded on a 1mL affinity column (GE Healthcare) conditioned with 20 mM Tris-HCl, 500 mM NaCl, 5 mM imidazole, pH 7.5 and the fractions (0.5 mL) collected and the sample were titred with spot test for assessing the concentration of colicin.

3.9.2.3. Affinity chromatography

Pellets were thawed and resuspended in 30 mL of 20 mM Tris-HCl, 500 mM NaCl, 5 mM imidazole, pH 7.5, and DNase and protease inhibitors (Fisher scientific, UK) were added and then lysed using an MSE Soniprep 150 (Wolf Laboratories, UK) and the cell debris separated by centrifugation (20 minutes 4000g).

The cell-free lysate was applied to a 5 mL Histrap column (GE Healthcare) conditioned with 20 mM Tris-HCl, 500 mM NaCl, 5 mM imidazole, pH 7.5, and the colicin was eluted over a 5 - 500 mM imidazole gradient using the Akta pure chromatography system (GE Healthcare, UK). Colicin containing fractions were identified by SDS-PAGE, pooled, dialysed overnight into 50 mM Tris-HCl, 200 mM NaCl, pH 7.5 and remaining contaminants removed by gel filtration chromatography on a HiPrep Sephacryl S-100 H column (GE Healthcare, UK) equilibrated in the same buffer.

3.9.2.4. SDS page

Protein lysates were run on SDS page gel to assess purity of samples during colicin production. Precast 10% SDS-PAGE gels (Mini-PROTEAN® TGX™, Biorad) were used. Samples were in reducing conditions: Laemni Buffer 4x was added to 20 µL of samples and then they were heated up to 95 °C for five minutes before loading the gel. The run was 45 minutes long, was performed using the Biorad electrophoresis cambers (Mini-PROTEAN Tetra System) and 120 V were used. Gel was stained using 50% methanol, 10% acetic acid, 0.25% Coomassie Brilliant Blue for 30 minutes, followed by three washes of destaining in 30% methanol, 10% acetic acid for at least 30 minutes.

4. Production and Purification of Colicin E9

This chapter focuses on the production and purification of the recombinant protein colicin E9. Colicin E9 is an antimicrobial protein that targets *E. coli* and this alternative to antibiotics will be soon tested in animal models (as mentioned in section 2.2.2 and 2.2.3). The goal was to set the optimization steps and parameters of upstream processing required to scale up production of colicin E9. Features considered included medium composition, temperature and length of production. A complex medium (LB broth) was compared with a fully synthetic medium (SM) to see if a chemically defined medium could ensure same concentrations of LB broth when producing colicin E9 but also improving the purification when using affinity chromatography. Small scale experiments for expression were performed and the two media were compared for protein yield in the lysates. Production was first carried out in batch mode and then in continuous steady state mode, using a chemostat configuration. Downstream purification of the protein was performed by affinity chromatography and breakthrough profiles were measured during loading in nickel affinity columns. Parameters and optimal conditions for production and purification were evaluated.

4.1. Production of colicin E9

4.1.1. Molecular biology background

Production of colicin E9 in the *E. coli* BL21(DE3)pLysS host involved the construction of a plasmid with the insertion of the genetic sequence for the expression of the colicin E9 (as mentioned in section 3.9.1.1). This insertion has an ampicillin resistance cassette for selection which has been fused in frame with the Lac operon. The Lac operon is widely used in molecular biology and its expression is controlled by presence of lactose in the medium. In the absence of lactose – which is a sugar that can be consumed by *E. coli* – in the growth medium is added Isopropyl β -D-1-thiogalactopyranoside (IPTG) which is a constant inducer as it is not consumed by *E. coli*. The host is then grown and induced with IPTG and the culture is collected and lysed to release the recombinant protein into the supernatant. Production of any recombinant proteins is influenced by many factors such as the medium used to grow the host, temperature, time and the length of induction as well as the concentration of inducer. Additionally, pH plays a major role in the final activity of the expressed protein that is active at between pH 5.5 and 7.5 and inactivated at higher pH.

4.1.2. Test expression of colicin E9 in LB and SM

Production of colicin E9 was tested (as referred in section 3.9.1.2) in growing *E. coli* BL21(DE3)pLysS in shake flasks at different conditions in different media, LB and SM: 37°C for 3 hours, 30°C for 6 hours or 30°C for 16 hours (overnight). All these conditions were tested using a working volume of 50 mL in a 250 mL flask with constant agitation of 120 rpm and inducing the culture with 1 or 0.3 mM of IPTG after the culture reached OD₆₀₀ 0.6. In this case, pH was not monitored during growth but only at the beginning and at the end of the process. Concentrations of colicin E9 in induced lysates were assessed by SDS-PAGE gels for a qualitative analysis and by spot test for a quantitative measurement of the expressed protein and the concentration equivalence is reported in the table 4.1. (as mentioned in section 3.9).

Dilution (log ₁₀)	-8	-7	-6	-5	-4	-3	-2	-1	0
Concentration	100	10	1	100	10	1	100	10	1
units	mg mL ⁻¹	mg mL ⁻¹	mg mL ⁻¹	µg mL ⁻¹	µg mL ⁻¹	µg mL ⁻¹	ng mL ⁻¹	ng mL ⁻¹	ng mL ⁻¹

Table 4.1 Dilutions and relative concentrations of colicin E9 producing a clear spot on a lawn of *E. coli*.

The best results for LB were achieved at 37°C for 3 hours with 1mM of IPTG, which yielded a concentration of colicin E9 of 1mg mL⁻¹. Using different concentrations of IPTG showed the same yield and not any improvements, as shown by SDS-PAGE gel (Fig. 4.1). Initial pH before induction was 6.5 and at the moment of collection of the lysate it was 5.8. The pH did not affect the final activity.

Induction for 6 or 16 hours in LB at 30 °C led to lower yields: after 6 hours the concentration of E9 was 100 µg mL⁻¹ and after 16 hours it was 10 µg mL⁻¹. This difference was not evident in the SDS PAGE gels (Fig. 4.1), but clearly showed during the spot tests.

Inducing *E. coli* BL21(DE3)pLysS with 0.3 or 1 mM of IPTG in synthetic medium at 30°C for 16 hours led to a yield of 1mg mL⁻¹ which was the best out of all the conditions tested for SM as confirmed by the SDS-PAGE gel (Fig. 4.1). Initial pH at the moment of induction was 6.8 and in the end of the process was ~6.

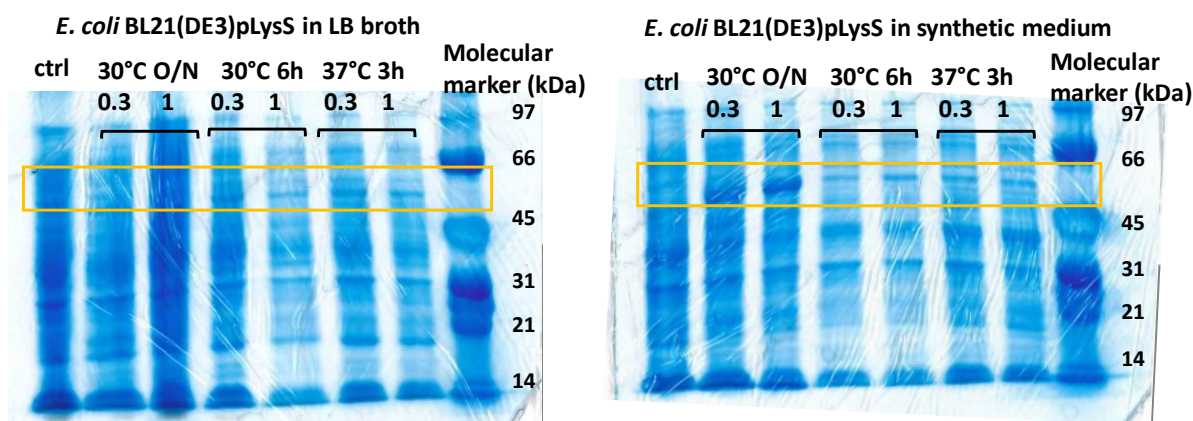


Figure 4. 1 Test expression of colicin in *E. coli* BL21(DE3)pLysS, in LB (left) and synthetic medium (right) at different conditions. In both the figures, in the far left there is the negative control (uninduced host strain) and on the right there are the lysates after induction at 30°C for 16 h and 6 h and at 37°C for 3h. The yellow rectangles show the height of the colicin and the different thickness of the band qualitatively shows that there is a difference in the final production due to the different conditions.

4.1.3. Growth curves and batch production of colicin E9 in lysates from LB and SM

Test expression conditions were used to produce colicin E9 in 1 litre bioreactors with a working volume of 0.5L and batch mode operation, without aeration. Growth of bacteria in LB was monitored every hour, from lag phase until the stationary phase when bacteria decreased their concentration. Concentration of colicin E9 was evaluated by spot test every hour. The host strain growing in LB reached Optical Density at 600 nm (OD_{600}) 0.6 in 3 hours, corresponding to $\sim 2 \times 10^8$ CFU mL^{-1} , and was induced with 1mM IPTG. After induction, OD_{600} and CFU count did not increase for the next hour but then the growth started again reaching $OD_{600} \sim 1.5$. Stationary phase was reached after 6 hours, when the OD_{600} decreased to $OD_{600} \sim 1.4$ (Fig. 4.2). Colicin E9 was produced in a basal level even before adding IPTG, at concentrations of the order of 10 ng mL^{-1} . After induction, concentration reached 1 mg mL^{-1} after 3 hours. The final concentration of colicin E9 in the lysate slightly decreased at the end of the stationary phase after 5 hours (Fig. 4.4).

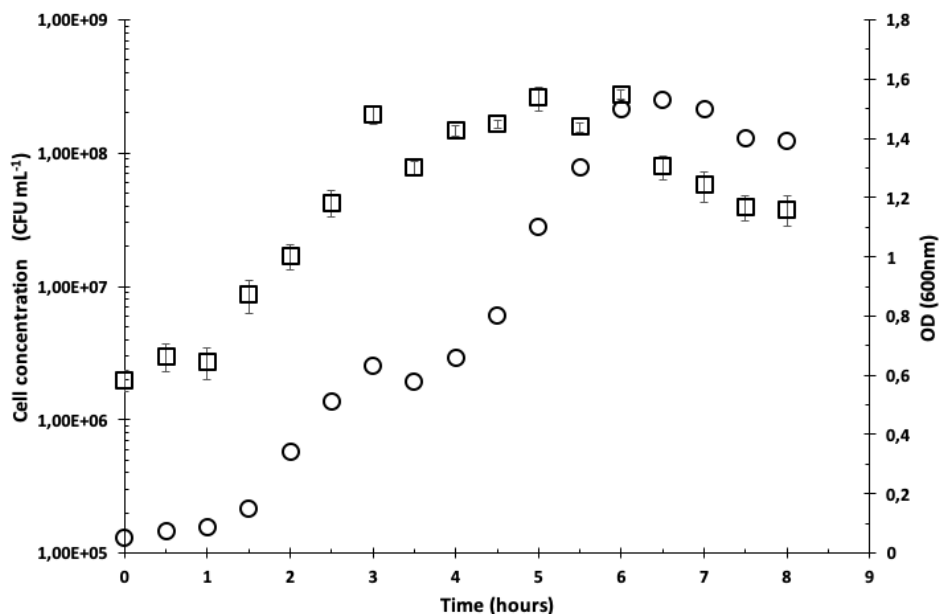


Figure 4. 2 Batch growth and colicin E9 production in LB broth. Empty squares (□) represent cell concentration (CFU mL⁻¹) ±SD (three technical repeats) and empty circles (○) represent OD₆₀₀.

Growth of *E. coli* and colicin E9 production in synthetic medium were measured every hour. After 4.5 hours bacteria reached OD₆₀₀ 0.6, corresponding to ~2x10⁸ CFU mL⁻¹, and IPTG was added to a final concentration of 1 mM. In synthetic medium as well, the CFU count did not increase for the following hour after induction, but then the growth restarted reaching OD₆₀₀ ~1.5. Stationary phase was reached after 8 hours, when the OD₆₀₀ decreased to OD₆₀₀ ~1.3. Final cell concentration was always ~1x10⁸ CFU mL⁻¹ (Fig. 4.3). Colicin E9 was produced in a basal level even before adding IPTG, at concentrations of the order of 10 ng mL⁻¹. After induction, the concentration reached 100 µg mL⁻¹ in 5 hours (Fig. 4.4) but the highest concentration of colicin E9 was measured after overnight induction, when it reached 1 mg mL⁻¹.

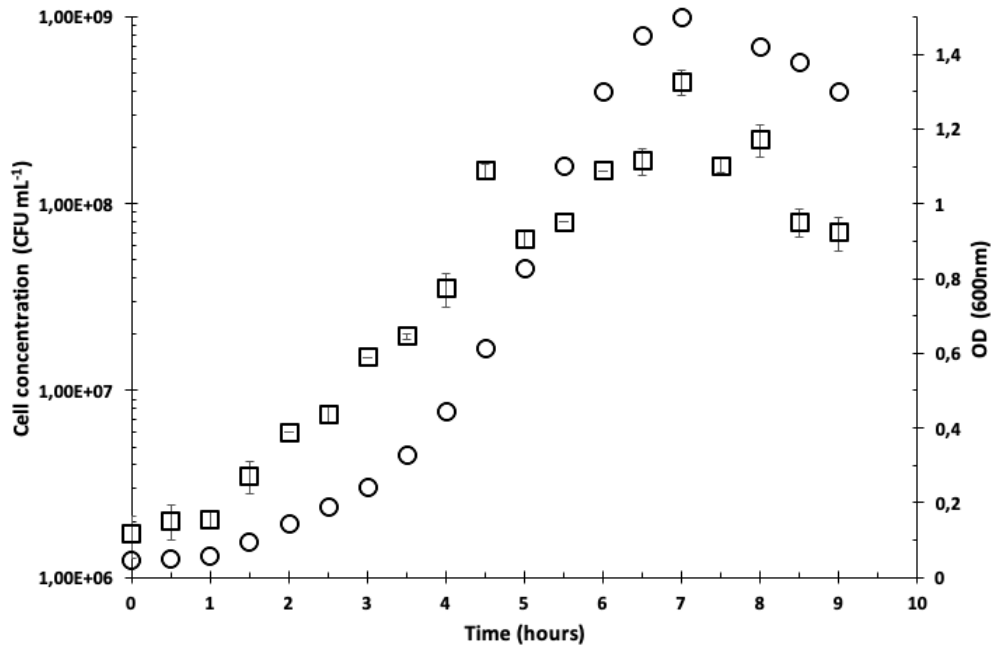


Figure 4. 3 Batch growth and colicin E9 production in SM. Empty squares (□) represent cell concentration (CFU mL⁻¹) and empty circles (○) represent OD₆₀₀. CFU concentration is the average ±SD (three technical repeats).

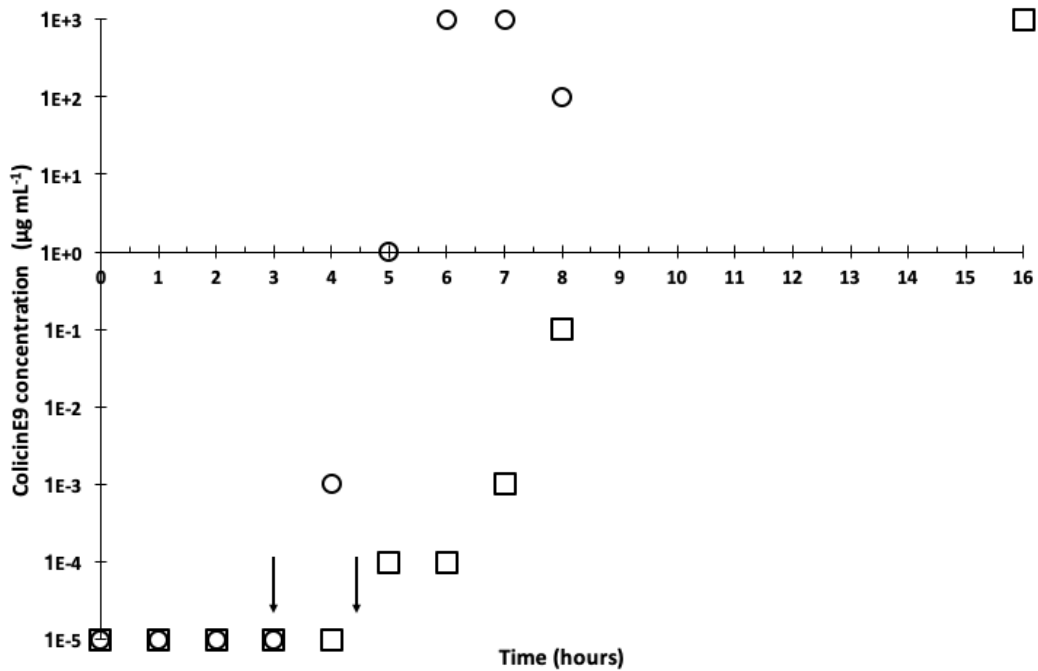


Figure 4. 4 Batch production of colicin E9 in LB (empty circles, ○) and in synthetic medium (empty squares, □). Arrows represent the moment of induction for LB (3hours) and synthetic medium (4.5 hours).

4.1.4. Continuous production of colicin E9 using chemostat mode in LB and synthetic medium

Production of colicin E9 in continuous mode was carried out using the chemostat system, where bacterial cells were maintained at steady state using the best conditions found earlier with the test expression (as mentioned in section 3.9.1.4). The best conditions for LB growth assessed in the earlier test expression experiments in shake flasks were an induction for a period of at least 3 hours with 1mM IPTG. The working volume in the bioreactor was 0.5 L; since the residence time (τ) was 3 h, the dilution rate was set at 0.33 h^{-1} and the corresponding media flowrate was then $\sim 167 \text{ mL h}^{-1}$ which corresponded to $\sim 2.8 \text{ mL min}^{-1}$. Optical density (OD_{600}) and cell concentration (CFU mL^{-1}) were sampled every hour for 8 hours and after 16 hours, pH was constantly monitored. The OD_{600} was maintained at an average value of 0.5. The cell concentration after reaching steady state was always above $1 \times 10^8 \text{ CFU mL}^{-1}$ (Fig. 4.5).

Production of colicin, as confirmed by spot testing, reached 1 mg mL^{-1} after 3 hours and remained steady during all the process (Fig. 4.7).

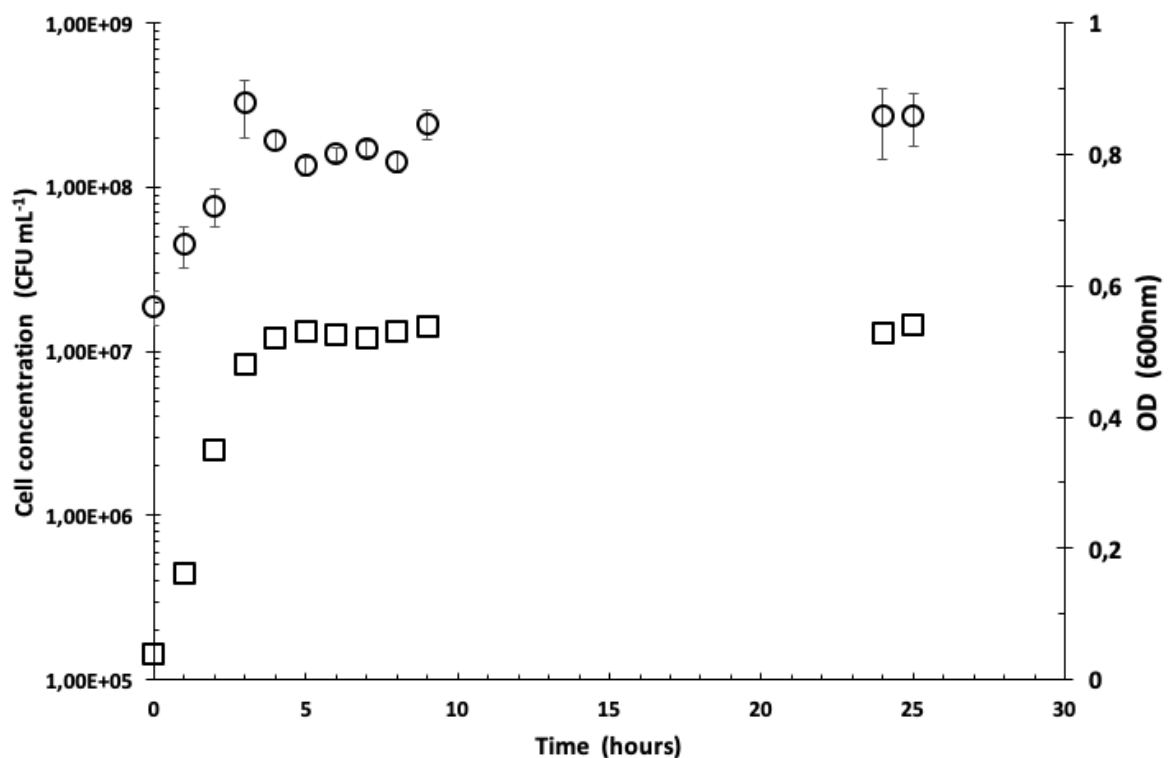


Figure 4. 5 Continuous production of colicin E9 in LB at 37°C, residence time 3 hours. The empty circles (○) represent the cell concentration and the empty squares (□) represent the OD_{600} during production. CFU concentration is the average $\pm SD$ (three technical repeats).

The best conditions assessed in the earlier test expression experiments in flasks using synthetic medium were tested using the continuous production with the chemostat process. The residence time (τ) in the reactor was 10 hours and using a 500 mL volume reactor the flowrate was 50 mL h⁻¹. *E. coli* was grown at 30°C and the OD₆₀₀ was maintained at an average value above 0.5 and the cell concentration was always above 1x10⁸ CFU mL⁻¹ (Fig. 4.6).

Production of colicin, as confirmed by spot testing, reached 1 mg mL⁻¹ only after overnight induction and was steady till the end of production (Fig. 4.7).

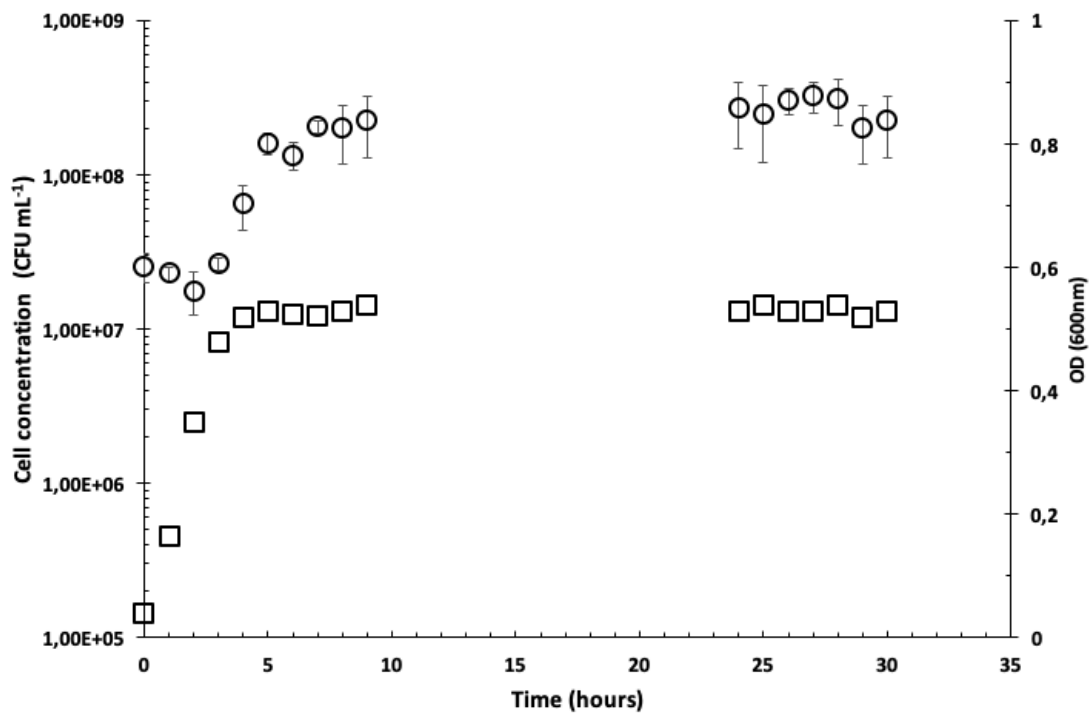


Figure 4. 6 Continuous production of colicin E9 in synthetic medium at 30°C, residence time 10 hours. The empty circles (○) represent the cell concentration (CFU mL⁻¹) and the empty squares (□) represent the OD600 during production. CFU concentration is the average \pm SD (three technical repeats).

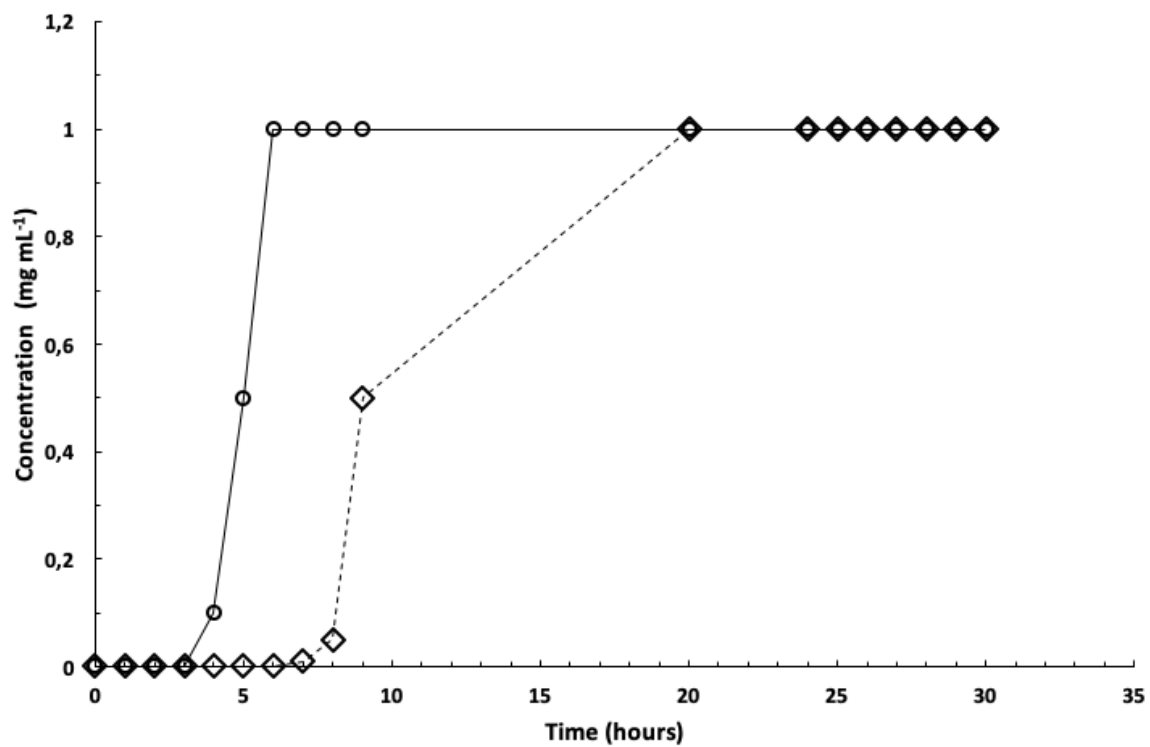


Figure 4. 7 Production of colicin E9 in LB (open circles, ○) and synthetic medium (open diamonds, ◇).

4.2. Purification of colicin E9 using nickel column

4.2.1. Difference in adsorption to nickel column of colicin produced in LB or SM

After the production of the protein and the collection of the induced host, cells were lysed, and the resulting lysate underwent further purification. The first step involved the separation of the recombinant protein from cell lysates by affinity chromatography, followed by a final polishing step of gel chromatography (as mentioned in sections 3.9.2.2 and 3.9.2.3). Isolation of colicin E9 from the lysate exploits the property of the His-tag sequence at the end of the protein that selectively binds to the nickel. Binding capacity is affected by many factors and one that can be controlled during operation is the flowrate. Breakthrough profiles of colicin E9 binding to 1mL nickel column were measured. The differences of adsorption of colicin E9 into nickel columns from lysates of LB and synthetic medium were tested. Different flowrates were tested, and the breakthrough curves measured.

The first flowrate tested using E9 from LB lysate was $0.167 \text{ mL min}^{-1}$, corresponding to 10 column volumes per hour (CV h^{-1}). There was total adsorption only for 0.5 mL and after that, the flow-through concentration sharply rose reaching the feed concentration after 3.5 mL. The second flowrate tested was 1 mL min^{-1} , corresponding to 60 CV h^{-1} , that was the flowrate suggested by the supplier. The adsorption was total till 0.5 mL, but then the binding was loose and the flow-through reached the feed concentration after 7 mL, forming a curve with shallow gradient (fig 4.8).

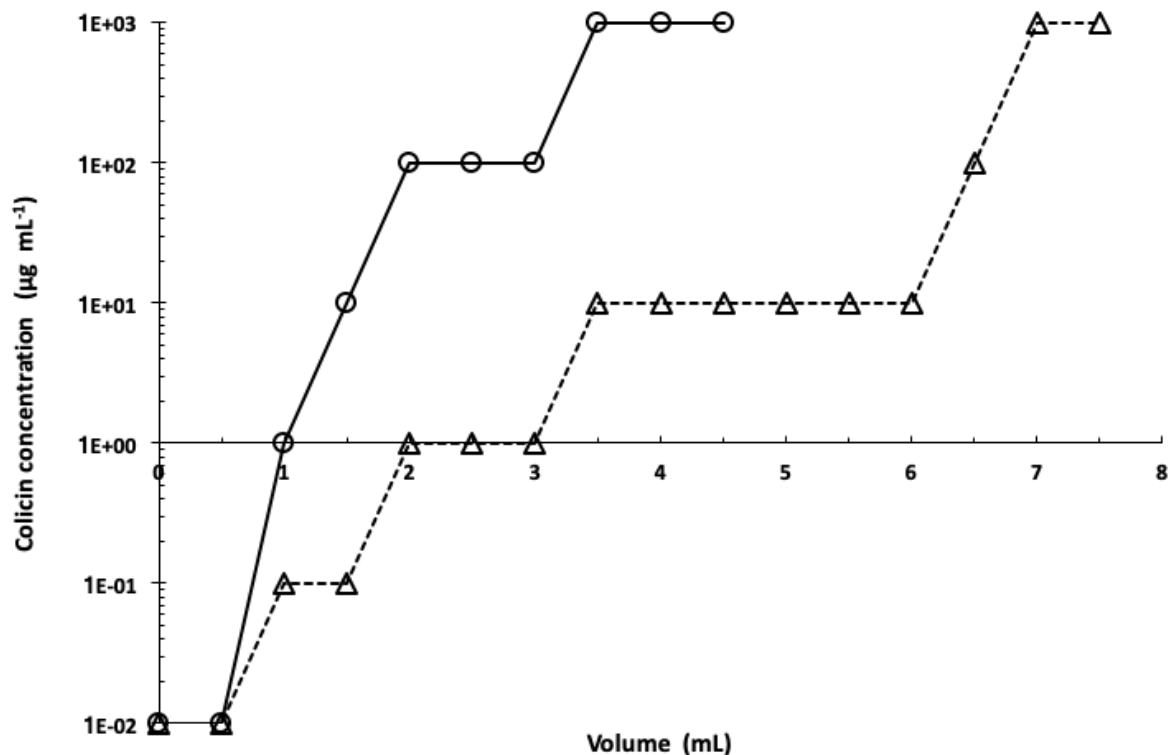


Figure 4. 8 Breakthrough curves of colicin E9 lysates from LB medium operated at 10 CV h⁻¹, empty circles and continuous line (○) and 60 CV h⁻¹, empty triangles and dashed line (Δ).

Also, for the synthetic medium lysate different flowrates were tested and the adsorption curve measured. At 1 CV h⁻¹ the adsorption was total till 1 mL and after 2.5 mL the flow-through from the column had the same concentration of the feed, showing a sharp rise of the curve. At 10 CV h⁻¹ the adsorption had more unabsorbed protein and the flow-through has the same concentration of the feed after 7mL and the curve is shallow (fig. 4.9).

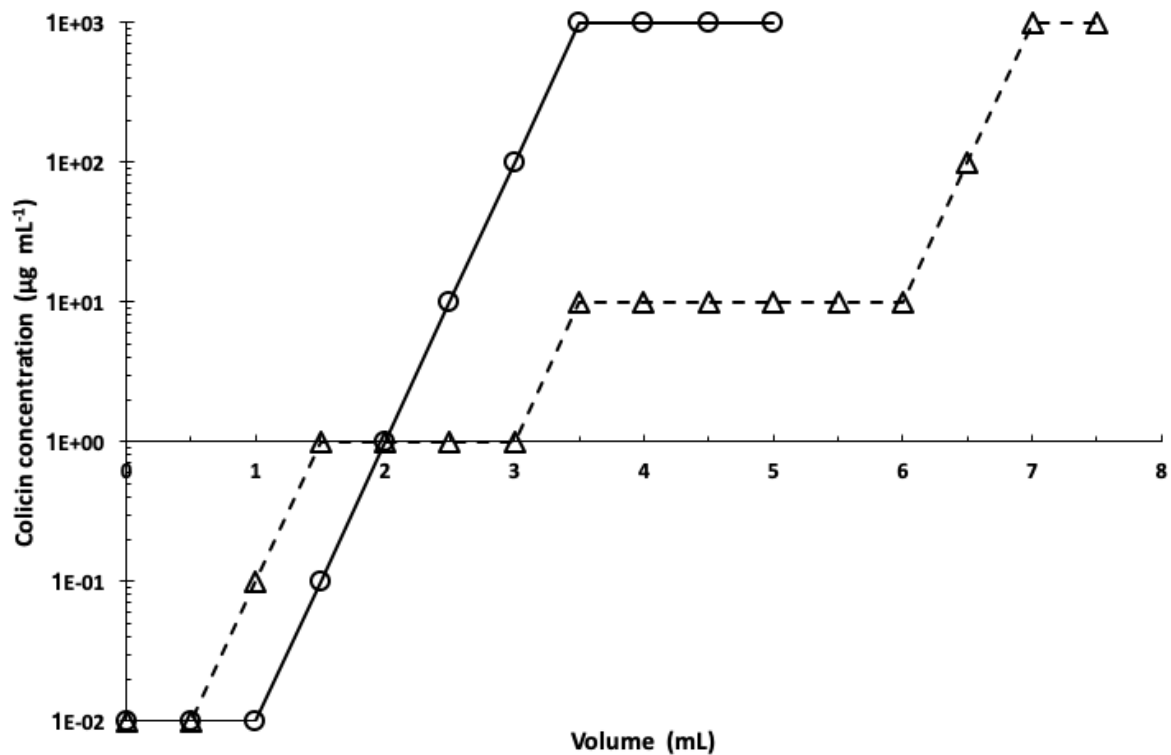


Figure 4. 9 Breakthrough curves of colicin E9 lysates from synthetic medium operated at 10 CV h^{-1} , empty circles and continuous line (○) and 60 CV h^{-1} , empty triangles and dashed line (Δ).

4.3. Discussion

Colicin E9 is a powerful bacteriocin with antimicrobial properties as it kills *E. coli* cells at very low concentrations. Its effect is visible at nanomolar range and it is a potentially interesting antimicrobial protein (Cascales et al., 2007; Gillor et al., 2004). Colicin E9 is an antimicrobial protein with a molecular weight of ~55kDa and, unlike bacteriophages, it does not replicate in the pathogen. So, it has a pharmacodynamic similar to a normal drug and it is necessary to have a high concentration in order to show therapeutic effects (Behens et al., 2017). Thus, scale up of production and purification is necessary for exploiting this therapeutic protein. This chapter dealt with optimization of parameters involved in the production of colicin E9. The goal was to find the best parameters for optimizing and increasing production and a comparison of final yields between LB broth and synthetic medium (SM) was performed.

The test expression was the first experiment to be designed, in conical shaking flasks. This showed the differences in final yield using a complex medium and a synthetic one, showed by SDS-PAGE gel filtration (Fig. 4.1) and by spot testing. *E. coli* growing in synthetic medium was slower in reaching the optimal cell concentration compared with cells growing in LB (Fig. 4.2 and 4.3). *E. coli* growing in synthetic medium had the same final protein concentration for colicin E9 compared with expression in LB, both reaching 1 mg mL^{-1} in the lysate. However, it was slower in starting the production and the synthetic medium lysate reached the concentration of 1 mg mL^{-1} after overnight induction. LB lysate reached the highest value of 1 mg mL^{-1} after 3 hours of induction and if the host was left growing longer, the final concentration dropped to $100 \text{ } \mu\text{g mL}^{-1}$, probably due to degradation of colicin E9 in the culture (Fig. 4.4). The different growth conditions, once the optimal parameters had been evaluated, were then validated in the chemostat system to achieve the best colicin production using a continuous process. One of the main parameters to control growth conditions during continuous production in the chemostat was the dilution rate. The dilution rate is the inverse of the residence time in the reactor and selecting a dilution rate allows control over the residence time. Dilution rate gives control over the growth rate of bacteria by controlling the feeding rate from the reservoir tank to the reactor (Peebo and Neubauer, 2018). For both LB and SM, the residence times were determined from previous experiments to determine conditions yielding the highest concentration of colicin E9: 3 hours for LB and 10 hours for SM. The set-up was simple, with a feed tank – where antibiotic and IPTG were added to the medium – that flowed fresh broth continuously into the reactor and a pump withdrawing induced cells at the same speed.

Again, the host growing in synthetic medium was slower than the one in LB broth to reach the ideal cell concentration - 7 hours compared to 3 hours -, to get to steady state and after adding IPTG it

needed a longer residence time to reach the same concentration of colicin. *E. coli* in LB needed only 3 hours to produce 1mg mL^{-1} of protein in steady state, while in synthetic medium it needed 10 hours, more than 3 times longer. This is an important discriminant during the production but can be improved by changing the medium composition, by adding nutrients that might boost production of colicin.

The advantage of using synthetic medium was visible during the isolation of the His-tagged protein from the lysate in a nickel column. Experiments to assess the breakthrough point were performed to see if different media would lead to different outcomes during the purification step in affinity column. The cultures were centrifuged, the pellets were then sonicated and centrifuged again. The supernatant was then collected and filtered through a $0.22\ \mu\text{m}$ filter. The samples were then ready for affinity chromatography using affinity column. The supplier instructions suggested operating at $1\ \text{mL min}^{-1}$ flowrate for $1\ \text{mL}$ nickel columns, corresponding to $60\ \text{CV h}^{-1}$. The total conditions tested were four: LB or synthetic medium at $60\ \text{column volumes per hour (CV h}^{-1})$ and $10\ \text{CV h}^{-1}$ to see if a slower flowrate could improve the adsorption of colicin E9 to the resin. As expected, LB lysates showed completely different breakthrough curves depending on the flowrates (Fig. 4.8). Defined medium lysates showed differences from LB ones: at $10\ \text{CV h}^{-1}$ it adsorbs more protein and has a higher absorption capacity (Fig. 4.9). At $60\ \text{CV h}^{-1}$ both synthetic medium and LB curves show the same trend, highlighting a low adsorption capacity at this flowrate. These experiments showed how flowrate and medium composition influence the adsorption of colicin E9 to the column.

This chapter showed results from optimization experiments indicating optimal conditions for colicin E9 production from a strain of *E. coli* BL21(DE3)pLysS using LB broth and SM. Overall LB showed faster production yields and a higher rate, but synthetic medium had better results during purification. Unfortunately, synthetic medium results are still far from results achieved using rich media like the Terrific Broth, but potentially it may be possible to increase protein expression rates by improving the medium recipe. Especially during the purification there are many parameters to control and this part is usually the bottleneck of the entire process. Future work will include measuring breakthrough curves of adsorption of colicin E9 using larger affinity column and finding the optimal recipe for synthetic medium, that could help having the same production rates of complex media and improving the overall purification process.

5. Production of Bacteriophages K and T3 in Batch and in Continuous Mode

This chapter is about production of bacteriophages K and T3, either in batch mode using shake flasks and 5 L reactors (as mentioned in section 5.2) or in continuous mode (as mentioned in section 5.3). Here are presented results of *Staphylococcus aureus* phage K and *Escherichia coli* phage T3 amplification and both hosts and phages were characterized by studying the growth curve for the bacteria and performing a one-step growth experiment for the bacteriophages (as mentioned in section 5.1). The lag phase, latent period, doubling time of bacteria, latent time and burst size of phages were measured. Phage amplification using different multiplicities of infection (MOI), i. e. the ratio of phage concentration to that of bacteria at the moment of infection, were performed and the effect of divalent salts such as ammonium sulphate and magnesium sulphate on the final titre were evaluated. These are the key parameters needed for phage production and most importantly to determine the conditions for process scaling-up for continuous production. Batch production of phage K and phage T3 were performed in shake flasks and using a 5L bioreactor. Continuous production of phage T3 was performed using a 3-stage bioreactor. The goal was to achieve high concentration of phages and comparing batch production with continuous production and evaluating the major parameters influencing phage productivity.

5.1. Life cycle parameters of bacteriophages and hosts

5.1.1. Growth curves of *S. aureus* and *E. coli*

Growth curves were obtained as described in section 3.3. Both the strains were grown at 37 °C in 250 mL shake flasks using a rotation speed of 120 rpm. The growth curve was started by diluting an overnight culture in 50 mL of fresh medium to an initial OD₆₀₀ of 0.05. 1 mL samples were collected every 30 minutes and OD₆₀₀ and CFU concentration measured. At these conditions *S. aureus* had a lag phase of 60 min, and exponential growth 90 minutes after inoculation (Fig. 5.1). This phase ended 4 h after inoculation and the cell concentration reached a plateau. The cell count showed an increase in cell concentration of ~2 log: starting from 4x10⁷ CFU mL⁻¹ and reaching ~3.4x10⁹ CFU mL⁻¹ during the stationary phase. After 4 h cell growth had stopped. There was a slight discrepancy between the data for OD₆₀₀ and measured CFU mL⁻¹ in determining when the exponential growth period came to an end by about 1.5 h. It was then possible to use the OD₆₀₀ as a surrogate indicator for exponential growth to decide when inoculating the phage for the infection.

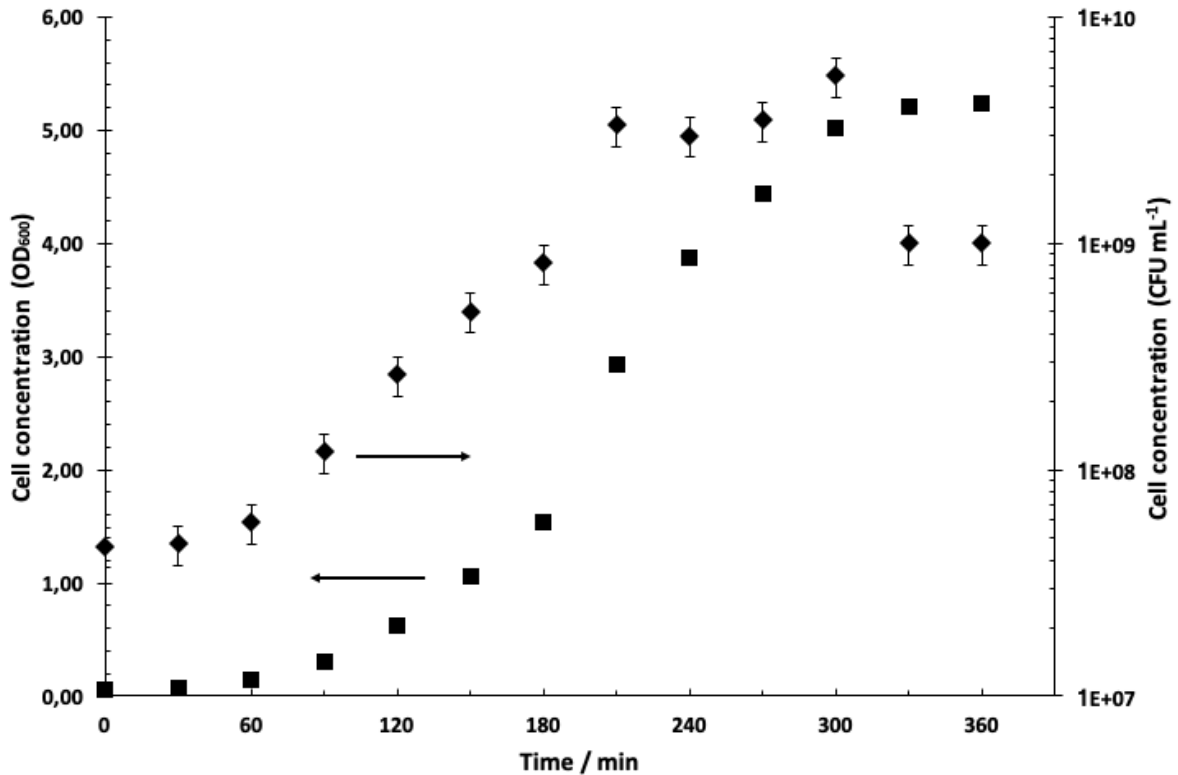


Figure 5. 1 Growth curve of *S. aureus* in BHI broth. Filled squares (■) represent the OD₆₀₀ while the filled diamonds (◆) represent the cell concentration (CFU mL⁻¹). CFU concentration is the average ± SD (three technical repeats). Measures above OD₆₀₀ 1 were repeated diluting the sample to have better accuracy.

E. coli grown in LB had a lag phase of 120 min, an exponential growth commenced 150 min following inoculation and stationary phase reached after 4.5 hours. The CFU count showed an increase in cell concentration of ~2 log: starting from 1x10⁷ CFU mL⁻¹ and reaching 3x10⁹ CFU mL⁻¹ at stationary phase.

There was a slight discrepancy between optical density measurements and CFU counts using the spot test in determining the beginning of the exponential growth phase: OD₆₀₀ measurements showed the start of the exponential growth phase between 90 and 120 min while the CFU mL⁻¹ concentration started rising only after 150 min (Fig. 5.2). Also in this case, OD₆₀₀ proved to be a good surrogate indicator of onset of exponential growth of the host and it was subsequently used for such a purpose and to decide at what point of the growth curve initiate the phage infection.

These growth curves were used as negative controls for the following experiments using bacteriophages (section 5.2).

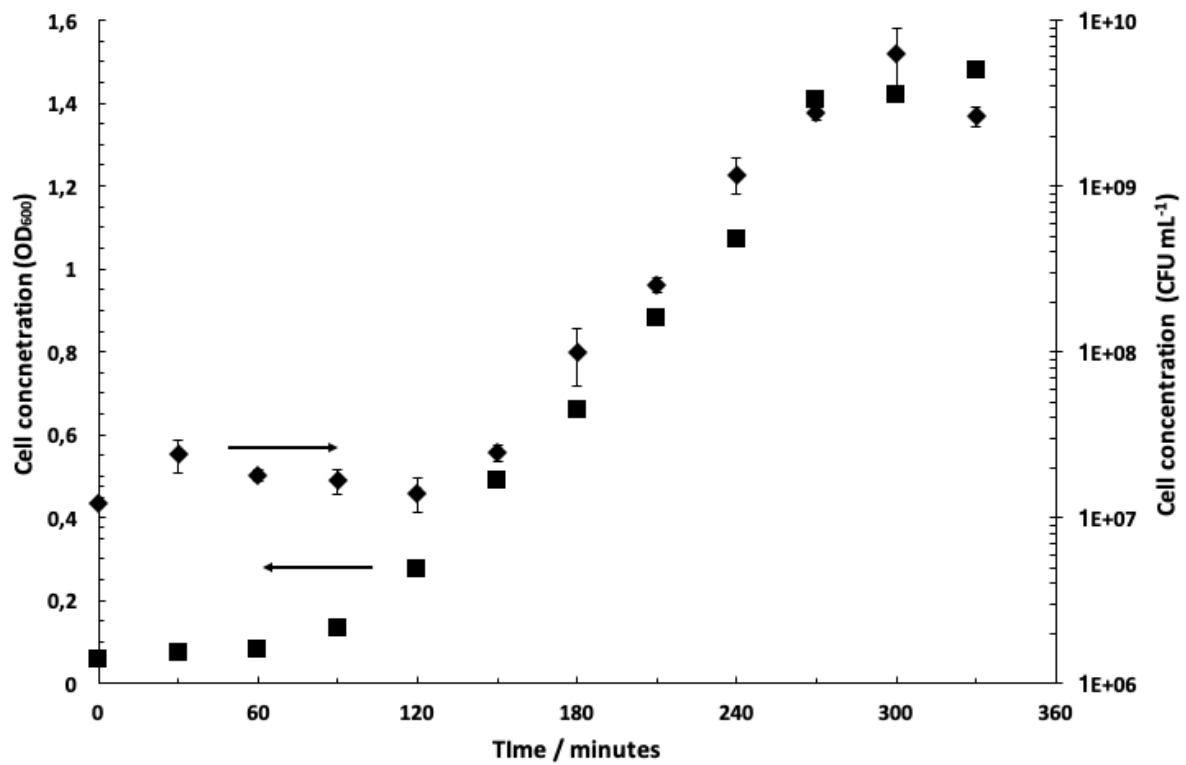


Figure 5. 2 Growth curve of *E. coli* in LB broth. Filled squares (■) represent the OD₆₀₀ while the filled diamonds (◆) represent the cell concentration (CFU mL⁻¹). CFU concentration is the average ± SD (three technical repeats). Measures above OD₆₀₀ 1 were repeated diluting the sample to have better accuracy.

5.1.2. One-step growth of Phage K and Phage T3

The one-step growth curve was determined as described in section 3.4.2 for phage K (in BHI) and for phage T3 (in LB) at 37°C. For both experiments, cells were infected by phages 10 minutes before the time zero in order to prepare the experiment. Phage K had a latency period of approximately 20 min and a rise period of 10 min, at which point when all the phages were released. The burst size was 100 ± 20 virions per infected cell (Fig. 5.3).

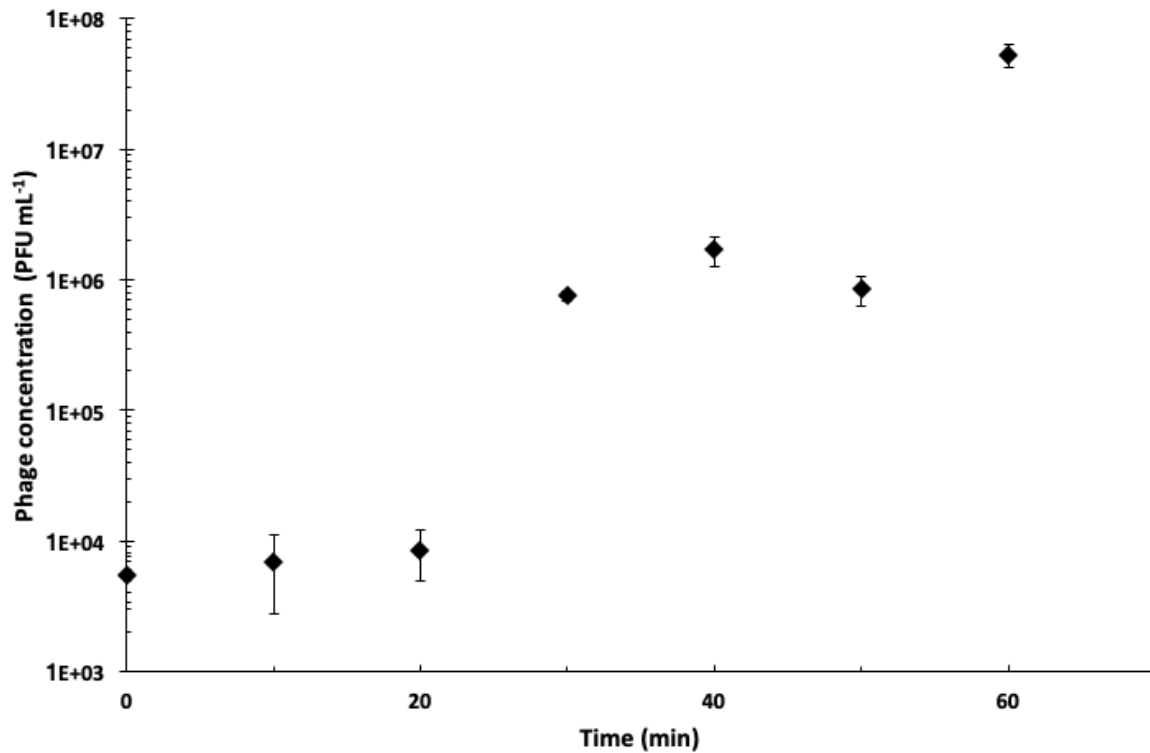


Figure 5. 3 One-step growth data for phage K grown in BHI broth at 37°C. Data are shown as mean \pm SD. PFU concentration is the average \pm SD (three technical repeats).

Phage T3 life cycle was a little quicker with a latency period of 15 minutes and here as well the infection happened 10 minutes before the time zero. The burst size was $\sim 90 \pm 20$ virions for each infected *E. coli* cell. The burst was complete in 10 minutes (Fig. 5.4).

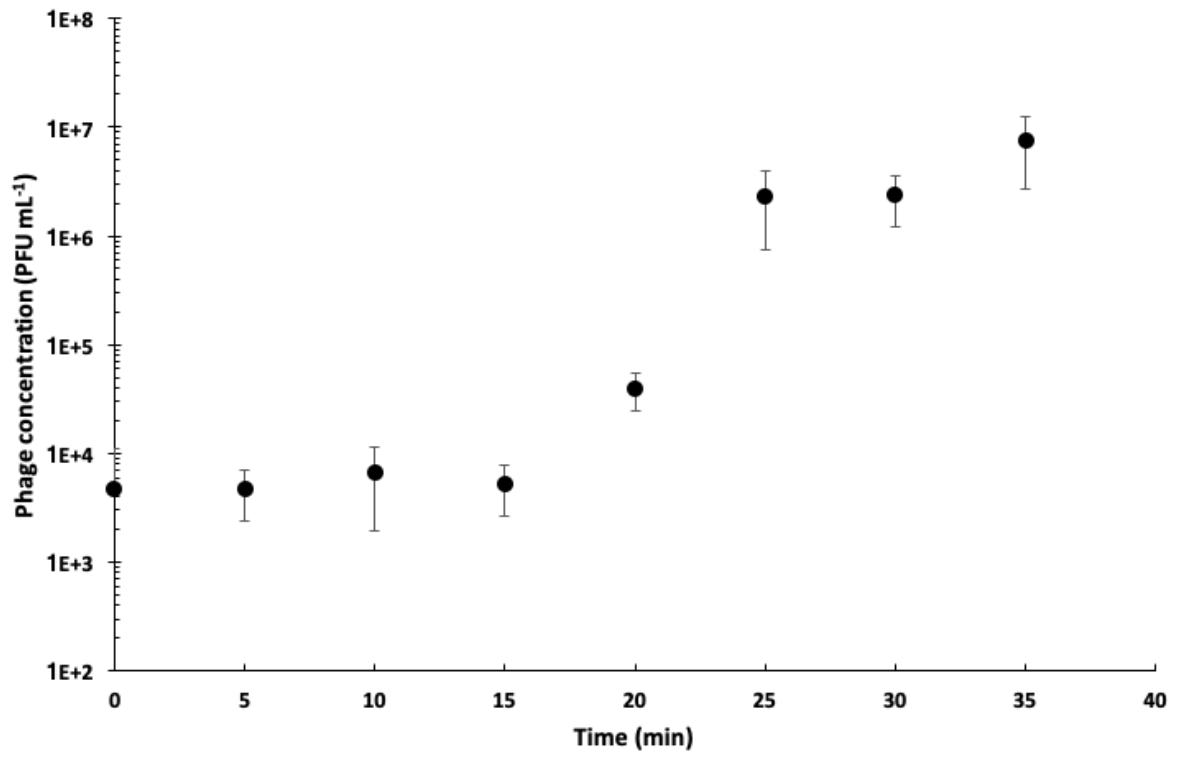


Figure 5. 4 One-step growth data for phage T3 grown in LB broth at 37°C. Data are shown as mean \pm SD. PFU concentration is the average \pm SD (three technical repeats).

5.2. Batch amplification of bacteriophages using different multiplicity of infection (MOI)

Phage K and phage T3 were produced in batch mode using a 5L bioreactor vessel using 2L working volume. Optical density for both the controls (no added phage) and the infected culture were assessed every 30 min. *S. aureus* was inoculated with phage after 90 min when the culture OD₆₀₀ was ~0.3. At this OD, the cell concentration for the control data was ~2x10⁸ CFU mL⁻¹ (Fig. 5.1). Multiplicities of infection (MOI) values used were 0.01, 0.1, 1 and 10 to assess the effect on phage amplification and which one yielded the highest concentration of bacteriophages. Infection with MOI 10 ended in less than one hour and produced less than 10⁸ PFU mL⁻¹. Infection with MOI 1 lysed all the host bacteria in 60 min after inoculation and the yield was ~5x10⁹ PFU mL⁻¹. The best results came from infections with MOI 0.01 and 0.1, which ended after 5 hours and resulted in phage concentrations of ~5x10¹⁰ PFU mL⁻¹ and ~1x10¹⁰ PFU mL⁻¹ respectively. Another infection with MOI 0.001 was made, but it was unsuccessful as it did not completely lyse the culture because phage K concentration was not high enough to take over the host cell culture and infect it before it reached the stationary phase (data not shown). All the concentrations of amplification using different MOI are summarized in table 5.1.

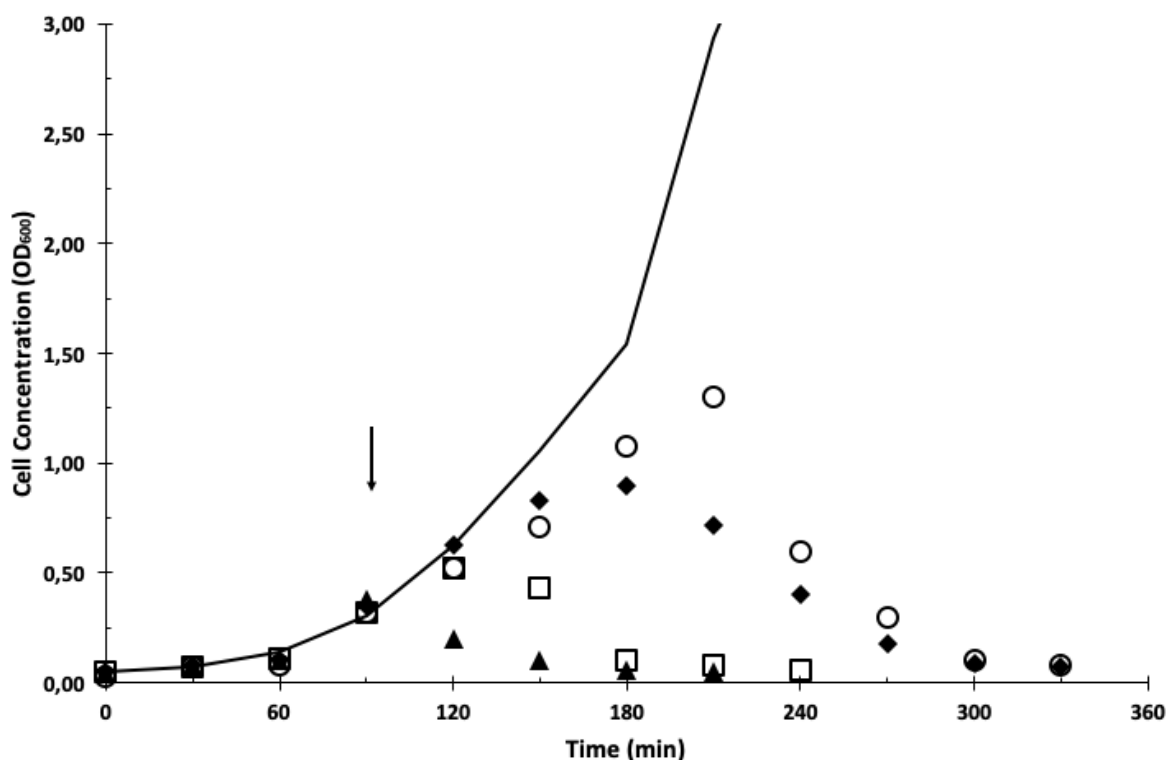


Figure 5. 5 Growth curve of *S. aureus* and amplification of phage K in BHI using different MOIs. Filled triangles (▲) represent MOI 10, empty squares (□) represent MOI 1, filled diamonds (◆) represent MOI 0.1 and empty circles (○) MOI 0.01. Black arrow represents the time of inoculum of the flask with bacteriophage to start infection. Negative control (growth curve of fig. 5.1) is the continuous line, which was cut for increasing clarity of the graph. Measures above OD₆₀₀ 1 were repeated diluting the sample to have better accuracy.

The effect of the divalent salt ammonium sulphate on the final titre was evaluated on the final titre of phage K (Clokic and Kropinski, 2009; Hotchin, 1955). The previous best conditions were repeated: phage was added to the culture at a MOI of 0.01 after 90 minutes and a final concentration of 2% ammonium sulphate was added. OD₆₀₀ reached ~1.6 (corresponding to ~1x10⁹ CFU mL⁻¹) before starting to slow the growth and it falling to values below 0.1 after a total time of 6 hours. Phage K was collected, filtered and titred and the final concentration reached the highest titre with phage K, always at least 1x10¹¹ PFU mL⁻¹(Fig. 5.6). Adding ammonium sulphate allowed growth for a longer period of time: the OD₆₀₀ without the salt rose up to ~1.2 and with ammonium sulphate rose up to ~1.6, hence more host cells were infected and lysed. Final titres are showed in table 5.1.

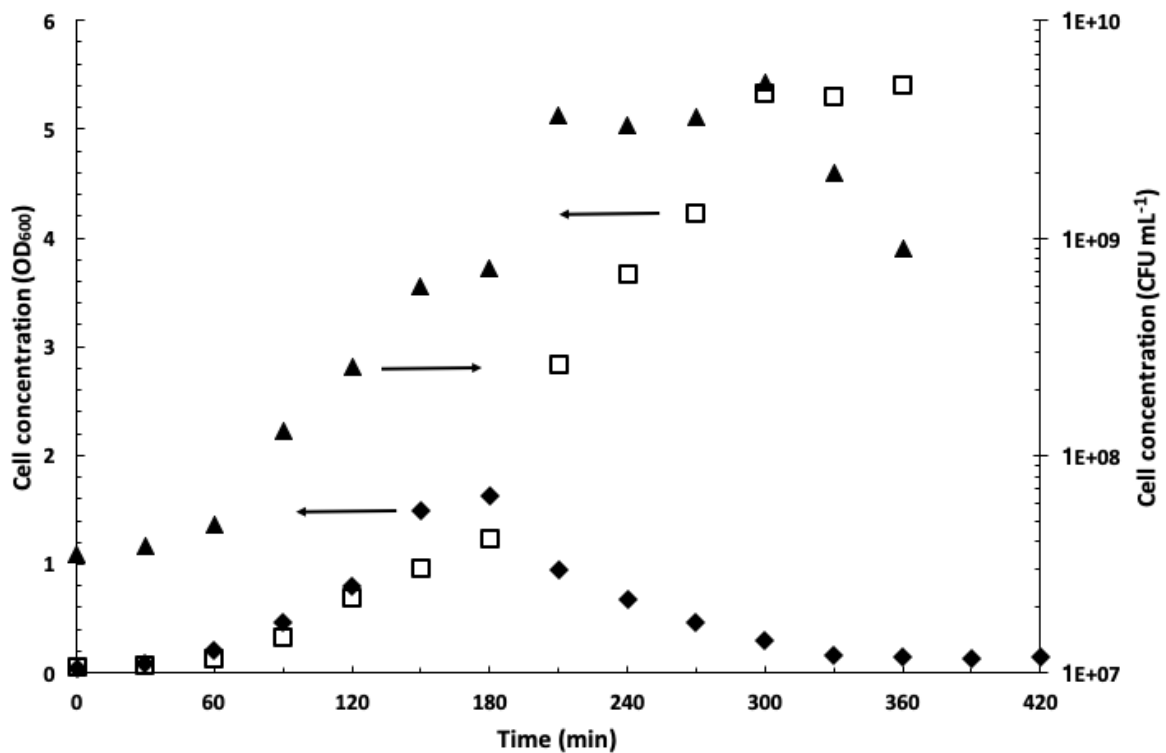


Figure 5. 6 Growth curve of *S. aureus* and amplification of phage K in BHI adding 2% ammonium sulphate, using a bioreactor with 2L working volume. MOI of infection was 0.01. Filled triangles (▲) represent cell concentration in CFU mL⁻¹, empty squares (□) represent OD₆₀₀ of control *S. aureus* and filled diamonds (◆) represent OD₆₀₀ of phage K amplification. Measures above OD₆₀₀ 1 were repeated diluting the sample to have better accuracy.

MOI	FINAL TITRE (PFU mL ⁻¹)
10	1x10 ⁸
1	5 x10 ⁹
0.1	1 x10 ¹⁰
0.01	5 x10 ¹⁰
0.001	n/a
0.01 + Ammonium sulphate	1 x10 ¹¹

Table 5.1 Summary of titres of Phage K using different Multiplicities of infection.

E. coli was infected when it got to OD₆₀₀ ~0.4 by phage T3 at different MOI 0.01, 0.1, 1 and 10. Host cultures infected by T3 phage showed different lysis time and different final phage concentrations. At MOI 10 the culture was cleared in 30 min and the final yield was ~5x10⁹ PFU mL⁻¹. At MOI 1 the culture was lysed in 90 min and the concentration of phage T3 after recovery was 1x10¹⁰ PFU mL⁻¹. MOI 0.1 took ~3 h to complete amplification of phages and the phage concentration increased further by 1 log, increasing to 1x10¹¹ PFU mL⁻¹. Infection with MOI 0.01 gave the best results despite taking ~3 h to lyse the culture, the final phage concentration was ~1x10¹¹ PFU mL⁻¹. Phage T3 is an effective lytic phage, it managed to lyse the cultures even at low MOI (even at MOI as low as 10⁻⁶) and yielding always ~1x10¹¹ PFU mL⁻¹ (Fig. 5.10). The effect of magnesium sulphate on phage T3 amplification was evaluated. The lysis time was no different to previous experiments, ~3 hours, but the final yield was the highest, ~2x10¹¹ PFU mL⁻¹ (data not shown).

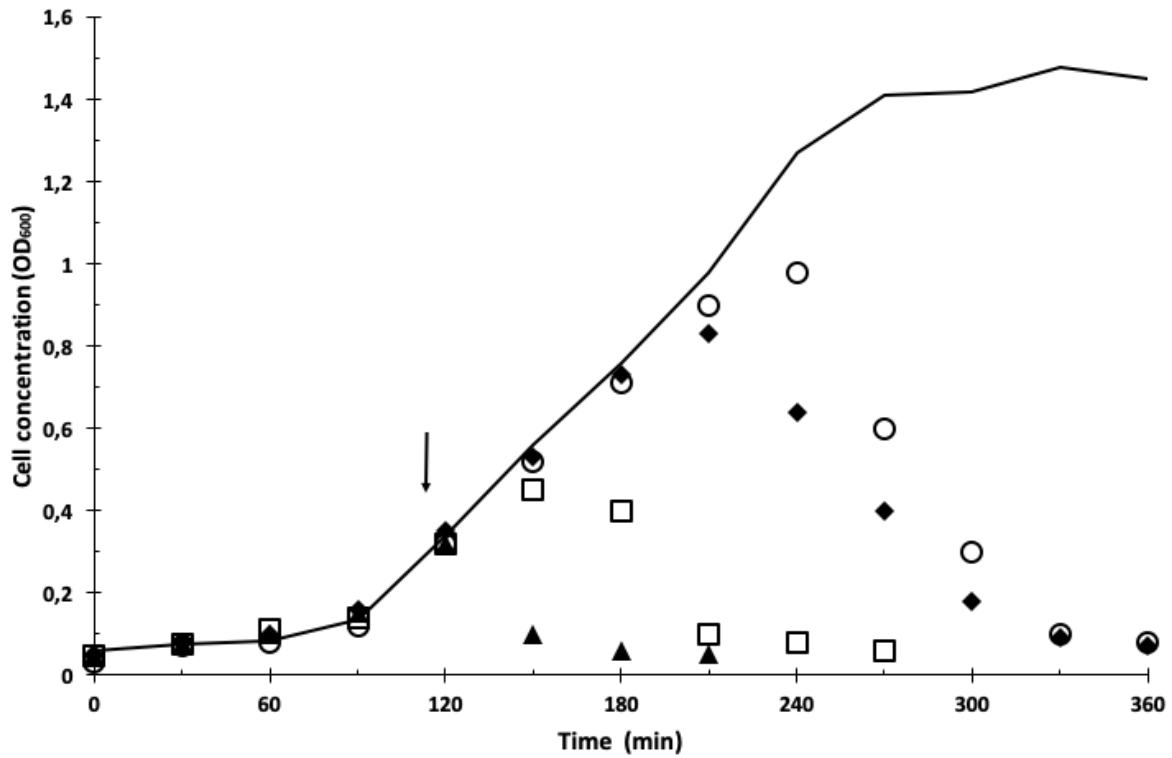


Figure 5. 7 Growth curve of *E. coli* and amplification of phage T3 in LB using different MOIs. The line represents negative control (growth curve showed in fig. 5.2), filled triangles (▲) represent MOI 10, empty squares (□) represent MOI 1, filled diamonds (◆) represent MOI 0.1 and empty circles (○) MOI 0.01. Black arrow represents the time of inoculation of flask with phage to start infection. Measures above $OD_{600} 1$ were repeated diluting the sample to have better accuracy.

MOI	FINAL TITRE (PFU mL ⁻¹)
10	5×10^9
1	1×10^{10}
0.1	1×10^{11}
0.01	1×10^{11}
0.01 + Magnesium sulphate	2×10^{11}

Table 5.2 Summary of titres of Phage T3 using different Multiplicities of infection

5.3. Continuous production of bacteriophage T3 using synthetic medium (SM)

Phage amplification in continuous mode has previously been evaluated in literature, however a well-defined synthetic medium and a process employing 3 reactors in series for production is novel. *E. coli* and T3 were chosen as model host and phage for the experiments. Continuous production of phages using 3 reactors in series allowed the decoupling of host growth and phage infection and amplification,

carried in individual reactors. The intermediate reactor was used for host-phage mixing and infection, whereas the final reactor operated in semi-batch mode or batch mode allowed completion of the phage amplification kinetics.

5.3.1. Characterization of *E. coli* and phage T3 growth in SM

Before performing the continuous production of the host in the new defined medium, the growth curve in shake flasks was performed to assess life cycle parameters in the new medium. The lag time of *E. coli* was 120 min and the logarithmic growth lasted 120 min and in total it took 4 h to reach the plateau. The cell concentration increased by ~2 log as the culture started from $\sim 10^7$ CFU mL⁻¹ during lag phase and reached $\sim 7 \times 10^8$ CFU mL⁻¹ at stationary phase. In this case as well, the optical density measurements were a reliable indication of the start of the exponential growth phase, but differences were observed for the start of the stationary phase. The OD₆₀₀ was ~1 after 3.5 h and kept rising till ~2 at 5.5 h, while the cell concentration remained stable to $\sim 6 \pm 2 \times 10^8$ CFU mL⁻¹ from 3.5 to 5.5 h (Fig. 5.8). Compared with growth in LB broth, here *E. coli* showed the same lag phase duration of 120 min but a faster growth, confirmed by the steeper growth curve. The stationary phase arrived late as well – 5.5 h compared 4.5 h with LB. The maximum cell concentration was lower than LB; the highest value for synthetic medium was $\sim 7 \times 10^8$ CFU mL⁻¹ while in LB the highest value was $\sim 5 \times 10^9$ CFU mL⁻¹.

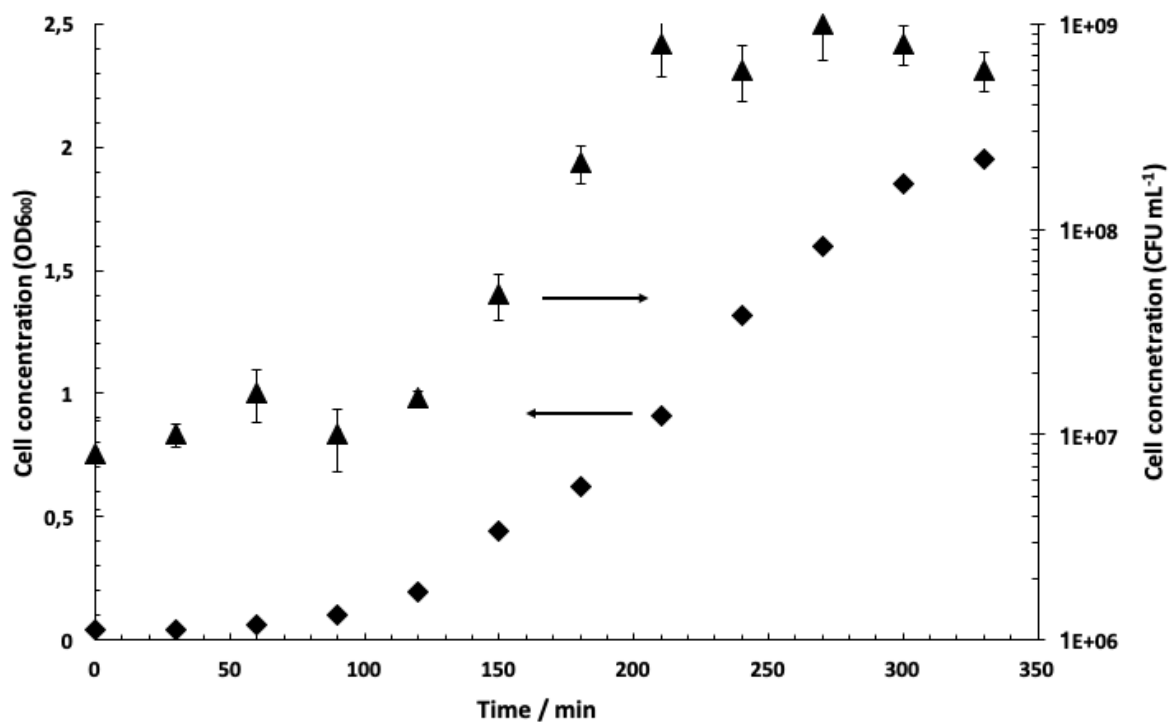


Figure 5. 8 Growth curve of *E. coli* in synthetic medium. Filled diamonds (◆) represent OD_{600} and filled triangles (▲) represent cell count ($CFU\ mL^{-1}$). Measures above $OD_{600}\ 1$ were repeated diluting the sample to have better accuracy. CFU concentration is the average \pm SD (three technical repeats).

The one-step growth experiment in synthetic medium showed a latency time of ~ 20 min and a slow release of virions during the rise period of 60 minutes. The burst was higher than in LB: ~ 700 virions per infected cell (Fig. 5.9).

Comparing synthetic medium data for the one-step growth with LB broth, the latency time was quite similar – 15 min in LB and 20 min in synthetic medium – but the release profile was very different: in LB all the virions were released in 10 min while in synthetic medium it took 60 min. This difference in time correlated with the measured burst size: ~ 100 phages per cell in LB and ~ 700 per cell in synthetic medium. Although still in the range of possible (in literature there are reports of burst sizes of 1000 virions per cell), the burst size of phage T3 in SM looked too high to be an actual number. It may be possible that the final number is the result of overlapping burst cycles in play.

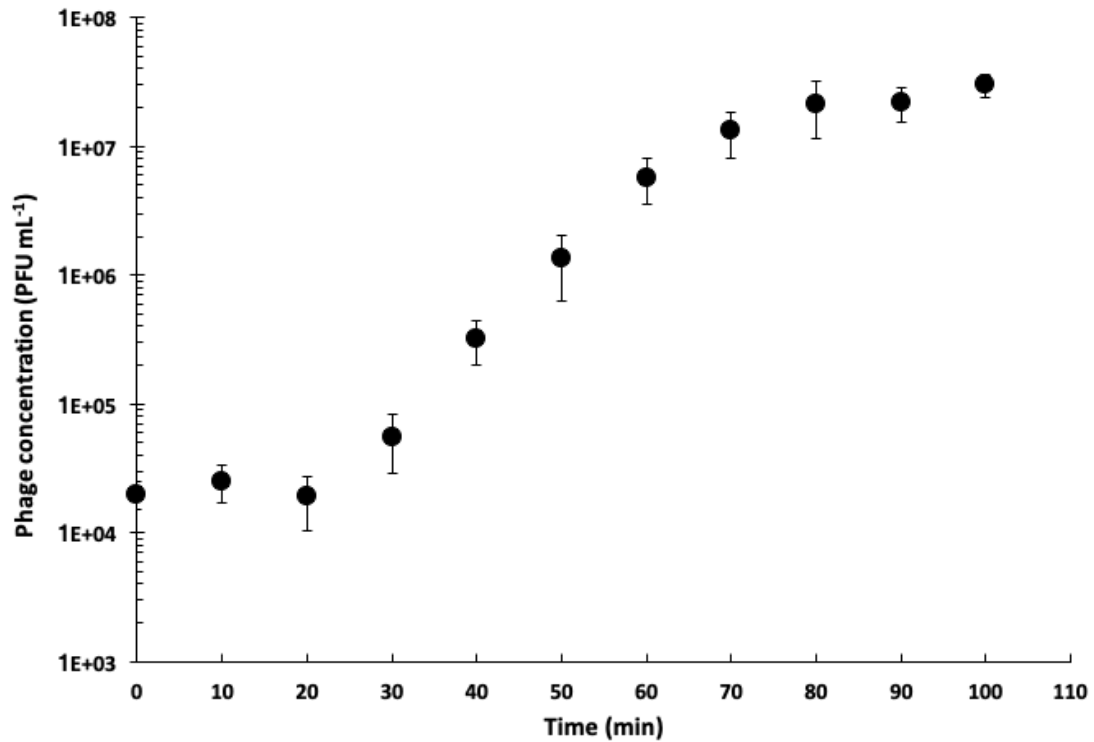


Figure 5.9 One-step growth data for phage T3 grown in synthetic medium. PFU concentration is the average \pm SD (three technical repeats).

5.3.1.1. Effect of different MOI on phage T3 titres in LB and Synthetic medium

Characterization of the effect of the MOI on the final concentration of T3 was performed for synthetic medium too. Here as well T3 phages could replicate even at a very low MOI and the final phage concentration was $\sim 1 \times 10^{10}$ PFU mL⁻¹ at MOI ranging from 10^{-1} to 10^{-6} (Fig. 5.10). This experiment shows the “infectivity working range” of phage T3 in the second reactor (see below). Despite the higher burst size in synthetic medium, the titres of phage T3 produced in synthetic medium are lower than those in LB and this could be because the moment of infection did not coincide with the best physiological of the host to get to a higher titre.

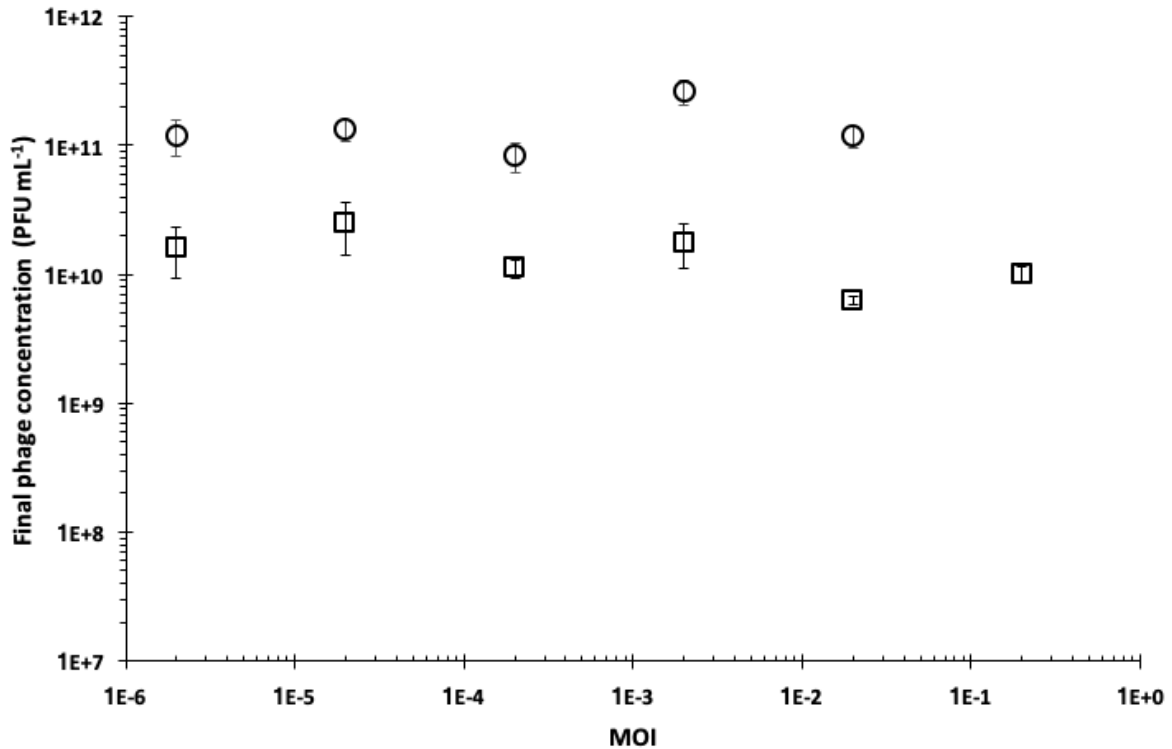


Figure 5.10 Final concentration of phage T3 after infection using different MOI in shake flasks. Empty circles (○) represent amplification in LB and empty squares (□) represent amplification in synthetic medium. PFU concentration is the average \pm SD (three technical repeats).

5.3.2. Continuous production of phage T3 using 3 reactor stages: Reactor 1 (R₁) and growth of the host culture

The host strain *E. coli* was grown at steady state in the reactor 1 (R₁) using different dilution rates (D₁) (as mentioned in section 3.5). Cell concentration and productivity of R₁ in relation to D₁ are reported in Fig. 5.11. Low dilution rates, corresponding to longer residence times, yielded the highest cell concentrations, specifically $\sim 2 \times 10^8$ CFU mL⁻¹ at D₁=0.1, $\sim 4 \times 10^8$ CFU mL⁻¹ at D₁=0.2 h⁻¹ and $\sim 1 \times 10^8$ CFU mL⁻¹ at D₁=0.3 h⁻¹. Higher dilution rates, corresponding to shorter residence times, yielded consistently lower cell concentrations. D₁= 0.4 h⁻¹, which corresponds to a residence time of 2.5 h produced $\sim 1 \times 10^7$ CFU mL⁻¹, D₁=0.5 h⁻¹ – residence time of 2 h – produced $\sim 5 \times 10^6$ CFU mL⁻¹ and finally D₁=0.6 h⁻¹, with a residence time of 100 minutes, produced 1×10^6 CFU mL⁻¹ (Fig. 5.11).

The productivity of the reactor is the number of cells produced per hour per unit volume, productivity is the product of dilution rate and cell concentration.

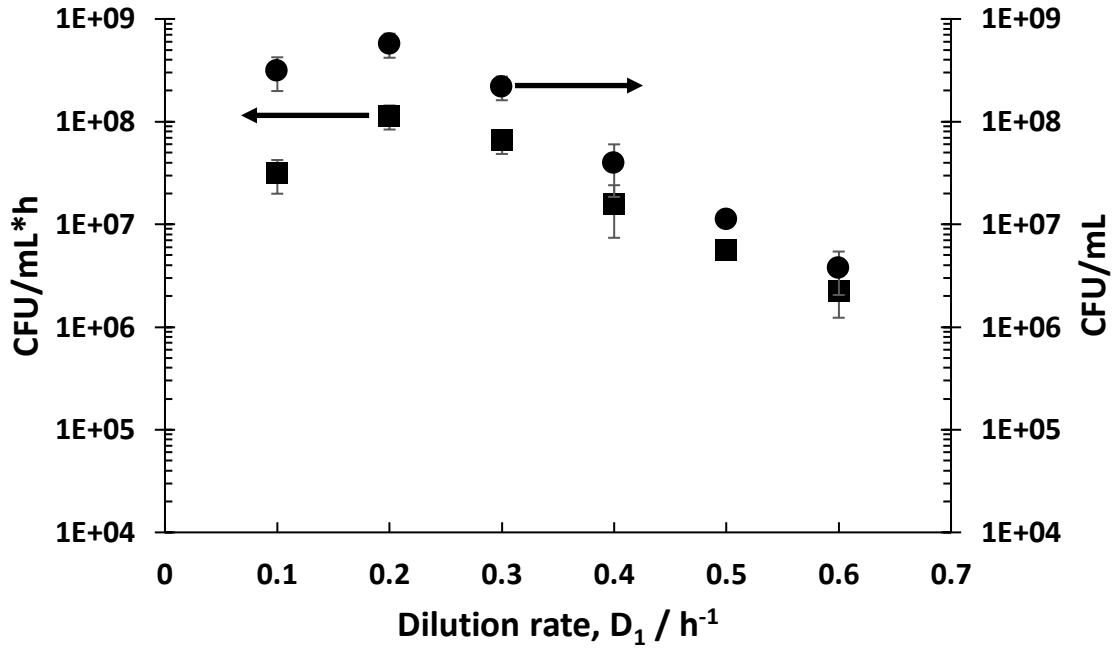


Figure 5. 11 Host bacterial cell productivity in reactor 1 (R1), as a function of different dilution rates in R1, filled squares (■). Concentration of host bacterial cells in R1, filled circles (●). Error bars represent one standard deviation. CFU concentration is the average \pm SD (three technical repeats) after steady state was achieved.

In the synthetic medium, glucose was the only carbon source, and this was monitored. The amount of sugar consumed depended on the residence time in the reactor, so it was dependent on the D_1 . For $D_1=0.1, 0.2$ and $0.3 h^{-1}$ the glucose was completely used-up by the bacteria and the glucose conversion was between 98 and 99%. Glucose conversion decreased by increasing D_1 : it was 60% at $D_1=0.4 h^{-1}$, 43% at $D_1=0.5 h^{-1}$ and 14% at $D_1=0.6 h^{-1}$ (Fig. 5.12).

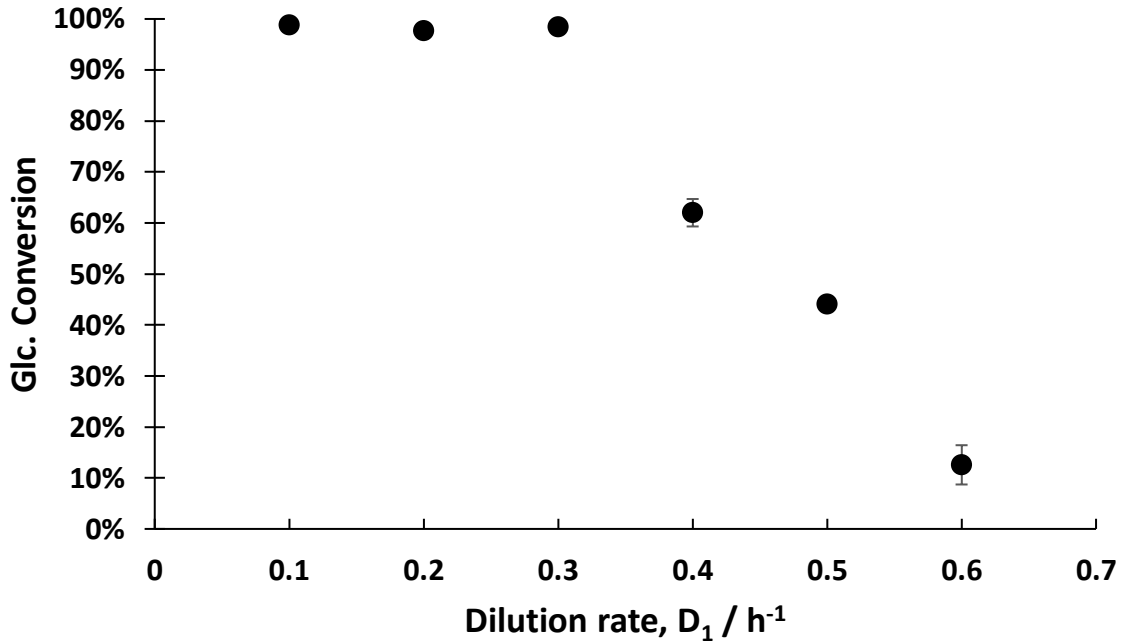


Figure 5. 12 Glucose conversion as a function of dilution rates in R1. The black filled circles (●) represent the percentage of glucose (compared with the inlet substrate concentration to R1) consumed by *E. coli* to produce new cells. The residence time in R1 was controlled using the dilution rate. Error bars represent one standard deviation. Glucose conversion values are the average \pm SD (three technical repeats) after steady state was achieved.

5.3.3. Continuous production of phage T3 using 3 reactor stages: Reactor 2 (R_2) – Infection reactor

The second reactor (R_2) served the dual purpose of acting as a mixing vessel and for initiating phage infection (as mentioned in section 3.5). Here phages had a short residence time, enough for adsorption and preliminary release of part of the phage progeny to keep the phage concentration constant. Two kinds of experiments were carried out. The first one intended to assess the productivity of phages in R_2 by changing D_1 and keeping D_2 constant at $4 h^{-1}$ – meaning that the residence time in R_2 was fixed at 15 min, about the same time as the lag time measured during the one-step growth experiment (Fig. 5.9). D_1 affects host cell physiology, so the experiment was carried out to assess the effect of host cell physiology on phage productivity rate. Concentration of phages produced at steady state in R_2 changed in relation to D_1 . If $D_1=0.1 h^{-1}$, phage T3 produced in R_2 was $\sim 1 \times 10^4$ PFU mL^{-1} ; at $D_1=0.2$ and $D_1=0.3 h^{-1}$ the concentration of phage T3 was $\sim 1 \times 10^5$ PFU mL^{-1} . At higher dilution rates, when higher glucose concentrations were coming out of R_1 , phage concentration increased by ~ 2 log. At $D_1=0.4 h^{-1}$ phages produced were $\sim 1 \times 10^7$ PFU mL^{-1} , at $D_1=0.5 h^{-1}$ $\sim 2 \times 10^7$ PFU mL^{-1} and at $D_1=0.6 h^{-1}$ the concentration was $\sim 8 \times 10^6$ PFU mL^{-1} (Fig. 5.13). Again, the productivity of R_2 was defined as the number of phages produced per hour per unit volume.

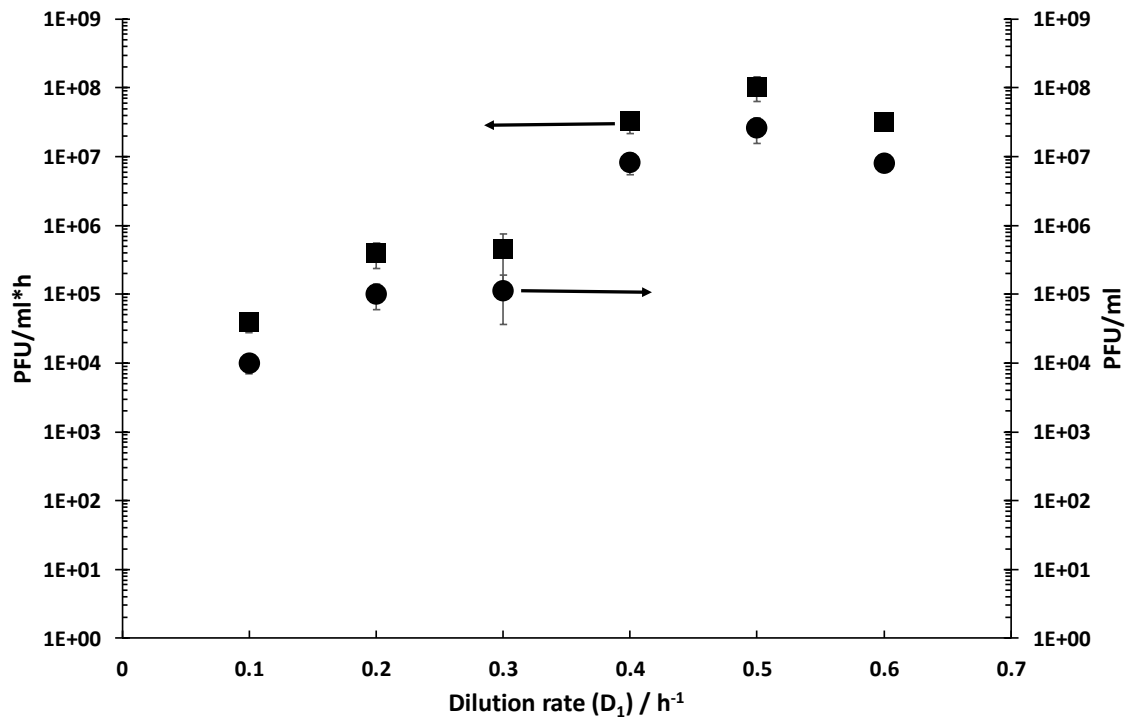


Figure 5.13 Phage productivity (■) in Reactor 2 (R2) as a function of the dilution rate (D_1) in Reactor 1 (R1). The dilution rate in R2 (D_2) was kept constant at a set value of $4 h^{-1}$. The filled circles (●) show the concentration of phages ($PFU mL^{-1}$) in R2 at steady state operation. PFU concentration is the average $\pm SD$ (three technical repeats) after steady state was achieved.

The second kind of experiments were set up to evaluate phage washout as a function of D_2 (Fig. 5.14). The D_1 values tested were 0.4, 0.5 and $0.6 h^{-1}$ and the D_2 values were 3, 4 and 6 with a residence time of 20, 15 and 10 min respectively. Phage T3 concentration decreased as the D_2 increased but there were still phage T3 virions being produced at $D_2 = 0.6 h^{-1}$ for all values of D_1 . At $D_2 = 3 h^{-1}$ phage concentrations converged to $\sim 3 \times 10^8 PFU mL^{-1}$ and by increasing the D_2 differences in phage concentration were observed. This was visible at $D_2 = 6 h^{-1}$, where phages T3 coming from R2 at $D_1 = 0.5 h^{-1}$ showed the highest concentration, $\sim 2 \times 10^6 PFU mL^{-1}$; when $D_1 = 0.6 h^{-1}$ it was $\sim 3 \times 10^5 PFU mL^{-1}$ and when $D_1 = 0.4 h^{-1}$ T3 concentration was $\sim 1 \times 10^5 PFU mL^{-1}$. Finally, wash out of phage T3 did not occur even with a residence time of 10 min in R2. It was difficult to control the dilution rate in R2 beyond $6 h^{-1}$ with the available set-up.

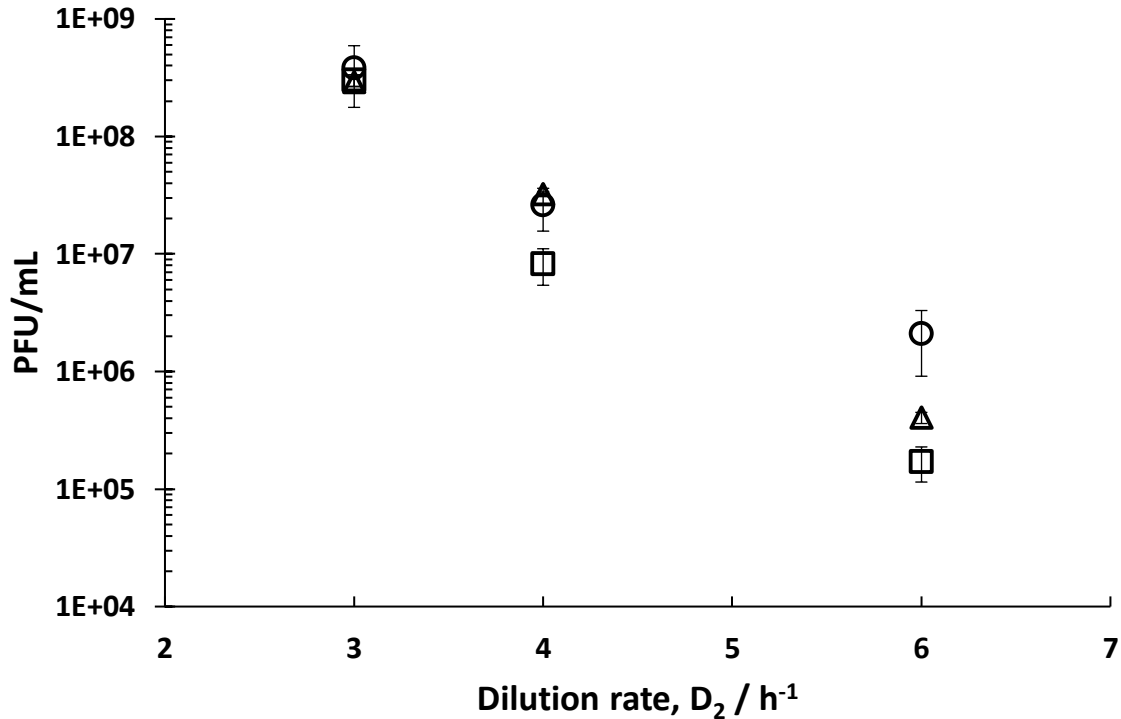


Figure 5. 14 Effect of bacteria physiology and dilution rate D_2 on phage titres in the second reactor (R_2). Empty circles (○) correspond to phages produced in R_2 when R_1 was operated at $D_1 = 0.5 h^{-1}$; Empty squares (□) correspond to phages produced in R_2 when R_1 was operated at $D_1 = 0.4 h^{-1}$ and empty triangles (△) correspond to phages produced in R_2 when R_1 was operated at $D_1 = 0.6 h^{-1}$. PFU concentration is the average \pm SD (three technical repeats) after steady state was achieved.

5.3.4. Continuous production of phage T3 using 3 reactors stages: Reactor 3 (R_3) – Amplification tank

In the third reactor (R_3) completion of phage T3 occurred with phage T3 coming from R_1 at D_1 ranging from 0.4 and 0.6 h^{-1} and from R_2 at D_2 ranging from 3 to 6 (as mentioned in section 3.5) (Fig. 5.15). Phage production in R_3 was operated in batch. Reactors were filled for 1 h and the volume of lysate depended on what dilution was operated in R_1 (ranging between 50 and 250 mL, as described in section 3.5), and then the flow of host and phages was redirected to a new vessel and so on. Incubation at 37 °C was carried on for 3 h until the culture was clear ($OD_{600} < 0.1$). The final phage concentration was similar to that of a batch amplification and reached $\sim 2 \times 10^{11}$ PFU mL^{-1} for phage T3 with $D_1 = 0.5 h^{-1}$ and $D_2 = 3 h^{-1}$. At $D_2 = 4$ and 6 h^{-1} , the final concentration was $\sim 5 \times 10^{10}$ PFU mL^{-1} . When D_1 was 0.4 h^{-1} the final phage concentration was lower, ranging from 5×10^9 and 1×10^{10} PFU mL^{-1} . When D_1 was 0.6 h^{-1} the final concentration of phage T3 was $\sim 1-3 \times 10^8$ PFU mL^{-1} . Table 5.3 summarizes all the conditions and final titres of phage T3.

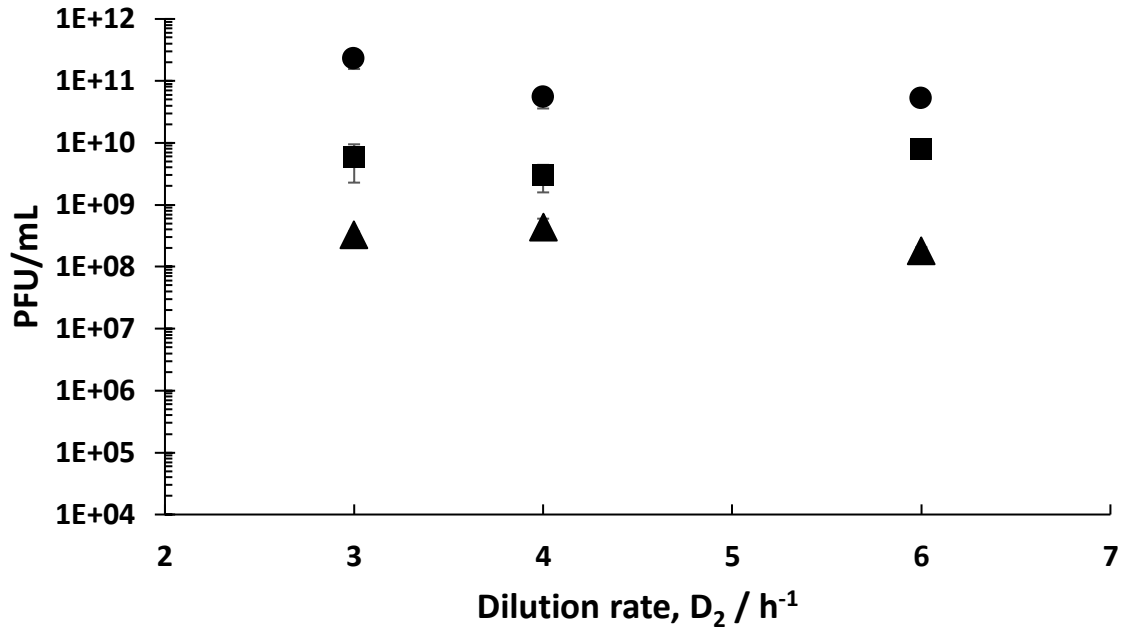


Figure 5. 15 Final phage titres in Reactor 3 (R_3) after overnight amplification following infection in R_2 using dilution rates (D_2). Filled round circles (\bullet) correspond to phages infected in R_2 when R_1 was operated at $D_1 = 0.5 h^{-1}$; Filled squares (\blacksquare) correspond to phages infected in R_2 when R_1 was operated at $D_1 = 0.4 h^{-1}$ and filled triangles (\blacktriangle) correspond to phages produced in R_2 when R_1 was operated at $D_1 = 0.6 h^{-1}$. PFU concentration is the average \pm SD (three technical repeats) after steady state was achieved.

5.4. Discussion

In this chapter, two bacteriophages have been evaluated in terms of factors affecting production. Lab scale production was improved by testing the best conditions for phage amplification, and experimentally determined parameters were used for scaling up production using a 5L reactor operated in batch mode. The first parameter that influences the outcome of the infection is the host cell concentration. Optical density is an effective method to follow the growth curve of bacteria, but it is not a completely reliable indicator of the actual cell concentration in the reactor. It was shown that *S. aureus* cells stopped doubling before the OD₆₀₀ reached a plateau and on the other hand, that *E. coli* cells did not actually start replicating while OD₆₀₀ was already increasing. It is thus necessary to measure OD₆₀₀ and the corresponding cell concentration allowing calibration of OD₆₀₀ and CFU mL⁻¹ of the host (Fig. 5.1, 5.2). The other main parameter influencing the final concentration of bacteriophages was the multiplicity of infection (MOI). MOI is the ratio between phages and bacteria at the moment of infection and it has been previously shown to have a significant impact on the amplification of phages (Abedon, 2009; Kasman et al., 2002). In this chapter it has been thoroughly investigated for both Phage K and phage T3. A high MOI such as 10 was not suitable for amplification of phages because it caused rapid lysis perhaps by lysis from without (Abedon, 2011). Lower MOI such as 1, gave fast lysis of the host culture but yielded a lower final concentration of phage K (Fig. 5.5). This may be explained due to phage amplification kinetics being 1st order with respect to the concentrations of phage and bacteria. The optimum concentration of phages may allow host replication cycles complete before lysis. Phage K amplifications gave the best results with infections started at MOI 0.1 or 0.01, reaching ~1x10¹¹ PFU mL⁻¹. Phage T3 showed the same trend: at high MOI such as 10 or 1 the lysis was fast, and the final phage concentration was low. At lower MOI, 0.1 or 0.01 the phage titres improved by ~2 log, getting again up to ~1x10¹¹ PFU mL⁻¹. T3, unlike phage K, was shown to be effective even at very low MOI: it was able to lyse the host culture till a MOI of 10⁻⁶ (Fig. 5.10). The effect of divalent salts was evaluated for both phages. Phage K was sensitive to the action of ammonium sulphate (Hotchin, 1955) and phage T3 to magnesium sulphate, both reaching the final titre of ~ 2x10¹¹ PFU mL⁻¹ after addition of these salts to the samples.

Subsequently, a defined medium (SM) was optimized, starting from one already described in literature (Li et al., 2010), for production of *E. coli* and the growth parameters were used for continuous production of phage T3. In SM, *E. coli* got to the same cell concentration, but the growth was slower compared with LB (Fig. 5.8). The main differences are on the phage production: even at low MOIs the highest concentration of phage T3 in a synthetic medium lysate was 3x10¹⁰ PFU mL⁻¹(Fig. 5.10). The one-step growth experiment showed a great difference compared with the LB one: the burst in

synthetic medium was ~700 virions, while in LB was ~100 and the rise period was 60 minutes instead of 10 (Fig. 5.9).

A new layout for continuous production was presented and the effect of operating conditions including dilution rate evaluated. Papers available in the open literature which described phage production using chemostats suggested that two reactors connected in series allowed decoupling the host growth and phage replication (Husimi et al., 1982b; Nabergoj et al., 2018) or other techniques such as the self-cycling fermentation allowed synchronisation of cell growth and phage replication (Sauvageau and Cooper, 2010; Storms, 2012). Here, continuous production of T3 phages was performed using 3 reactors connected in series. The novelty lies in the second reactor, working as a mixing and infection tank for host and phages. Its role is to let phages and host cell get in contact and to let adsorption happen but releasing some new phages at the same time to avoid phage washout.

In the first reactor, once steady state was reached, cells were synchronised and were ready to be infected in the second reactor. Dilution rate was the parameter used to control host growth – and thus its physiology - and at the same time allowed ease of control (Fig. 5.11). Using glucose as the only carbon source allowed to clearly see the effect of host cell growth physiological differences on phage amplification kinetics by varying the dilution rate (Fig. 5.12). A perceived weakness of continuous production of bacteriophages has been the low titre, due to the chemostat layout and the need to get a balance between phage amplification and the host culture not to be completely lysed by phages (Nabergoj et al., 2018). The direct consequence of chemostat continuous production was the poor yield and difficulty in controlling the MOI. The results of this chapter show that the titre of phages clearly depends on the physiological state of the host (Fig. 5.13) and that at steady state there was no washing out below D_2 6 h^{-1} , that corresponds to 15 min of residence time (Fig. 5.14). Comparing phage production rates in R_2 operating at a dilution rate D_2 of 6 h^{-1} showed an increase in phage titres from $6.8 \times 10^4 \text{ PFU mL}^{-1}$ (D_1 0.6 h^{-1}) to $1.7 \times 10^5 \text{ PFU mL}^{-1}$ (D_1 0.4 h^{-1}) and the highest value at $2.1 \times 10^6 \text{ PFU mL}^{-1}$ operating R_1 at the optimum dilution rate D_1 of 0.5 h^{-1} . This was indicative of the different phage amplification rates given by the different physiology of cells coming out R_1 . The third reactor was used as the real amplification tank. Here, phages could amplify for several hours to complete the amplification cycle. This depended on the amount of residual glucose allowing uninfected host cells to replicate and the physiological state of the host and the phage concentration from the second reactor. Initially, the second reactor was meant to be a “controller” of the MOI before the amplification. The goal was to maintain a low MOI, between 0.1 and 0.01, to get the highest final phage T3 concentration. The expected result was different: according to previous experiments, a low MOI yields better phage amplifications. The expected result should have been a higher final titre when D_2 was 4 or 6 h^{-1} . The real outcome of the experiment was that the 3 h^{-1} as the best D_2 , achieving a MOI

of ~ 1 in R_2 and a final concentration of $\sim 2 \times 10^{11}$ PFU mL^{-1} in R_3 , whilst it was $\sim 6 \times 10^{10}$ PFU mL^{-1} at D_2 6 h^{-1} ($p < 0.05$ using a two-sample t-test, 95% confidence interval for the difference in means was $1.3 \times 10^{11} - 2.1 \times 10^{11}$ PFU mL^{-1}) (Fig. 5.15). The final titre did not depend only on the MOI but also on the physiological state of the host and due to the mass action law, the more phages available for infection the higher the final titre.

Reactor 1	Reactor 2	Reactor 3
Dilution Rate (h^{-1})	Dilution Rate (h^{-1})	Production of phages (PFU mL^{-1})
0.1	n/a	n/a
0.2	n/a	n/a
0.3	n/a	n/a
0.4	3	1×10^{10}
0.4	4	5×10^9
0.4	6	1×10^{10}
0.5	3	2×10^{11}
0.5	4	5×10^{10}
0.5	6	5×10^{10}
0.6	3	5×10^8
0.6	4	5×10^8
0.6	6	1×10^8

Table 5.3 Summary of conditions tested and final titres of Phage T3 in reactor 3.

Another aspect of this continuous production process for phage T3 was that it was carried out in synthetic medium used previously (Li et al., 2010) with a slight change in the sugar composition. Here the glucose was the only carbon source and the concentration was low enough to show changes influenced by different dilution rates. Previous studies using chemostats to investigate the effect of host physiology have used complex media where it was unclear which limiting factor affected the host organism growth rate (Nabergoj et al., 2017). The final titre of phage T3 after continuous production, at the optimal parameters, was higher than the batch amplification using shaking flasks (Fig. 5.10).

This medium has also less issues related to purification, as the entire composition is controlled and there is less variety than a complex medium such as LB broth.

Bacteria host growth parameters here measured were used in a separate paper to build a mathematical model for phage production. Data from bacterial growth were fitted with Monod kinetics and phage growth parameters (adsorption constant, burst size, and latency period) were fitted in a mathematical model (built by Dr. D. J. Malik) simulating the key features of the production process (Mancuso *et al.*, 2018).

In this chapter key parameters driving phage amplification and influencing the final titre were evaluated. A new continuous production method was described, overcoming limitations, allowing fine control over host cell growth in the first reactor, low MOI infections in the second reactor and amplification yielding high titre phages in the third reactor. The use of a synthetic medium did not affect the final titre of phage T3 may help improve the downstream purification processes needed to produce purified phage for human therapeutic use.

6. Purification of Phage Lysates Using Ultrafiltration

This chapter presents results of phage lysate purification using batch ultrafiltration (UF) using phage K and phage T3. The goal was to remove impurities in lysates composed mostly of host cell proteins and nucleic acids and finally exchange the medium of the lysate with fresh buffer. Both phages were amplified in complex media, brain heart infusion (BHI) for phage K and Lysogeny Broth (LB) for phage T3. After the infection and lysis of the host, the lysates were clarified using centrifugation ($4000 \times g$) and microfiltration using $0.22 \mu\text{m}$ filters. Batch UF was conducted using dead-end filtration in a stirred cell (SC) using 100 kDa or 300 kDa MWCO membranes or using tangential flow filtration (TFF, also called cross-flow filtration, CFF) using flat sheet membranes of 100 kDa MWCO. The cut-off of 100 kDa or 300 kDa allows separation of impurities of the lysates such as host cell proteins and nucleic acids, that will be removed in the permeate, from the phages, that are expected to remain in the retentate.

The fouling of the membrane is a common issue in membrane separation processes and it is caused by concentration polarization: proteinaceous solutes tend to accumulate at the membrane surface forming a layer that affects filtration rates. In SC concentration polarization effects are minimised by applying a shear force across the membrane surface using agitation of an impeller; in the TFF the feed liquid stream flows tangentially across the membrane surface minimising solute accumulation due to permeate flow across the membrane surface. Parameters influencing the filtration were assessed, e.g. the membrane pore size and the permeate flowrates over time. A comparison of recovery of phages in the retentate was also performed. Anion exchange binding capacities were evaluated before and after UF and gel filtration was used as the analytical method for assessing the degree of purity of the final phage samples (although for the Gram-negative derived phage T3 the level of endotoxins achieved was not considered in this Chapter, but will be discussed further in Chapter 7).

6.1. Ultrafiltration using a stirred cell for purifying bacteriophage lysates

6.1.1. Characterization of membranes and shear stress in the stirred cell

Polyethersulfone (PES) membranes with different cut-offs, 100 kDa and 300 kDa MWCO, were characterized in the SC (as mentioned in section 3.6.1) (Fig. 6.1). A constant transmembrane pressure of 1 bar was applied in the SC and dextran standards (guaranteed by the specialty supplier to be close to be monodisperse) of increasing molecular weight were filtered (as described in section 3.6.1). The shear stress was calculated using a model described previously (Kosvintsev et al., 2005). Although parameters such as cell geometry, blade dimension etc. affect shear stress in the cell, only two

parameters were varied during the experiments: the viscosity of the fluid (BHI and LB) and rotation speed of the impeller. Viscosity of the media was measured, and the impeller of the SC was set at two different rotational speeds such that the shear force across the membrane was either ~10 Pa (low shear) or ~20 Pa (high shear).

6.1.1.1. Characterization of Merck Millipore membranes– 100 and 300 kDa MWCO

The 100 kDa MWCO Merck Millipore membranes in the SC at shear rate of 20 Pa showed the following rejection rates for 5.2 kDa (7%), 23.8 kDa (8%) and 48kDa (10%). For the same MW dextran size, at lower shear (10 Pa), the rejection was 7%, 14% and 24% respectively. The rejection was 34% at 20 Pa for the 148 kDa MW dextran whilst at 10 Pa the rejection was 54%. Over the 90% of the 668 kDa MW dextran was rejected by the 100 kDa MWCO membrane, with insignificant differences between the two shear stress values: 93% at 20 Pa and 96% at 10 Pa.

The 300 kDa MWCO membrane showed a different rejection profile. Smaller MW dextran molecules of 5.2 kDa, 23.8 kDa and 48 kDa mostly passed through the membrane at 20 Pa, with a typical rejection around ~5%. At 10 Pa rejection was greater at 13%, 18% and 21% respectively. The rejection was 34% for the 148 kDa MW dextran molecule at 10 Pa and 24% at 20 Pa. At 20 Pa 83% rejection of 668 kDa MW was observed for the 300 kDa MWCO membrane and at 10 Pa the rejection was 89%. The rejection profiles clearly showed that the filtration profile of the UF membrane depended on the membrane cut-off and was influenced by the shear stress at the membrane surface.

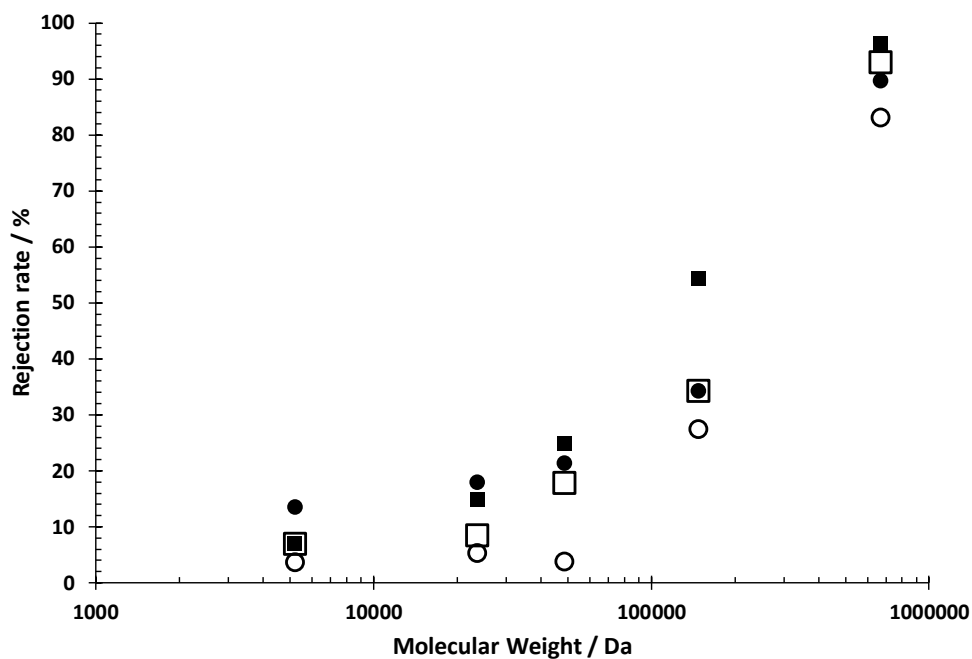


Figure 6. 1 Percentage rejection of different MW dextrans in the stirred cell using Millipore membranes of 100 kDa or 300 kDa MWCO at high or low shear. Open squares (□) represent 100 kDa MWCO at high shear, filled squares (■) 100 kDa MWCO at low shear. Open circles (○) represent 300 kDa MWCO membrane at high shear, filled circles (●) 300 kDa MWCO at low shear. Values are the average \pm SD (three technical repeats (SD too small to be seen)).

6.1.1.2. Characterization of Alfa Laval membrane – 100 kDa MWCO

Alfa Laval 100 kDa MWCO membranes in the SC showed slightly lower rejection of dextran molecules of 668 kDa MW, 83% at 20 Pa and 86% at 10 Pa compared with the 100 kDa Millipore membranes. Smaller MW dextran molecules 5.8 kDa and 23.8 kDa rejection rates were of 4% and 9% at 20 Pa whilst they were 9% and 13% at 10 Pa.

The effect of surface shear was evident for dextran of MW 48 kDa and 148 kDa. The 48 kDa molecules had a rejection value of 12% at 20 Pa and 20% at 10 Pa whilst the 148 kDa molecules at 10 Pa shear were rejected at ~36% and 51% at 20 Pa shear.

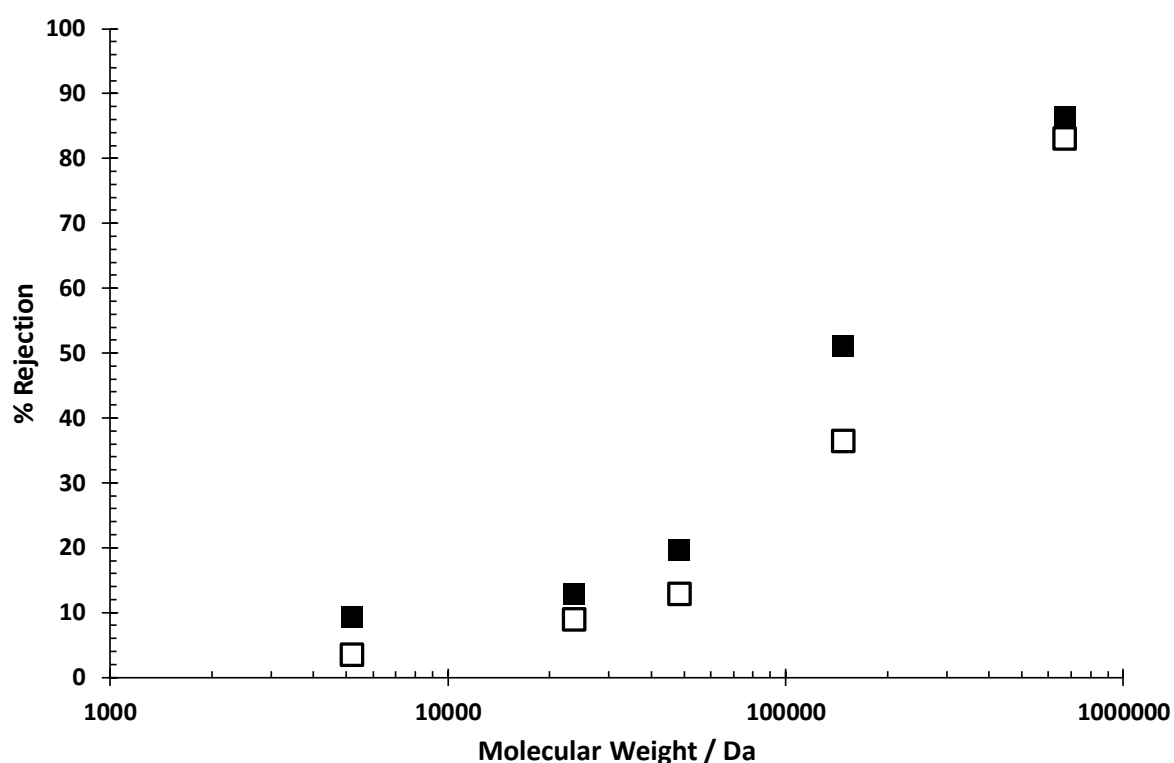


Figure 6. 2 Percentage rejection of different MW dextran solutions in the stirred cell with Alfa Laval membranes of 100 kDa at high or low shear. Open squares (\square) represent high shear, filled squares (\blacksquare) low shear. Values are the average \pm SD (three technical repeats (SD too small to be seen)).

6.1.2. Phage recovery after UF in the SC and viability of phages over time

6.1.2.1. Phage K lysate in BHI

Phage K lysate was subjected to filtration in the SC using either the 100 kDa or 300 kDa MWCO membranes and employing different shear rates using different rotation speeds of the impeller (as mentioned in section 3.6.2).

Phage K has a capsid size of 80 nm (Fig. 6.4) and a 100 kDa MWCO membrane retained 100% of the phages in the retentate. Using a 300 kDa MWCO membrane caused a loss of 2% of the initial concentration of phage K in the permeate.

At the maximum rotational speed, the shear stress in the SC was 20 Pa and the viability of phages decreased by ~1 log after 60 min and ~2 log after 2 h. The initial concentration of viable phage K diminished by 99% in 2 h. Decreasing the rotation speed of the impeller and exposing the phage to a lower shear stress (10 Pa) resulted in reduction in phage K viability loss to ~0.5 log after 60 min and ~1 log after 2 h, equating a reduction of 50 and 90% of the initial phage titre (Fig. 6.3).

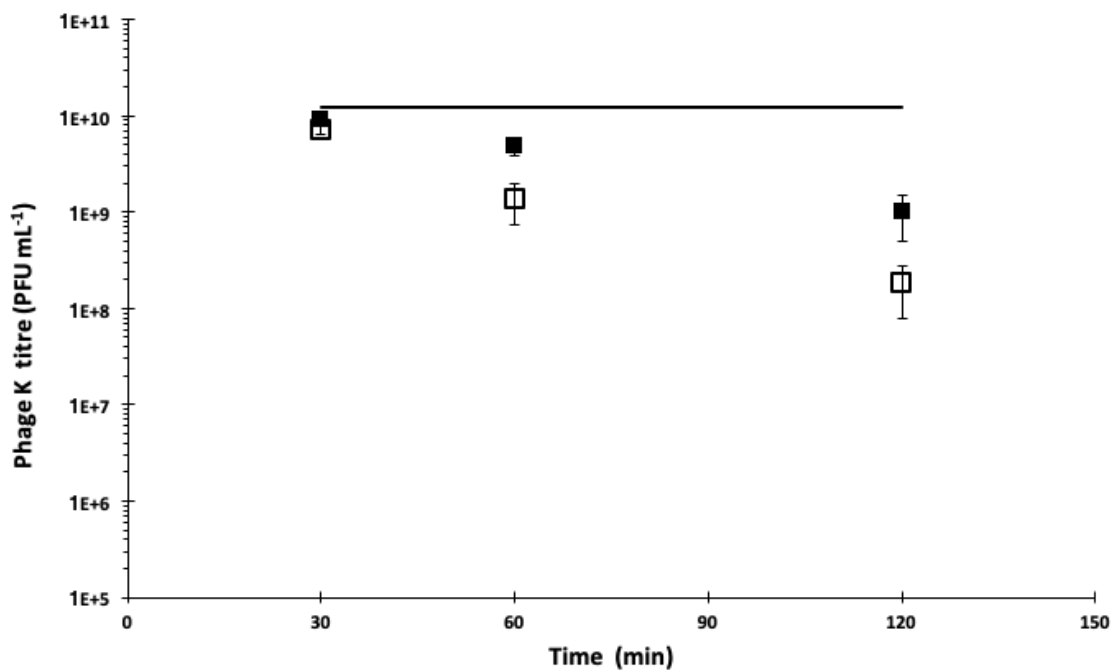


Figure 6. 3 Time series data showing viability of phage K in the stirred cell exposed to different shear stress levels over time. Empty squares (□) represent high shear, filled (■) squares low shear and the continuous line represents the negative control. PFU concentration is the average \pm SD (three technical repeats).

Cryo-TEM images visually confirmed that the loss of activity of phages was a consequence of detachment of the head from the tail caused by the shear stress (Fig. 6.4).

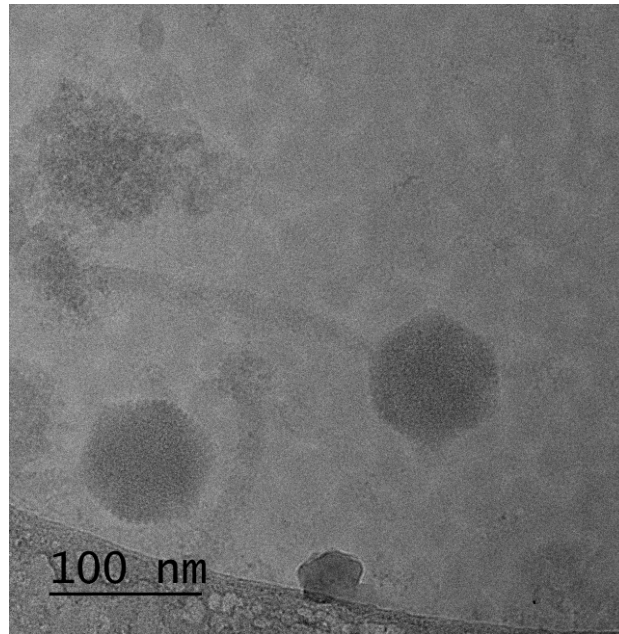


Figure 6. 4 Cryo-TEM image of phage K after ultrafiltration in the stirred cell. The effect of shear stress is visible as the capsid is detached from the tail of phage K.

6.1.2.2. Phage T3 lysate in LB medium

T3 phages did not show any significant viability loss over time due to exposure to shear stress and phage titre remained ~100%. Viability of phage T3 is maintained during UF in the SC either at 10 Pa and 20 Pa shear stress (Fig. 6.5) and no morphological changes were seen at the cryo-TEM images (Fig. 6.6). Despite a slightly smaller capsid head (~65 nm) and a short tail, hardly visible from cryo-TEM images (Fig. 6.6), only 3% of T3 phages were found in the permeate when filtered using a 300 kDa MWCO membrane, while the total rejection was noted using a 100 kDa MWCO membrane.

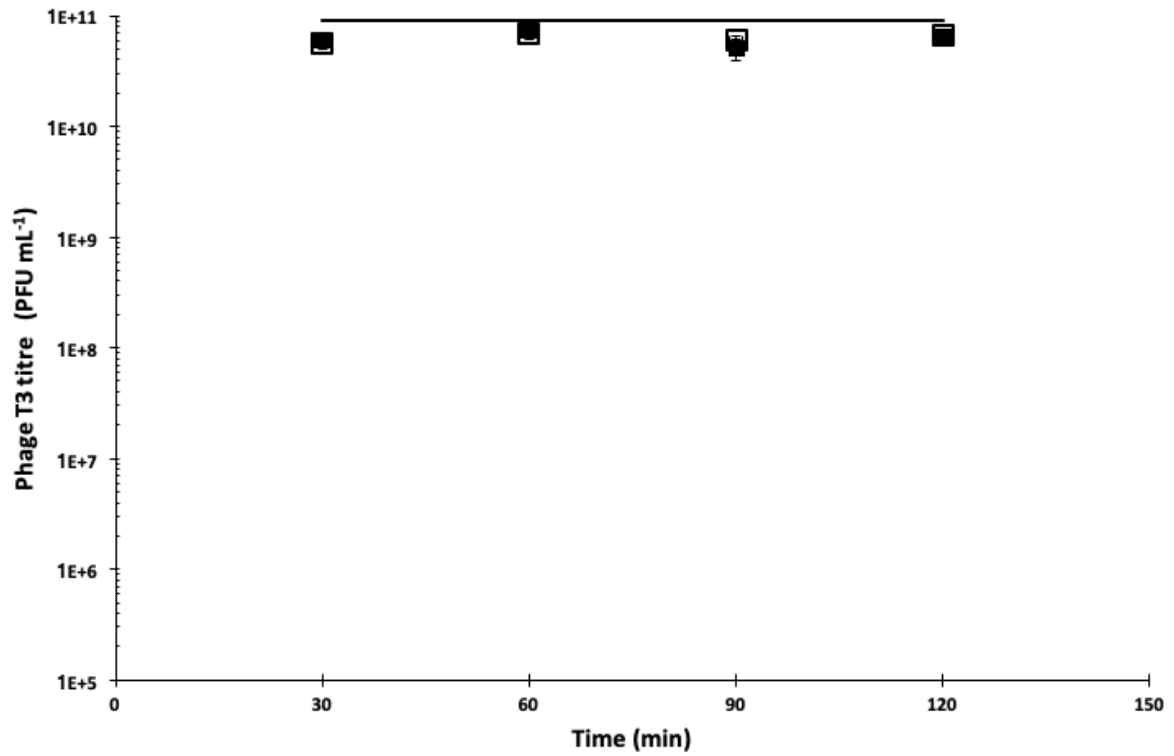


Figure 6. 5 Time series data showing viability of T3 phages in the stirred cell exposed to different shear stress levels over time. Empty squares (□) represent high shear, filled (■) squares low shear and the continuous line represents the negative control. PFU concentration is the average \pm SD (three technical repeats).

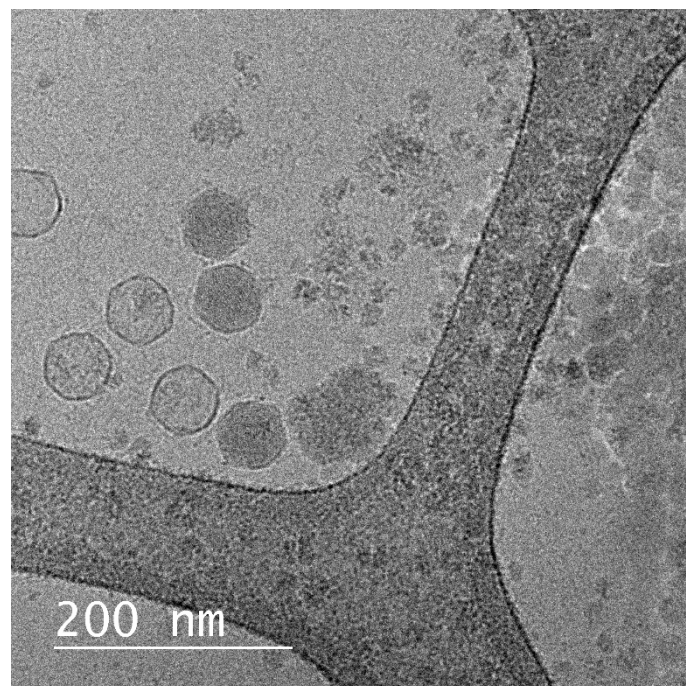


Figure 6. 6 Cryo-TEM image of T3 phages after ultrafiltration.

6.2. Cross-flow filtration (CFF): batch ultrafiltration (UF)

6.2.1. Viability of phage K in CFF

CFF is typically used to process large production volumes (as mentioned in sections 2.3.3.2.3 and 3.6.3). The feed sample flows across the membrane, the surface shear reduces the concentration polarization effect that is typical of ultrafiltration processes. Exposure to shear in the CFF cell did not affect the phage K concentration. The starting initial concentration was 2×10^{10} PFU mL⁻¹ and the viability remained constant over a period of 20 h. Ultrafiltration at transmembrane pressures ~ 0.5 bars did not affect the titre of phage K in the CFF.

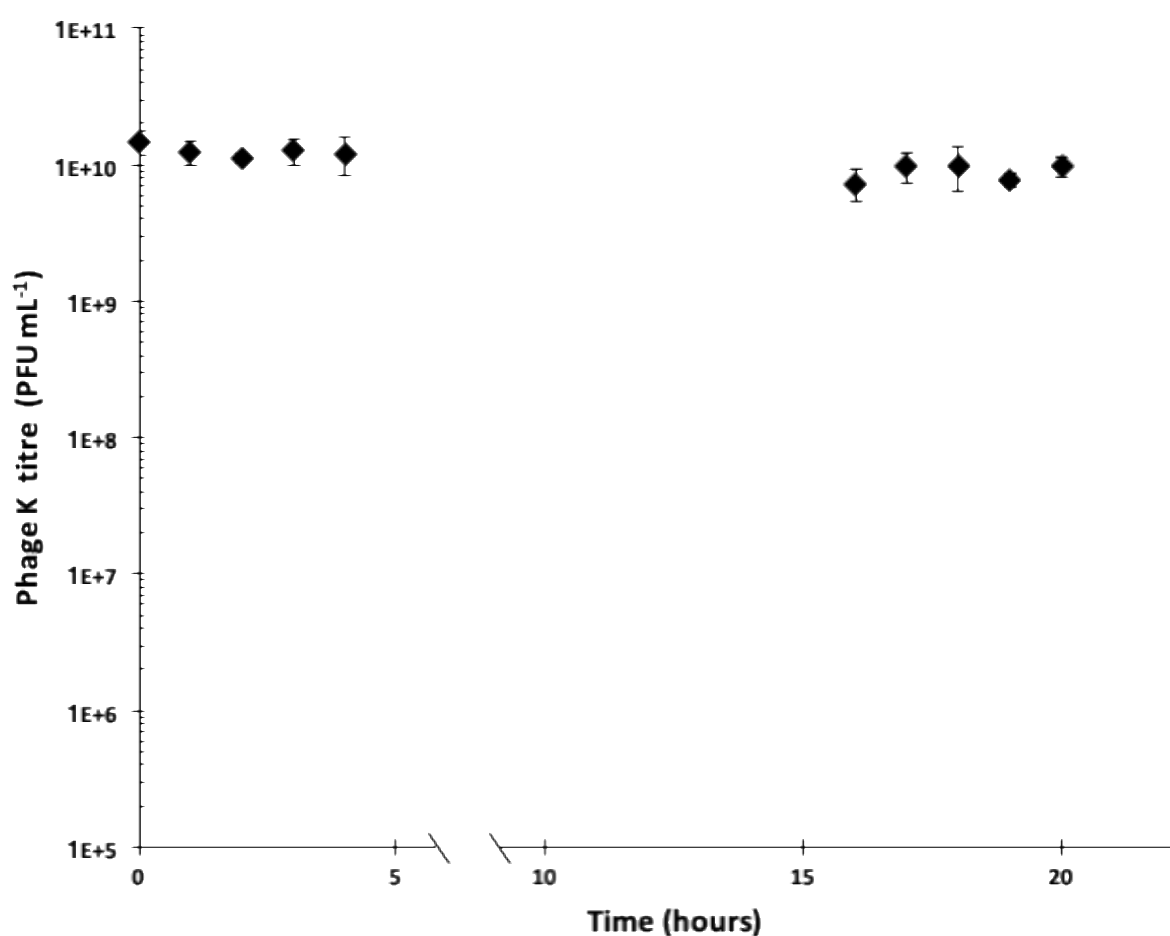


Figure 6. 7 Viability of phage K purified using a 100 kDa MWCO membrane using the crossflow apparatus measured over time. PFU concentration is the average \pm SD (three technical repeats).

6.2.2. Viability of phage T3 in the CFF

Phage T3 lysates in LB were filtered in CFF. The feed had a starting initial concentration of phage T3 of 8×10^{10} PFU mL⁻¹. Viability of this phage was not affected by batch UF using CFF over a period of 20 hours as it ranged between 4×10^{10} PFU mL⁻¹ and 9×10^{10} PFU mL⁻¹.

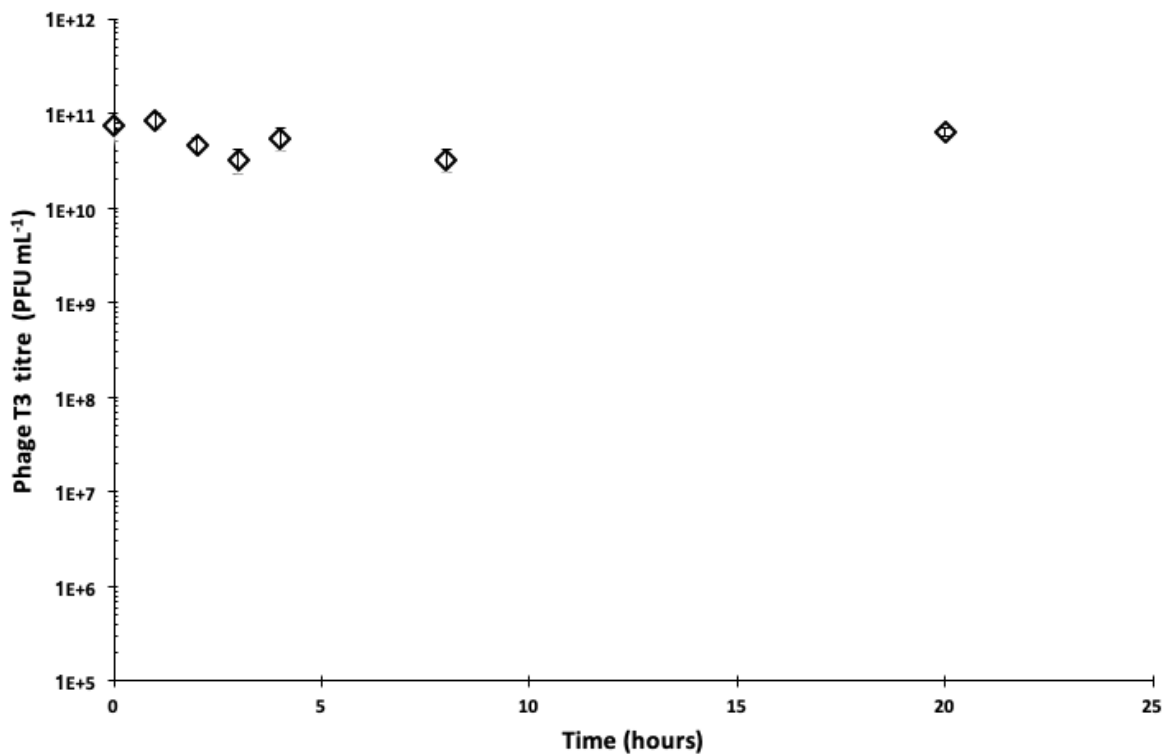


Figure 6. 8 Viability of phage T3 purified using a 100 kDa MWCO membrane using the crossflow apparatus measured over time. PFU concentration is the average \pm SD (three technical repeats).

6.2.3. Permeate flux using CFF

6.2.3.1. Permeate flux of water

Alfa Laval PES flat sheet membrane of 100 kDa MWCO was used for batch ultrafiltration in CFF. Transmembrane pressure was set at 0.5 bars and after conditioning, water permeate fluxes were measured. The starting initial water permeate flux was $12 \text{ Lh}^{-1}\text{m}^{-2}$ and $11.8 \text{ Lh}^{-1}\text{m}^{-2}$ after 30 min. Flux started to decrease after 1 hour, when it reached $\sim 11.6 \text{ Lh}^{-1}\text{m}^{-2}$ and then it kept decreasing at 90 and 120 min to ~ 11.4 and $\sim 11.2 \text{ Lh}^{-1}\text{m}^{-2}$ respectively. Permeate flux reached a steady value of $\sim 11 \text{ Lh}^{-1}\text{m}^{-2}$ after 3 h and remained constant at this value for 20 h (data not shown). Permeate fluxes of phage K in BHI and T3 in LB were measured at the same transmembrane pressure of 0.5 bars. The reduction in

flux is typically attributed to the membrane compression under pressure which affects the membrane permeability.

6.2.3.2. Permeate flux of sterile BHI and phage K lysate in BHI broth

Sterile BHI broth showed lower but constant fluxes over time. In 1 hour the permeate flowrate was $\sim 2.1 \text{ Lh}^{-1}\text{m}^{-2}$ and maintained a constant value for a 16 hours period. Lower flux might be due to higher viscosity of BHI compared with deionised water, measured as $\sim 2.1 \text{ mPa}\cdot\text{s}$ at 25°C (Fig. S.1).

The phage K lysate in BHI broth showed lower fluxes, starting at $\sim 2.1 \text{ Lh}^{-1}\text{m}^{-2}$ after 1 hour and reaching and slowly decreasing the permeate flowrates to $\sim 1.4 \text{ Lh}^{-1}\text{m}^{-2}$ after 3 hours. The polarization effect on the membrane is evident after 16 hours, when the flux reached $\sim 0.8 \text{ Lh}^{-1}\text{m}^{-2}$ (Fig. 6.8).

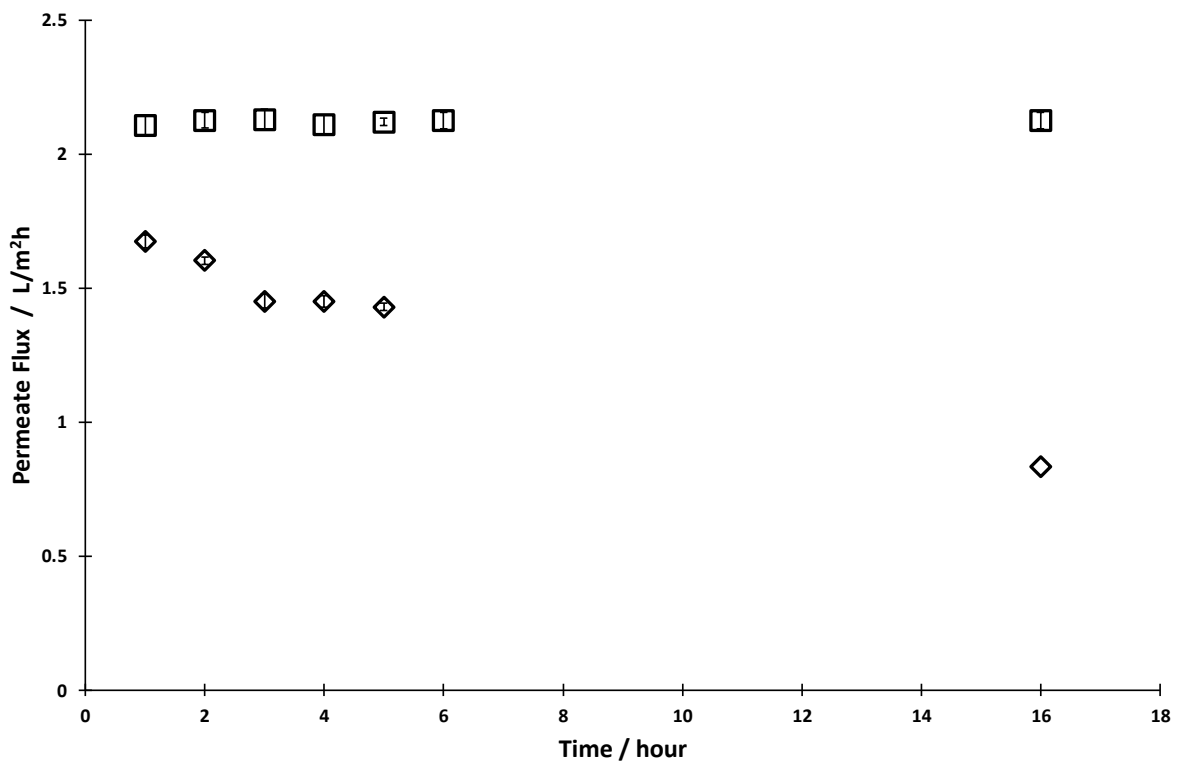


Figure 6. 9 Permeate flux of sterile BHI (empty squares, □) and phage K lysate in BHI (empty diamonds, ◇) in the CFF apparatus. Values are the average \pm SD (three technical repeats. Transmembrane pressure $\Delta P= 0.5 \text{ bar}$.

6.2.3.3. Permeate fluxes of sterile LB and phage T3 lysates in LB

Sterile LB broth permeate flux was $\sim 3 \text{ Lh}^{-1}\text{m}^{-2}$ after 1 h and the flux remained steady for a 16 h of operation. Phage T3 lysate permeate flux showed the effect of concentration polarization on the membrane resulting in a reduction in the flux from $\sim 2.2 \text{ Lh}^{-1}\text{m}^{-2}$ after 1 h of operation to ~ 1.8 and $\sim 1.6 \text{ Lh}^{-1}\text{m}^{-2}$ after 2 and 3 h respectively. After 16 h of operation the flux was $\sim 1.5 \text{ Lh}^{-1}\text{m}^{-2}$.

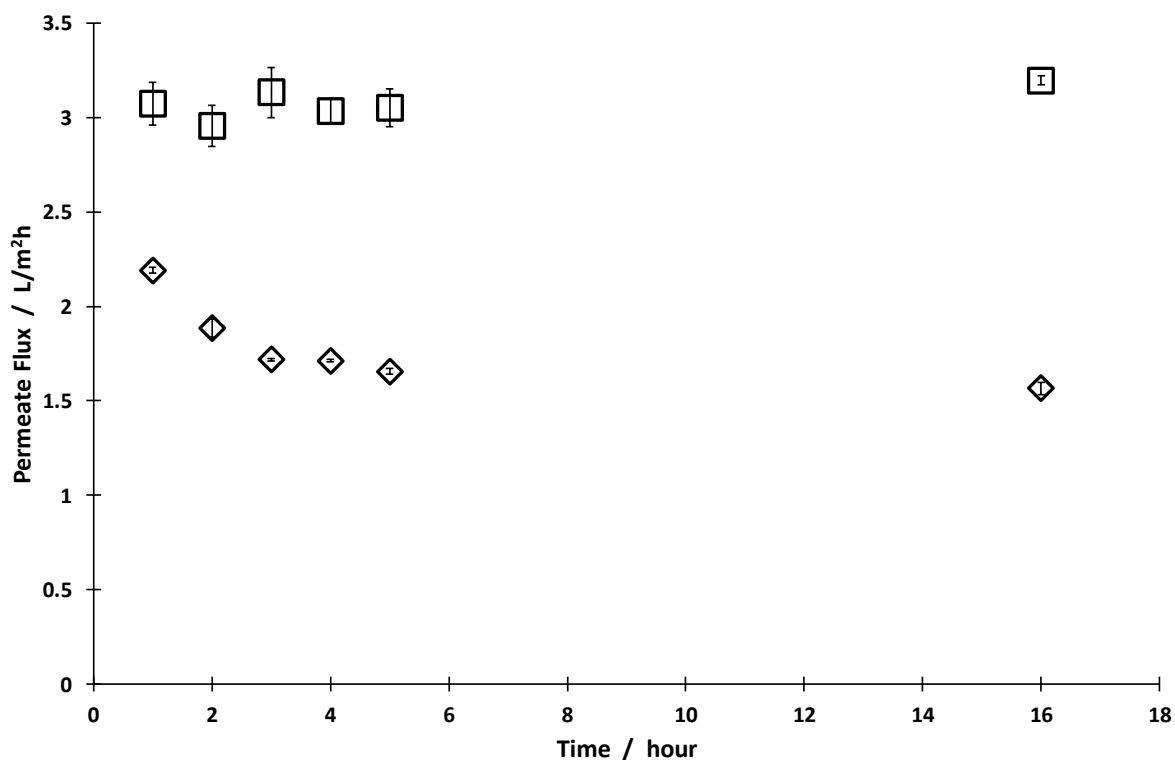


Figure 6. 10 Permeate flowrates of sterile LB (empty squares, \square) and phage T3 lysate in LB (empty diamonds, \diamond) in the cross-flow apparatus. Values are the average \pm SD (three technical repeats. Transmembrane pressure $\Delta P=0.5$ bar.

6.3. Assessment of purity of samples

Batch UF was carried on until the feed volume reached $\frac{1}{4}$ of the initial volume and then fresh buffer was used to replenish the feed tank. This process was repeated at least five times to swap the complex medium with fresh buffer. UV readings at 260 and 280 nm of the retentate samples were used as a real time method to assess the purity of retentate samples and size exclusion chromatography (SEC) was used as an analytical tool to confirm that all the nucleic acids and host cell proteins had been eliminated by UF and therefore was used as an indicator of the purity of the sample (as mentioned in sections 2.3.3.3.4 and 3.8.1).

6.3.1. Size Exclusion Chromatography to assess purity of retentate phage samples

A S-100 gel filtration column (GE Healthcare, UK) was used. The pore channels are 10^5 MWCO and hence the same order of size of the membrane pores: phages were expected to elute in the void volume and all the proteins smaller than 100 kDa were expected to diffuse into the pores. The retention time of molecules of sizes less than 100 kDa would vary depending on their size.

Different samples were analysed using SEC: the phage lysates after centrifugation and filtration through $0.2\ \mu\text{m}$ and purified phages after UF through 100 kDa MWCO and after swapping of buffer.

Chromatograms of both phage K and phage T3 showed a similar outcome. The chromatograms of the lysate showed a peak in the void volume indicative of the phage and a higher peak of contaminants able to access the SEC column, e.g. proteins smaller than 100 kDa.

The chromatograms of the phage samples purified using UF showed no contamination associated peaks, free from host cell proteins (Fig. 6.11 and 6.12).

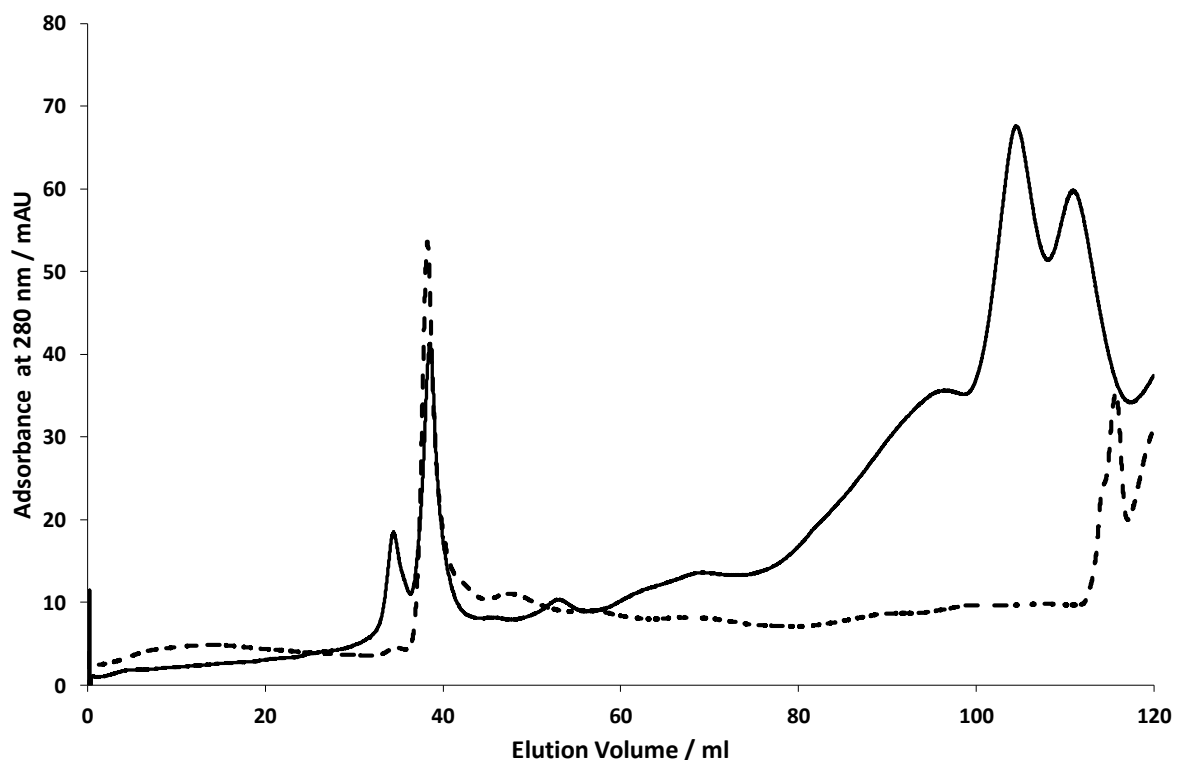


Figure 6. 11 Gel filtration chromatography of Phage K lysate (solid line) and Phage K after batch ultrafiltration (dashed line).

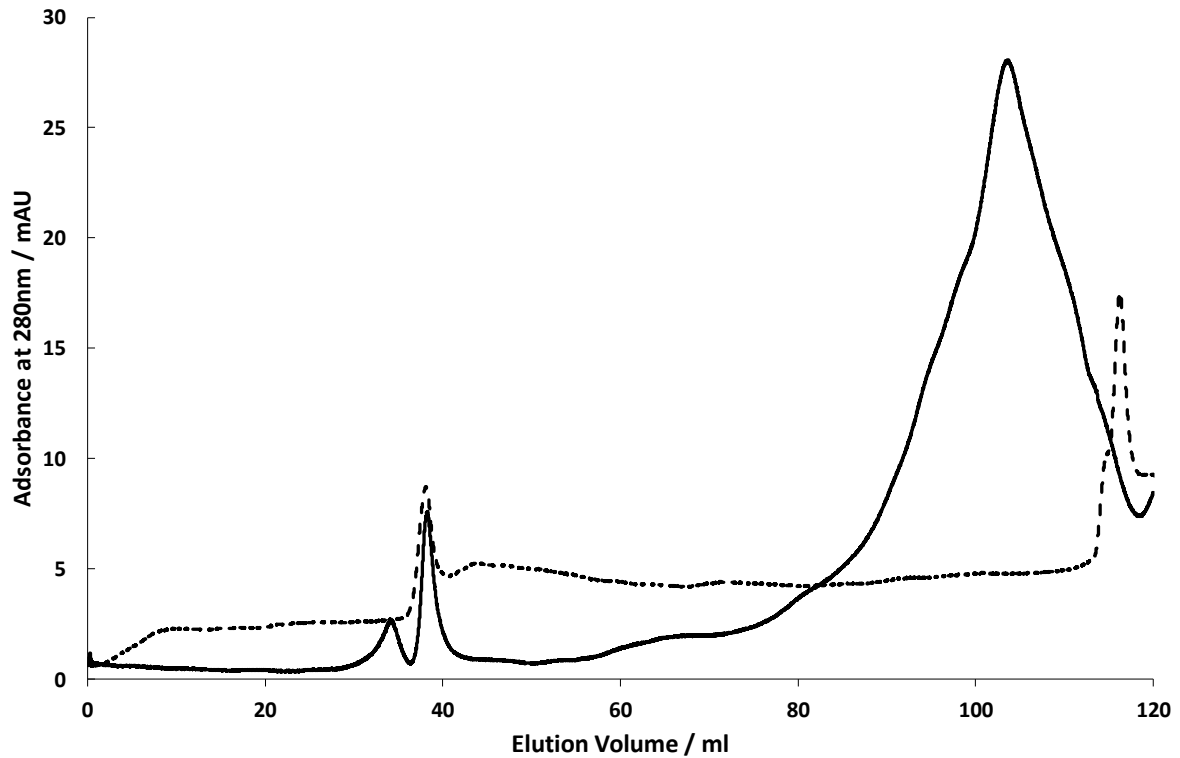


Figure 6. 12 Gel filtration chromatography of Phage T3 lysate (solid line) and Phage T3 after batch ultrafiltration (dashed line).

6.4. Ion exchange isotherms of phage K and phage T3 before and after UF

Ion exchange chromatography can be used to purify bacteriophages, by loading the virions into the column and eluting them with a gradient of salt. A polishing step, such as ultrafiltration, before chromatography can help improving the performances of the column and load more bacteriophages into it. Isotherm curves can help measuring the differences of performance of the resin when in contact with a crude lysate or a purified one, by measuring the concentration of phages that can bind to one gram of resin (as mentioned in sections 2.3.4.2 and 3.8.3).

Ion exchange isotherms were obtained for phage K binding to a strong anion exchange quaternary amine (QA) resin. Phage binding from samples of lysate of phage K were compared with sample purified using batch UF. The isotherm of phage K was found to be linear (log-log plot) and did not saturate the resin at the phage concentration used during experimentation which covered typical phage lysate concentrations. There was a $\sim 1 \log_{10}$ difference in adsorption between UF filtered phages and those from the lysate (Fig. 6.13). This suggests that UF could be used as a polishing step to reduce contaminants and hence improve the downstream ion exchange chromatography polishing step.

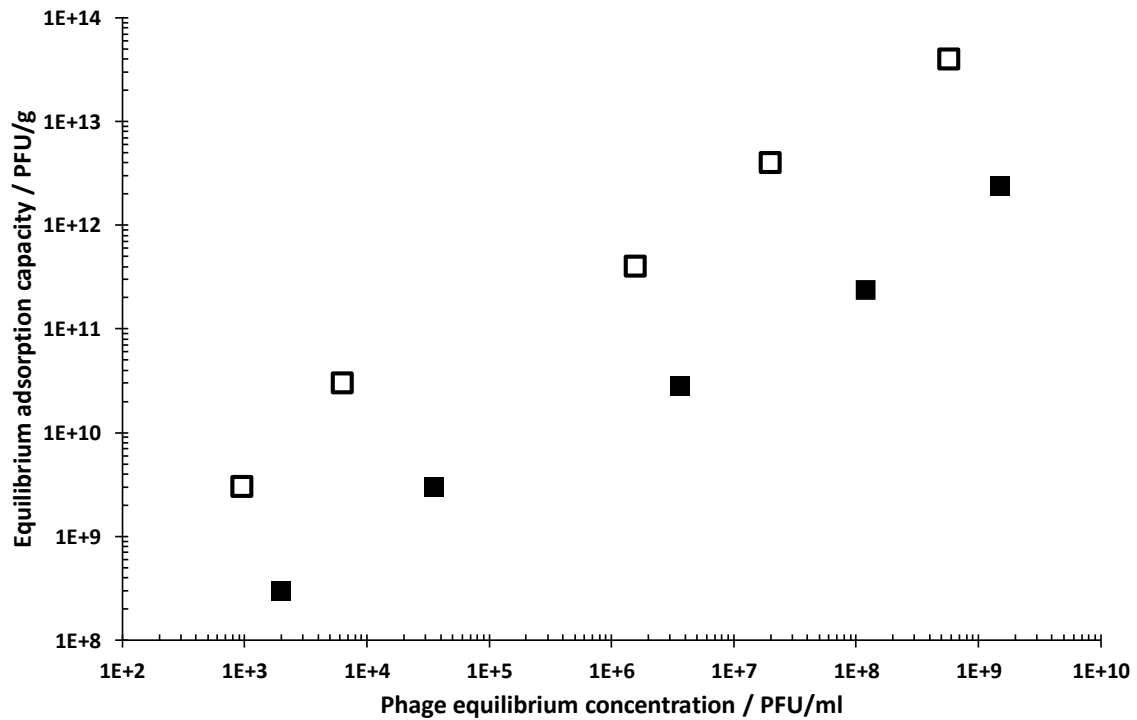


Figure 6. 13 Ion exchange isotherm curves of phage K before (phage K lysate, filled squares, ■) and after batch ultrafiltration (empty squares, □).

Equilibrium adsorption capacity of phage T3 lysate and after batch UF was measured using QA as well. Isotherms were found to be linear (log-log plot) and did not saturate the resin over typical phage lysate concentrations used. Phages purified by batch UF showed higher binding capacity to the QA by $\sim 1 \log_{10}$ (Fig. 6.14). This suggests higher phage T3 binding to the QA resin after batch UF (ion exchange results will be investigated further in Chapter 7).

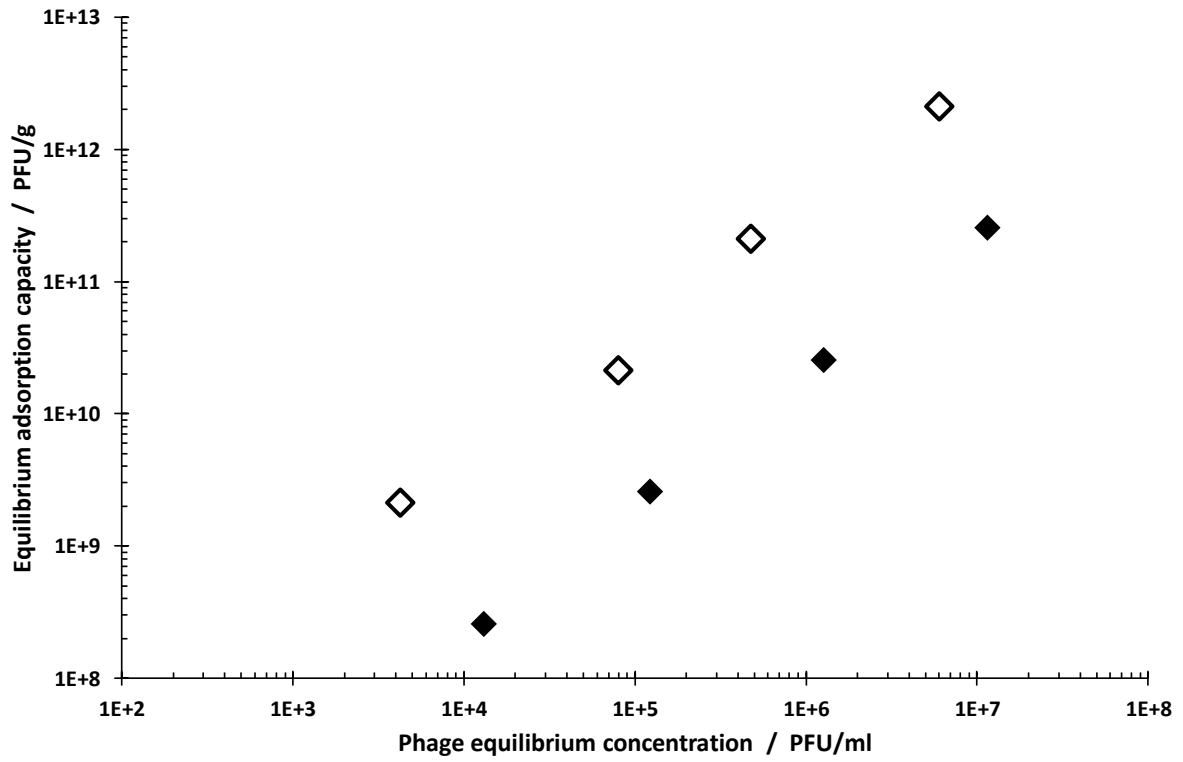


Figure 6. 14 Ion exchange isotherm of phage T3 before (phage T3 lysate, filled squares, ■) and after batch ultrafiltration (empty squares, □).

6.5. Discussion

Ultrafiltration is a widely used method for purifying and concentrating biological solutions. It has been studied and used mostly for proteins and viral vectors (Nestola et al., 2014; Parada et al., 2007; Pyo et al., 2001) and with the spread of phage therapy, it has been applied to bacteriophages as well (Boratynski et al., 2004; Bourdin et al., 2014). Normal “dead-end” filtration, is the most common way of using ultrafiltration in the laboratory environment, where flow is perpendicular to the membrane (van Reis and Zydney, 2007). The main problem in this kind of filtration is membrane fouling due to pore blockage and the decrease of separation efficiency (Kelly and Zydney, 1997). For bacteriophages, that are produced using complex media such as BHI and LB this is a relevant issue. One way to prevent or at least slow the fouling of the membrane is to create a surface shear force that sweeps the membrane surface and continuously regenerates it. This shear force is created by the rotation of an impeller resulting in liquid sweeping the surface; the higher the shear the better the regeneration of the membrane (Becht et al., 2008) thereby resulting in improvement in membrane permeability (Figs. 6.1 and 6.2). The shear stress affects the viability of long tailed phages like the *Myoviridae* Phage K. The shear forces result in detachment of the capsid head from the tail of the phage, as shown by TEM imaging (Fig. 6.4) and the concentration of viable virions decreases over time, resulting in a $\sim 2 \log_{10}$ loss over 2 h (Fig. 6.3). Results reported here showed how phage T3, a *Podoviridae* with a short tail, was not affected at all by the shear stress in the SC, even applying a 20 Pa shear stress for 2 h (Figs. 6.5 and 6.6). TFF allowed UF without loss of phage K viability with UF operation for more than 20 h (Fig. 6.7). TFF was better than dead-end filtration and is easily scalable. It can process large volumes of crude lysate samples. It can be put at the end of the continuous production line and start, after clarification, purifying the freshly produced phages to have a continuous process. UF was performed as a batch process with retentate recirculated until the same volume got to $\frac{1}{4}$ of the initial volume. After that, the retentate was replenished with fresh buffer and the process was repeated 5 times, until only the 0.1% of the initial medium was left and the rest had been swapped with buffer. This process exposed the membrane to a high concentration of impurities rejected by the membrane and concentrated-up during the feed volume reduction and the permeate flux decreased quickly in the first few hours of ultrafiltration before getting to a constant value. Batch UF was heavily affected by concentration polarisation that slowed the process and the membrane needed regeneration or replacement (Jungbauer, 2013). There are other ways to run a TFF process for UF, such as diafiltration, where fresh buffer is added continuously to the feed tank (these results are discussed in the next chapter).

Gel chromatography (SEC) was used to assess purity of the samples following UF and buffer exchange and showed that all the proteins and nucleic acids had been filtered through the membrane. The SEC

column used had pores of 100 kDa MWCO, meaning that all the molecules larger than 100 kDa eluted in the void volume and anything smaller passed slowly through the column. The difference between UF phages and phages from lysate was clearly seen, samples from lysate showed a typical peak attributed to the phages at 40 mL, whereas the diffuse peak due to impurities disappeared after UF.

UF was found to be a good intermediate step before chromatography, which is typically considered a bottleneck in the purification. It is also more expensive and using UF for phage purification before chromatography can improve the performance of the column. Here, the anion exchange binding capacity was measured, using a strong anion exchanger, a quaternary amine (QA) resin. Isotherms were measured to show the binding capacity of the phages to a QA resin. Both phage K and phage T3 bind differently to the resin depending on the purity of the sample. A purified sample binds to the resin with $\sim 1 \log_{10}$ greater binding capacity compared to phages in the crude lysate (for phage T3 this aspect will be investigated further in Chapter 7). Isotherms showed that the resin was not fully saturated by the phages over the concentration range explored during experimentation, which were $\leq 10^{11}$ PFU mL⁻¹. This suggests that ion exchange can be exploited for purifying and also concentrating phages in the same step (Oksanen et al., 2012; Smrekar et al., 2011b) and that UF can help improve this process.

The QA resin has a higher operational binding capacity to purified phage samples because there are less impurities competing for the binding sites in the resin. This is important because performing UF before ion exchange chromatography can help increase the loading of phages on the column, achieving better recovery and provide better performance.

In summary, ultrafiltration was shown to be a useful unit operation for purifying crude phage lysates allowing buffer exchange and concentration of phage samples. Furthermore, it was an essential intermediate step before ion exchange chromatography purification to enhance the binding capacity of the QA resin. The effect of shear stress associated phage damage to phage K was shown using the SC operated in dead-end filtration. The advantages of TFF were shown allowing purification of tailed phages such as phage K without loss of phage titre.

7. Removal of Endotoxins From Phage T3 Lysates

In the previous chapter, UF was used to remove major contaminants from phage lysates after clarification. In this chapter, major attention is put on lipopolysaccharide (LPS) contamination in phage lysate produced in a Gram-negative host (as mentioned in sections 2.3.5 and 3.7).

LPS, or endotoxin, is the name of a complex molecule that is constitutive of the Gram-negative bacteria membrane and contributes to the structure and stability. It is a potent immunostimulant that can cause severe adverse reactions in the human body and any medical product must have less than 5 endotoxin units per mL (EU mL⁻¹) (European Pharmacopoeia, 2010).

This chapter focuses on different separation techniques for endotoxin removal from *E. coli* phage T3 lysates. The goal was to investigate how much endotoxin can be removed by using ultrafiltration in batch mode or diafiltration mode. Endotoxin removal from lysates using LB and synthetic medium (SM) to grow *E. coli* and amplify phage T3 was assessed. Liquid-liquid extraction (LLE) using 1-octanol was used to remove residual endotoxin following the ultrafiltration step. Anion exchange chromatography was evaluated as a unit operation either instead of LLE or after UF to enhance the removal of endotoxin.

7.1. Ultrafiltration (UF) to reduce endotoxin from phage lysate

7.1.1. Batch ultrafiltration

7.1.1.1. Permeate flowrate measurements of LB and Synthetic Medium (SM)

T3 phages were propagated either in LB or SM, reaching concentration from 5×10^{10} PFU mL⁻¹ to 2×10^{11} PFU mL⁻¹ (as described in chapter 5). Lysates were centrifuged $4000 \times g$ to remove cellular debris and subsequently underwent ultrafiltration through a 100 kDa MWCO membrane and the permeate fluxes were measured (like described in chapter 6). The physical dimensions of phage T3 are considerably larger than the nominal average pore size of the membrane which would suggest that the phage should stay in the retentate whilst any impurities (e.g. intracellular host proteins and DNA) smaller than the membrane pore size would pass through the membrane in the permeate. During filtration runs when the retentate volume reached $\frac{1}{4}$ of the starting initial batch volume, fresh make-up buffer was added to bring it back to the initial starting volume. This resulted in complete swapping of the buffer during batch UF.

Higher permeate flux was recorded for phage lysates in synthetic medium in comparison with LB broth (Fig. 7.1). In the first hour of filtration, the permeate flux with synthetic medium was $2.7 \text{ L h}^{-1}\text{m}^{-2}$ compared with and $\sim 2.2 \text{ L h}^{-1}\text{m}^{-2}$ for LB broth. UF of synthetic medium was faster at time point 3 hours however, the difference slowly decreased and after 5 hours of filtration both synthetic medium and LB broth permeate flowrate was $\sim 1.7 \text{ L h}^{-1}\text{m}^{-2}$. The reduction in permeate flux is attributed to membrane fouling and is commonly referred to in membrane literature as concentration polarisation. Once the flux reached $\sim 1.7 \text{ L h}^{-1}\text{m}^{-2}$ fluxes for both LB and synthetic medium remained similar over the next 24 hours decreasing to a final value of $1.56 \text{ L h}^{-1}\text{m}^{-2}$ (Fig. 7.1).

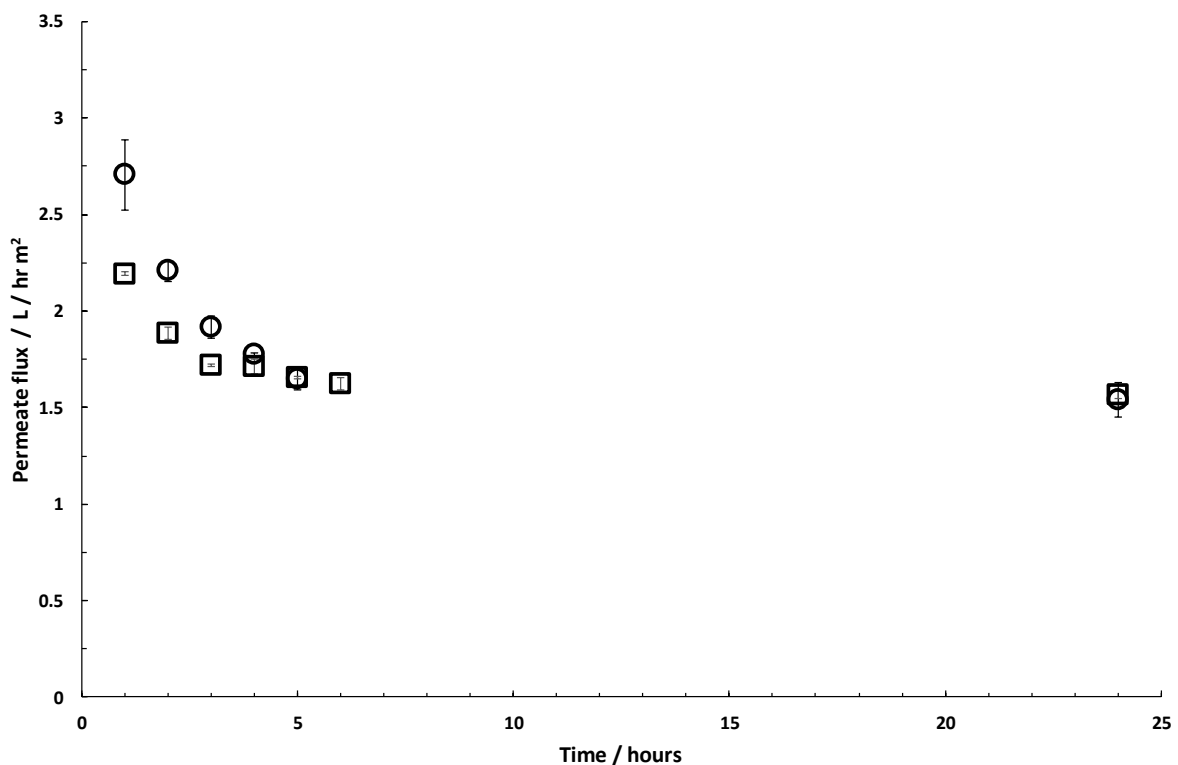


Figure 7. 1 Permeate fluxes for batch ultrafiltration of phage T3 lysates produced in LB (\square) or synthetic medium (\circ). Values are the average \pm SD (three technical repeats. Transmembrane pressure $\Delta P= 0.5 \text{ bar}$).

7.1.1.2. Reduction in endotoxin concentration by batch ultrafiltration for T3 phages produced in LB or synthetic medium

Swapping the growth medium with SM buffer during batch ultrafiltration using the 100 kDa membrane and keeping phage T3 in the retentate resulted in a significant decrease in the measured concentration of endotoxin in the retentate by $\sim 2 \log_{10}$. The phage T3 sample produced in LB had an initial endotoxin concentration of $\sim 7 \times 10^6 \text{ EU mL}^{-1}$ which decreased to $\sim 1.6 \times 10^5 \text{ EU mL}^{-1}$ after 24 hours of ultrafiltration

(Fig. 7.2). The endotoxin concentration in the phage T3 lysate produced in synthetic medium started at $\sim 4 \times 10^6$ EU mL⁻¹ and reduced to $\sim 9 \times 10^4$ EU mL⁻¹ (Fig. 7.2).

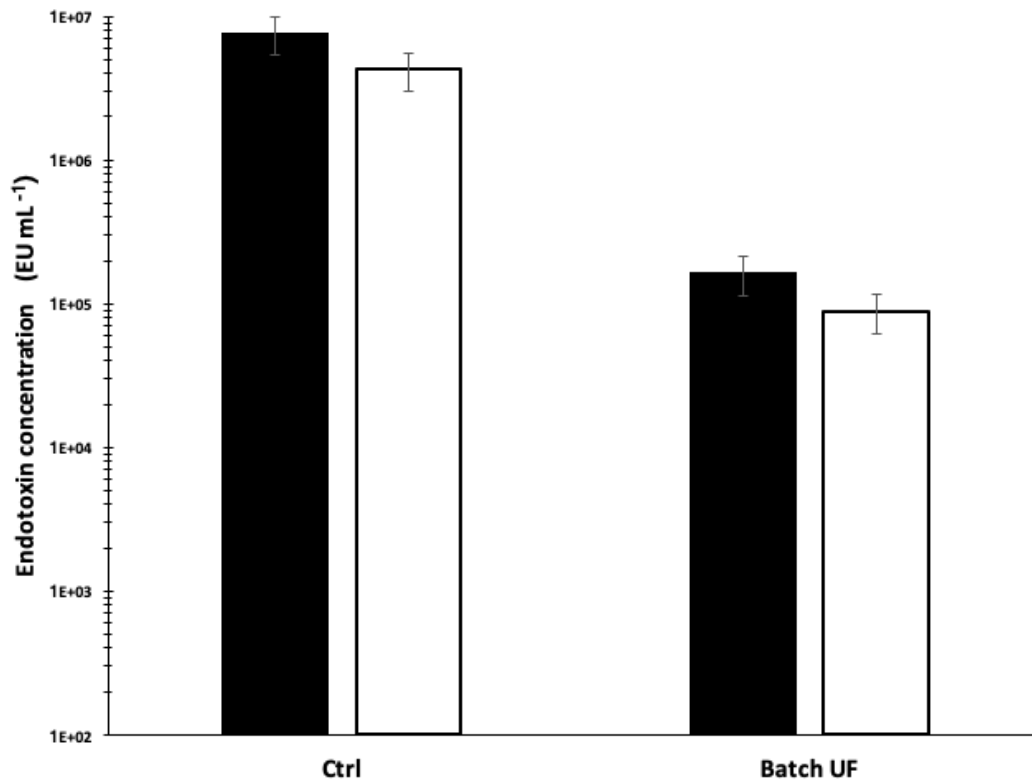


Figure 7. 2 Endotoxin concentration before and after batch ultrafiltration in LB broth (filled columns) and synthetic medium (empty columns). Endotoxin concentration is the average \pm SD (three technical repeats).

7.1.2. Purification of T3 phage lysate using diafiltration

7.1.2.1. Permeate flowrates of LB and Synthetic medium

Operating the ultrafiltration system in diafiltration mode (as mentioned in section 3.6.3.2) allowed fresh SM buffer to constantly replenish the liquid in the feed tank without change in the liquid level due to permeate passing through the membrane. Addition of fresh buffer ensured that the concentration of macromolecules retained in the retentate did not increase due to a volume reduction which may result in greater concentration polarisation at the membrane surface and affect the endotoxin filtration efficiency.

Diafiltration resulted in higher filtration rates for both LB broth and synthetic medium compared with batch ultrafiltration. Permeate fluxes were similar ~ 3 L h⁻¹m⁻² for both SM and LB after 1 hour of filtration and there was only a slight difference between the fluxes for LB and SM after 5 hours. After

24 hours of filtration, the permeate fluxes were similar for LB and synthetic medium, $\sim 1.6 \text{ L h}^{-1}\text{m}^{-2}$ compared to $1.5 \text{ L h}^{-1}\text{m}^{-2}$ (Fig. 7.3).

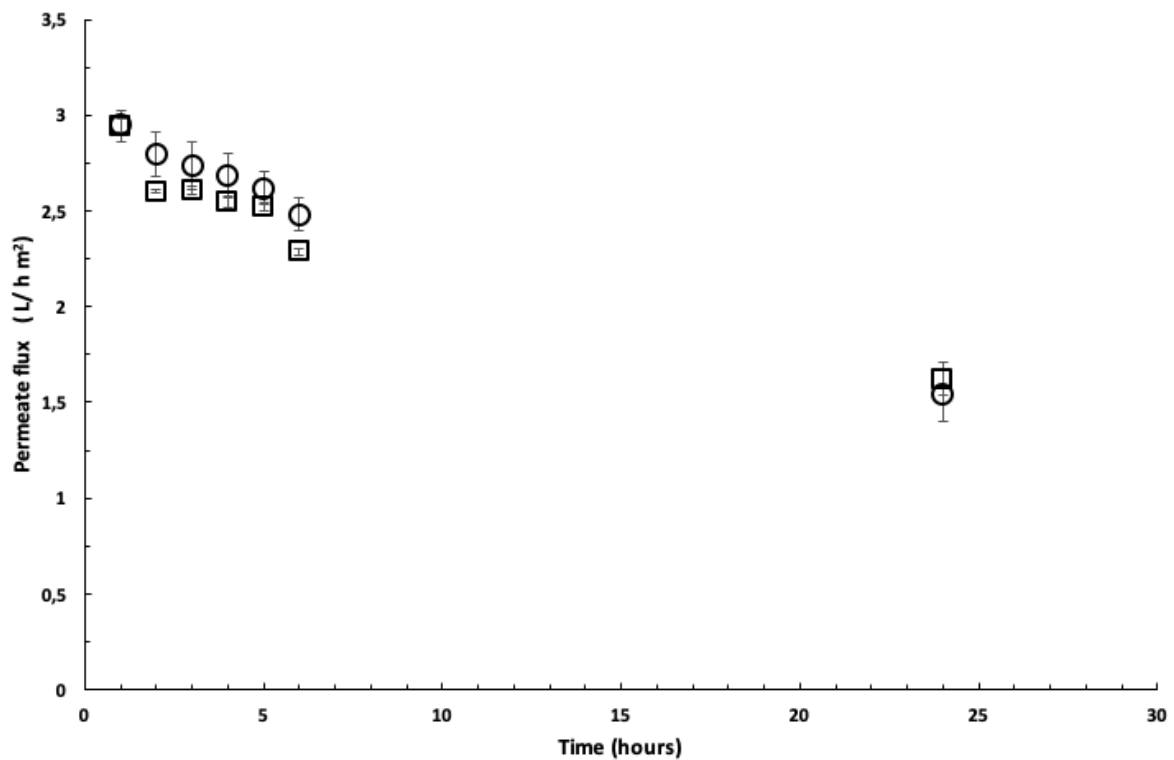


Figure 7. 3 Permeate fluxes for diafiltration of phage T3 lysates produced in LB (□) or synthetic medium (○). Values are the average of three technical repeats \pm SD. Transmembrane pressure $\Delta P= 0.5$ bar.

7.1.3. Comparison of endotoxin levels after diafiltration for LB and SM

Time series data was gathered for the endotoxin concentration (measured every hour) during the diafiltration process for LB and SM. A steep decrease in the solution endotoxin concentration was observed. Endotoxin concentration decreased from $\sim 1 \times 10^7 \text{ EU mL}^{-1}$ to $\sim 1 \times 10^5 \text{ EU mL}^{-1}$ with 2 hours of LB diafiltration. The rate of endotoxin removal decreased significantly following the initial drop and after 24 hours of diafiltration (~ 3 batch volumes of buffer exchanged) the concentration had reached $\sim 1 \times 10^4 \text{ EU mL}^{-1}$ (Fig. 7.4).

Endotoxin concentration in the synthetic medium lysate sample reached $\sim 1 \times 10^4 \text{ EU mL}^{-1}$ after 4 hours of diafiltration, corresponding to 2 diavolumes of SM buffer exchange, and did not decrease significantly thereafter even after 24 hours and 3 batch volumes of buffer exchange the final endotoxin concentration remained $\sim 8 \times 10^3 \text{ EU mL}^{-1}$.

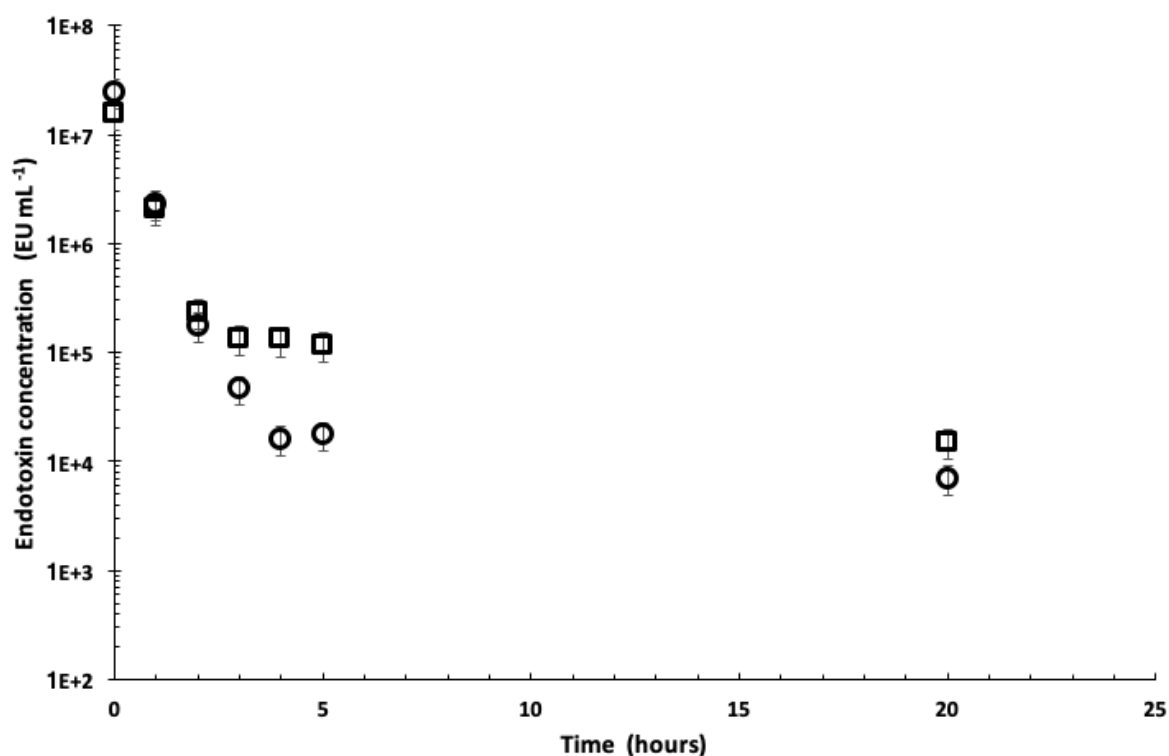


Figure 7. 4 Endotoxin concentration in LB lysate (□) and synthetic medium lysate during diafiltration (○). Values are the average of three technical repeats \pm SD.

7.2. Removal of endotoxin from T3 phage lysates using Liquid-Liquid extraction

Endotoxin removal from T3 lysates was evaluated using liquid-liquid extraction employing 1-octanol as the extractant organic solvent (Szermer-Olearnik and Boratyński, 2015). Phage T3 lysate was mixed with different volumes of 1-octanol, agitated on a shaking platform at 300 rpm for 1 hour and then separated from the organic phase (as described in section 3.7.1). Preliminary experiments were carried out to investigate the effect of different volume ratios of octanol: lysate, contact time and multiple exchanges of fresh organic solvent on residual aqueous endotoxin concentration in the lysate.

7.2.1. Effect of different volume ratios of octanol: lysate on endotoxin removal

Different volume ratios of octanol: lysate (phage T3 in LB) were mixed together for 3 hours and the residual aqueous endotoxin concentration was measured at the end of the contact time (as described in section 3.7.1). When 4.5 mL of octanol was contacted with 0.5 mL of LB lysate (i.e. 90 % v/v octanol) the concentration of endotoxin in the lysate was reduced to $\sim 1 \times 10^2$ EU mL⁻¹. Using different octanol

volume fractions (80 % v/v, 40 % v/v, 20 % v/v and 10 % v/v) the final endotoxin concentration ranged between 6×10^2 EU mL⁻¹ and 1×10^3 EU mL⁻¹.

Differences in endotoxin removal were observed if the sample was phage T3 in LB lysate or if it was previously purified and swapped in buffer by UF in batch. The initial concentration of endotoxin was different: $\sim 1 \times 10^7$ EU mL⁻¹ in the lysate and $\sim 1 \times 10^5$ EU mL⁻¹ for the purified sample. However, the final measured endotoxin concentration in the aqueous phase was of the same order regardless of the initial endotoxin concentration. Employing 90 % v/v, the final endotoxin concentration reached $\sim 4 \times 10^2$ EU mL⁻¹, while at different octanol concentrations in the final volume (80 % v/v, 40 % v/v, 20 % v/v and 10 % v/v) the endotoxin concentration was between 2×10^3 EU mL⁻¹ and 4×10^3 EU mL⁻¹ (Fig. 7.5).

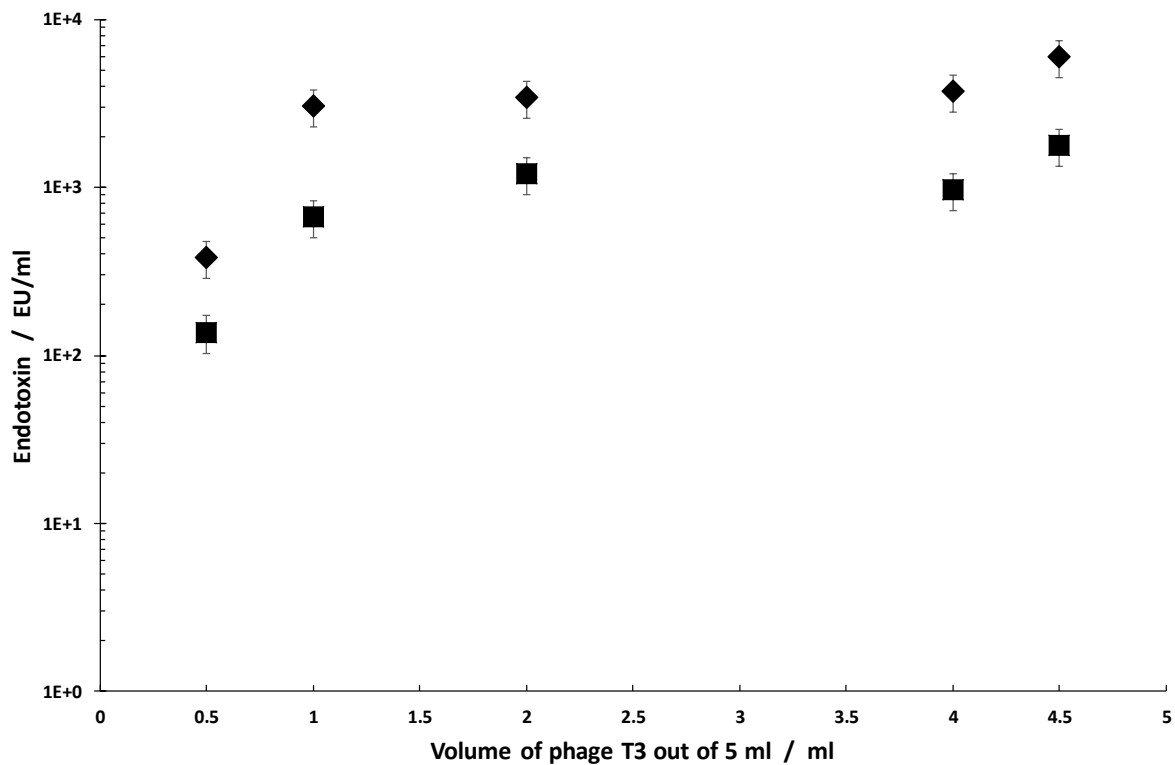


Figure 7. 5 Endotoxin concentration after liquid-liquid extraction using different volume ratios of 1-octanol/phage T3. Filled squares (■) represent endotoxin concentration in phage T3 lysates and filled diamonds (◆) represent endotoxin concentration in phage T3 after batch UF. Endotoxin concentration is the average \pm SD (three technical repeats).

7.2.2. LLE using multiple equilibrium stages

The volume ratio between the aqueous (containing phage lysate) and the organic phases was kept constant at 50:50. Following initial contact (equilibrium stage 1), the retentate aqueous phase was separated from the 1-octanol extract phase and mixed with fresh pure 1-octanol (equilibrium stage 2) and agitated again for a period of 3 hours. The separation of the aqueous phase and contact with fresh solvent step was repeated for a total of 4 times (i.e. 4 equilibrium stages were employed connected in cross-current mode). In the first extraction stage, the endotoxin concentration decreased by ~ 3 \log_{10} , from $\sim 1 \times 10^7$ EU mL⁻¹ to $\sim 5 \times 10^3$ EU mL⁻¹, in the second it was lowered further and reached $\sim 3 \times 10^2$ EU mL⁻¹, however subsequent extraction using a third and fourth extraction stage did not result in any further reduction in the endotoxin concentration (Fig. 7.6).

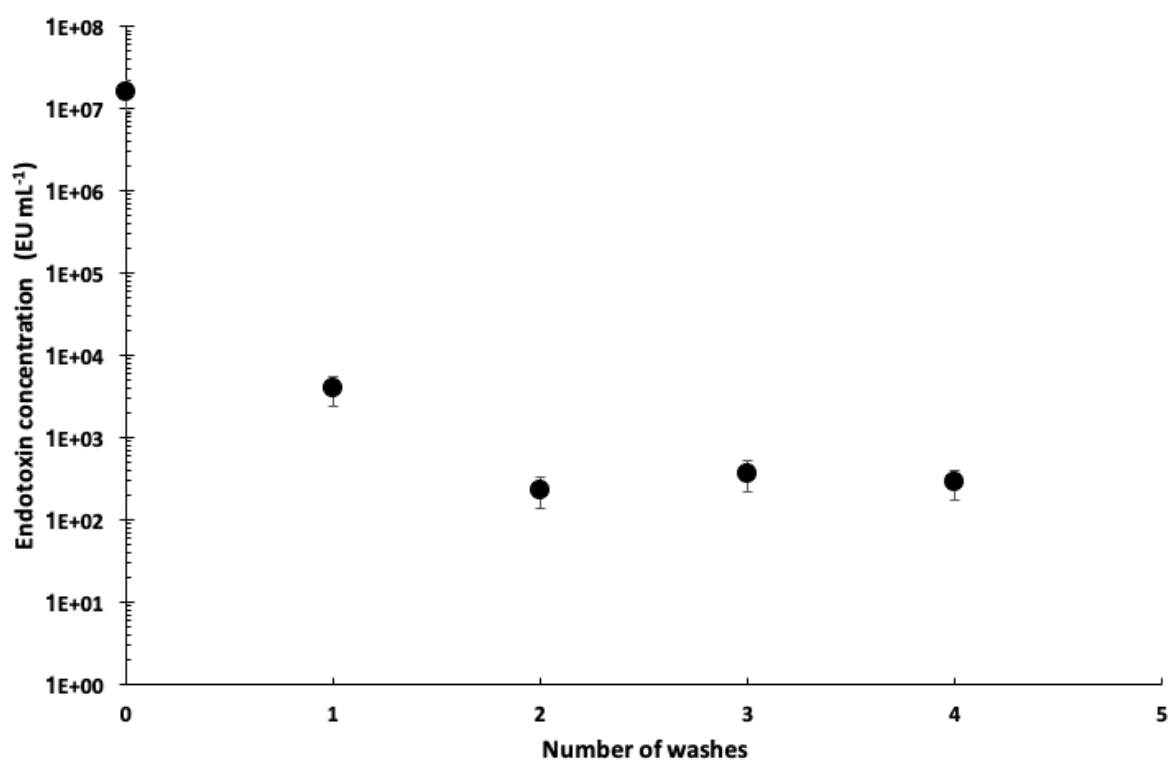


Figure 7. 6 Endotoxin concentration in phage T3 lysate after multiple liquid-liquid extraction cross-current equilibration steps. Endotoxin concentration is the average \pm SD (three technical repeats).

7.2.3. LLE using multiple equilibrium stages using higher mass transfer mixing

Improving the interfacial mass transfer area to facilitate endotoxin exchange between the aqueous and octanol phase was achieved by mixing the aqueous phase with an equivalent volume of octanol in an agitated vessel. Time series data was collected to investigate the rate of endotoxin removal from the aqueous phase with a starting initial endotoxin concentration of $\sim 5 \times 10^3$ EU mL⁻¹. An initial phage

lysate was diluted in SM buffer 1:1000 to have an initial LPS concentration of $\sim 1 \times 10^3$ EU mL⁻¹ and then mixed with 1-octanol (50:50 v/v) for 20 hours and samples were taken at regular time intervals and endotoxin concentration was measured.

After 1 hour the LPS concentration reached $\sim 1 \times 10^3$ EU mL⁻¹ and did not subsequently decrease significantly reaching $\sim 7 \times 10^2$ EU mL⁻¹ after 6 hours of contact and thereafter remaining at this level after 20 hours (Fig. 7.7).

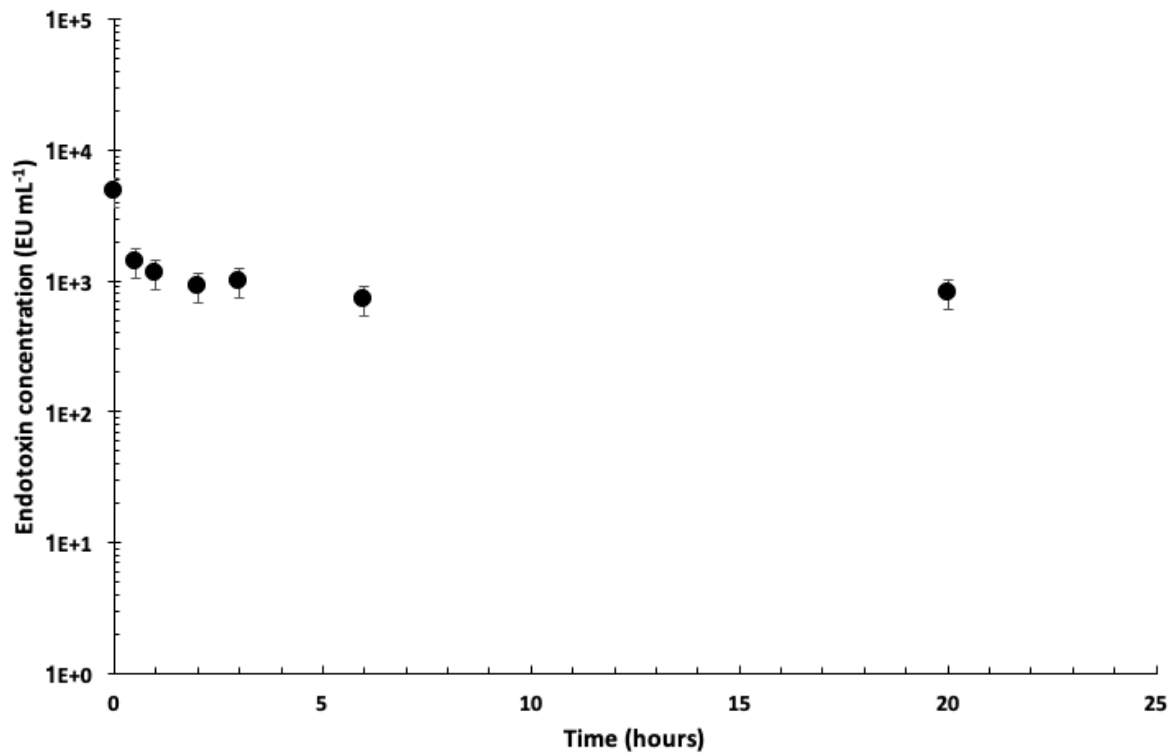


Figure 7. 7 Endotoxin concentration in phage T3 lysate over time using enhanced mixing. Values are the average of three technical repeats \pm SD.

7.3. Measurement of aggregation of T3 phages in the presence of endotoxin

The phage T3 sample purified using batch UF had a residual endotoxin concentration of $\sim 10^5$ EU mL⁻¹. Nanoparticle tracking analysis (NTA) measurements (using Malvern NanoSight, described in section 3.4.6) showed that the sample had a wide size distribution, ranging from 150 nm to 900 nm. Cryo-TEM images confirmed that aggregates of phage T3 clusters were present in solution (Fig. 7.9). Samples that had undergone diafiltration (either phage T3 produced in LB or SM) had a final endotoxin concentration of 10^4 EU mL⁻¹. NTA measurements showed a narrower peak at 180 ± 52 nm for phage T3 sample purified from LB using diafiltration. Finally, the phage T3 sample purified by LLE using 1-octanol showed the lowest endotoxin concentration $\sim 10^2$ EU mL⁻¹ and NTA measurements showed that the sample had a peak $\sim 65 \pm 46$ nm (Fig. 7.8).

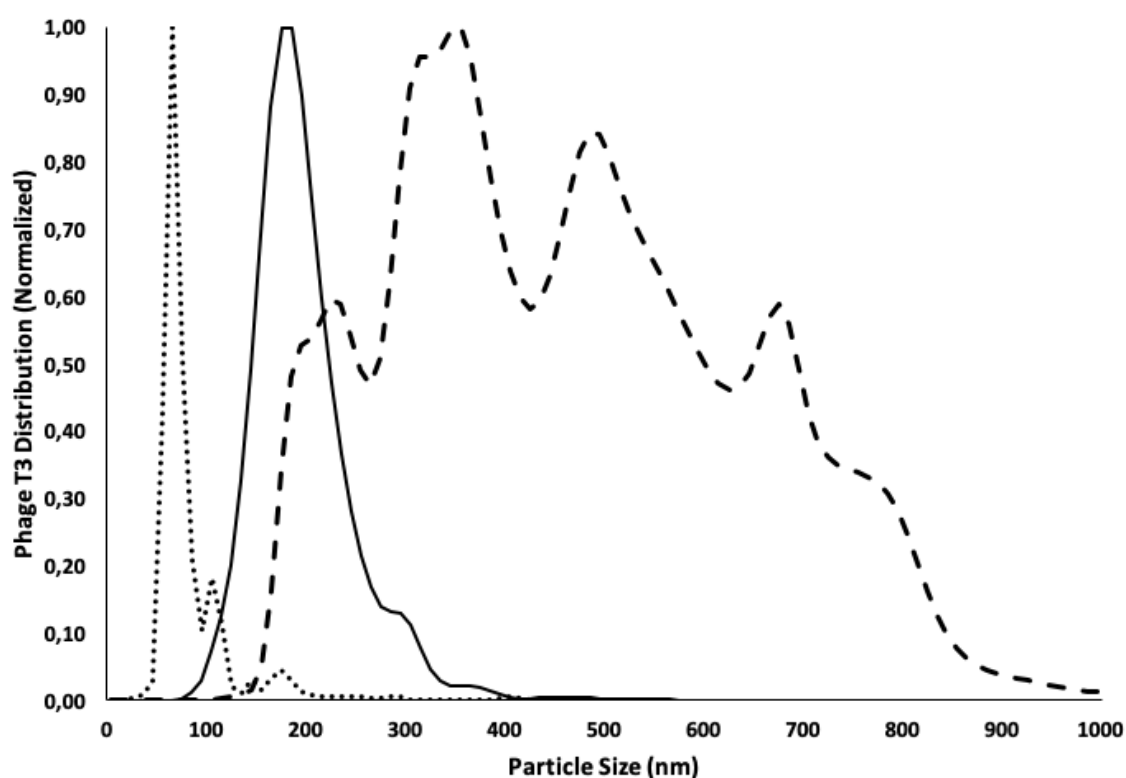


Figure 7. 8 Size distribution and aggregation state of phage T3 samples after different purification methods: liquid-liquid extraction in 1-octanol (dotted line), diafiltration (continuous line) and batch ultrafiltration (dashed lines).

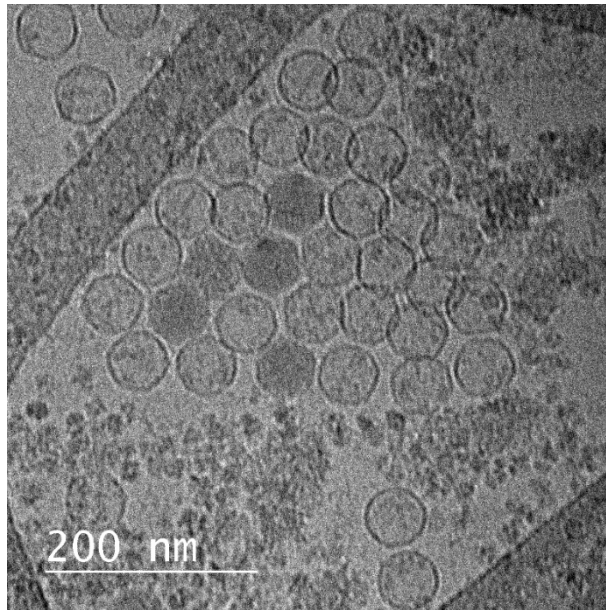


Figure 7. 9 Cryo-TEM image of phage T3 after batch ultrafiltration.

If the purest sample of phage T3, the one after LLE, is mixed with pure lipopolysaccharide (LPS) endotoxin (1 mg mL^{-1} corresponds to $\sim 10^6 \text{ EU mL}^{-1}$) the phage T3 peak at 55 nm was seen to disappear suggesting aggregation of phages. The sample showed a similar distribution to the UF batch sample (Fig. 7.10).

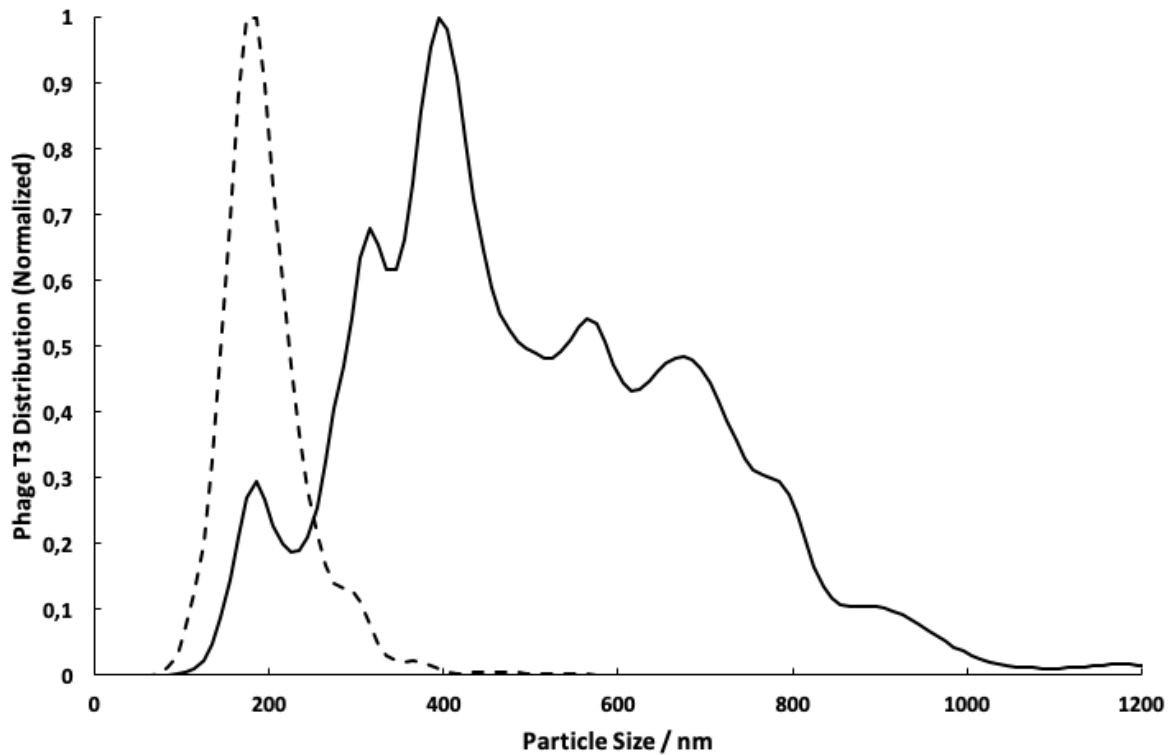


Figure 7. 10 Particle size distribution and aggregation state of phage T3 sample, before (dashed line) and after diafiltration followed by addition of pure endotoxins (continuous line).

7.4. Removal of endotoxin from phage lysates using anion exchange resins

7.4.1. Ion exchange equilibrium isotherm data

Ion exchange equilibrium adsorption isotherms were obtained for T3 binding to a strong anion exchange quaternary amine (QA) resin (as described in sections 3.8.2 and 3.8.3). Binding of phage T3 samples purified using diafiltration were compared with crude lysates. Interact of endotoxin with quaternary amine (QA) resin was measured.

The adsorption of pure LPS to the QA resin was measured and equilibrium adsorption isotherm data plotted. The isotherm was found to be linear (log-log plot) up to 5×10^8 EU g^{-1} before the resin was saturated (Fig. 7.11). This suggests that ion exchange chromatography could be used as a polishing step to remove endotoxin from phage lysates samples.

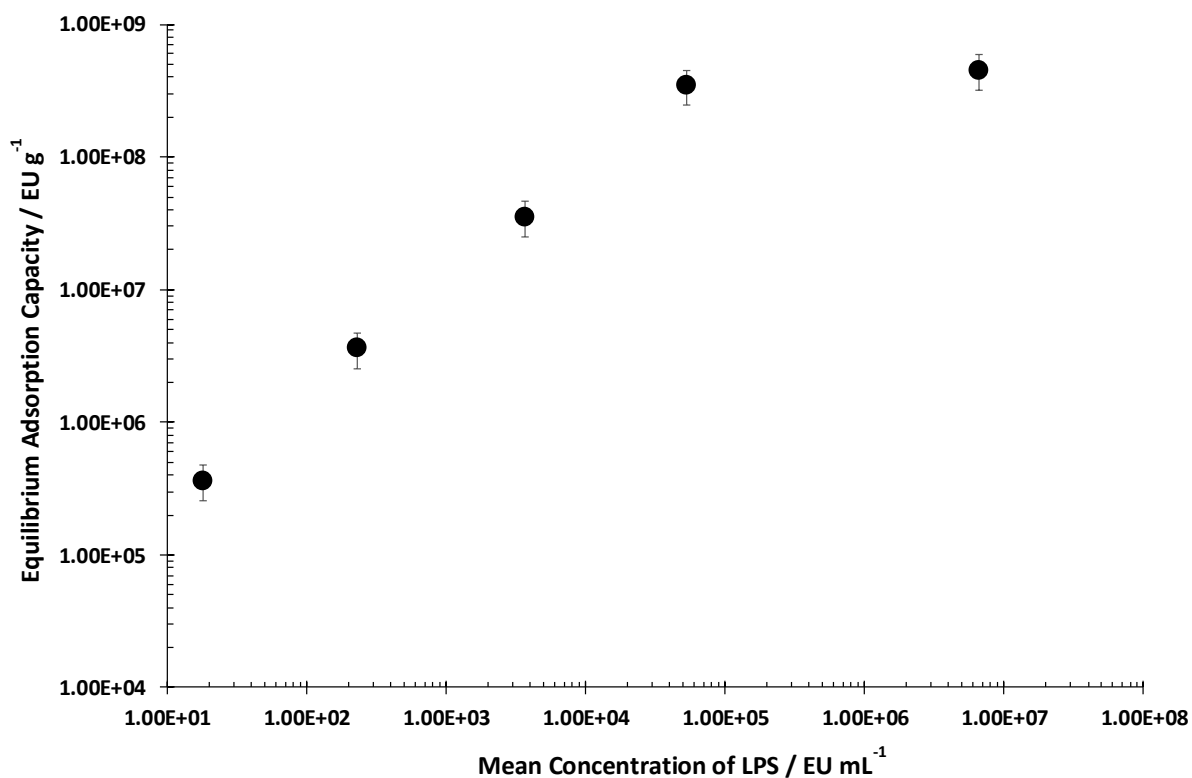


Figure 7. 11 Isothermal curves of adsorption of pure LPS to QA resin. Values are the average \pm SD of three technical repeats.

The equilibrium adsorption capacity of phage T3 purified in different ways was measured using a quaternary amine (QA) resin. The adsorption capacity was measured for the crude lysate from LB broth (reported in chapter 6) and also for T3 samples purified using diafiltration. Phage binding to the resin for the sample purified using diafiltration was compared with the same sample spiked with LPS to see its effect on phage-resin interaction.

The isotherms were found to be linear (log-log plot) and did not saturate the resin over the phage concentration range explored during experimentation. Phages purified using diafiltration showed lower adsorption in comparison with the same sample spiked with LPS. This suggested interaction between the endotoxin bound phage and the resin. Higher levels of other contaminants competing with the anion exchange binding sites may explain the lower binding of phage for the crude samples (Fig 7.12).

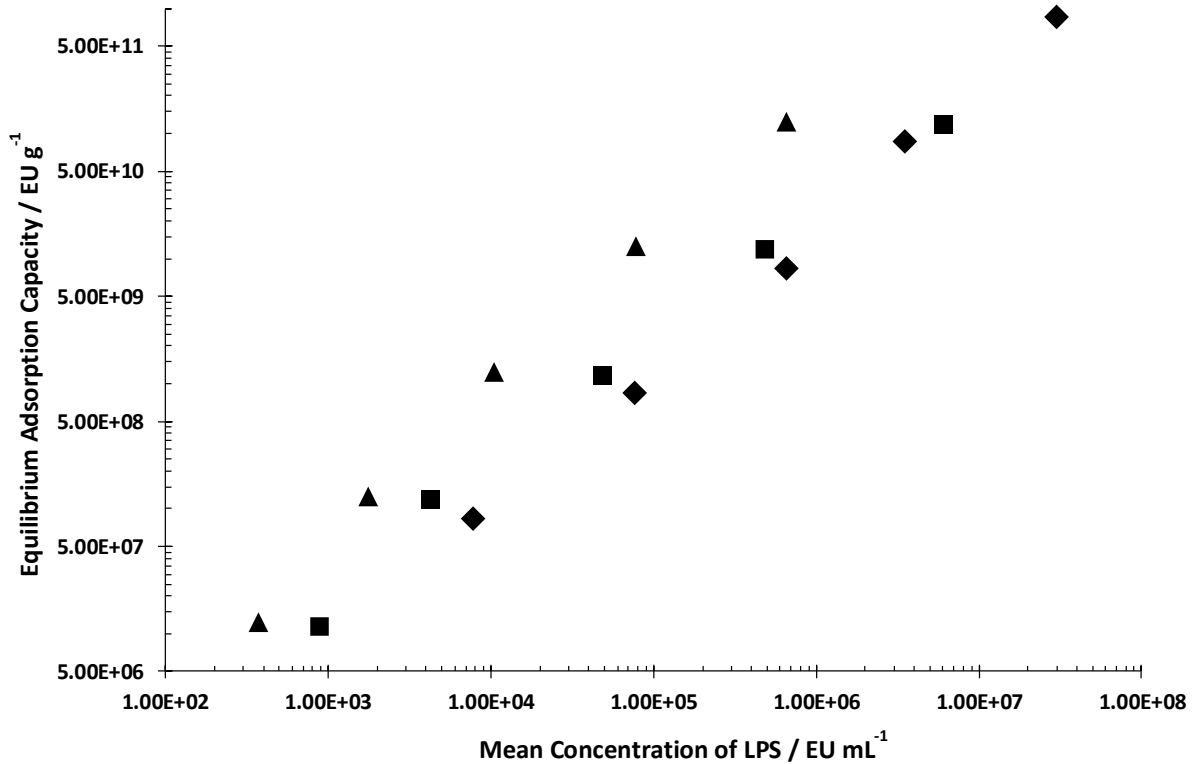


Figure 7. 12 Isothermal curves of adsorption of different phage T3 samples to QA resin. The black diamonds (◆) represent the phage T3 lysate, the black squares (■) the diafiltrated T3 and the black triangles (▲) represent the diafiltrated sample + LPS.

The presence of LPS in the sample affects phage binding to the QA resin (Figs. 7.12). Removal of endotoxin using QA ion exchange chromatography may permit separation of phage from endotoxin including endotoxin bound to the phage using a reverse chromatography approach. To test this hypothesis, phage T3 sample purified using LLE (with endotoxin concentration $\sim 10^2$ EU mL⁻¹) was loaded onto a QA ion exchange column (as described in section 3.8.2). Elution was performed with a step-wise gradient elution using two 0.5 M steps to 1 M of NaCl – and the elution fractions were assayed for LPS and phage presence.

During the loading phase, T3 phages were found not to bind to the QA resin and were eluted in the void volume. The LPS concentration in these samples remained the same perhaps due to phage bound endotoxin being dragged with the phage.

Endotoxin was found to elute using the 0.5 M NaCl gradient revealing a total amount of endotoxin of 9×10^3 EU and a further 1×10^3 EU eluted using the 1M NaCl gradient. This suggested that the concentration of endotoxin was $\sim 2 \log_{10}$ higher than originally measured in the initial sample loaded onto the column (Fig. 7.13).

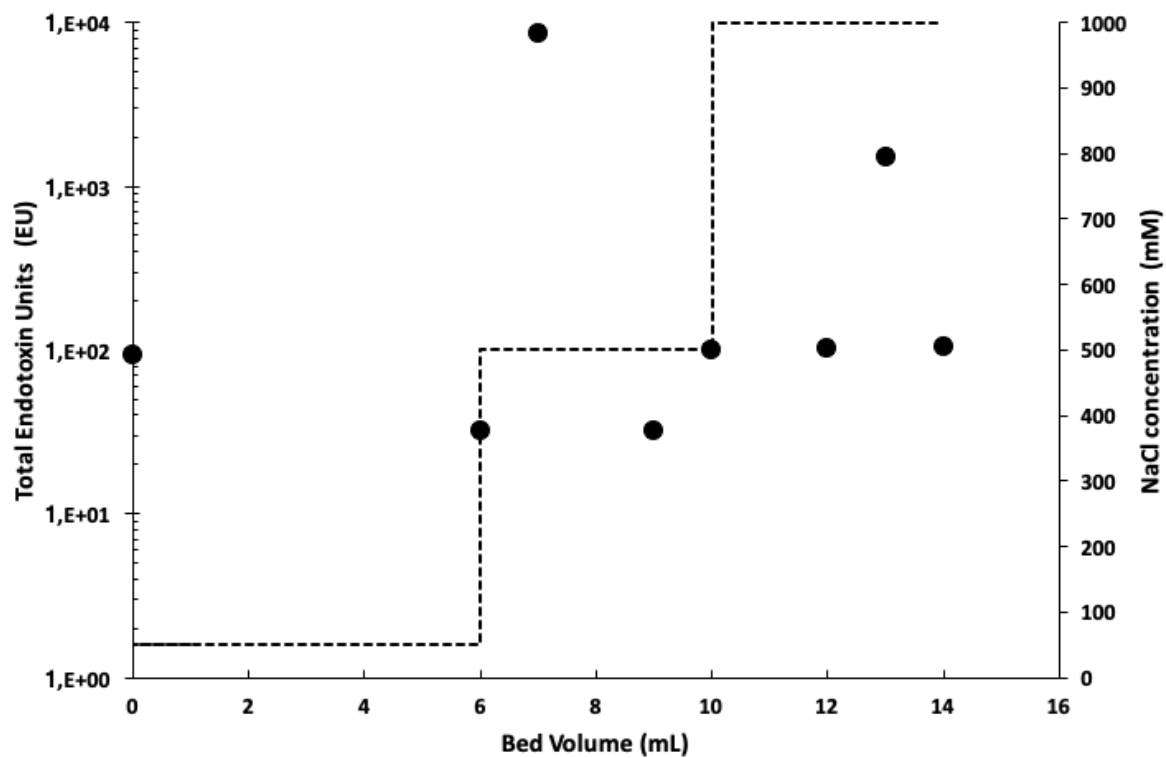


Figure 7. 13 Loading and elution of phage T3 sample (after LLE) and endotoxin from QA ion exchange column. Filled circles (●) represent endotoxin units (EU) and the dashed line the NaCl concentration.

7.5. Discussion

Batch ultrafiltration is a way of purifying phage lysates and it is increasingly being recognised as a standard unit operation in the downstream purification process flow sheet for phage purification. The process is highly scalable and is able to cope with a high volumetric capacity operating either semi-continuously or in batch mode as tangential flow filtration. Concentration polarisation results in membrane fouling and reduction in the operating performance including lower membrane permeate flux and reduction in the endotoxin removal rates over time which necessitates regularly stopping the process and cleaning of the membrane to regenerate the membrane surface. Over time the membrane performance degrades, and the membrane needs replacement.

Operating the process in diafiltration mode reduces the degree of concentration polarisation and allows better removal of endotoxin. Continuous addition of fresh buffer helps to dilute the feed impurities allowing better permeation through the membrane reducing the rate of membrane fouling and improving the overall process performance.

The most obvious benefits of diafiltration include higher filtration rates which reduces the process cycle time. Alternatively, operation at lower transmembrane pressures would allow improvement in separation performance. Major impurities such as intracellular host proteins and nucleic acids can easily be removed using a 100 kDa membrane and diafiltration gave better results for the removal of endotoxin from the lysates achieving endotoxin reduction in less time compared with batch ultrafiltration. Using batch ultrafiltration the decrease in endotoxin was ~ 2 log compared with ~ 3 log reduction using diafiltration.

Operating the membrane separation step under dilute conditions (favoured by diafiltration) may reduce the tendency of endotoxins to aggregate and form micelles which would not pass through a 100 kDa MWCO membrane and remain with the phage in the retentate (Petsch and Anspach, 2000). Diafiltration allowed operation at low ionic strength, preventing the formation of excessively big micelles (Li and Luo, 1998) and it leading to better endotoxin removal.

Differences between filtration rates were observed for phages in a complex medium like LB broth or using a synthetic medium (SM). Higher filtration rates were observed for synthetic medium compared with LB using batch ultrafiltration, however, both eventually showed similar filtration fluxes and the final endotoxin concentration achieved in the samples was similar.

Important differences were observed between LB and synthetic medium using diafiltration. Although the final endotoxin concentration in the purified retentate from LB and synthetic medium was $\sim 10^4$ EU mL⁻¹ faster removal rates were observed for the synthetic medium lysate taking ~ 4 hours of

filtration time, while for the LB sample it took around 24 hours of diafiltration to get to the same final concentration. Reduction in process cycle times may be an important advantage during industrial production of phages.

Diafiltration seems to be a good method for reducing a significant proportion of the endotoxin load from crude lysates whilst also removing intracellular proteins and other dissolved contaminants that are permeable to the membrane. Liquid-liquid extraction (LLE) using 1-octanol may subsequently be used to reduce endotoxin concentration further to reach the 5 EU mL⁻¹ target limit (Szermer-Olearnik and Boratyński, 2015). This method seems well-suited for endotoxin polishing and can easily be scaled-up; further work is however needed to investigate LLE equilibria and mass transfer kinetics to allow design of suitable contacting units employing cross-current or counter-current contacting arrangements. Preliminary data reported here showed the effect of contact time, volume of solvent and number of extraction steps on endotoxin reduction using phage T3. For phage T4 in previous studies showed that after LLE with octanol the endotoxin concentration could be reduced to below the 5 EU mL⁻¹ threshold limit. In the case of phage T3, multiple equilibrium stages may be required to achieve the same results, due to endotoxin bound to the phage which re-equilibrates with the solution. Using a ratio of 1-octanol to phage T3 90:10 v/v the final concentration of endotoxin in the phage sample was reduced to ~10² EU mL⁻¹. The rate of endotoxin mass transfer was quite fast using the well-mixed contacting system (stirred tank) – with a few hours the transfer was complete, and equilibrium was reached between the phage bound endotoxin, endotoxin in solution and endotoxin in octanol. Simple dilution of phage containing endotoxin solutions using a buffer resulted in re-equilibration of the endotoxin (Fig. 7.6).

There is a difference between two experiments that is interesting: in the sections 7.2.2 and 7.2.3, as showed in figures 7.6 and 7.7, despite in both the initial LPS concentrations were ~5x10³ EU mL⁻¹, the concentrations after different ways of LLE were different. This can be explained by the differences in the sample: in figure 7.6 the initial endotoxin concentration was the result of a previous LLE extraction, while in figure 7.7 it was the result of a simple dilution from a more concentrated sample. So, the initial LPS concentration measured in figure 7.6 was closer to the real amount of LPS in the sample, while the initial concentration measured in figure 7.7 is the lower than the real one and is the result of the equilibrium reached between phages and endotoxins. This was the first evidence of the presence of more endotoxin units that the LAL kit could not detect because of the interaction between phage T3 and LPS. Final endotoxin concentrations are reported in table 7.1.

Purification Method	Final Endotoxin concentration (EU ml ⁻¹)	
	LB	SM
Lysate (t0)	7x10 ⁶	4x10 ⁶
Batch Ultrafiltration	1.5x10 ⁵	9x10 ⁴
Diafiltration	1x10 ⁴	8x10 ³
Liquid-liquid Extraction (octanol)	1x10 ²	1x10 ²
LLE + Ion Exchange Chromatography	50	50

Table 7.1 Final concentrations of endotoxins before and after different purification methods.

Nanoparticle tracking analysis (NTA) measurements showed that phage T3 aggregates at high concentrations and is monodispersed when diluted at lower concentrations (Cinquerrui et al., 2018). It is known from literature that endotoxin molecules may facilitate the formation of bridges between proteins and LPS might be the cause of aggregation of phage T3 (Li and Luo, 1998; de Oliveira Magalhães et al., 2007). Dynamic light scattering was used to assess changes in the phage sample size distribution by keeping the concentration of phage T3 above 10⁹ PFU mL⁻¹, but after removing most of the endotoxins, although at different levels. Phage T3 was seen to be monodispersed after LLE with octanol: the major peak was found at 65 nm and there was a smaller one at 130 nm, suggesting that phage T3 sample was not seriously aggregated and either single or doublets of virions were present in the sample. Aggregation of phage T3 after batch ultrafiltration was confirmed using Cryo-TEM imaging: the sample had an endotoxin concentration of ~1x10⁵ EU mL⁻¹. Confirmation of the role of endotoxin in facilitating phage aggregation was shown by addition of pure LPS to a T3 phage sample (previously purified using diafiltration). The diafiltered sample initially showed a single peak at 220 nm. After mixing with pure LPS for 1 hour at 37°C, that peak at 220 nm disappeared, and the size distribution became significantly broader suggesting phage aggregation.

Aggregation of phages have previously been observed and discussed by researchers (Szermer-Olearnik et al., 2017). Phages aggregates were found to respond to different ionic concentrations; the phages had been purified using LLE extraction with 1-octanol (Szermer-Olearnik et al., 2017). In the present work, aggregation is reported in a previous purification step and aggregates are broken in a different way.

The LPS adsorption isotherm showed significant endotoxin binding at pH 7.2 ± 0.2 to quaternary amine (QA) resins. Phage T3 binding to the QA resin depended on the presence of impurities such as host cell proteins and LPS competing with phages for the binding sites. Phage T3 sample purified using diafiltration with low residual endotoxin was found not to bind to the QA. Phage bound endotoxin

may play a role in phage binding to the QA functional groups. Addition of LPS to the diafiltered phage sample increased phage binding to the QA resin by $\sim 1 \log_{10}$. It is proposed that phage T3 does not bind to QA by itself, LPS bound to the phage is responsible for this interaction (Fig. 7.14, shows a model of the interaction between LPS, phage T3 and QA resin).

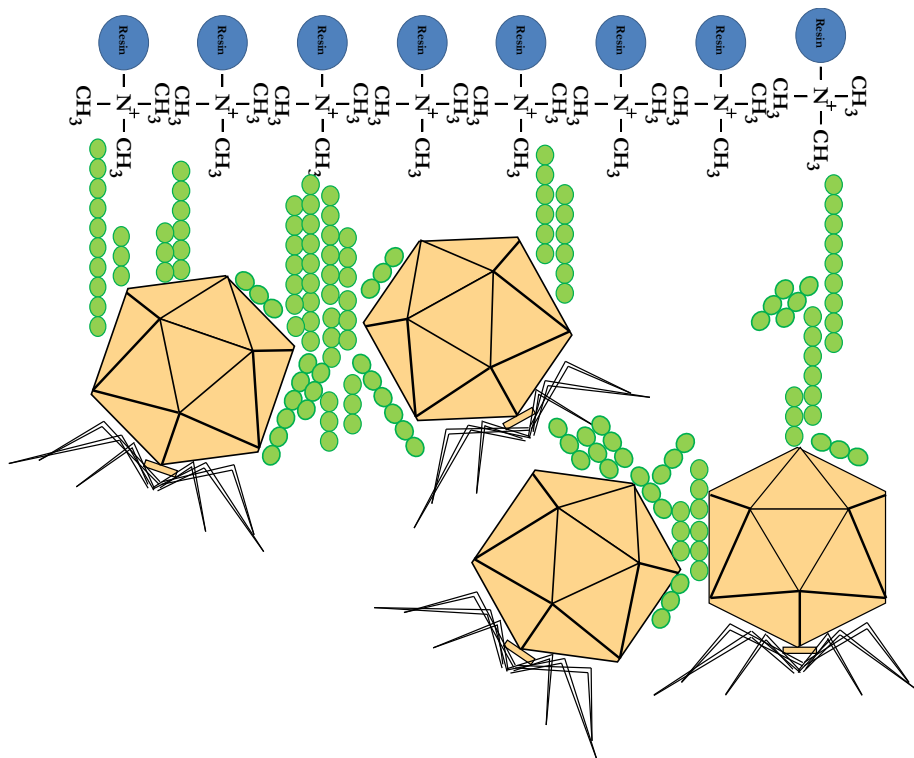


Figure 7. 14 Schematic model of interaction between phage T3, LPS molecules (green circles) and QA resin.

The LLE purified phage T3 sample with a low concentration of endotoxin ($\sim 10^2$ EU mL⁻¹) was found not to bind to the QA resin due to the role of endotoxin in facilitating interaction between the phage and the resin functional groups. This suggests that “negative chromatography” may be used to facilitate the removal of phage from endotoxin containing samples. Phage T3 sample purified using LLE was loaded on a QA anion exchange column. The phage did not bind to the resin and passed through the column in void volume. The amount of LPS in the collected phage sample was found to be the same as that in the original feed sample. Also, a much higher amount of endotoxins ($\sim 10^4$ EU) were eluted from the column using step-wise NaCl gradients using 0.5M and 1M steps. This result supports earlier findings reported in literature where it was noted that after performing LLE using 1-octanol, there was a higher concentration of LPS in the organic phase than present in the original solution (Szermer-Olearnik and Boratyński, 2015). The results reported here suggest that phage T3 has endotoxin bound to it, that are not detectable by the LAL test, but still present in the sample and which was removed

by the anion exchange resin during reverse chromatography. This effect may be exploited as a final polishing step in the purification of phages.

In summary, this chapter provides important data on the suitability of methods for endotoxin reduction from crude phage lysates. The benefits of using a synthetic medium rather than a complex medium were shown using ultrafiltration operated in diafiltration mode. Diafiltration is able to remove intracellular proteins and DNA and allows buffer exchange as well as reducing endotoxin concentration from $\sim 10^7$ EU mL⁻¹ in the crude lysate to less than 10^4 EU mL⁻¹. LLE using 1-octanol as the extracting solvent is capable of reducing endotoxin concentration from 10^4 EU mL⁻¹ following diafiltration to $\sim 10^2$ EU mL⁻¹. QA anion exchange may be used as polishing step to remove endotoxin but further investigation is needed to elucidate the role of endotoxin bound to the phage and its interaction with the QA functional groups.

8. Conclusions and Future Work

This thesis focused on bioprocessing of antimicrobials, such as the recombinant protein colicin E9 and especially bacteriophages, phage K and T3. They are all potential alternatives to antibiotics but, in the past, little attention has been put on the large-scale production and purification of phages and bacteriocins. Bacteriophages show more potential and they are far ahead on the way to be used in the future as the clinical trials currently ongoing.

Issues relative to upstream and downstream processes have been highlighted, such as poor titre when a too high MOI is used or when continuous production is carried out using a chemostat setting. Different ways to overcome them have been proposed: overall, one of the main problems for continuous production of phages – the low yield – was overcome thanks to the new layout with three reactors here proposed, reaching a production of 2×10^{11} PFU mL⁻¹, the same concentration reached for batch productions.

Besides, continuous production of recombinant protein colicin E9 was performed and the same concentrations of complex media, 1 mg mL⁻¹, were achieved using a chemically defined medium. These were important achievements towards the scaling-up of production of bacteriophages and recombinant proteins, because continuous processing allows large scale production with a small footprint.

Furthermore, ultrafiltration was demonstrated to be a useful method to polish phage samples before chromatography, allowing on average a binding to the resin of $1 \log_{10}$ higher compared with the crude lysate. Another main problem in phage purification – endotoxin contamination – was addressed using liquid-liquid extraction, reaching 1×10^2 EU mL⁻¹ and new insights about LPS-phage T3 interaction were proposed: a phage sample purified from endotoxins has a polydispersity closer to 1 compared with samples with a higher concentration of LPS.

Results showed here are all about model protein/viruses and above them all, major attention has been put on phage T3. Further work needs to be done to confirm these results with other proteins and phages and to build a model and a platform that could be used for any phage or protein.

8.1. Future work

8.1.1. Bacteriocins

8.1.1.1. Production

In chapter 4 a synthetic medium (SM) was used to produce colicin E9, giving good results but still not as good as when using a complex medium. Future work should focus on improving the composition of SM and to find even better conditions for improving *E. coli* growth rates thus improving production and yields of colicin E9.

One of the paths to follow when improving medium recipe could be to test the autoinduction defined medium, in which glycerol and lactose and glucose are used as carbon sources. An autoinduction defined medium exploits the catabolite repression of *E. coli*, which uses firstly the glucose and the glycerol to rapidly grow. Finally, when these carbon sources are consumed, *E. coli* uses lactose and the Lac operon inside the cells is activated (Studier, 2005).

8.1.1.2. Purification

Chapter 4 dealt with purification of colicin E9 and showed how different production media can influence the purification process. Future work will involve the scale-up of purification, starting from using larger affinity columns. Expanded bed chromatography could be used, as it is effective on viscous samples and crude extracts (Lali, 2002).

8.1.2. Bacteriophages

8.1.2.1. Production

Chapter 5 showed production of phages in batch mode, using shaking flasks and bioreactors and production in continuous mode using new settings. Most of the recent papers dealing with continuous production of phages used two reactors connected in series (Nabergoj et al., 2018; Storms, 2012) and in this thesis, three reactors were used. Future work should prove that the three-stages continuous production is a method of producing phages that can be used for other lytic phages. Furthermore, the first two reactors were mostly studied as they influence the most the outcome of the production and in the future work better understanding of the process, especially in the 3rd reactor should be achieved. Furthermore, optimizing the synthetic medium used, minimizing the concentration of reagents but maintaining the high final titre.

Here, the only quality check on the new phages produced was the spot test: new T3 phages were always able to infect the host strain. In the future work the genomic stability of the produced phages over time must be controlled to assure a uniform and constant product.

8.1.2.2. Purification

Ultrafiltration using 100 kDa flat sheet membranes was one of the most exploited methods for purifying phages as showed in chapter 6 and 7. Improvements of binding capacity to an ion exchange resin after UF were demonstrated for phage K. Future work should focus on analysing the effects of UF on chromatography using membranes with larger pores, i.e. between 300 kDa and 750kDa.

UF was used along liquid-liquid extraction (LLE) to remove LPS from phage T3 samples. It was hypothesized that LPS molecules bind directly to phage T3 by combining LLE and ion exchange chromatography data. It will be interesting to assess if the LPS-phage interaction is a constant for phages produced from Gram-negative hosts and if there is correlation between different species such as *Salmonella*, *Pseudomonas* or *Klebsiella* which are the main antibiotic resistant bacterial pathogens clinicians are facing.

In chapter 7 the best method to remove octanol was dialysis in ethanol, but it has many limitations as it is not scalable, ethanol is likely going to decrease viability of phages. Alternatives to dialysis, such as chromatography, should be investigated. This will be useful to design a process flowchart that could be used for all phages, to assess if it is better to start with ultrafiltration and then using LLE and then removing octanol using ultrafiltration again or using first LLE and after removing octanol and exchanging buffer in one step by using diafiltration. LLE needs to be scaled up: in future work other methods for LLE can be used, such as counter current columns, which ensure a large volumes processing.

9. References

- Abedon, S.T. (2009). Kinetics of phage-mediated biocontrol of bacteria. *Foodborne Pathog. Dis.* 6, 807–815.
- Abedon, S.T. (2011). Lysis from without. *Bacteriophage* 1, 46–49.
- Abedon, S.T., Kuhl, S.J., Blasdel, B.G., and Kutter, E.M. (2011). Phage treatment of human infections. *Bacteriophage* 1, 66–85.
- Adam, O., Vercellone, A., Paul, F., Monsan, P.F., and Puzo, G. (1995). A nondegradative route for the removal of endotoxin from exopolysaccharides. *Anal. Biochem.* 225, 321–327.
- Adams Mark H. (1959). *Bacteriophages*. New York, Interscience Publishers.
- Aida, Y., and Pabst, M.J. (1990). Removal of endotoxin from protein solutions by phase separation using triton X-114. *J. Immunol. Methods* 132, 191–195.
- Akbar, B. J., and Jalal, K.C.A. (2010). Mechanism in the Clot Formation of Horseshoe Crab Blood during Bacterial Endotoxin Invasion. *Journal of Applied Sciences*, Vol. 10, 1930–1936.
- Amarillas, L., Lightbourn-Rojas, L., Angulo-Gaxiola, A.K., Basilio Heredia, J., González-Robles, A., and León-Félix, J. (2018). The antibacterial effect of chitosan-based edible coating incorporated with a lytic bacteriophage against *Escherichia coli* O157:H7 on the surface of tomatoes. *J. Food Saf.* e12571.
- Amons, R., and Schier, P.I. (1981). Removal of sodium dodecyl sulfate from proteins and peptides by gel filtration. *Anal. Biochem.* 116, 439–443.
- Asenjo, J.A., and Andrews, B.A. (2009). Protein purification using chromatography: Selection of type, modelling and optimization of operating conditions. *J. Mol. Recognit.* 22, 65–76.
- Assenberg, R., Wan, P.T., Geisse, S., and Mayr, L.M. (2013). Advances in recombinant protein expression for use in pharmaceutical research. *Curr. Opin. Struct. Biol.* 23, 393–402.
- Atterbury, R.J. (2009). Bacteriophage biocontrol in animals and meat products. *Microb. Biotechnol.* 2, 601–612.
- Balciunas, E.M., Castillo Martinez, F.A., Todorov, S.D., Franco, B.D.G. de M., Converti, A., and Oliveira, R.P. de S. (2013). Novel biotechnological applications of bacteriocins: A review. *Food Control* 32, 134–142.
- Baldwin, D., and Summer, N. (2012). Process for Continuous Production of Bacteriophage. US Pat.

8,252,519 2.

Bales, R.C., Hinkle, S.R., Kroeger, T.W., Stocking, K., and Gerba, C.P. (1991). Bacteriophage Adsorption during Transport through Porous Media: Chemical Perturbations and Reversibility. *Environ. Sci. Technol.* 25, 2088–2095.

Batas, B., and Chaudhuri, J.B. (1996). Protein refolding at high concentration using size-exclusion chromatography. *Biotechnol. Bioeng.* 50, 16–23.

Becht, N.O., Malik, D.J., and Tarleton, E.S. (2008). Evaluation and comparison of protein ultrafiltration test results: Dead-end stirred cell compared with a cross-flow system. *Sep. Purif. Technol.* 62, 228–239.

Becker, D., Selbach, M., Rollenhagen, C., Ballmaier, M., Meyer, T.F., Mann, M., and Bumann, D. (2006). Robust Salmonella metabolism limits possibilities for new antimicrobials. *Nature* 440, 303.

Behens, H.M., Six, A., Walker, D., and Kleantous, C. (2017). The therapeutic potential of bacteriocins as protein antibiotics. *Emerg. Top. Life Sci.* 1, 65–74.

Bertani, G. (1953). Lysogenic versus Lytic Cycle of Phage Multiplication. *Cold Spring Harbor Symposia on Quantitative Biology*, 18, 65–70.

Bertani, G., and Nice, S.J. (1953). Study on Lysogenesis. *J Bacteriol.* 67, 202–209.

Blondeau, K., Boze, H., Jung, G., Moulin, G., Galzy, P. (1994). Physiological approach to heterologous human serum albumin production by *Kluyveromyces lactis* in chemostat culture. *Yeast*, 10, 1297–1303.

Bonilla, N., Rojas, M.I., Netto Flores Cruz, G., Hung, S.-H., Rohwer, F., and Barr, J.J. (2016). Phage on tap—a quick and efficient protocol for the preparation of bacteriophage laboratory stocks. *PeerJ* 4, e2261.

Bononi, I., Balatti, V., Gaeta, S., and Tognon, M. (2008). Gram-negative bacterial lipopolysaccharide retention by a positively charged new-generation filter. *Appl. Environ. Microbiol.* 74, 6470–6472.

Boratynski, J., Syper, D., Weber-Dabrowska, B., Lusiak-Szelachowska, M., Pozniak, G., and Gorski, A. (2004). Preparation of endotoxin-free bacteriophages. *Cell. Mol. Biol. Lett.* 9, 253–259.

Bosák, J., Micenková, L., Hala, M., Pomorská, K., Kunova Bosakova, M., Krejci, P., Göpfert, E., Faldyna, M., and Šmajš, D. (2018). Colicin FY inhibits pathogenic *Yersinia enterocolitica* in mice. *Sci. Rep.* 8, 1–12.

- Bourdin, G., Schmitt, B., Guy, L.M., Germond, J.E., Zuber, S., Michot, L., Reuteler, G., and Brüßow, H. (2014). Amplification and purification of T4-Like *Escherichia coli* phages for phage therapy: From laboratory to pilot scale. *Appl. Environ. Microbiol.* 80, 1469–1476.
- Brandenburg, K., Mayer, H., Koch, M.H.J., Weckesser, J., Rietschel, E.T., and Seydel, U. (1993). Influence of the supramolecular structure of free lipid A on its biological activity. *Eur. J. Biochem.* 218, 555–563.
- Branston, S.D., Wright, J., and Keshavarz-Moore, E. (2015). A non-chromatographic method for the removal of endotoxins from bacteriophages. *Biotechnol. Bioeng.* 112, 1714–1719.
- Bull, J.J., Millstein, J., Orcutt, J., and Wichman, H. a (2006). Evolutionary feedback mediated through population density, illustrated with viruses in chemostats. *Am. Nat.* 167, E39–E51.
- Burcham, C.L., Florence, A.J., and Johnson, M.D. (2018). Continuous Manufacturing in Pharmaceutical Process Development and Manufacturing. *Annu. Rev. Chem. Biomol. Eng.* 9, 253–281.
- Burns, D.B., and Zydney, A.L. (1998). Effect of solution pH on protein transport through ultrafiltration membranes. *Biotechnol. Bioeng.* 64, 27–37.
- Burova, E., and Ioffe, E. (2005). Chromatographic purification of recombinant adenoviral and adeno-associated viral vectors: Methods and implications. *Gene Ther.* 12, S5–S17.
- Cademartiri, R., Anany, H., Gross, I., Bhayani, R., Griffiths, M., and Brook, M.A. (2010). Immobilization of bacteriophages on modified silica particles. *Biomaterials* 31, 1904–1910.
- Cairns, B.J., Timms, A.R., Jansen, V. a a, Connerton, I.F., and Payne, R.J.H. (2009). Quantitative models of in vitro bacteriophage-host dynamics and their application to phage therapy. *PLoS Pathog.* 5, 1–10.
- Canchaya, C., Fournous, G., Chibani-Chennoufi, S., Dillmann, M.L., and Brüßow, H. (2003). Phage as agents of lateral gene transfer. *Curr. Opin. Microbiol.* 6, 417–424.
- Capparelli, R., Parlato, M., Borriello, G., Salvatore, P., and Iannelli, D. (2007). Experimental phage therapy against *Staphylococcus aureus* in mice. *Antimicrob. Agents Chemother.* 51, 2765–2773.
- Carlton, R.M. (1999). Phage Therapy : Past History and Future Prospects. *Arch. Immunol. Ther. Exp. (Warsz)*. 47, 267–274.
- Cascales, E., Buchanan, S.K., Duche, D., Kleantous, C., Lloubes, R., Postle, K., Riley, M., Slatin, S., and Cavard, D. (2007). Colicin Biology. *Microbiol. Mol. Biol. Rev.* 71, 158–229.
- Cavallaro, A.S., Mahony, D., Commins, M., Mahony, T.J., and Mitter, N. (2011). Endotoxin-free

purification for the isolation of Bovine Viral Diarrhoea Virus E2 protein from insoluble inclusion body aggregates. *Microb. Cell Fact.* 10, 57.

Ceglarek, I., Piotrowicz, A., Lecion, D., Miernikiewicz, P., Owczarek, B., Hodyra, K., Harhala, M., Górski, A., and Dąbrowska, K. (2013). A novel approach for separating bacteriophages from other bacteriophages using affinity chromatography and phage display. *Sci. Rep.* 3, 1–6.

Center for Health Policy at Brookings (2015). Promoting Continuous Manufacturing in the Pharmaceutical Sector. www.brookings.edu/events/promoting-continuous-manufacturing-in-the-pharmaceutical-sector

Chan, B.K., and Abedon, S.T. (2015). Bacteriophages and their enzymes in biofilm control. *Curr. Pharm. Des.* 21, 85–99.

Cinquerrui, S., Mancuso, F., Vladisavljević, G.T., Bakker, S.E., and Malik, D.J. (2018). Nanoencapsulation of Bacteriophages in Liposomes Prepared Using Microfluidic Hydrodynamic Flow Focusing. *Front. Microbiol.* 9, 2172.

Clokier, M.R.J., and Kropinski, A.M. (2009). *Bacteriophages: methods and protocols*. Springer Protocols.

Coates, A.R., Halls, G., and Hu, Y. (2011). Novel classes of antibiotics or more of the same? *Br. J. Pharmacol.* 163, 184–194.

Cummins, P.M., Rochfort, K.D., and Connor, B.F.O. (2011). *Protein Chromatography*. 681, 209–223.

Cutler, S.A., Lonergan, S.M., Cornick, N., Johnson, A.K., and Stahl, C.H. (2007). Dietary inclusion of colicin E1 is effective in preventing postweaning diarrhea caused by F18-positive *Escherichia coli* in pigs. *Antimicrob. Agents Chemother.* 51, 3830–3835.

de Kraker, M.E.A., Wolkewitz, M., Davey, P.G., and Grundmann, H. (2011). Clinical Impact of Antimicrobial Resistance in European Hospitals: Excess Mortality and Length of Hospital Stay Related to Methicillin-Resistant *Staphylococcus aureus* Bloodstream Infections. *Antimicrob. Agents Chemother.* 55, 1598–1605.

de Kraker, M.E.A., Stewardson, A.J., and Harbarth, S. (2016). Will 10 Million People Die a Year due to Antimicrobial Resistance by 2050? *PLoS Med.* 13, 1–6.

de Oliveira Magalhães, P., Lopes, A.M., Mazzola, P.G., Rangel-Yagui, C., Penna, T.C. V, and Pessoa, A. (2007). Methods of endotoxin removal from biological preparations: A review. *J. Pharm. Pharm. Sci.* 10, 388–404.

Delcour, A.H. (2009). Outer Membrane Permeability and Antibiotic Resistance. *Biochim Biophys Acta*. 1794, 808–816.

Demain, A.L., and Vaishnav, P. (2011). Production of Recombinant Proteins by Microbes and Higher Organisms. *Compr. Biotechnol. Second Ed.* 3, 333–345.

Domingo-Calap, P., Georgel, P., and Baham, S. (2016). Back to the future: bacteriophages as promising therapeutic tools. *Hla* 87, 133–140.

Doorne, H. Van (1993). Sorption of Bacterial Endotoxin and Retention of Bacteria by Positively Charged Membrane Filters. *J. Parenter. Sci. Technol.* 47, 192-198.

Dosmar, M. (2006). An Experimental Approach to Optimization of Ultrafiltration. *BioProcess Tech.* 434, 44–54.

Drider, D., FimLand, G., Hechard, Y., McMullen, L.M., and Prevost, H. (2006). The Continuing Story of Class IIa Bacteriocins. *Microbiol. Mol. Biol. Rev.* 70, 564–582.

Dullah, E.C., and Ongkudon, C.M. (2017). Endotoxin Characterization – Effects of Metal Ions on Endotoxins Zeta Potential under Various Concentrations and pH Conditions. *Transactions on Science and Technology*, 4, 432–436.

Duong-Ly, K., and Gabelli, S.B. (2015). Affinity Purification of a Recombinant Protein Expressed. *Anal Chem.* 25, 368–379.

Earnshaw, W.C., and Harrison, S.C. (1977). DNA arrangement in isometric phage heads. *Nature* 268, 598–602.

European Centre for Disease Prevention and Control (2015). Antimicrobial resistance surveillance in Europe 2014. Annual Report of the European Antimicrobial Resistance Surveillance Network (EARS-Net). Stockholm: ECDC; 2015.

Ellis, E.L., and Delbrück, M. (1939). the Growth of Bacteriophage. *J. Gen. Physiol.* 22, 365–384.

El-Moghazy, A.N.A. (2011). Factors affecting endotoxin removal from aqueous solutions by ultrafiltration process. *J. Sci. Ind. Res. (India)*. 70, 55–59.

El-Sayed, M.M.H., and Chase, H.A. (2010). Simulation of the breakthrough curves for the adsorption of α -lactalbumin and β -lactoglobulin to SP Sepharose FF cation-exchanger. *Biochem. Eng. J.* 49, 221–228.

European Medicine Agency (2015). Workshop on the therapeutic use of bacteriophages_summary. 44, 2.

Etzel, M.R., and Riordan, W.T. (2009). Viral clearance using monoliths. *J. Chromatogr. A* 1216, 2621–2624.

European Pharmacopoeia (2010). Bacterial endotoxins. *Eur. Pharmacop.* 5.0 161.

Fahim, H.A., Khairalla, A.S., and El-Gendy, A.O. (2016). Nanotechnology: A valuable strategy to improve bacteriocin formulations. *Front. Microbiol.* 7:1385.

Food and Drug Administration (2012). Guidance for Industry Pyrogen and Endotoxins Testing. 1–10.

Felsovalyi, F., Mangiagalli, P., Bureau, C., Kumar, S.K., and Banta, S. (2011). Reversibility of the adsorption of lysozyme on silica. *Langmuir* 27, 11873–11882.

García, P., Rodríguez, L., Rodríguez, A., and Martínez, B. (2010). Food biopreservation: Promising strategies using bacteriocins, bacteriophages and endolysins. *Trends Food Sci. Technol.* 21, 373–382.

Gerba, C.P., and Hou, K. (1985). Endotoxin removal by charge-modified filters. *Appl. Environ. Microbiol.* 50, 1375–1377.

Gésan-Guiziou, G., Daufin, G., Boyaval, E., and Le Berre, O. (1999). Wall shear stress: effective parameter for the characterisation of the cross-flow transport in turbulent regime during skimmed milk microfiltration. *Lait* 79, 347–354.

Gillor, O., Kirkup, B.C., and Riley, M.A. (2004). Colicins and microcins: the next generation antimicrobials. *Adv. Appl. Microbiol.* 54, 129–146.

Gori, G. (1965). Continuous Cultivation of Virus in Cell Suspensions by Use of the Lysostat. *Appl. Microbiol.* 13, 909–917.

Gräslund, S., Nordlund, P., Weigelt, J., Hallberg, B.M., Bray, J., Gileadi, O., Knapp, S., Oppermann, U., Arrowsmith, C., Hui, R., et al. (2008). Protein production and purification. *Nat. Methods* 5, 135–146.

Guo, S., Kiefer, H., Zhou, D., Guan, Y.H., Wang, S., Wang, H., Lu, Y., and Zhuang, Y. (2016). A scale-down cross-flow filtration technology for biopharmaceuticals and the associated theory. *J. Biotechnol.* 221, 25–31.

Hammami, R., Fernandez, B., Lacroix, C., and Fliss, I. (2013). Anti-infective properties of bacteriocins: An update. *Cell. Mol. Life Sci.* 70, 2947–2967.

Hanke, A.T., and Ottens, M. (2014). Purifying biopharmaceuticals: Knowledge-based chromatographic process development. *Trends Biotechnol.* 32, 210–220.

Hankin, M.E. (1896). L'action bactéricide des eaux de la Jumna et du Gange sur le vibron du choléra.

Ann. Inst. Pasteur 10,511–523.

Heerden, C., D. and Nicol, W. (2013). Continuous and batch cultures of *Escherichia coli* KJ134 for succinic acid fermentation: metabolic flux distributions and production characteristics. *Microbial cell Factories* 12,80.

Hershey, A. D., and Chase, M. (1952). Independent functions of viral protein and nucleic acid in growth of bacteriophage. *J. Gen. Physiol.* 36, 39–56.

Heunis, T.D.J., Botes, M., and Dicks, L.M.T. (2010). Encapsulation of *Lactobacillus plantarum* 423 and its bacteriocin in nanofibers. *Probiotics Antimicrob. Proteins* 2, 46–51.

Hidayat, B.J., Eriksen, N.T. and Wiebe, M.G. (2006). Acid phosphatase production by *Aspergillus niger* N402A in continuous flow culture. *FEMS Microbiol. Lett.*, 254, 324–331.

Hirsch, A. (1950). The Assay of the Antibiotic Nisin. *Microbiology* 4, 70–83.

Hoffmann, S., Peterbauer, A., Schindler, S., Fennrich, S., Poole, S., Mistry, Y., Montag-Lessing, T., Spreitzer, I., Löschner, B., Van Aalderen, M., et al. (2005). International validation of novel pyrogen tests based on human monocytoid cells. *J. Immunol. Methods* 298, 161–173.

Horne, M.T. (1970). Coevolution of *Escherichia coli* and Bacteriophages in chemostat culture. *Science* 168, 992-993.

Hotchin, B.Y.J.E. (1955). The Use of Ammonium Sulphate in the Production of Lysates of *Staphylococcus* Phage K of High Titre. *J. Gen. Microbiol.* 13, 185–189.

Husimi, Y. (1989). Selection and evolution of bacteriophages in cellstat. *Adv Biophys.* 25, 1–43.

Husimi, Y., Nishigaki, K., Kinoshita, Y., Tanaka, T., Husimi, Y., Nishigaki, K., Kinoshita, Y., and Tanaka, T. (1982a). Cellstat—A continuous culture system of a bacteriophage for the study of the mutation rate and the selection process at the DNA level. *Rev. Sci. Instrum.* 53, 517.

Jacobson, H., and Jacobson, L. (1966). Virustat, a device for continuous production of viruses. *Appl. Microbiol.* 14, 940–952.

Jault, P., Leclerc, T., Gabard, J., and Fanneau de la Horie, G.C. (2017). Evaluation of phage therapy for the treatment of *Escherichia coli* and *Pseudomonas aeruginosa* burn wound infections (Phase I - II clinical trial). <https://clinicaltrials.gov/ct2/show/NCT02116010>.

Jault, P., Leclerc, T., Jennes, S., Pirnay, J.P., Que, Y.-A., Resch, G., Rousseau, A.F., Ravat, F., Carsin, H., Le Floch, R., et al. (2018). Efficacy and tolerability of a cocktail of bacteriophages to treat burn wounds

infected by *Pseudomonas aeruginosa* (PhagoBurn): a randomised, controlled, double-blind phase 1/2 trial. *Lancet Infect. Dis.* 19, 35–45.

Jennes, S., Merabishvili, M., Soentjens, P., Pang, K.W., Rose, T., Keersebilck, E., Soete, O., François, P.M., Teodorescu, S., Verween, G., et al. (2017). Use of bacteriophages in the treatment of colistin-only-sensitive *Pseudomonas aeruginosa* septicaemia in a patient with acute kidney injury—a case report. *Crit. Care* 21, 2016–2018.

Jeon, J., Ryu, C.M., Lee, J.Y., Park, J.H., Yong, D., and Lee, K. (2016). In vivo application of bacteriophage as a potential therapeutic agent to control OXA-66-like carbapenemase-producing acinetobacter baumannii strains belonging to sequence type 357. *Appl. Environ. Microbiol.* 82, 4200–4208.

Joerger, R.D. (2003). Alternatives to antibiotics: Bacteriocins, antimicrobial peptides and bacteriophages. *Poult. Sci.* 82, 640–647.

Johansson, H., Jägersten, C., and Shiloach, J. (1996). Large scale recovery and purification of periplasmic recombinant protein from *E. coli* using expanded bed adsorption chromatography followed by new ion exchange media. *J. Biotechnol.* 48, 9–14.

Jozala, A.F., Geraldes, D.C., Tundisi, L.L., Feitosa, V. de A., Breyer, C.A., Cardoso, S.L., Mazzola, P.G., de Oliveira-Nascimento, L., Rangel-Yagui, C. de O., Magalhães, P. de O., et al. (2016). Biopharmaceuticals from microorganisms: from production to purification. *Brazilian J. Microbiol.* 47, 51–63.

Jungbauer, A. (2013). Continuous downstream processing of biopharmaceuticals. *Trends Biotechnol.* 31, 479–492.

Kaca, W., Roths, R.I., and Rabi, S.B. (1994). Hemoglobin, a Newly Recognized Lipopolysaccharide (LPS)-binding Protein That Enhances LPS Biological Activity substrate. *Journal of Biological Chemistry* 269, 25078–25084.

Kapoor, G., Saigal, S., and Elongavan, A. (2017). Action and resistance mechanisms of antibiotics: A guide for clinicians. *J. Anaesthesiol. Clin. Pharmacol.* 33, 300–305.

Kasman, L.M., Kasman, A., Westwater, C., Dolan, J., Schmidt, M.G., and Norris, J.S. (2002). Overcoming the Phage Replication Threshold: a Mathematical Model with Implications for Phage Therapy. *J. Virol.* 76, 5557–5564.

Kelly, S.T., and Zydney, A.L. (1997). Protein fouling during microfiltration: Comparative behavior of different model proteins. *Biotechnol. Bioeng.* 55, 91–100.

Kick, B., Behler, K.L., Severin, T.S., and Weuster-Botz, D. (2017). Chemostat studies of bacteriophage

M13 infected *Escherichia coli* JM109 for continuous ssDNA production. *J. Biotechnol.* 258, 92–100.

Klaenhammer, T.R. (1993). Genetics of bacteriocins produced by lactic acid bacteria. *FEMS Microbiol. Rev.* 12, 39–85.

Konstantinov, K.B., and Cooney, C.L. (2014). White Paper on Continuous Bioprocessing. *J. Pharm. Sci.* 104, 813-820.

Kosvintsev, S.R., Gasparini, G., Holdich, R.G., Cumming, I.W., and Stillwell, M.T. (2005). Liquid - Liquid membrane dispersion in a stirred cell with and without controlled shear. *Ind. Eng. Chem. Res.* 44, 9323–9330.

Kutter, E., De Vos, D., Gvasalia, G., Alavidze, Z., Gogokhia, L., Kuhl, S., and Abedon, S. (2010). Phage Therapy in Clinical Practice: Treatment of Human Infections. *Curr. Pharm. Biotechnol.* 11, 69–86.

Kutter, E. and Sulakvelidze, A. (2005). Bacteriophage therapy in humans In: Kutter E, Sulakvelidze A, eds. *Bacteriophages: Biology and Application*. Boca Raton: CRC Press, 2005:381-436.

Lali, A. (2002). Expanded Bed Affinity Chromatography - Methods for Affinity-Based Separations of Enzymes and Proteins. M.N. Gupta, ed. (Basel: Birkhäuser Basel), pp. 29–64.

Levin, J., and Bang, F.B. (1968). Clottable protein in *Limulus*; its localization and kinetics of its coagulation by endotoxin. *Thomb. Diath. Haemorrh.* 19, 186—197.

Lewin (2009). *Genes VII*. Oxford University Press.

Li, L., and Luo, R.G. (1998). Use of Ca^{+2} to re-aggregate lipopolysaccharide (LPS) in hemoglobin solutions and the subsequent removal of endotoxin by ultrafiltration. *Biotechnol. Tech.* 12, 119–122.

Li, M., Su, Z.G., and Janson, J.C. (2004). In vitro protein refolding by chromatographic procedures. *Protein Expr. Purif.* 33, 1–10.

Li, Z., Kessler, W., Heuvel, J. van den, and Rinas, U. (2010). Simple defined autoinduction medium for recombinant protein production in *E. coli* T7 expression system. *Appl. Microbiol. Biotechnol.* 91, 1203-13.

Liu, Z.; Hou, J.; Martínez, J.L.; Petranovic, D.; Nielsen, J. (2013). Correlation of cell growth and heterologous protein production by *Saccharomyces cerevisiae*. *Appl. Microbiol. Biotechnol.* 97, 8955–8962

Luria, S.E., Delbrück, M., and Anderson, T.F. (1943). Electron Microscope Studies of Bacterial Viruses. *J. Bacteriol.* 46, 57–77.

Mack, L., Brill, B., Delis, N., and Groner, B. (2014). Endotoxin depletion of recombinant protein preparations through their preferential binding to histidine tags. *Anal. Biochem.* 466, 83–88.

Malik, D.J., Sokolov, I.J., Vinner, G.V.K., Mancuso, F., Cinquerrui, S., Vladisavljevic, G.T., Clokie, M.R.J.J., Garton, N.J., Stapley, A.G.F.F., and Kirpichnikova, A. (2017). Formulation, Stabilisation and Encapsulation of Bacteriophage for Phage Therapy. *Adv. Colloid Interface Sci.* 249, 100–133.

Mancuso, F., Shi, J., and Malik, D.J. (2018). High Throughput Manufacturing of Bacteriophages Using Continuous Stirred Tank Bioreactors Connected in Series to Ensure Optimum Host Bacteria Physiology for Phage Production. *Viruses* 10, 1–19.

Merabishvili, M., Pirnay, J., Verbeken, G., Chanishvili, N., Tediashvili, M., Lashkhi, N., Glonti, T., Krylov, V., Mast, J., Parys, L. Van, et al. (2009). Quality-Controlled Small-Scale Production of a Well-Defined Bacteriophage Cocktail for Use in Human Clinical Trials. *PLoS One* 4, 1–10.

Michaelidis, C.I., Fine, M.J., Lin, C.J., Linder, J.A., Nowalk, M.P., Shields, R.K., Zimmerman, R.K., and Smith, K.J. (2016). The hidden societal cost of antibiotic resistance per antibiotic prescribed in the United States: An exploratory analysis. *BMC Infect. Dis.* 16, 1–8.

Mueller, M., Lindner, B., Kusumoto, S., Fukase, K., Schomm, A.B., and Seydel, U. (2004). Aggregates are the biologically active units of endotoxin. *J. Biol. Chem.* 279, 26307–26313.

Nabergoj, D., Modic, P., and Podgornik, A. (2017). Effect of bacterial growth rate on bacteriophage population growth rate. *Microbiologyopen* 7, 1–10.

Nabergoj, D., Kuzmi, N., Drakslar, B., and Podgornik, A. (2018). Effect of dilution rate on productivity of continuous bacteriophage production in cellstat. 3649–3661.

Nestola, P., Martins, D.L., Peixoto, C., Roederstein, S., Schleuss, T., Alves, P.M., Mota, J.P.B., and Carrondo, M.J.T. (2014). Evaluation of novel large cut-off ultrafiltration membranes for adenovirus serotype 5 (Ad5) concentration. *PLoS One* 9, 1–22.

Nieth, A., Verseux, C., Barnert, S., Süß, R., and Römer, W. (2015). A first step toward liposome-mediated intracellular bacteriophage therapy. *Expert Opin. Drug Deliv.* 5247, 1–14.

O’Neill, J. (2014). Review on Antimicrobial Resistance. *Antimicrobial Resistance: Tackling a Crisis for the Health and Wealth of Nations, 2014.* <https://amr-review.org/>

O’Neill, J. (2016). *Tackling Drug-Resistance Infections Globally: Final Report and Recommendations.* 1, 52-63. <https://amr-review.org/>

Ohno, N., and Morrison, D.C. (1989). Lipopolysaccharide interaction with lysozyme. Binding of

lipopolysaccharide to lysozyme and inhibition of lysozyme enzymatic activity. *J. Biol. Chem.* 264, 4434–4441.

Oksanen, H.M., Domanska, A., and Bamford, D.H. (2012). Monolithic ion exchange chromatographic methods for virus purification. *Virology* 434, 271–277.

Ongkudon, C.M., Chew, J.H., Liu, B., and Danquah, M.K. (2012). Chromatographic Removal of Endotoxins: A Bioprocess Engineer's Perspective. *ISRN Chromatogr.* 2012, 1–9.

Pantel, L., Florin, T., Dobosz-Bartoszek, M., Racine, E., Sarciaux, M., Serri, M., Houard, J., Campagne, J.M., de Figueiredo, R.M., Midrier, C., et al. (2018). Odilorhabdins, Antibacterial Agents that Cause Miscoding by Binding at a New Ribosomal Site. *Mol. Cell* 70, 83–94.e7.

Parada, J.L., Caron, C.R., Medeiros, A.B.P., and Soccol, C.R. (2007). Bacteriocins from lactic acid bacteria: Purification, properties and use as biopreservatives. *Brazilian Arch. Biol. Technol.* 50, 521–542.

Paulová, L.; Hyka, P.; Branská, B.; Melzoch, K.; Kovar, K. (2012). Use of a mixture of glucose and methanol as substrates for the production of recombinant trypsinogen in continuous cultures with *Pichia pastoris* Mut+. *J. Biotechnol.*, 157, 180–188.

Payne, Robert J H and Jansen, V. (2001). Understanding Bacteriophage Therapy as a Density-dependent Kinetic Process. *J. Theor. Biol.* 208, 37–48.

Peebo, K., and Neubauer, P. (2018). Application of Continuous Culture Methods to Recombinant Protein Production in Microorganisms. *Microorganisms* 6, 56.

Petsch, D., and Anspach, F.B. (2000). Endotoxin removal from protein solutions. *J. Biotechnol.* 76, 97–119.

Pirnay, G.V.J., Lavigne, R., Jennes, S., and Vos, D. De (2014). Call for a Dedicated European Legal Framework for Bacteriophage Therapy. *Arch. Immunol. Ther. Exp.*, 117–129.

Pirnay, J., Verbeken, G., Rose, T., Jennes, S., Zizi, M., Huys, I., Lavigne, R., Merabishvili, M., Vaneechoutte, M., Buckling, A., et al. (2012). Introducing yesterday's phage therapy in today's medicine. *Futur. Med.* 379–390.

Pirnay, J., Blasdel, B.G., Bretaudeau, L., Buckling, A., Chanishvili, N., Clark, J.R., and Corte-real, S. (2015). Quality and Safety Requirements for Sustainable Phage Therapy Products. 2173–2179.

Pirnay, J.P., De Vos, D., Verbeken, G., Merabishvili, M., Chanishvili, N., Vaneechoutte, M., Zizi, M., Laire, G., Lavigne, R., Huys, I., et al. (2011). The phage therapy paradigm: Prêt-à-porter or sur-mesure?

Pharm. Res. 28, 934–937.

Pyo, S.H., Lee, J.H., Park, H.B., Hong, S.S., and Kim, J.H. (2001). A large-scale purification of recombinant histone H1.5 from *Escherichia coli*. *Protein Expr. Purif.* 23, 38–44.

Raetz, C.R.H., and Whitfield, C. (2008). Lipopolysaccharide Endotoxins. *Annu Rev Biochem.* 71, 1–57.

Rahimzadeh, M., Sadeghizadeh, M., Najafi, F., Arab, S., and Mobasheri H., (2016). Impact of heat shock step on bacterial transformation efficiency. *Mol. Biol. Res. Commun.* 5, 257-261.

van Reis, R., and Zydney, A. (2007). Bioprocess membrane technology. *J. Memb. Sci.* 297, 16–50.

Rhoads, D.D., Wolcott, R.D., Kuskowski, M.A., Wolcott, B.M., Ward, L.S., and Sulakvelidze, A. (2009). Bacteriophage therapy of venous leg ulcers in humans: results of a phase I safety trial. *J. Wound Care* 18, 237–243.

Rose, T., Verbeken, G., Vos, D. De, Merabishvili, M., Vanechoutte, M., Jennes, S., Zizi, M., and Pirnay, J. (2014). Experimental phage therapy of burn wound infection : difficult first steps. *Int. j. Burns Trauma* 4, 66–73.

Roslansky, P.F., and Novitsky, T.J. (1991). Sensitivity of Limulus ameocyte lysate (LAL) to LAL-reactive glucans. *J. Clin. Microbiol.* 29, 2477–2483.

Saksena, S., and Zydney, A.L. (1993). Effect of solution pH and ionic strength on the separation of albumin from immunoglobulins (IgG) by selective filtration. *Biotechnol. Bioeng.* 43, 960–968.

Sarker, S.A., Berger, B., Deng, Y., Kieser, S., Foata, F., Moine, D., Descombes, P., Sultana, S., Huq, S., Bardhan, P.K., et al. (2016). Oral application of *Escherichia coli* bacteriophage: safety tests in healthy and diarrheal children from Bangladesh. *Environ. Microbiol.* 19, 237–250.

Sauvageau, D., and Cooper, D.G. (2010). Two-stage, self-cycling process for the production of bacteriophages. *Microb. Cell Fact.* 9, 81.

Schooley, R.T., Biswas, B., Gill, J.J., Hernandez-Morales, A., Lancaster, J., Lessor, L., Barr, J.J., Reed, S.L., Rohwer, F., Benler, S., et al. (2017). Development and use of personalized bacteriophage-based therapeutic cocktails to treat a patient with a disseminated resistant *Acinetobacter baumannii* infection. *Antimicrob. Agents Chemother.* 61, e00954-17.

Schomm, A.B., Brandenburg, K., Loppnow, H., Zähinger, U., Rietschel, E.T., Carroll, S.F., Koch, M.H., Kusumoto, S., and Seydel, U. (1998). The charge of endotoxin molecules influences their conformation and IL-6-inducing capacity. *J Immunol.* 161, 5464–5471.

Schwarz, H., Gornicec, J., Neuper, T., Parigiani, M.A., Wallner, M., Duschl, A., and Horejs-Hoeck, J. (2017). Biological activity of masked endotoxin. *Sci. Rep.* 7, 1–11.

Seydel, U., Hawkins, L., Schomm, A.B., Heine, H., Scheel, O., Koch, M.H.J., and Brandenburg, K. (2003). The generalized endotoxic principle. *Eur. J. Immunol.* 33, 1586–1592.

Shallcross, L.J. and Davies, S.C. (2014). Antibiotic overuse: a key driver of antimicrobial resistance. *Br. J. Gen. Pract.* 64, 604–605.

Shin, J.M., Ateia, I., Paulus, J.R., Liu, H., Fenno, J.C., Rickard, A.H., and Kapila, Y.L. (2015). Antimicrobial nisin acts against saliva derived multi-species biofilms without cytotoxicity to human oral cells. *Front. Microbiol.* 6, 617.

Shlaes, D.M., and Bradford, P.A. (2018). Antibiotics—From There to Where? *Pathog. Immun.* 3, 19.

Siddiqui, A.R., and Bernstein, J.M. (2010). Chronic wound infection: Facts and controversies. *Clin. Dermatol.* 28, 519–526.

Sidhu, P.K., and Neha, K. (2017). Bacteriocin-nanoconjugates as emerging compounds for enhancing antimicrobial activity of bacteriocins. *J. King Saud Univ. - Sci.*, in press.

Skidmore, G.L., and Chase, H.A. (1990). Two-component protein adsorption to the cation exchanger S Sepharose®FF. *J. Chromatogr. A* 505, 329–347.

Smrekar, F., Ciringer, M., Jančar, J., Raspor, P., Štrancar, A., and Podgornik, A. (2011a). Optimization of lytic phage manufacturing in bioreactor using monolithic supports. *J. Sep. Sci.* 34, 2152–2158.

Smrekar, F., Ciringer, M., Strancar, A., and Podgornik, A. (2011b). Characterisation of methacrylate monoliths for bacteriophage purification. *J. Chromatogr. A* 1218, 2438–2444.

Srivastava, P.; Mukherjee, K.J. (2005). Kinetic studies of recombinant human interferon-alpha (rhIFN- α) expression in transient state continuous cultures. *Biochem. Eng. J.*, 26, 50–58.

Storms, Z.J. (2012). Bioprocessing with Bacteriophages Using Self- Cycling Fermentation. PhD Thesis, McGill University, Montreal, Quebec, Canada.

Storms, Z.J. (2014). Impact of the cell life-cycle on bacteriophage T4 infection. *FEMS Microbiol. Lett.* 353, 63-68.

Studier, F.W. (2005). Protein production by auto-induction in high-density shaking cultures. *Protein Expression and Purification*, 41, 207–234.

Su, W., and Ding, X. (2015). Methods of Endotoxin Detection. *J. Lab. Autom.* 20, 354–364.

Sweadner, K.J., Forte, M., and Nelsen, L.L. (1977). Filtration removal of endotoxin (pyrogens) in solution in different states of aggregation. *Appl. Environ. Microbiol.* 34, 382–385.

Swinehart, D.F. (1962). The Beer-Lambert Law. *J. Chem. Educ.* 39, 333.

Szermier-Olearnik, B., and Boratyński, J. (2015). Removal of endotoxins from bacteriophage preparations by extraction with organic solvents. *PLoS One* 10, 1–10.

Szermier-Olearnik, B., Drab, M., Makosa, M., Zembala, M., Barbasz, J., Dabrowska, K., and Boratyński, J. (2017). Aggregation/dispersion transitions of T4 phage triggered by environmental ion availability. *J. Nanobiotechnology* 15, 1–15.

Thabit, A.K., Crandon, J.L., and Nicolau, D.P. (2015). Antimicrobial resistance: impact on clinical and economic outcomes and the need for new antimicrobials. *Expert Opin. Pharmacother.* 16, 159–177.

Tomono, T., Hirai, Y., Okada, H., Adachi, K., Ishii, A., Shimada, T., Onodera, M., Tamaoka, A., and Okada, T. (2016). Ultracentrifugation-free chromatography-mediated large-scale purification of recombinant adeno-associated virus serotype 1 (rAAV1). *Mol. Ther. - Methods Clin. Dev.* 3, 15058.

Trautner, B., Hull, R., and Darouiche, R. (2007). Colicins prevent colonization of urinary catheters. *J Antimicrob Chemother* 56, 413–415.

Tripathi, N.K., and Shivastava, A. (2018). Scale up of biopharmaceuticals production (Elsevier Inc.), 133-172.

Tsonos, J., Vandenheuvell, D., Briers, Y., Greve, H. De, Hernalsteens, J., and Lavigne, R. (2014). Hurdles in bacteriophage therapy : Deconstructing the parameters. *Vet. Microbiol.* 171, 460–469.

Twort, F.W. (1915). An investigation on the nature of ultra-microscopic viruses. *Lancet* 2, 1241–1243.

Vaiphei, S.T., Pandey, G., Mukherjee, K.J. (2009). Kinetic studies of recombinant human interferon-gamma expression in continuous cultures of *E. coli*. *J. Ind. Microbiol. Biotechnol.* 36, 1453–1458.

Van Belleghem, J.D., Merabishvili, M., Vergauwen, B., Lavigne, R., and Vanechoutte, M. (2017). A comparative study of different strategies for removal of endotoxins from bacteriophage preparations. *J. Microbiol. Methods* 132, 153–159.

Velur Selvamani, R.S.; Friehs, K.; Flaschel, E. (2014). Extracellular recombinant protein production under continuous culture conditions with *Escherichia coli* using an alternative plasmid selection mechanism. *Bioprocess Biosyst. Eng.*, 37, 401–413.

Ventola, C.L. (2015). The antibiotic resistance crisis: part 1: causes and threats. *P T A Peer-Reviewed J.*

Formul. Manag. 40, 277–283.

Verbeke, G., Vos, D. De, Vaneechoutte, M., Zizi, M., and Pirnay, J. (2007). European regulatory conundrum of phage therapy. *Future Microbiol.* 2, 485–491.

Verheest, C., Pauwels, K., Mahillon, J., Helinski, D.R., and Herman, P. (2010). Contained use of Bacteriophages: Risk Assessment and Biosafety Recommendations. *Appl. Biosaf.* 15, 32–44.

Vieu, J.F. (1961). Intérêt des bactériophages dans le traitement de staphylococcies. *Vie Med.* 823–829.

Vinner, G.K., Vladislavljević, G.T., Clokie, M.R.J., and Malik, D.J. (2017). Microencapsulation of *Clostridium difficile* specific bacteriophages using microfluidic glass capillary devices for colon delivery using pH triggered release. *PLoS One* 12, 1–27.

Walker, D., and McCaughey, L. (2016). Pulmonary administration of pyocins for treating bacterial respiratory infections. WO/2016/046218

Wallis, R., Moore, G.R., James, R., and Kleanthous, C. (1995). Protein-Protein Interactions in Colicin E9 DNase-Immunity Protein Complexes. 1. Diffusion-Controlled Association and Femtomolar Binding for the Cognate Complex. *Biochemistry* 34, 13743–13750.

Ward, P.P., Cunningham, G.A., and Conneely, O.M. (1997). Commercial production of lactoferrin, a multifunctional iron-binding glycoprotein. *Biotechnol. Genet. Eng. Rev.* 14, 303–320.

Werner, M.H., Clore, G.M., Gronenborn, A.M., Kondoh, A., and Fisher, R.J. (1994). Refolding proteins by gel filtration chromatography. *FEBS Lett.* 345, 125–130.

Who (2014). Antimicrobial resistance. *Bull. World Health Organ.* 61, 383–394.

Wilson, M.J., Haggart, C.L., Gallagher, S.P., and Walsh, D. (2001). Removal of tightly bound endotoxin from biological products. *J. Biotechnol.* 88, 67–75.

Wingfield, P.T. (2016). Overview of the Purification of Recombinant Proteins. *Curr. Protoc. Protein Sci.* 2015 80:6.1.1-35.

World Medical Association Declaration of Helsinki (2013). Ethical Principles For Scientists Requirements and Research Protocols - 9th (Fortalez amendment). 29–32.

Wurm, F.M. (2004). Production of recombinant protein therapeutics in cultivated mammalian cells. *Nat. Biotechnol.* 22, 1393–1398.

Yamakami, K., Tsumori, H., Sakurai, Y., Shimizu, Y., Nagatoshi, K., and Sonomoto, K. (2013). Sustainable inhibition efficacy of liposome-encapsulated nisin on insoluble glucan-biofilm synthesis by

Streptococcus mutans. *Pharm. Biol.* 51, 267–270.

Yu, L.X. (2008). Pharmaceutical Quality by design: Product and Process Development, Understanding, and Control. *Pharm. Res.* 25, 781–791.

Zakharova, M.Y., Kozyr, A. V, Ignatova, A.N., Vinnikov, I.A., Shemyakin, I.G., and Kolesnikov, A. V (2005). Purification of filamentous bacteriophage for phage display using size-exclusion chromatography. *Biotechniques.* 38, 2–4.

Zhao, M., Vandersluis, M., Stout, J., Haupts, U., Sanders, M., and Jacquemart, R. (2018). Affinity chromatography for vaccines manufacturing: Finally ready for prime time? *Vaccine* 37, 5491-5503.

Ziv, N., Brandt, N.J., and Gresham, D. (2013). The Use of Chemostats in Microbial Systems Biology. *J. Vis. Exp.* 80, 1–10.

10. Supplementary Results

10.1. Viscosity of BHI and LB broth

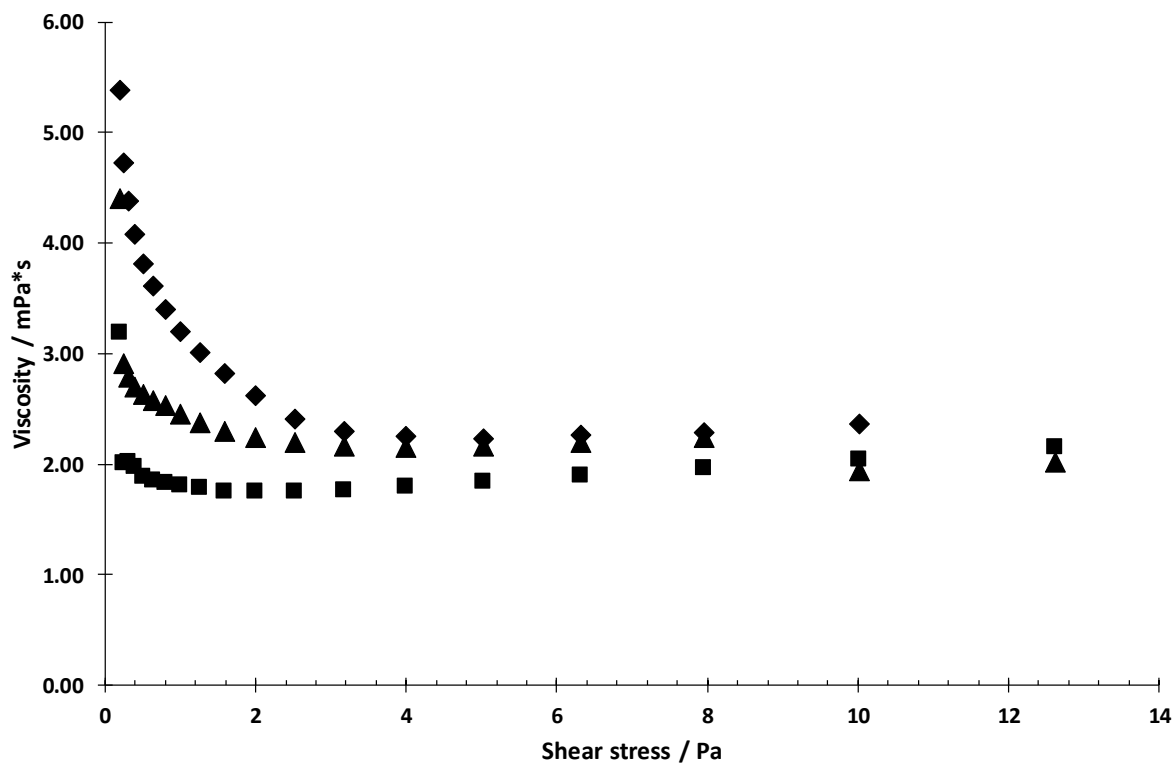


Figure S. 1 Viscosity measures of BHI at 25° C measured using a rheometer with cone-plate configuration. Final viscosity value is the average of the values taken from 4 to 10 Pa from the three independent measures taken from three different samples.

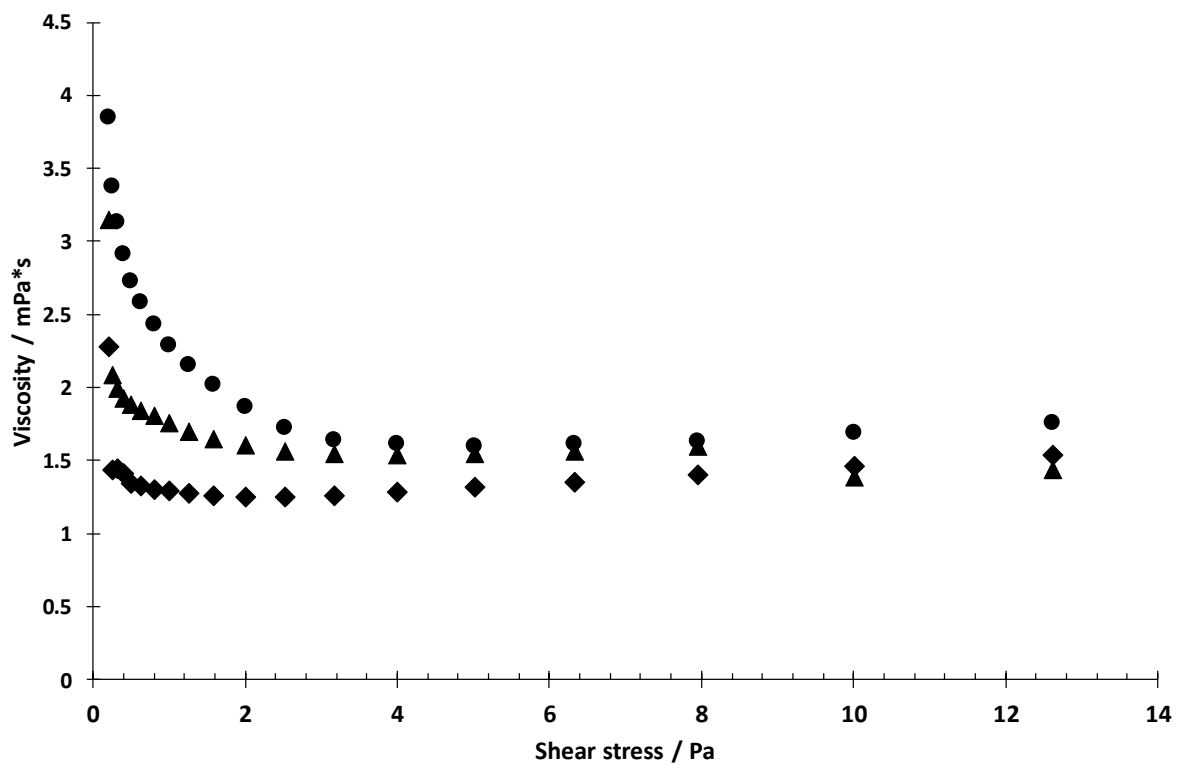


Figure S. 2 Viscosity measures of LB at 25° C measured using a rheometer with cone-plate configuration. Final viscosity value is the average of the values taken from 4 to 10 Pa from the three independent measures taken from three different samples.

10.2.3. Tangential Flow Filtration Experimental set-up



Figure S. 5 Operative tangential flow filtration apparatus.

10.3. Composition of the synthetic medium

Name	Working concentration	Sterilization method
MgSO₄	0.586 g L ⁻¹	121 °C autoclave
Glucose	2.94 g L ⁻¹	Filtration (0.22 µm)
Na₂MoO₄ ·H₂O	2.1 mg L ⁻¹	121 °C autoclave
Trace elements	2.5mg L ⁻¹ CoCl ₂ ·6H ₂ O	121 °C autoclave
	15 mg L ⁻¹ MnCl ₂ ·4H ₂ O	
	1.5 mg L ⁻¹ CuCl ₂ ·2H ₂ O	
	3 mg L ⁻¹ H ₃ BO ₃	
	33.8 mg L ⁻¹ Zn(CH ₃ COO) ₂ ·2H ₂ O	
	14.10 mg L ⁻¹ Titriplex III	
(NH₄)₂HPO₄	4 g L ⁻¹	121 °C autoclave
KH₂PO₄	13.3 g L ⁻¹	121 °C autoclave
Citric Acid	1.5542 g L ⁻¹	121 °C autoclave
Fe(III) citrate	0.1008 g L ⁻¹	121 °C autoclave
Trizma Base	To bring pH to 7	121 °C autoclave

Table S.1 Composition of synthetic medium for continuous production of *E. coli*

10.4. Adsorption of Phage T3 at different dilution rates

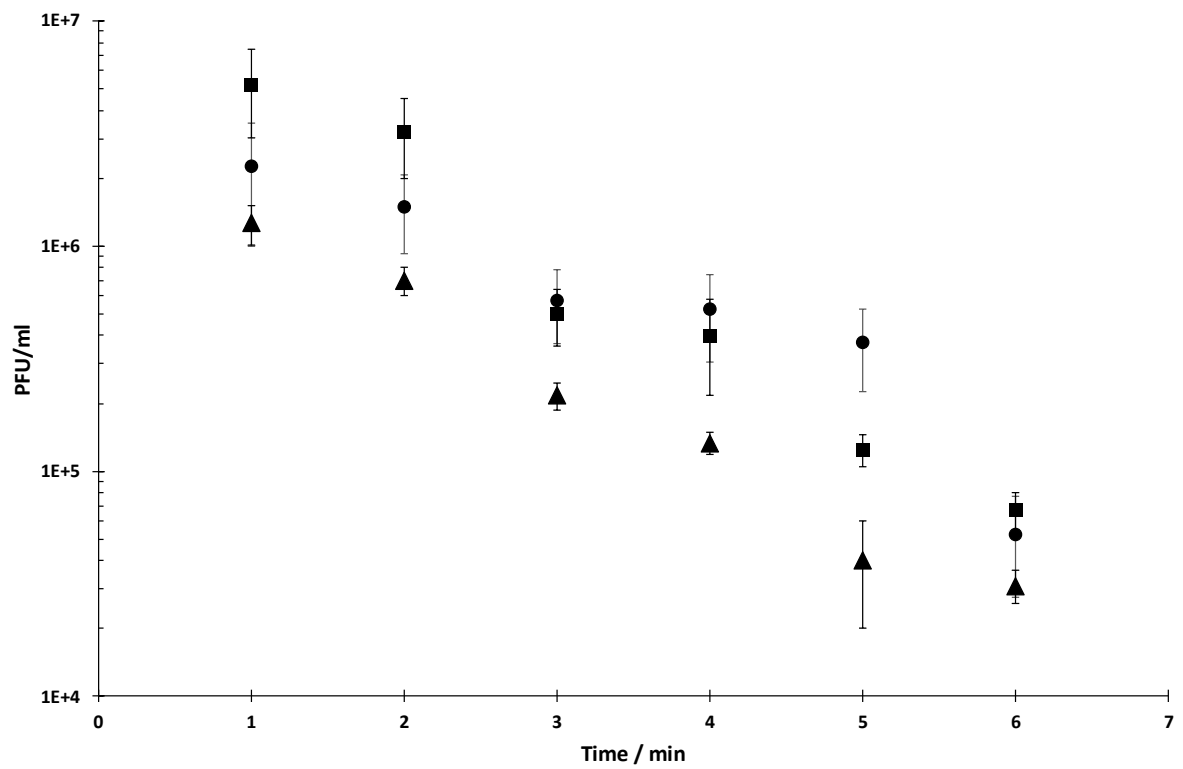


Figure S. 6 Adsorption rates of phage T3 at different dilution rates. Filled circles (●) represent adsorption at $D1=0.5\text{ h}^{-1}$, filled squares at $D1=0.4\text{ h}^{-1}$ (■) and filled triangles (▲) at $D1=0.6\text{ h}^{-1}$.

10.5. One-step of Phage T3 at different dilution rates

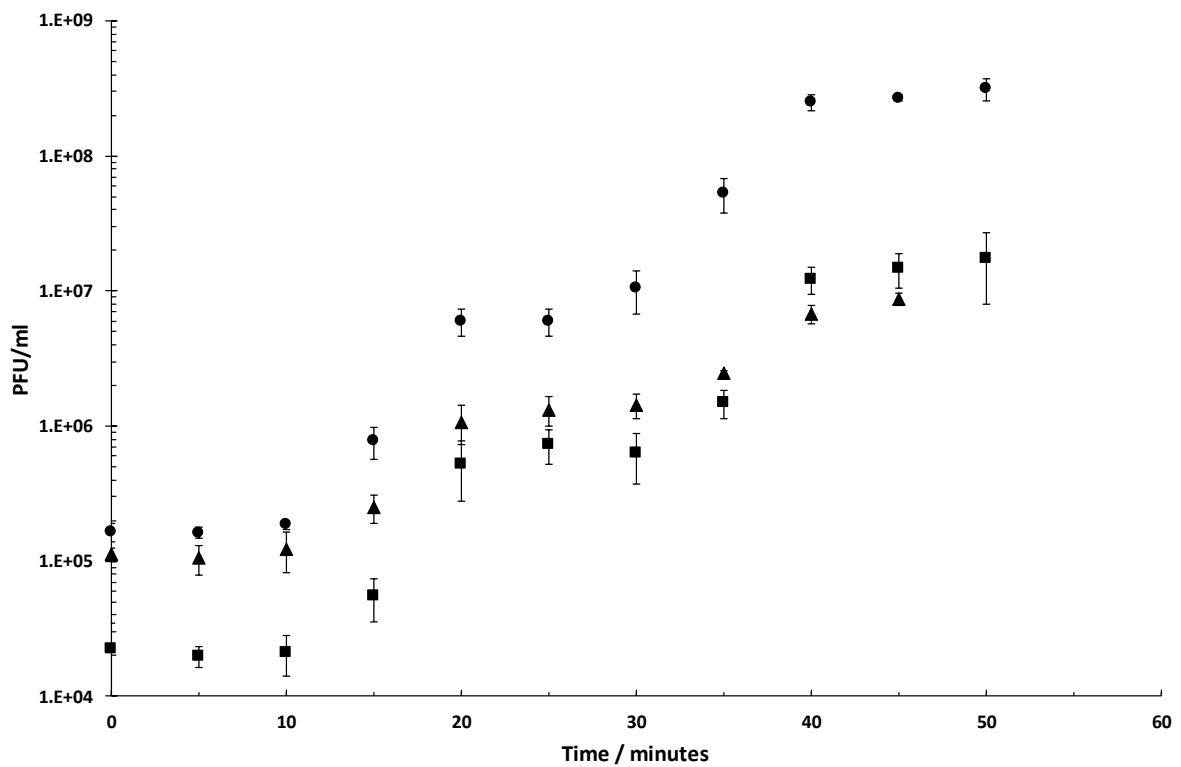


Figure S. 7 One-step of phage T3 at different dilution rates. Filled circles (●) represent adsorption at $D1=0.5\text{ h}^{-1}$, filled squares at $D1=0.4$ (■) and filled triangles (▲) at $D1=0.6\text{ h}^{-1}$.

10.6. Cesium Chloride purification for phage T3 and Phage K

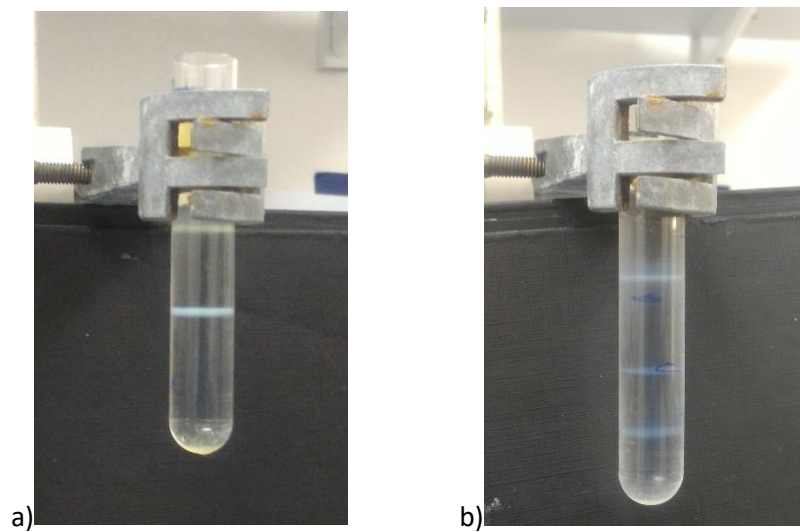


Figure S.8 CsCl separation for phage K (a) and phage T3 (b) with the typical bands due to different gradients.

10.7. Calibration curves

10.7.1. Dextran refractive index

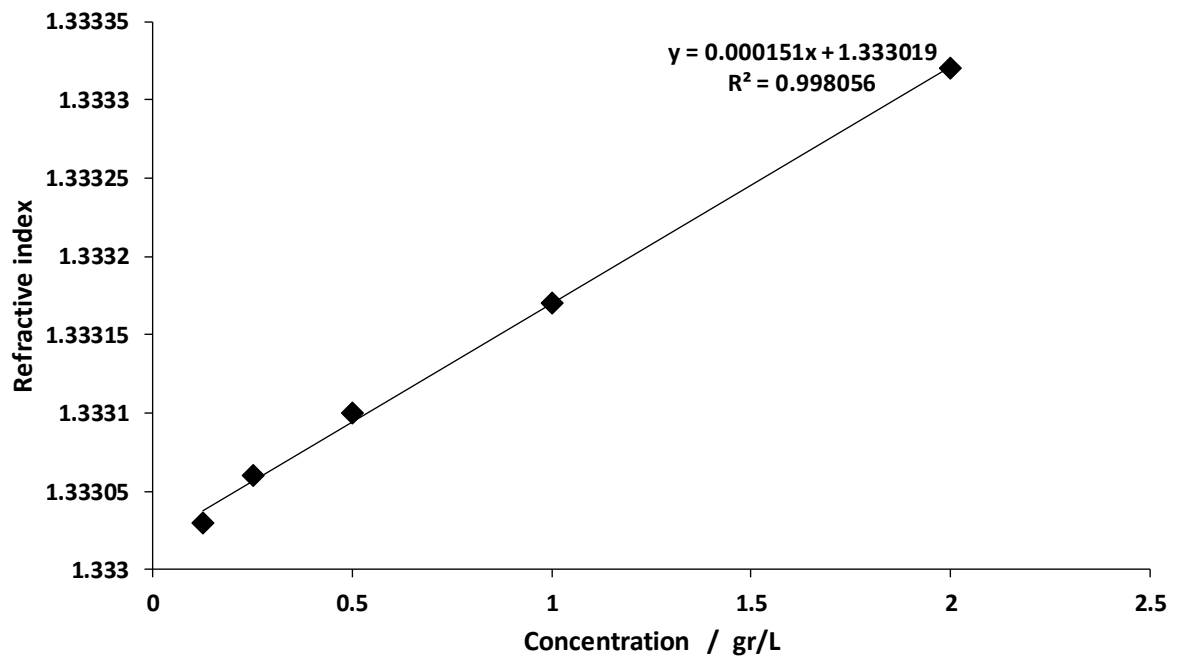


Figure S. 9 Calibration curve correlating dextran refractive index to their concentration in the solution.

10.7.2. Peristaltic pump

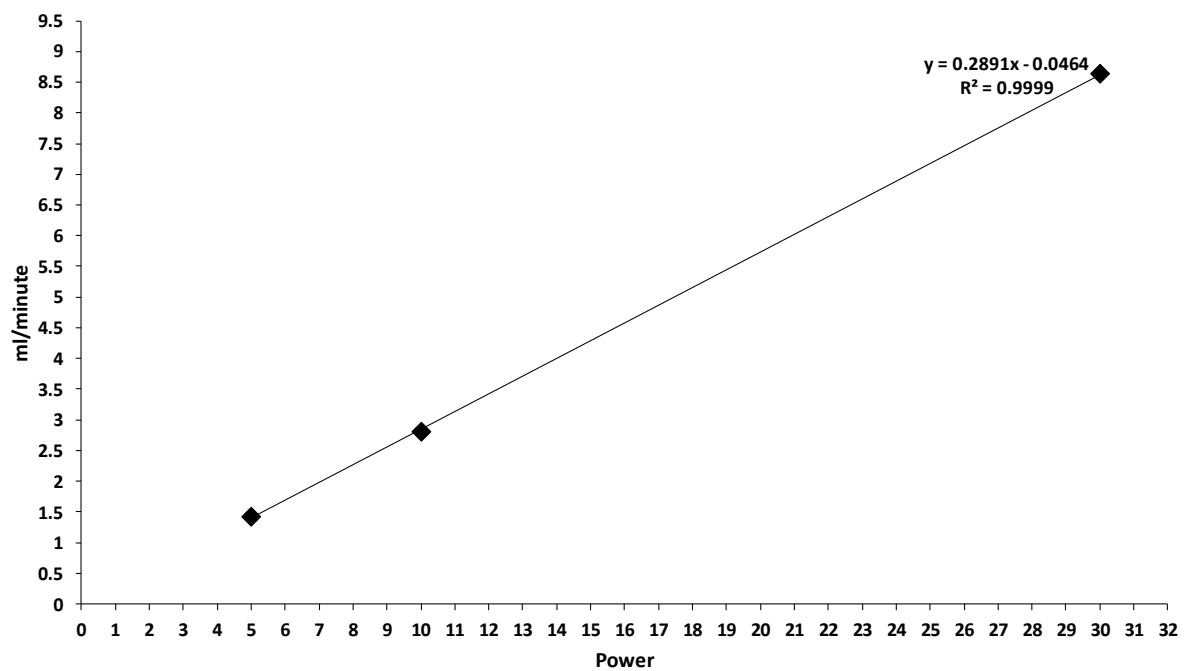


Figure S. 10 Calibration curve correlating peristaltic pump power to flowrate of deionised water.

10.7.3. Analox

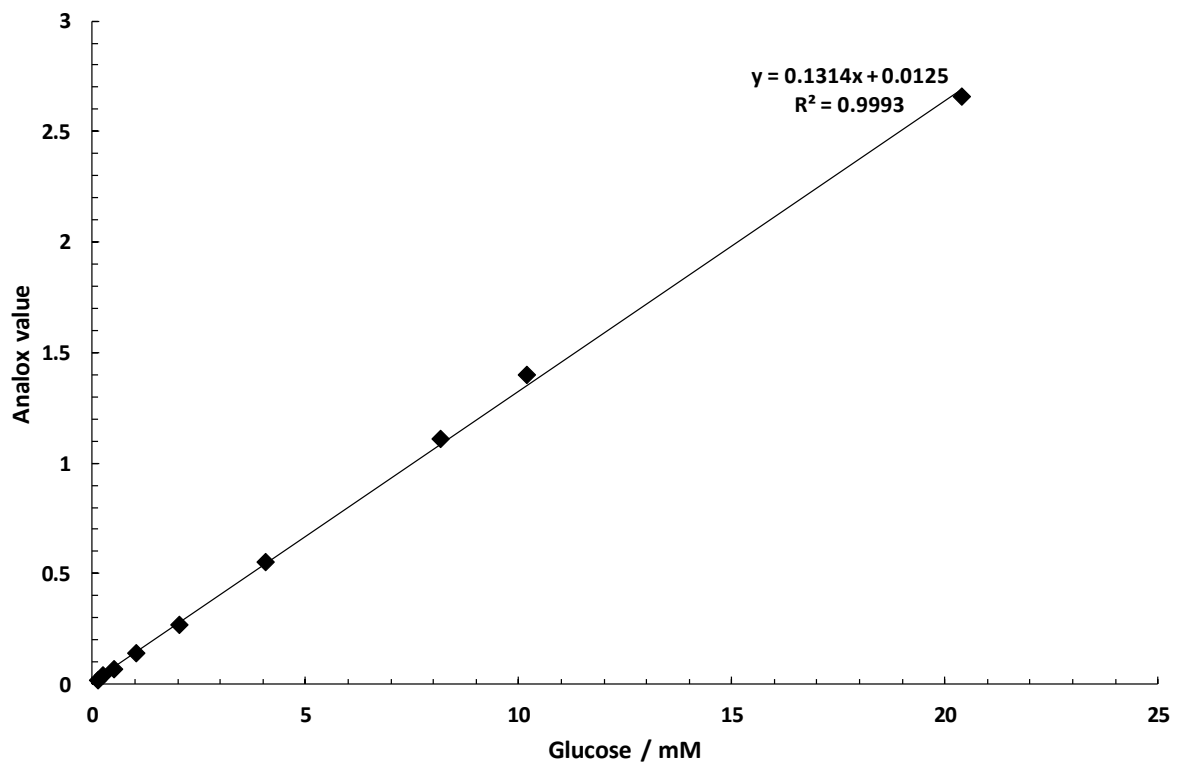


Figure S. 11 Calibration curve correlating Analox voltage outcome to glucose concentration (mM).

10.7.4. Protein standards at SEC

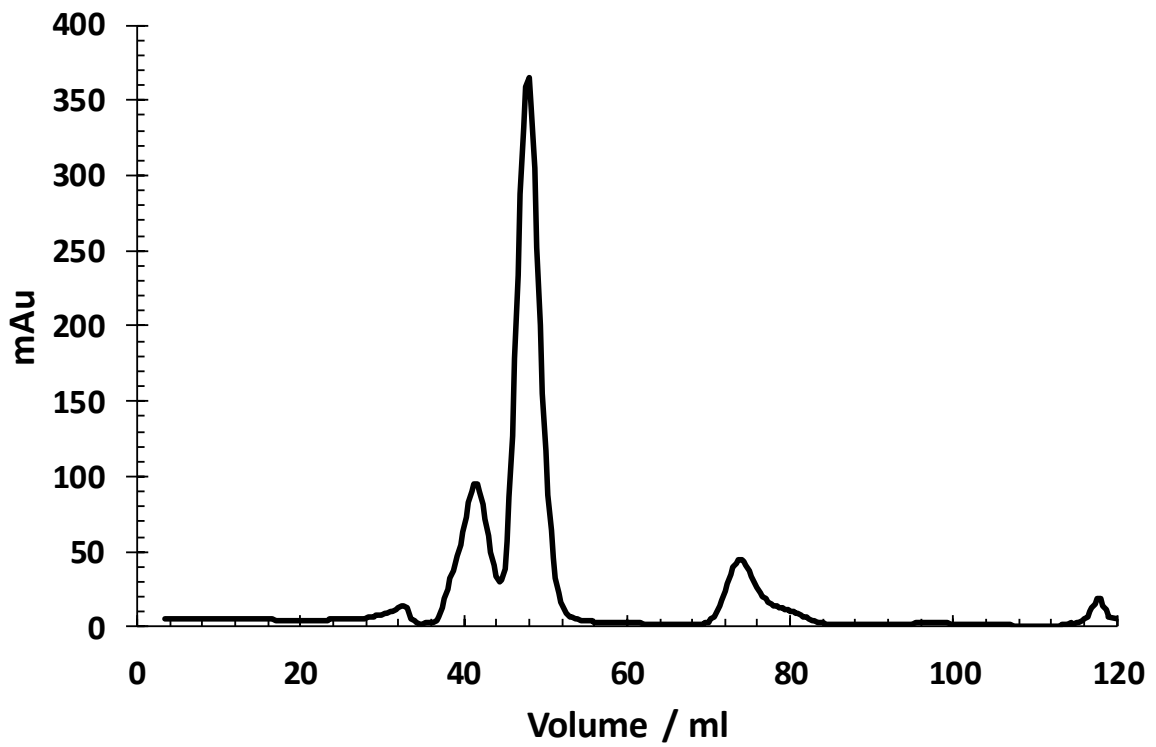


Figure S. 12 Elution of protein standards in SEC using S-100 column. The proteins eluted are IgG (160 kDa), BSA (67 kDa) and cytochrome C (12,4 kDa).